



LEHIGH
UNIVERSITY

Library &
Technology
Services

The Preserve: Lehigh Library Digital Collections

Learning control and repetitive control of flexible planar variable input speed linkages mechanisms.

Citation

Al-Ghanem, Khaled - Lehigh University. *Learning Control and Repetitive Control of Flexible Planar Variable Input Speed Linkages Mechanisms*. 2004, <https://preserve.lehigh.edu/lehigh-scholarship/graduate-publications-theses-dissertations/theses-dissertations/learning-6>.

Find more at <https://preserve.lehigh.edu/>

This document is brought to you for free and open access by Lehigh Preserve. It has been accepted for inclusion by an authorized administrator of Lehigh Preserve. For more information, please contact preserve@lehigh.edu.

NOTE TO USERS

This reproduction is the best copy available.

UMI[®]

Learning Control and Repetitive Control of Flexible Planar Variable Input Speed Linkages Mechanisms

By

Khaled Al-Ghanem

Presented to the Graduate and Research Committee
of Lehigh University

in Candidacy for the Degree of
Doctor of Philosophy

in

The Department of Mechanical Engineering
and Mechanics

Lehigh University

August 2004

UMI Number: 3154552

INFORMATION TO USERS

The quality of this reproduction is dependent upon the quality of the copy submitted. Broken or indistinct print, colored or poor quality illustrations and photographs, print bleed-through, substandard margins, and improper alignment can adversely affect reproduction.

In the unlikely event that the author did not send a complete manuscript and there are missing pages, these will be noted. Also, if unauthorized copyright material had to be removed, a note will indicate the deletion.

UMI[®]

UMI Microform 3154552

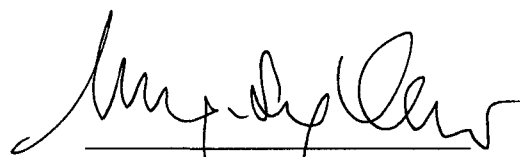
Copyright 2005 by ProQuest Information and Learning Company.

All rights reserved. This microform edition is protected against unauthorized copying under Title 17, United States Code.

ProQuest Information and Learning Company
300 North Zeeb Road
P.O. Box 1346
Ann Arbor, MI 48106-1346

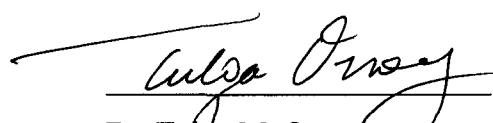
Approved and recommended for acceptance as a dissertation in partial fulfillment of the requirements for the degree of Doctor of Philosophy.

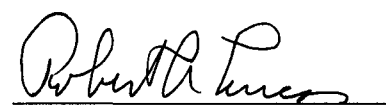
August 19, 2004
Date

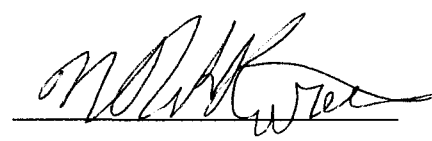

Dr. Meng-Sang Chew
(Dissertation Advisor)

August 19, 2004
Accepted Date

Committee Members


Dr. Tulga M. Ozsoy
(Committee Chairperson)


Dr. Robert A. Lucas


Dr. N. Duke Perreira

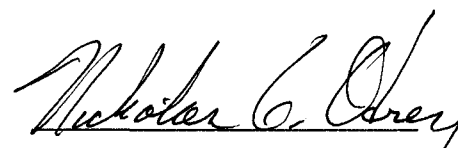

Dr. Nick Oudrey

Table of Contents

List of figures	vii
List of tables	xiii
List of symbols	xiv
Abstract	1
Introduction	3
Chapter 1: Literature review	10
1.1 Yan and Chen – 1 st paper	11
1.2 Yan and Chen – 2 nd paper	12
1.3 Yan and Soong	13
1.4 Yan and Chen – 3 rd paper	13
Chapter 2: Theory of learning control and repetitive control methods	15
Chapter 3: Case 1: Path generation with timing	23
3.1 Applying learning and repetitive control methods	24
3.2 System's control	26
3.3 System's model	28
3.4 System's specifications	29
3.4.1 Specifications of the flexible slider-crank	
Mechanism	29
3.4.2 Flexible elements	30

3.5 Timing simple path	33
3.5.1 Results of timing simple path	35
3.6 Timing dwell path	43
3.6.1 Results of timing dwell path	45
3.7 Discussion of results	53
Chapter 4: Case 2: Constant output velocity	55
4.1 Applying learning and repetitive control methods	56
4.2 Results of constant output velocity	60
4.3 Discussion of results	68
Chapter 5: Case 3: Minimizing output acceleration	70
5.1 Applying learning and repetitive control methods	71
5.2 Results of minimizing output acceleration	76
5.3 Discussion of results	82
Chapter 6: Case 4: Minimizing dissipated energy	84
6.1 Applying learning and repetitive control methods	85
6.2 System's model	89
6.3 System's specifications	91
6.3.1 Specifications of the rigid slider-crank mechanism ..	92
6.4 Results of minimizing dissipated energy	93
6.5 Discussion of results	99
Chapter 7: Case 5: Minimizing input torque	101

7.1 Applying learning and repetitive control methods	102
7.2 Results of minimizing input torque	106
7.3 Discussion of results	112
Chapter 8: Case 6: Flexible six-bar mechanism used in scanning	
machine	116
8.1 Constant input speed scanning machine	117
8.2 Applying learning and repetitive control methods	120
8.3 System's model	127
8.3.1 Specifications of the system	131
8.4 Results of the six-bar scanning machine	134
8.5 Discussion of results	150
Chapter 9: Case 7: Flexible slider-crank mechanism used in scanning	
machine	154
9.1 Applying learning and repetitive control methods	155
9.2 System's model	162
9.2.1 Specifications of the system	164
9.3 Results of flexible slider-crank mechanism	166
9.4 Discussion of results	185
Chapter 10: Conclusion	189
Appendix A: Derivation of the optimized input	191
Appendix B: Derivation of the equations of motion of the flexible	

slider-crank mechanism by Lagrange's equations	193
Appendix C: Derivation of the equations of motion of the rigid	
slider-crank mechanism by Lagrange's equations	199
Appendix D: Derivation of the equations of motion of the flexible	
six-bar Stephenson mechanism by Lagrange's equations ...	204
Part 1: Determining the critical damping of a simple cantilever ...	204
Part 2: Lagrange's equations of motion	207
Appendix E: Derivation of the equations of motion of the flexible	
slider-crank mechanism by Lagrange's equations	229
References	237
Vita	241

List of Figures

Figure 3.1: Block diagram of the controlled system	27
Figure 3.2: Flexible slider-crank mechanism	28
Figure 3.3: Output displacement versus time for the simple path case	34
Figure 3.4: Absolute error versus repetitions using learning control	35
Figure 3.5: Input angle versus time using learning control	36
Figure 3.6: Output displacement versus time using learning control	37
Figure 3.7: Output displacement versus repetitions using learning control	38
Figure 3.8: Absolute error versus repetitions using repetitive control	39
Figure 3.9: Input angle versus time using repetitive control	40
Figure 3.10: Output displacement versus time using repetitive control	41
Figure 3.11: Output displacement versus repetitions using repetitive control	42
Figure 3.12: Output displacement versus time for the dwell path case	44
Figure 3.13: Absolute error versus repetitions using learning control	45
Figure 3.14: Input angle versus time using learning control	46
Figure 3.15: Output displacement versus time using learning control	47
Figure 3.16: Output displacement versus repetitions using learning control ..	48
Figure 3.17: Absolute error versus repetitions using repetitive control	49
Figure 3.18: Input angle versus time using repetitive control	50
Figure 3.19: Output displacement versus time using repetitive control	51

Figure 3.20: Output displacement versus repetitions using repetitive control	52
Figure 4.1: Percentage error versus repetitions using learning control	60
Figure 4.2: Input angle versus time using learning control	61
Figure 4.3: Output velocity versus time using learning control	62
Figure 4.4: Output velocity versus repetitions using learning control	63
Figure 4.5: Percentage error versus repetitions using repetitive control	64
Figure 4.6: Input angle versus time using repetitive control	65
Figure 4.7: Output velocity versus time using repetitive control	66
Figure 4.8: Output velocity versus repetitions using repetitive control	67
Figure 5.1: Acceleration function versus repetitions using learning control ..	76
Figure 5.2: Input angle versus time using learning control	77
Figure 5.3: Output displacement versus time using learning control	78
Figure 5.4: Acceleration function versus repetitions using repetitive control	79
Figure 5.5: Input angle versus time using repetitive control	80
Figure 5.6: Output displacement versus time using repetitive control	81
Figure 6.1: Rigid slider-crank mechanism	91
Figure 6.2: Power function versus repetitions using learning control	93
Figure 6.3: Input angle versus time using learning control	94
Figure 6.4: Output displacement versus time using learning control	95
Figure 6.5: Power function versus repetitions using repetitive control	96
Figure 6.6: Input angle versus time using repetitive control	97

Figure 6.7: Output displacement versus time using repetitive control	98
Figure 7.1: Torque function versus repetitions using learning control	106
Figure 7.2: Input angles versus time using learning control	107
Figure 7.3: Output displacement versus time using learning control	108
Figure 7.4: Torque function versus repetitions using repetitive control	109
Figure 7.5: Input angles versus time using repetitive control	110
Figure 7.6: Output displacement versus time using repetitive control	111
Figure 8.1: Six-bar Stephenson mechanism	118
Figure 8.2: Normalized output velocity versus input angle	120
Figure 8.3: Velocity error versus repetitions using learning control	134
Figure 8.4: Input angles versus time using learning control	135
Figure 8.5: Output displacement of the slider versus time using learning control	136
Figure 8.6: Output velocity of the slider versus time using learning control ..	137
Figure 8.7: Output velocity of the slider versus repetitions using learning control	138
Figure 8.8: Maximum deflection of the flexible links 1, 2 and 4 versus time using learning control	139
Figure 8.9: Motor's output torque to the mechanism versus time using learning control	140
Figure 8.10: Frequency content of the flexible links 1, 2 and 4, and the input	

torque using learning control	141
Figure 8.11: Velocity error versus repetitions using repetitive control	142
Figure 8.12: Input angles versus time using repetitive control	143
Figure 8.13: Output displacement of the slider versus time using repetitive control	144
Figure 8.14: Output velocity of the slider versus time using repetitive control	145
Figure 8.15: Output velocity of the slider versus repetitions using repetitive control	146
Figure 8.16: Maximum deflection of the flexible links 1, 2 and 4 versus time using repetitive control	147
Figure 8.17: Motor's output torque to the mechanism versus time using repetitive control	148
Figure 8.18: Frequency content of the flexible links 1, 2 and 4, and the input torque using repetitive control	149
Figure 9.1: Flexible slider-crank mechanism	155
Figure 9.2: Velocity error versus repetitions using learning control	166
Figure 9.3: Input angles versus time using learning control	167
Figure 9.4: Output displacement of the slider versus time using learning control	168
Figure 9.5: Output velocity of the slider versus time using learning control ..	169

Figure 9.6: Output velocity of the slider versus repetitions using learning control	170
Figure 9.7: Maximum deflection of the flexible links 1 and 2 versus time using learning control	171
Figure 9.8: Motor's output torque to the mechanism versus time using learning control	172
Figure 9.9: Frequency content of the flexible links 1 and 2, and the input torque using learning control	173
Figure 9.10: Velocity error versus repetitions using repetitive control	174
Figure 9.11: Input angles versus time using repetitive control	175
Figure 9.12: Output displacement of the slider versus time using repetitive control	176
Figure 9.13: Output velocity of the slider versus time using repetitive control	177
Figure 9.14: Output velocity of the slider versus repetitions using repetitive control	178
Figure 9.15: Maximum deflection of the flexible links 1 and 2 versus time using repetitive control	179
Figure 9.16: Motor's output torque to the mechanism versus time using repetitive control	180
Figure 9.17: Frequency content of the flexible links 1 and 2, and the input	

torque using repetitive control	181
Figure 9.18: Velocity error versus repetitions of the final modified inputs	
using repetitive control	182
Figure 9.19: A comparison between the six-bar Stephenson mechanism and	
the slider-crank mechanism, used in scanning machines	184
Figure B.1: Flexible slider-crank mechanism	193
Figure C.1: Rigid slider-crank mechanism	199
Figure D.1: A flexible cantilever deflected on the X-Y plane	204
Figure D.2: The flexible Six-bar Stephenson Mechanism	207
Figure D.3 (a,b): The deflected links with respect to the local coordinate	
system	208
Figure E.1: Flexible slider-crank mechanism	229

List of Tables

Table 3.1: Links specifications of the flexible slider-crank mechanism	30
Table 6.1: Links specifications of the rigid slider-crank mechanism	92
Table 8.1: Physical and mechanical properties of CARILON® Thermoplastic Polymer DP R1000	132
Table 8.2: Links specifications of the flexible six-bar Stephenson mechanism	133
Table 9.1: Links specifications of the flexible six-bar Stephenson mechanism	165
Table 9.2: Comparison between the six-bar Stephenson mechanism and the slider-crank mechanism used in scanning machines	183

List of Symbols

A	Area
\underline{A}	System parameter matrix
\underline{B}	System parameter matrix
C	Cosine
c	Damping constant
\underline{D}	Differentiating matrix
E	Modulus of elasticity
e	Error vector
f	Frequency
I	Area moment of inertia, mass moment of inertia
K_d	Derivative gain
K_e	Motor back EMF
K_p	Proportional gain
K_t	Motor torque constant
k	Spring stiffness
m	Mass
N	Gear ratio
n	Safety factor
Q	Minimizing error weighting matrix

q	Weight coefficient, magnitude function
R	Length
\underline{R}	Projection matrix
R_s	Armature resistance
S	Sine
\underline{S}	Minimizing change in the input weighting matrix
S_{NL}	No load speed
S_y	Yield strength
T	Torque
T_F	Friction torque
T_{PK}	Peak torque
U	Input angles vector
U_s	Strain energy
V	Motor's voltage
V^*	Desired output velocity
x	Initial conditions vector
Y	Output displacement vector
Y^*	Desired output vector
y	Deflection
δU	Difference in the input between repetitions
ζ	Damping ratio

θ	Crank angle
θ_r	Reference angles
μ	Coefficient of friction
ρ	Density
$\underline{\Phi}$	System parameter matrix
$\underline{\phi}$	Initial conditions and input angles matrix
ψ	Mode shape
$\dot{\psi}$	Motor's speed
ω	Frequency
ω_n	Natural frequency

Abstract

This study is a theoretical investigation of applying learning control and repetitive control in variable input speed planar linkages mechanisms that perform different tasks. Simulations of a flexible slider-crank mechanism and a flexible six-bar Stephenson mechanism are provided with taking into account the elasticity of links. Seven different cases were studied, where the elasticity of the system is presented as a vibrated mass attached to the mechanism by a spring and a dashpot, or as bendable links that vibrate laterally during motion.

Learning control method and its extension, repetitive control, were applied to the system for modifying the input by tracking the output error to achieve some desired output. Another task was to minimize a cost function that depends on the system's output according to a specific criterion. Minimizing the output error and the cost function was carried out by learning the effect of the system's input on the system's output resulting from repeated motion of the mechanism.

Three cases were studied using two degrees of freedom system, a slider-crank mechanism with a flexibly attached mass to the slider that goes in a repeated rectilinear motion. The three cases were: path generation with timing, constant output velocity, and minimizing output acceleration.

Two more cases were studied using one degree of freedom slider-crank mechanism. This model carried variable load depending on the displacement and velocity of the slider. The mechanism's task was to run in a manner that minimizes a specific cost function depending on the output motion. The two cases, which were examined, are as follows: minimizing the dissipated energy in the system, and minimizing input torque to the mechanism.

The last two cases were dedicated to the study and comprising of the performance of two kinds of flexible mechanisms that were used in scanning machines to generate constant output velocity; a six-bar Stephenson mechanism and a slider-crank mechanism.

A comparison study between the learning control and the repetitive control will be discussed at the end of this dissertation.

Introduction

Rotary linkages mechanisms are widely used in industrial fields. Usually they are used to convert constant input rotational motion into reciprocal, rotational, or oscillatory output motion. In addition, some mechanisms are used to convert rotational motion driven by a motor to rectilinear motion appearing as a slider moves along a straight course.

Nearly all applications of rotary mechanisms consider that the input motion has constant speed, which means driving these kinds of mechanisms needs a reasonably large flywheel to cancel the effect of inertia of moving parts, and they need a constant input power motor. Analyzing these types of mechanisms is based on the assumption that the mechanism is strictly rigid and consists of unbendable parts. However, in reality, there is some elasticity in all links and joints, making the whole system vibrate in the plane of motion. Besides this flexibility, there are more factors affecting the motion of the mechanism such as inertial forces, fluctuation of the speed of driving motor, friction between moving surfaces, impact that occurs in joints, among others. All these components disturb the system, which ends up with unexpected and undesirable output motion. Therefore, the need of controlling mechanisms arises to improve their performance and to minimize the disturbance on the system.

The classical control is a great improvement on a mechanism's performance, but it is still constrained by the assumption that links are stiff and unbendable. This ideal assumption makes the practical use of classical control inefficient and ineffective, especially when dealing with large mechanisms that go under relatively large deflections and vibrations. For this reason, the simple control adds more complexity to the whole system without significant income.

The new method, which is the learning control, deals with these kinds of systems that are characterized by doing cyclical motion with the same state at the beginning of each cycle. It learns how the output is affected by the input, while taking into account the other disturbing factors. It tracks the error and minimizes it until reaching some low level, which improves the overall performance of the system.

As an extension of this technique, a repetitive control method may be used. It does not require typical initial conditions at each repetition, which makes the system go in a continuous motion. It takes into account the changes in the initial conditions at each repetition, and it keeps converging the output motion to the desired output.

These two methods modify the input speed of the motor that drives the system. They enhance the mechanism performance by varying the input speed and changing the whole mechanism into a variable input speed mechanism.

Variable input speed mechanisms are the smart generation of innovative mechanisms. They are simple, accurate, light in weight, and much more efficient than the old-fashioned mechanisms used in industry.

These evolutionary mechanisms also allow for using new materials in manufacturing mechanisms. There is no need to use steel links anymore. Most of the old mechanisms are made of steel, even when used for non-heavy duty, to minimize bending in links. But with the new smart mechanisms, light and thin plastic links can be used; however, links bend. Moreover, light materials used in constructing smart mechanisms lead to the use of small motors instead of using larger ones to drive the heavy mechanisms and their flywheels.

These modern mechanisms have many applications at the present time, especially for the newest technology. It is important in minor systems that require precise and accurate motion, such as assembling electric appliances that consist of tiny elements. Moreover, printing and scanning processes demand some fast and accurate instruments that are able to complete the task perfectly. These kinds of jobs allow small errors and insignificant vibrations that could ruin the overall work.

Also, some other applications that do not require much accuracy can benefit from the smart mechanisms. The task that needs to be done by the old-style mechanisms could be done exactly the same way by the smart machines with the advantage of

minimizing input power, dissipation in energy, effect of external loads, or any other unwanted destructive factors.

The objective of this study is to revolutionize the old image of mechanisms that do routine jobs by constant input speed, and upgrade them to modern and clever variable input speed mechanisms that perform different tasks done by one mechanism. Also, this study shows how the input speed can be adjusted by using adaptive control, which modifies input speed continuously to enhance mechanism performance.

In this study, different cases have been examined theoretically to show the ability of these new kinds of mechanisms to perform certain jobs brilliantly. These different cases represent highly non-linear dynamic systems that go under repeated motion, and have one, two, or an infinite number of degrees of freedom as will be shown in later chapters. All simulations provided have been done by using MATLAB.

Seven different cases have been studied, which are: path generation with timing, constant output velocity, minimizing output acceleration, minimizing dissipated energy in the system, minimizing input torque, scanning process by six-bar mechanism, and scanning process by slider-crank mechanism. In all cases, two

methods of adaptive control were examined; learning control method, and its extension, repetitive control method.

Chapter 1 is a literature review investigation showing the history of variable input speed mechanisms and its control methods. There are few studies that address this new topic.

Chapter 2 describes the theory behind adaptive control method used in controlling the seven cases examined in this study. It discusses and presents the derivation of the learning control method and repetitive control method.

Chapter 3 presents the first studied case, which is the path generation with timing. In this case, the two methods of adaptive control bring the output displacement of the system to a specific path designated by a number of precision points. This desired output could be expressed as a function of time. It could be a simple or more complicated path involving dwell segments.

Chapter 4 shows the second case, which is producing rectilinear constant output velocity in a portion of the cycle, which repeats itself. The control methods adjust the input at each repetition, so they end up with the constant velocity between the two designated points of the concerned region.

Chapter 5 demonstrates the third case: minimizing output acceleration of the system. It has a different concept from the first two cases. The control methods learn to anticipate the output acceleration, which is a high fluctuating function, varying widely with time. However, the output acceleration cannot be zero, so it is minimized to the lowest possible level.

Chapter 6 points up the fourth case, which tries to save the energy of the system. It minimizes the wasted energy that is dissipated in the motor and the dashpot involved in the system. It keeps the same periodic motion with doing this.

Chapter 7 explains the fifth case, which deals with input torque to the mechanism. The system has variable external load, depending on the input angle to the mechanism and the angular velocity. The controlled system has to achieve the optimum input speed that minimizes required torque for driving the mechanism. In sequence, this minimum input torque minimizes the size of the motor.

Chapter 8 discusses the mechanism used in scanning machines and explains the improvement of the famous mechanism, which is six-bar Stephenson mechanism, often used in constant output velocity applications, such as scanning or printing processes. The adaptive control takes a role in developing the output from this mechanism by adjusting the speed of motor that drives this machine.

Chapter 9 presents an alternate machine, the slider-crank mechanism, which handles scanning process efficiently by employing adaptive control methods. This outstanding machine exclusively has several advantages of using learning and repetitive control methods in controlling smart mechanisms.

Chapter 10 concludes this study. The derivation of governing equations for systems have been used, and the list of simulating programs are attached as appendices at the end of this study.

Chapter 1

Literature Review

The variable input speed mechanism, which is the latest branch in machinery science, is a very new topic. Several studies have been done on cams, which are driven by a motor that is controlled by using learning and repetitive control methods. The studies focus on bringing the actual output displacement of a highly non-linear vibration system to a desired output displacement that is designated by a number of precision points.

Most research that has been done in this area, has been addressed to cams, which are the simplest mechanisms that could be used in driving systems. They consist of one small rotary part that has insignificant inertia, and its profile can be shaped as required to produce any kind of motion. On the other hand, linkages mechanisms, which consist of a number of links, have little research behind them. The complexity of controlling linkages mechanisms, which have at least three moving parts, is due to the great inertia of links, which often are made of steel. Moreover, synthesizing linkages mechanisms for path generation purposes is unfeasible unless adding numerous number of links, a process that converts simple mechanisms to massive machines.

The earliest work done in controlling linkages mechanisms was in year 2000. Only four published papers came into view in this field. They used simple classical control in controlling the driving motor.

The innovative idea in this study is to use learning and repetitive control methods instead of the classical control for improving a mechanism's performance to overcome all disturbing factors on the controlled systems.

1.1 Yan and Chen – 1st Paper

In April 2000, Yan and Chen published the first work in controlling variable input speed linkages mechanisms [1]. They proposed a new concept by varying the speed of the crank of a rigid slider-crank mechanism to obtain the desired output motion. They used a servomotor as the power input of the mechanism. By properly designing the input speed of the mechanism, the output motion passes through the desired trajectory. They worked on three different cases of output motion according to several criteria. They showed three cases: path generation with timing, constant output velocity, and minimizing the peak acceleration. The optimized input speed was obtained by analytically determining the optimized input angles at equal time steps, and then the time derivative of these points was computed numerically to determine the input speed. They fed these angle points to the controller as reference data.

Yan and Chen simplified the servomotor as a first-order system. The system characteristics were determined from Bode diagram by applying different frequencies to the system, while the PID controller gains were determined by computer simulation to meet the desired performance index.

First, the case of path generation with timing allowed the system to pass through five selected points at prescribed timing. These points were located at the extreme positions at 0° and 360° , and at some three middle points on the trajectory. These five points were designated carefully to ensure smoothness of the output motion. In the second case, which is the constant output velocity, Yan and Chen forced the system to go with constant output velocity in a short time period of the forward stroke. The minimizing peak acceleration case was performed by determining numerically the optimized input points that minimize the output peak acceleration, and then, applying these points in driving the motor. In all cases, they characterized input motion by ten precision points leading the system's motion. In addition, they verified their theoretical work by experimental results.

1.2 Yan and Chen – 2nd Paper

In April 2000, Yan and Chen published their second paper on variable input speed linkages mechanisms [2]. The second paper has the same conception employed in the first published work. Yan and Chen considered the case of path generation with timing utilized in the industrial field. At this time, they used the same concepts for

the servomotor and controller, but with a six-bar Watt drag-link mechanism. They verified in that work that it is able to use these kinds of mechanisms in deep-drawing and precision-cutting processes by adjusting the output speed, that is, the cutting speed. They provided two cases of fast constant output speed and slow constant output speed of the cutting tool.

1.3 Yan and Soong

In September 2001, Yan and Soong presented a new method for four-bar linkages that satisfies the kinematic design requirements of the system and also attains trade-off of dynamic balance [3]. They showed that by properly designing the speed trajectory of the input link, the disk counterweight of moving links, and the link's dimensions of the given mechanism, the expected output motion and dynamic balancing could be obtained. The main target was to reach the dynamic balance by optimizing the input speed of the mechanism. This optimized input speed minimized a cost function, which consisted of the shaking forces and moments. A servomotor was used to provide the system with the desired input speed. Yan and Soong proved theoretically that by varying input speed, the shaking forces and moments can be minimized.

1.4 Yan and Chen – 3rd Paper

In June 2002, Yan and Chen replicated their work done on the Watt mechanism, except that they replaced the six-bar Watt mechanism by the Stevenson mechanism

[4]. They showed theoretically the feasibility of varying the input speed to make the ram's motion suitable for both deep-drawing and precision-cutting processes, which are the same as those in the previous cases of fast and slow constant output speeds.

Chapter 2

Theory of Learning Control and Repetitive Control Methods

The learning control method is a cyclical process that generally modifies the input commands at each repetition. It starts all cycles with typically the same initial conditions or with insignificant difference in the state of the system. The process behind learning control is to inspect and identify the effect of the system's input on the system's output directly, regardless of any internal actions in the system. In the course of time, the feedback data provide the learning process with more information on the system's performance, which makes the identifying development more efficient and also makes the input capable of being modified during the system's action, as more feedback data are gained. As the learning process makes more progress in identifying the system's output, the predicted next repetition output comes closer to the actual output, and consequently, the learning method gives better results.

The repetitive control method is considered an extension and improvement of the learning control method. It is a powerful technique that deals with systems that are unable to be stopped when they start moving, or ones that do not start each cycle with the same initial conditions. The repetitive method works like the learning method, except that it does not require the same initial conditions at each repetition.

It takes into account the differences in the initial conditions in manipulating the feedback from the system to make the learning process more efficient.

While the learning control method seeks some kind of relation between the system's input and the output, the repetitive method looks for a relation between both the input and the initial conditions, and the output simultaneously.

If we consider the learning control method is a special case of the repetitive control method, then the theory behind both methods is the same, except that the initial conditions term is canceled at the end of the derivation of learning control method.

To clarify how these two methods work, assume that a closed loop system has input commands and feedback p times per a repetition, and the system does not have the same initial conditions at each repetition, so the system output can be expressed as

$$Y_i = \underline{A}_i x_i(0) + \underline{B}_i U_i + e_i$$

$$Y_i = [y_i(\Delta t) \quad y_i(2\Delta t) \quad y_i(3\Delta t) \quad \cdots \quad y_i((p-1)\Delta t) \quad y_i(p\Delta t)]^T$$

$$U_i = [u_i(0) \quad u_i(\Delta t) \quad u_i(2\Delta t) \quad \cdots \quad u_i((p-2)\Delta t) \quad u_i((p-1)\Delta t)]^T$$

Where Y_i is the system output vector of length p , A_i ($p \times n$) and B_i ($p \times p$) are the system parameter matrices to be estimated, x_i is the initial conditions vector of

length n , U_i is the system input vector of length p , and e_i is the error vector of length p due to the estimating process, all at the i^{th} repetition.

The system parameter matrices A and B can be initiated arbitrarily. However, the starting assumption of these matrices has a considerable effect on identifying process progression. Therefore, it is suggested to start with the identity matrices, since the final parameter matrices are unpredictable.

For simplicity, the system parameter matrices A and B , as well as the initial conditions and system input vectors, can be combined in two main matrices:

$$\underline{\Phi}_i = [\underline{A}_i \underline{B}_i]$$

$$\phi_i = [x_i(0) \quad U_i]^T$$

Therefore, the estimated output vector is written as follows:

$$Y_i = \underline{\Phi}_i \phi_i$$

where the error vector is neglected at this point.

This new parameter matrix will go under modifying process at the end of each repetition. The process updates the matrix as more feedback is collected after each repetition. The updated system parameter matrix is in this form¹:

$$\underline{\Phi}_{i+1} = \underline{\Phi}_i + (Y_i - \underline{\Phi}_i \phi_i) \frac{\phi_i \underline{R}_i}{1 + \phi_i^T \underline{R}_i \phi_i}$$

$$\underline{R}_{i+1} = \underline{R}_i - \frac{\underline{R}_i \phi_i \phi_i^T \underline{R}_i}{1 + \phi_i^T \underline{R}_i \phi_i}$$

Initially, Φ_1 is estimated as the identity matrix. R_1 can be estimated as $\alpha \Phi_1$, where α is a large positive number².

As more information pertaining to the system is acquired, the estimated output that comes from matrices calculations becomes closer to the system's actual output. In sequence, the error term decreases and Φ_i becomes closer to Φ_{i+1} . At this moment, a good estimation for the next repetition output can be obtained by employing the current system parameter matrix, as shown by these equations:

¹ For complete derivation, see Ref. [34].

² An exact form of R_1 is provided in Ref. [34].

$$Y_i = \underline{\Phi}_i \phi_i + E_i$$

$$e_{i+1} \approx 0$$

2.1

$$\Rightarrow \underline{\Phi}_{i+1} \approx \underline{\Phi}_i$$

$$\Rightarrow Y_{i+1} \approx \underline{\Phi}_i \phi_{i+1}$$

At this point, when the actual output can be predicted, an optimization process will play a role. The purpose of the optimization is to find the best next repetition input, which minimizes the difference between the next repetition output and the desired output.

For explaining the optimizing process, consider a cost function J that needs to be minimized:

$$J = \frac{1}{2} e_{i+1}^T Q e_{i+1} + \frac{1}{2} \delta U_{i+1}^T S \delta U_{i+1}$$

$$e_{i+1} = Y^* - Y_{i+1} \quad 2.2$$

$$\delta U_{i+1} = U_{i+1} - U_i$$

where Q and S are weighting matrices and Y^* is the desired output vector.

Substituting Y_{i+1} from 2.1 into 2.2 and performing the optimization process to minimize J give³,

$$\begin{aligned} \delta U_{i+1} &= \left(\underline{B}_i^T \underline{Q} \underline{B}_i + \underline{S} \right)^{-1} \underline{B}_i^T \underline{Q} \left(Y^* - Y_i - \underline{A}_i (x_{i+1}(0) - x_i(0)) \right) \\ U_{i+1} &= U_i + \delta U_{i+1} \end{aligned} \quad 2.3$$

In fact, Matrix Q in 2.2 works to put more effort in minimizing the error, while S tries to minimize the input differences between repetitions.

Notice that in equation 2.3, the absence of matrix S leads to trouble in manipulating the optimization process when calculating the inverse of the first bracket. Therefore, it is important to have S as a non-zero matrix. Moreover, S is intentionally used to minimize the changes in the system's input between any consecutive repetitions.

Reducing changes in the system's input keeps the system parameter matrix applicable in estimating the next repetition output and keeps the learning process within its range. If the system's input varies widely, then the learning and identifying processes become unfeasible. Therefore, it is very important to

³ For complete derivation, see appendix A.

maintain that the differences in the input are small enough to be tracked and do not produce unexpected output.

Another use of matrix S is to keep some specific input points unchanged during the optimizing system's input. For example, if the system's final state is specific and not to be changed during the recurring motion, then the input at these points has to be fixed to make them incapable of modification. This can be done by setting very large values at elements of matrix S corresponding to these points of input. Note that Q and S are symmetric and positive definite.

Equations 2.3 represent the general case of repetitive control, where the initial conditions are not the same at each repetition. They can be simplified to match the special case when each repetition starts with the same initial conditions, which is the learning control method.

$$\delta U_{i+1} = (\underline{B}_i^T \underline{Q} \underline{B}_i + \underline{S})^{-1} \underline{B}_i^T \underline{Q} (\underline{Y}^* - \underline{Y}_i)$$

Observe that matrix A is not involved in the case of learning control because of the cancellation of the initial conditions term.

If the desired output is to minimize the cost function according to a specific criterion, such as minimizing the output acceleration, then, the output that needs to be learned (Y) is the output acceleration, and the desired output (Y^*) becomes zeros vector. In fact, the actual output, which is the output acceleration, will never reach the desired output, which is the zeros vector, but it converges until it reaches the lowest possible level.

Chapter 3

Case 1: Path Generation with Timing

Path generation task is one of the most important applications performed by a mechanism. It is defined as “*the control of a point in the plane such that it follows some prescribed path*⁴”. Timing path generation, which is more precise than path generation, correlates a mechanism’s output to time. It prescribes the desired output motion as a function of time. The path prescription is designated by some precision points to determine the position of the driven link with respect to time. In slider-crank mechanism, the input to the system is the input angles of the driving link, while the output is the slider’s displacement measured from a reference point.

In constant input speed mechanisms, the number of precision points depends on the type of mechanism. As the number of links increases, the maximum number of precision points increases. In fact, number of links limits this number of precision points. In the case of the slider-crank mechanism, the maximum precision points are three. This means that it is impossible to synthesize a slider-crank mechanism that passes through four arbitrarily timed precision points.

⁴ Ref 32, page 79.

3.1 Applying learning and repetitive control methods

As mentioned in chapter 2, learning control method requires fixed initial conditions at the beginning of each cycle. Therefore, the mechanism will start each repetition with zero input angle and zero angular velocity. In repetitive control method, the initial conditions at each new repetition are the same as the final conditions of the previous repetition. For this system, the output displacement of the slider is the function needed to be learned; therefore, it is described by,

$$Y_i = \underline{A}_i x_i(0) + \underline{B}_i U_i$$

where Y is the output displacement vector, A and B are the parameter matrices, x is the initial conditions vector, and U is the input angles vector, all at the i^{th} repetition. The above equation, which is used for the repetitive method, is the general case where the initial conditions are changeable.

As a first estimation of input angles to the mechanism at the first repetition, a straight line, which is constant input speed, is used to operate the mechanism. Mainly, the weighting matrix Q in equation 2.2, which minimizes the error, is set very small for the first ten repetitions. This makes the learning method capable of enhancing identifying process and making the changes in the input more efficient for later repetitions. Otherwise, the modifying process of the input angles will

produce erratic output, which requires more repetitions to relate it to the input, and in sequence, more time to bring it back to the desired output.

At the end of the repetitions devoted to expanding learning development, the process of optimizing the input will be done simultaneously with the learning process at the end of each repetition. The output data that is collected will be used in optimizing the input for minimizing proposed cost function. The cost function for this case can be written as follows:

$$J = \frac{1}{2} \mathbf{e}_{i+1}^T \mathbf{Q} \mathbf{e}_{i+1} + \frac{1}{2} \delta \mathbf{U}_{i+1}^T \mathbf{S} \delta \mathbf{U}_{i+1}$$

$$\mathbf{e}_{i+1} = \mathbf{Y}^* - \mathbf{Y}_{i+1}$$

Minimizing this cost function successfully brings the actual output to the desired output in few repetitions. The next repetition's optimized input is,

$$\mathbf{U}_{i+1} = \mathbf{U}_i + \delta \mathbf{U}_{i+1}$$

$$\delta \mathbf{U}_{i+1} = \left(\mathbf{B}_i^T \mathbf{Q} \mathbf{B}_i + \mathbf{S} \right)^{-1} \mathbf{B}_i^T \mathbf{Q} \left(\mathbf{Y}^* - \mathbf{Y}_i - \mathbf{A}_i (\mathbf{x}_{i+1}(0) - \mathbf{x}_i(0)) \right)$$

The absolute error, which shows how the actual output converges to the desired output, is defined as the maximum absolute difference between the desired output and the actual output at some designated points at each repetition, where the excluded points belong to the uncontrollable regions that are boarded by extreme positions of the slider. This uncontrollability is due to the excessive vibrations of the attached mass. When the mechanism comes to the dead-center positions, where the input angle is 0° or 180° , the displacement of the attached mass becomes bigger than the slider's displacement. Moreover, the ratio between the slider's output velocity and mechanism's input angular velocity reaches its minimum at these extreme positions. For this reason, controlling output velocity at these positions requires large changes in input angular velocity and leads to enormous input torque.

At these extreme positions, nothing can be done to control the output displacement. Although these points are uncontrollable, the input angles at these points are modified to prepare the system to go smoothly to minimize the error at the preferred regions.

3.2 System's control

In this studied case, a simple variable input speed mechanism passes through 50 timed precision points. By varying the input speed of the motor, the output motion goes through the desired timed output. A PD controller is used to control the input

speed of the motor. The block diagram of the controlled system is shown in figure 3.1.

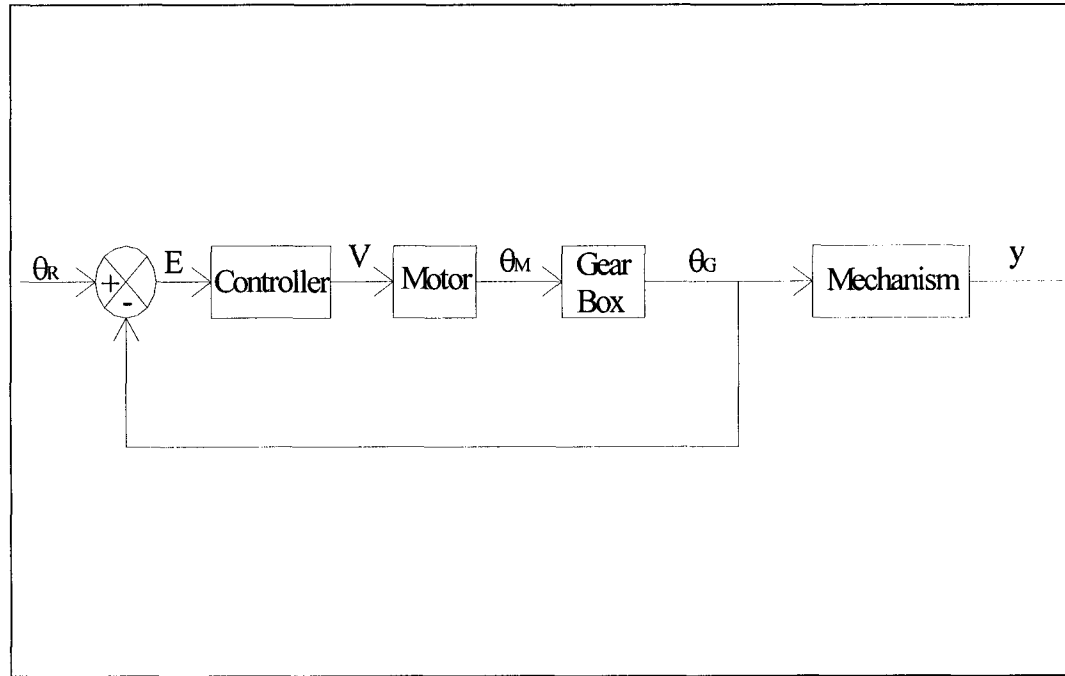


Figure 3.1: Block diagram of the controlled system

The input to the system is the referenced mechanism's angles. The error is fed into a PD controller to adjust the voltage that drives the motor. And then a gearbox reduces the speed of the motor to match the mechanism's speed. The mechanism's output is the displacement of the attached mass measured from the position of the slider at the head dead center position of the mechanism, which occurs when the angle of the driving link is zero.

3.3 System's model

The mechanism used in this case is a slider-crank mechanism with flexibly attached mass. The links are assumed to be rigid, while the whole elasticity of the system is concentrated at the flexible element that joins the attached mass with the slider, as shown in figure 3.2. The system moves in the horizontal plane where the weights are ignored.

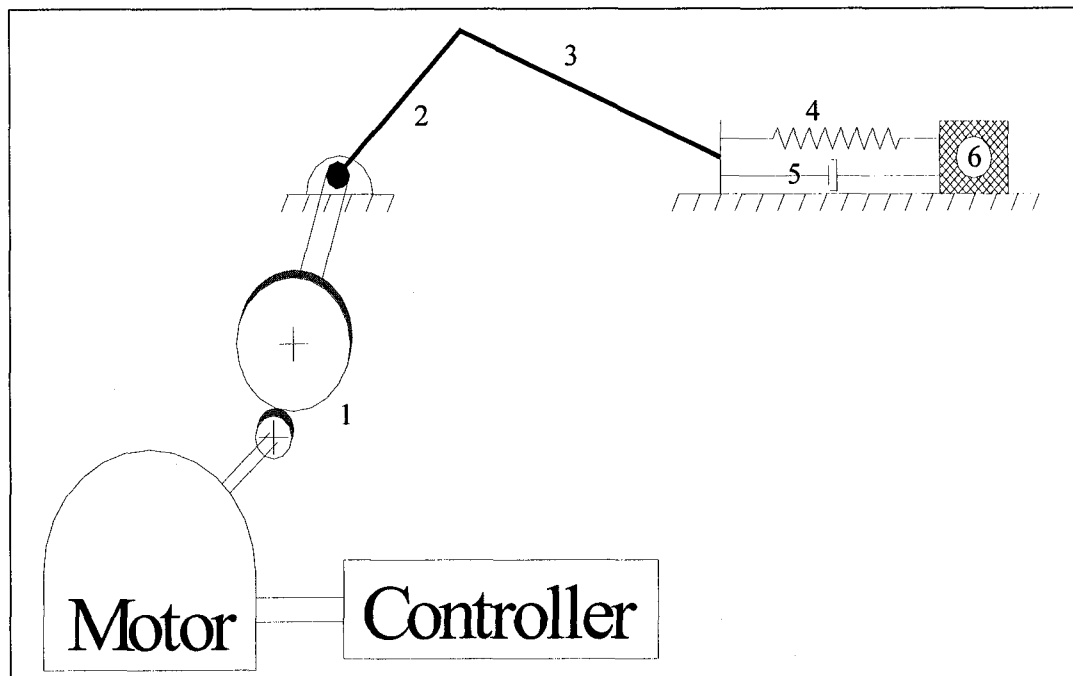


Figure 3.2: Flexible slider-crank mechanism

A coulomb friction is assumed to occur at the contact surfaces of the mechanism with the ground. The joints connecting links are assumed to be smooth, and no

friction is involved between them. The static and dynamic friction coefficients are assumed to be the same and equal to 0.1.

3.4 System's specifications

The proportional gain (K_p) is 100, while the derivative gain (K_d) is 2.4. The motor specifications are as follows:

K_t : Motor torque constant,	0.0297 N.m/amp.
K_e : Motor back EMF,	0.0297 V.s/rad
R_s : Armature resistance,	2.53 Ω
T_{PK} : Peak torque,	0.2232 N.m
S_{NL} : No load speed,	627.6 rad/s
T_F : Friction torque,	0.0042 N.m

3.4.1 Specifications of the flexible slider-crank mechanism

1. Gears, gear ratio (N) = 2.
2. Crank link.
3. Driven link.

Table 3.1: Links specifications of the flexible slider-crank mechanism

Link #	Length (m)	Mass (Kg)	Moment of inertia (Kg.m ²)
2	0.10	0.062832	$234.38 \times 10^{-6}^*$
3	0.15	0.094248	176.71×10^{-6}

Moment of inertia of motor's shaft and gears are included in moment of inertia of link 2 (\bar{I}_1).

4. Spring, $k = 25 \text{ N/m}$.
5. Dashpot, $c = 0.1 \text{ Kg/s}$, damping ratio (ζ) = 0.1.
6. Attached mass, $m = 0.01 \text{ Kg}$.

The mechanism's average input speed is 60 rpm.

3.4.2 Flexible elements

The damping ratio (ζ) is selected to be 0.1, which is a reasonable choice to estimate internal damping in the system. The spring's stiffness is determined to be such that it shrinks the uncontrollable regions at the extreme positions of the slider. Therefore, the displacement transmissibility between the mechanism's slider and the attached mass should be around 1.015.

If we assume the slider goes in a periodic motion with amplitude of 0.1 m, and frequency of 1 Hz, then

$$\text{Displacement Transmissibility} = \sqrt{\frac{1+(2\zeta r)^2}{(1-r^2)^2+(2\zeta r)^2}}$$

$$r = \frac{\omega}{\omega_n} = \frac{\omega}{\sqrt{\frac{k}{m}}}$$

For the assigned values, the stiffness of the spring is selected to be 25 N/m, and ω_n is 50 rad/s, which is around 8 Hz. According to Nyquist frequency, the sampling points have to be at least two times the maximum frequency of the system, which means at least 16 sampling points per repetition. In this case, 50 sampling points are used to make sure that aliasing is excluded.

The equations of motion for this system were performed by employing Lagrange's Equations. The complete derivation of the governing equations is provided in appendix B.

The equations of motion in matrix form are

$$\begin{bmatrix} \bar{I}_1 + m_2 R_1^2 & -m_2 R_1 r_2 C_{\theta+\phi} & 0 & -R_1 C_\theta \\ -m_2 R_1 r_2 C_{\theta+\phi} & I_2 + m_2 r_2^2 & 0 & R_2 C_\phi \\ 0 & 0 & m_3 & 0 \\ R_1 C_\theta & -R_2 C_\phi & 0 & 0 \end{bmatrix} \begin{bmatrix} \ddot{\theta} \\ \ddot{\phi} \\ \ddot{x} \\ \lambda \end{bmatrix}$$

$$= \begin{bmatrix} E_1 \\ E_2 \\ -\mu m_3 g \operatorname{sign}(\dot{x}) + c(R_1 \dot{\theta} S_\theta + R_2 \dot{\phi} S_\phi - \dot{x}) + k(R_1 + R_2 - R_1 C_\theta - R_2 C_\phi - x) \\ R_1 \dot{\theta}^2 S_\theta - R_2 \dot{\phi}^2 S_\phi \end{bmatrix}$$

$$E_1 = \frac{NK_t}{R_s} (V - K_e N \dot{\theta}) - c R_1 S_\theta (R_1 \dot{\theta} S_\theta + R_2 \dot{\phi} S_\phi - \dot{x}) - m_2 R_1 r_2 \dot{\phi}^2 S_{\theta+\phi} - k(R_1 + R_2 - R_1 C_\theta - R_2 C_\phi - x) R_1 S_\theta$$

$$E_2 = -c R_2 S_\phi (R_1 \dot{\theta} S_\theta + R_2 \dot{\phi} S_\phi - \dot{x}) - m_2 R_1 r_2 \dot{\theta}^2 S_{\theta+\phi} - k(R_1 + R_2 - R_1 C_\theta - R_2 C_\phi - x) R_2 S_\phi$$

$$V = K_p (\theta_r - \theta) + K_d (\dot{\theta}_r - \dot{\theta})$$

where S and C denote the sine and cosine of the angles, \bar{I}_1 is the total moment of inertia of the motor shaft, gears and driving link, V is the motor input voltage, θ_r is the reference input angle.

Two different cases were studied in timing path generation: a simple path case and dwell path case.

3.5 Timing simple path

This case is commonly used with slider-crank mechanism as it simply consists of rise and return segments. Regularly, in constant input speed mechanisms, the proposed path is symmetric around the mid-point, and the slider is driven to go between extreme positions routinely.

In this studied case, the output motion, which is the displacement of the vibrated attached mass, has to go through the precision points that specify the desired output path as shown in figure 3.3. The path is represented by polynomials of degree 7 to satisfy the continuity of motion up to the third derivative. The absolute error at each repetition is defined as,

$$e = \left| Y_j^* - Y_j \right|_{\max}, \quad \begin{cases} 3 \leq j \leq 29 \\ 33 \leq j \leq 49 \end{cases}$$

where j denotes the output data point number. Notice that the excluded points in determining absolute error referred to the uncontrollable extreme positions.

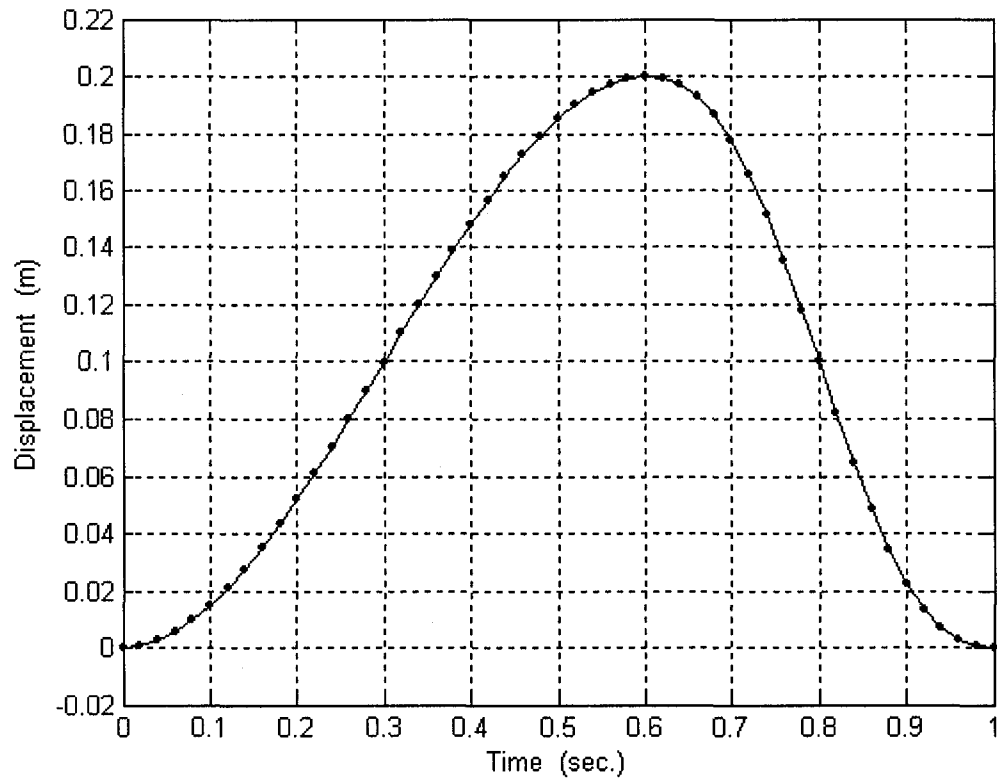


Figure 3.3: Output displacement versus time for the simple path case

3.5.1 Results of timing simple path

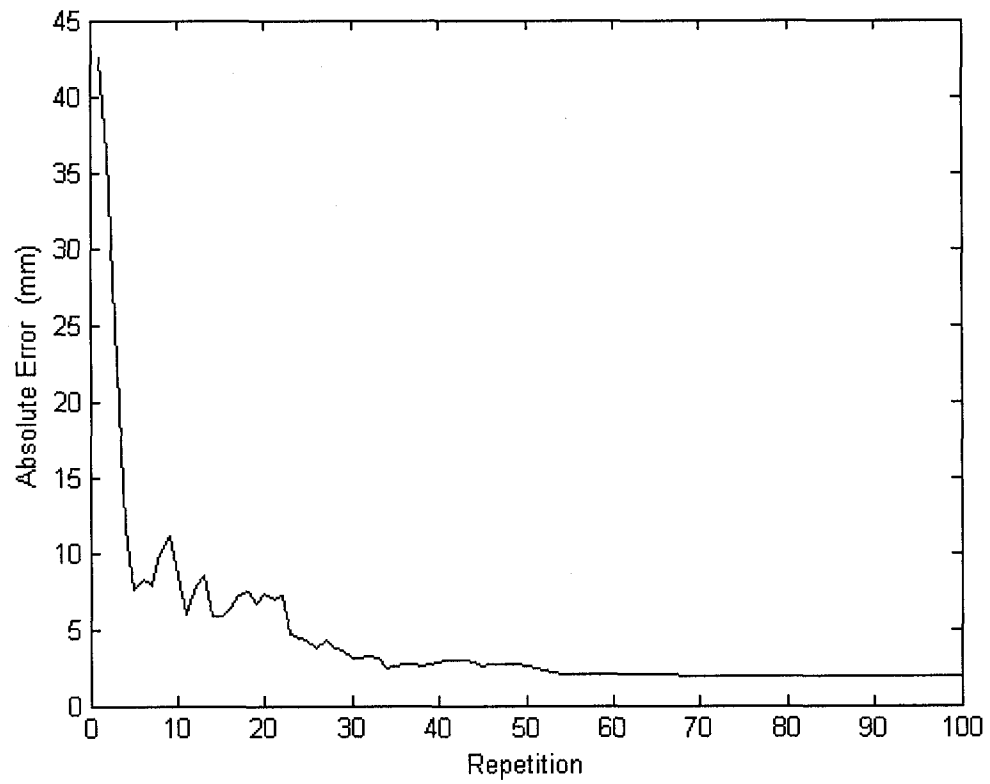


Figure 3.4: Absolute error versus repetitions using learning control

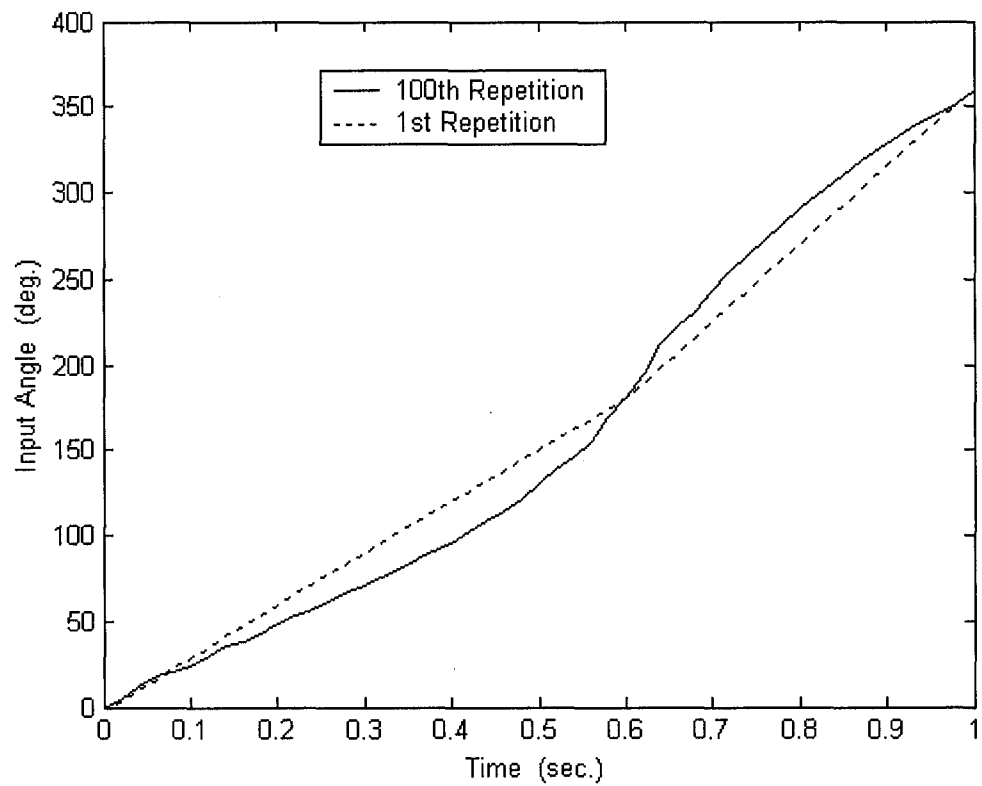


Figure 3.5: Input angle versus time using learning control

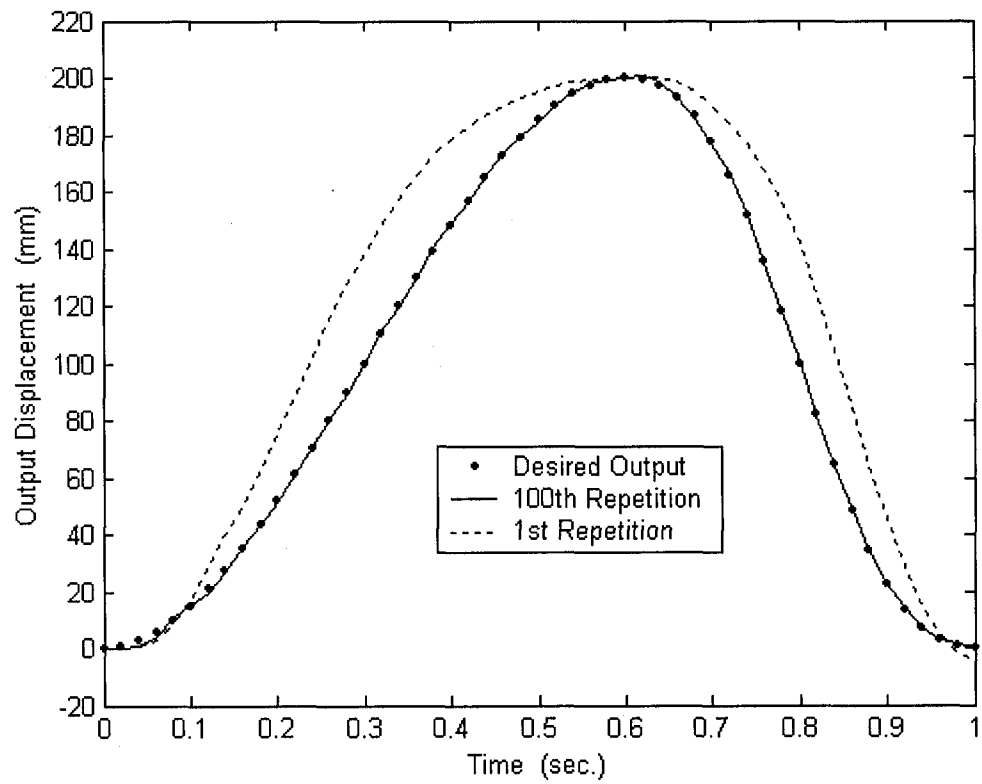


Figure 3.6: Output displacement versus time using learning control

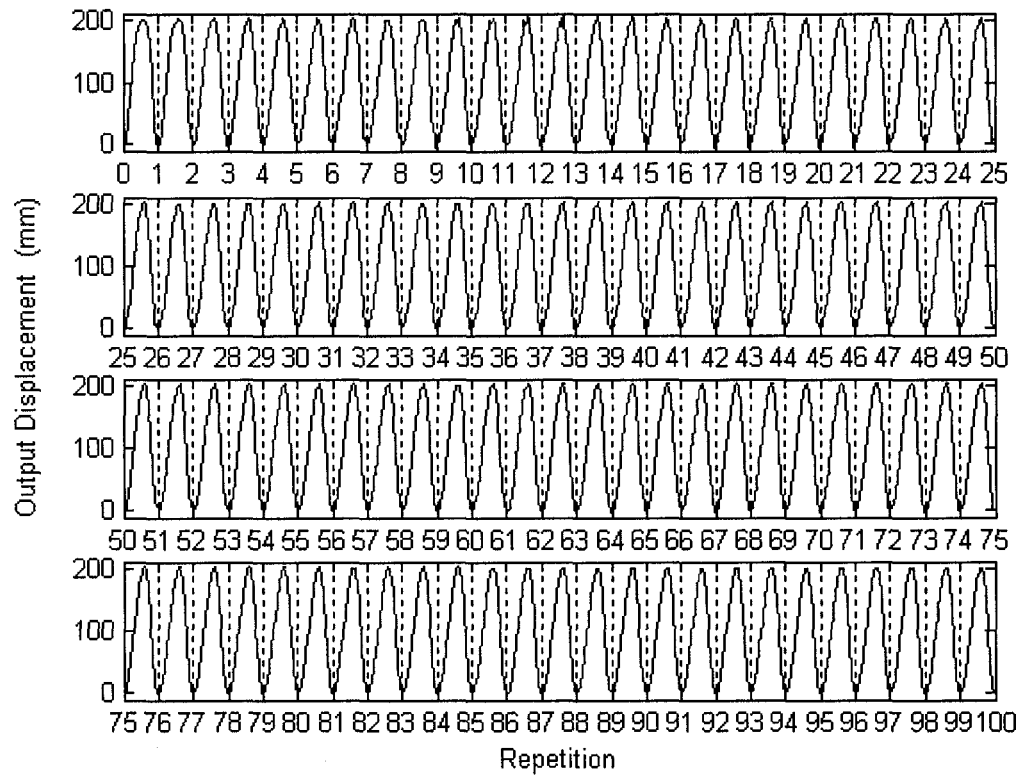


Figure 3.7: Output displacement versus repetitions using learning control

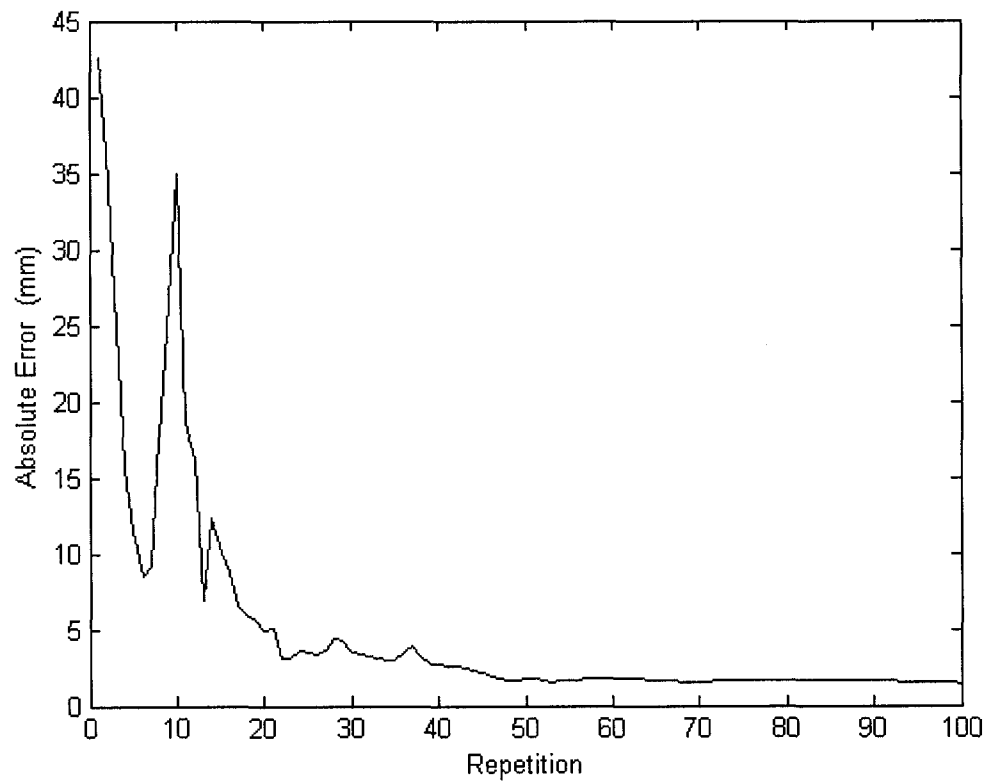


Figure 3.8: Absolute error versus repetitions using repetitive control

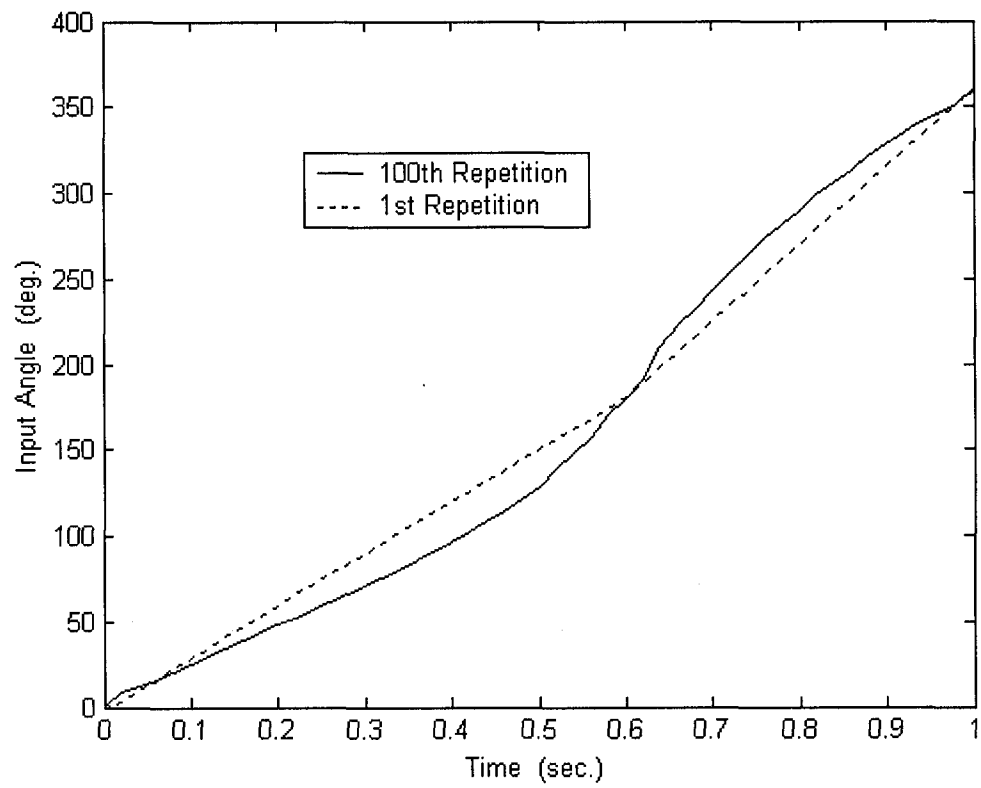


Figure 3.9: Input angle versus time using repetitive control

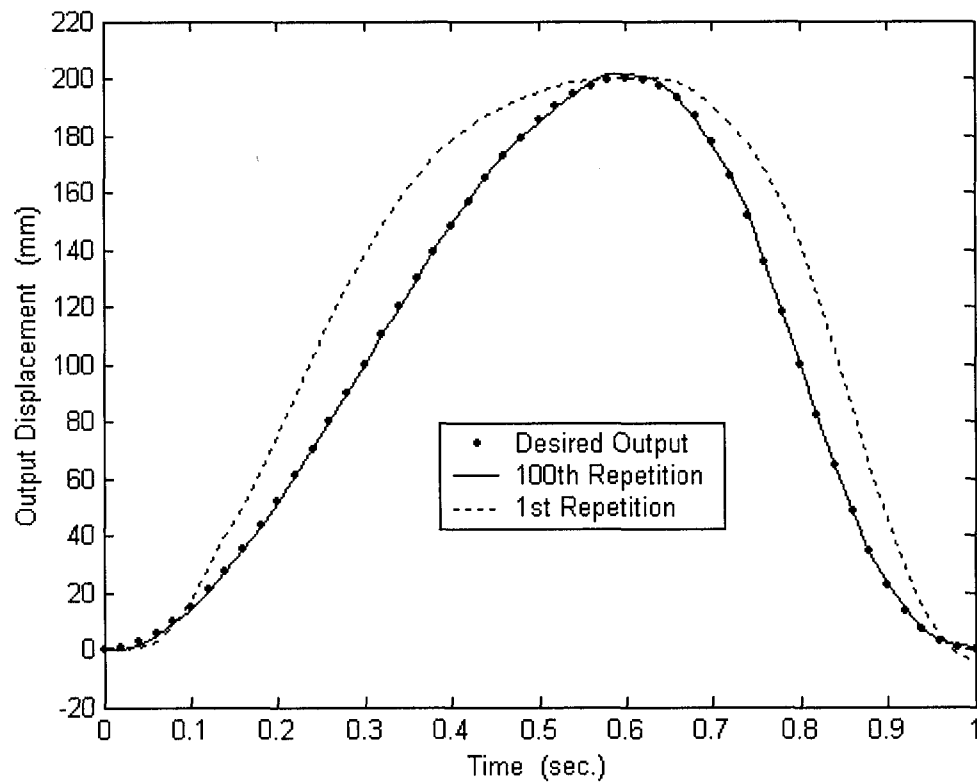


Figure 3.10: Output displacement versus time using repetitive control

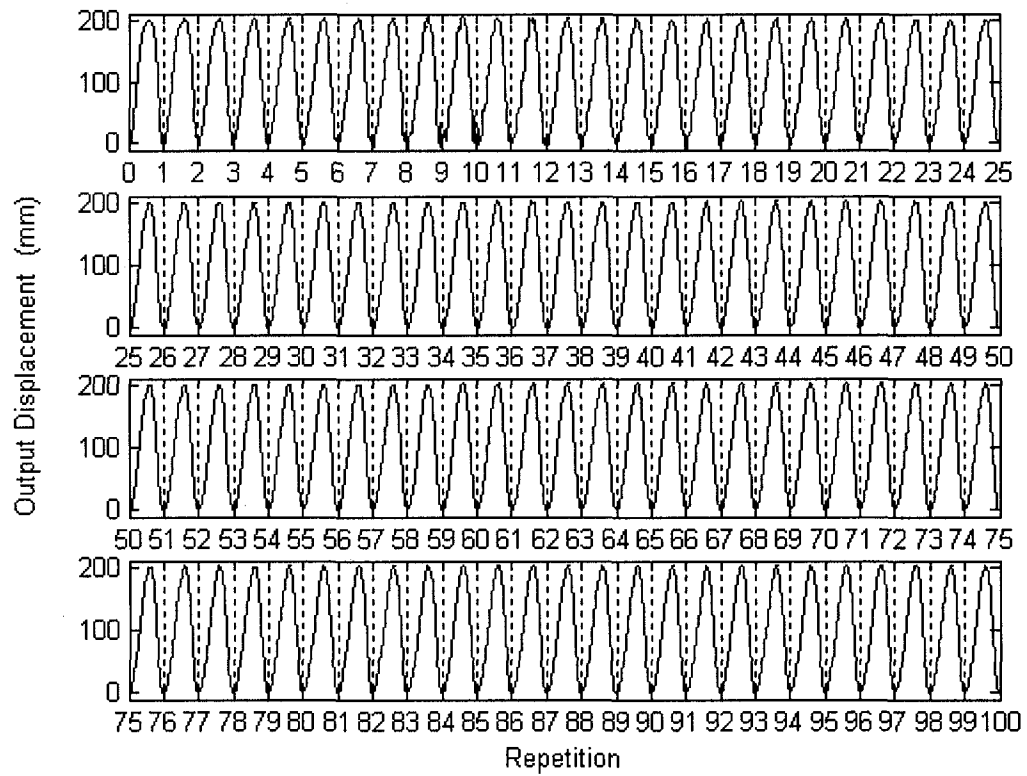


Figure 3.11: Output displacement versus repetitions using repetitive control

3.6 Timing dwell path

Timing dwell path is much more complicated than the simple one. It consists of rise, dwell, rise, and return segments as shown in figure 3.12. This type of mechanism has an output motion that does not dwell during the motion. However, it is important to examine the control methods in such complex cases. This unusual case tries to find the maximum feasibility of the control methods to learn the system's behavior and optimize the input speed to generate this uncommon output path. The path is represented by a polynomial of degree 11 to satisfy the continuity of the motion up to the third derivative. The absolute error at each repetition is defined as,

$$e = \left| Y_j^* - Y_j \right|_{\max}, \quad \left\{ \begin{array}{l} 3 \leq j \leq 34 \\ 38 \leq j \leq 49 \end{array} \right\}$$

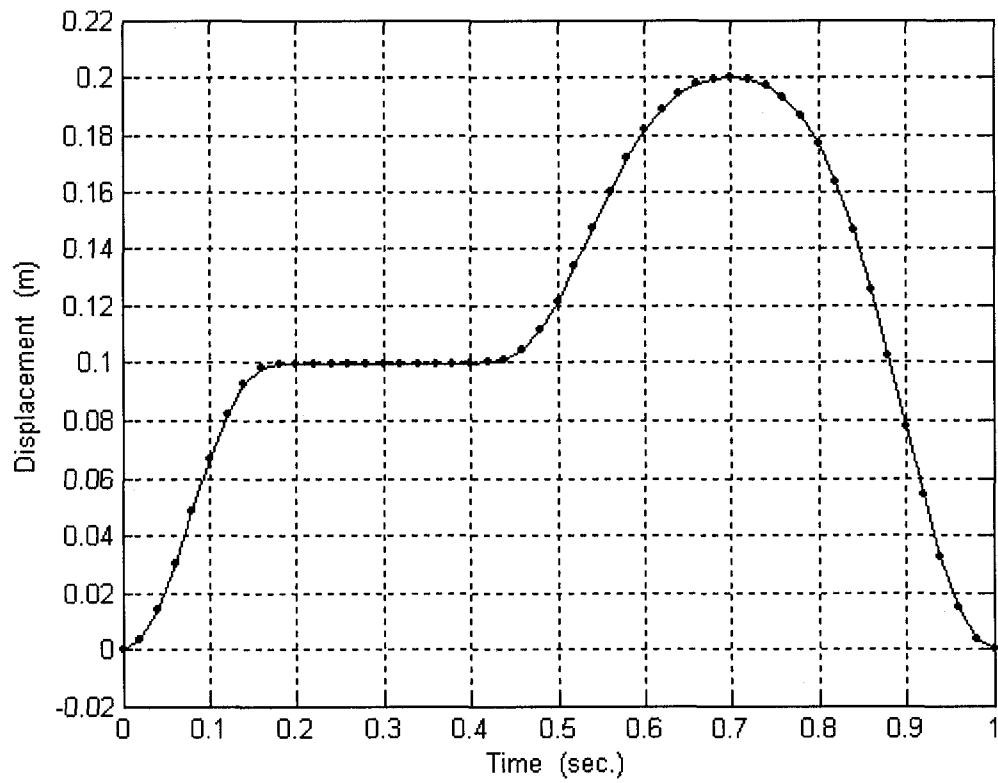


Figure 3.12: Output displacement versus time for the dwell path case

3.6.1 Results of timing dwell path

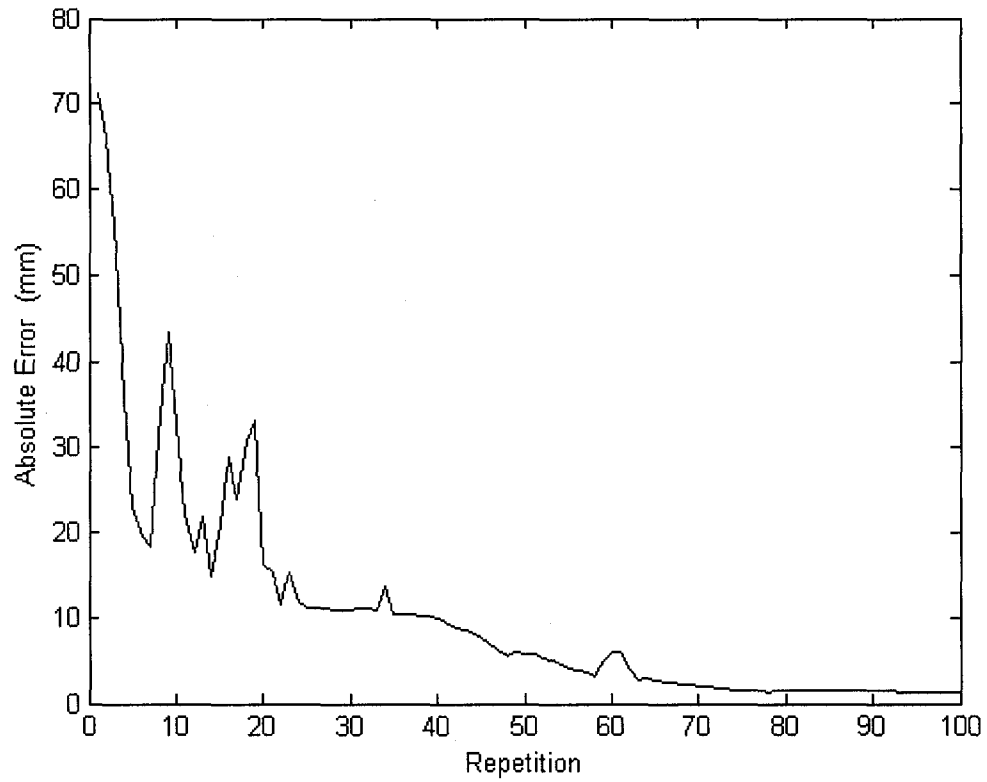


Figure 3.13: Absolute error versus repetitions using learning control

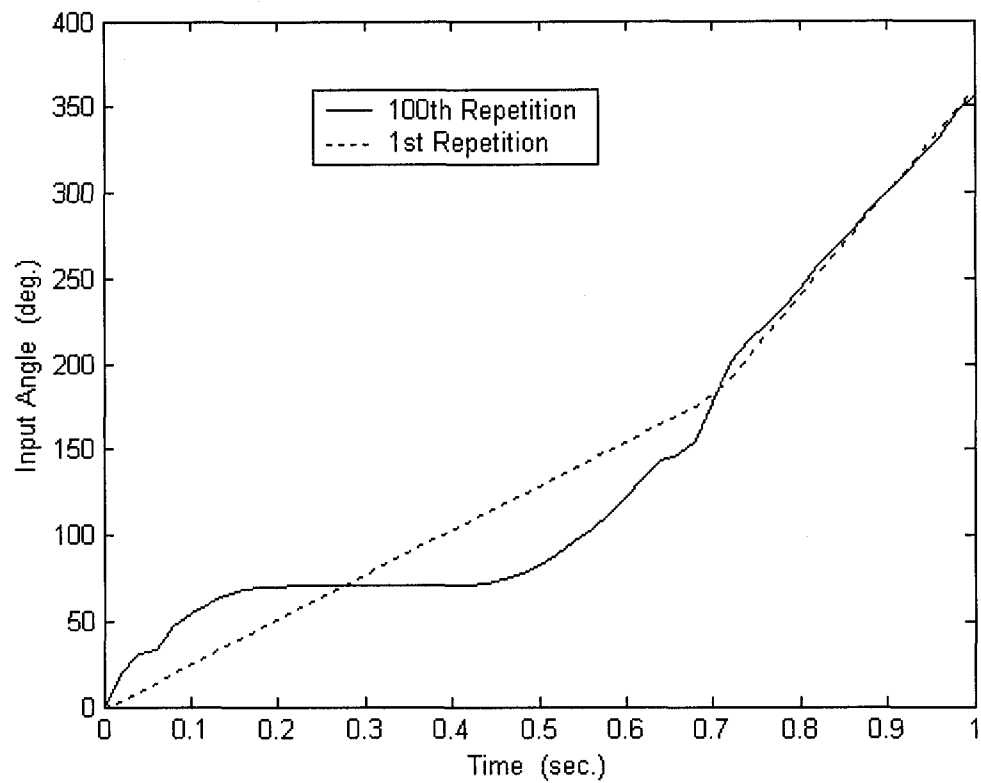


Figure 3.14: Input angle versus time using learning control

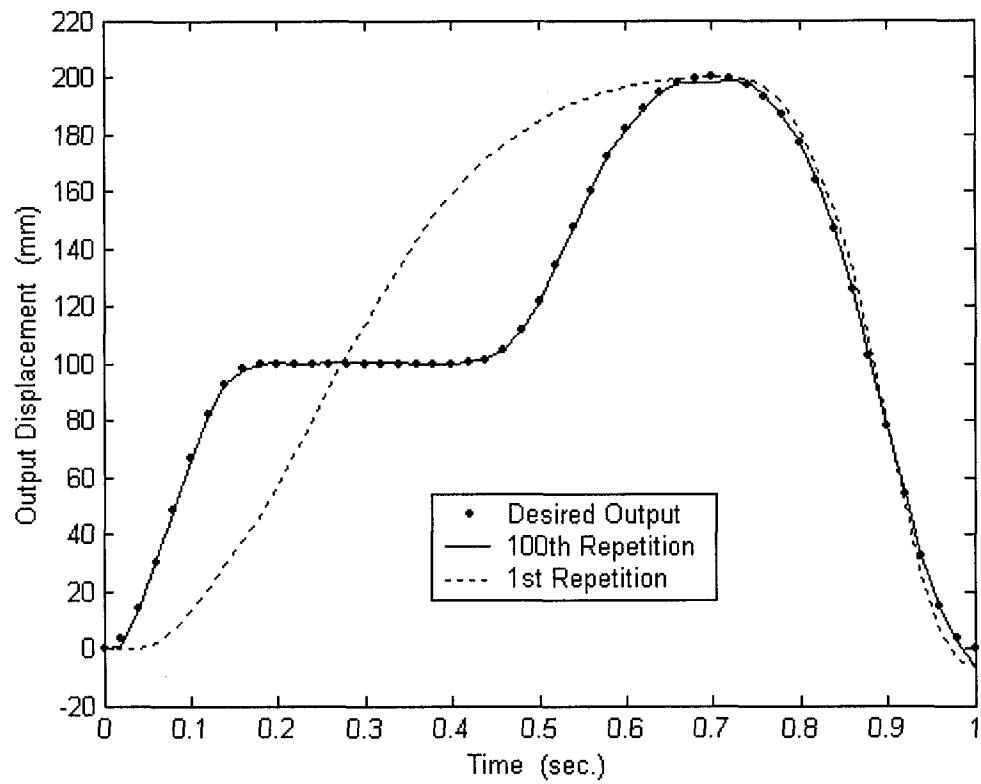


Figure 3.15: Output displacement versus time using learning control

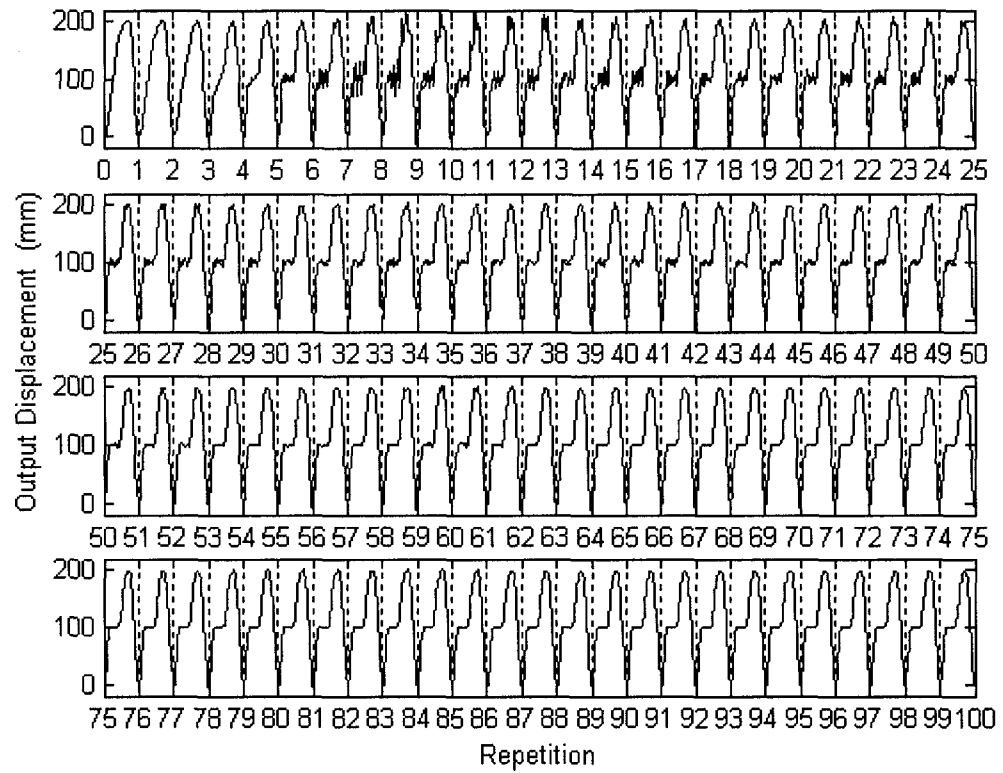


Figure 3.16: Output displacement versus repetitions using learning control

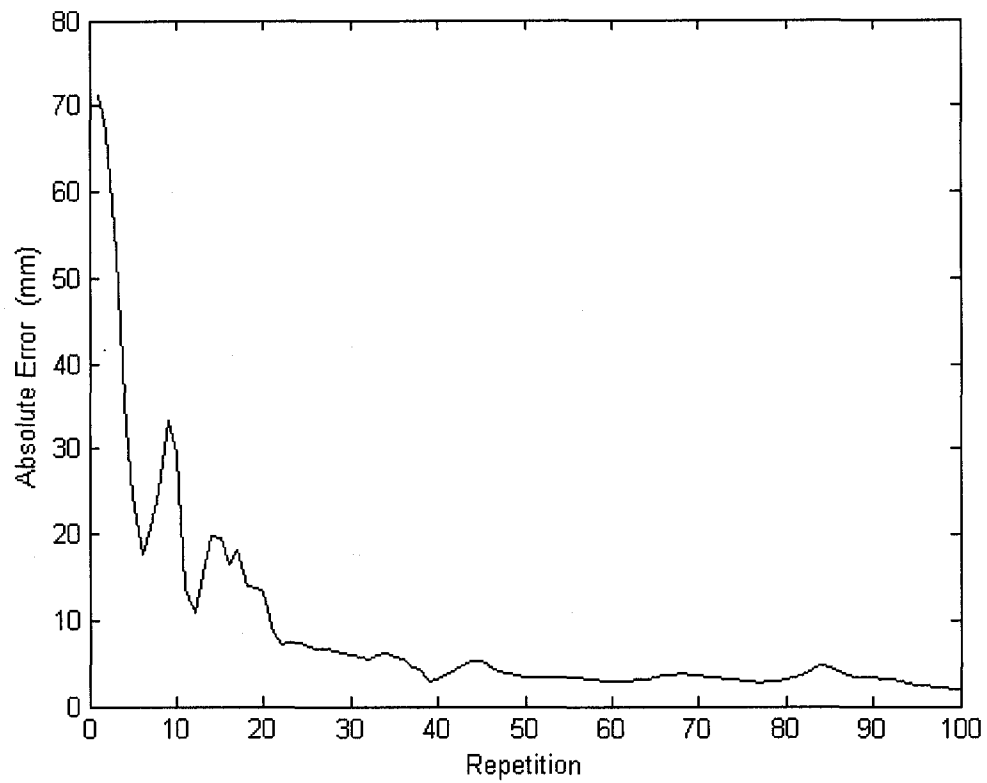


Figure 3.17: Absolute error versus repetitions using repetitive control

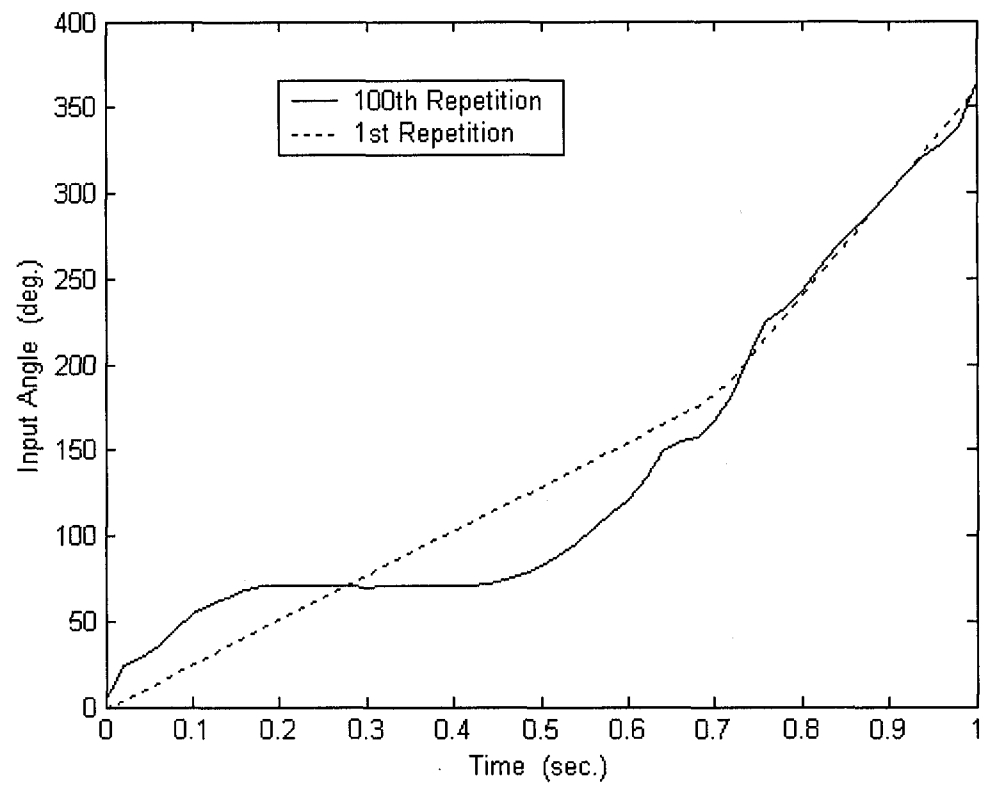


Figure 3.18: Input angle versus time using repetitive control

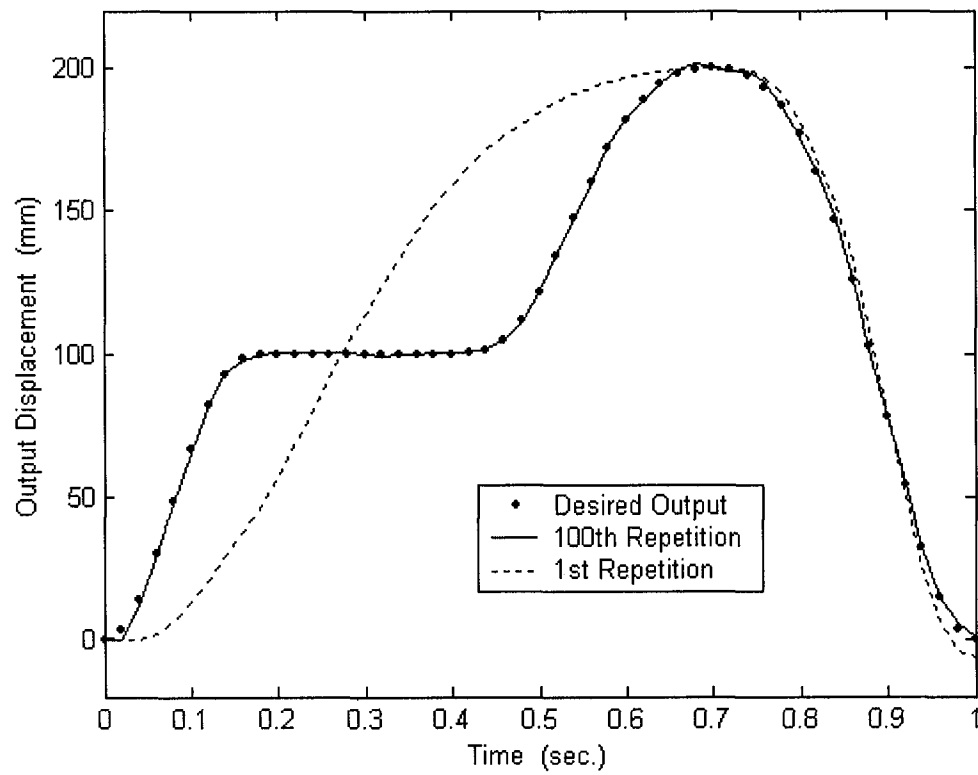


Figure 3.19: Output displacement versus time using repetitive control

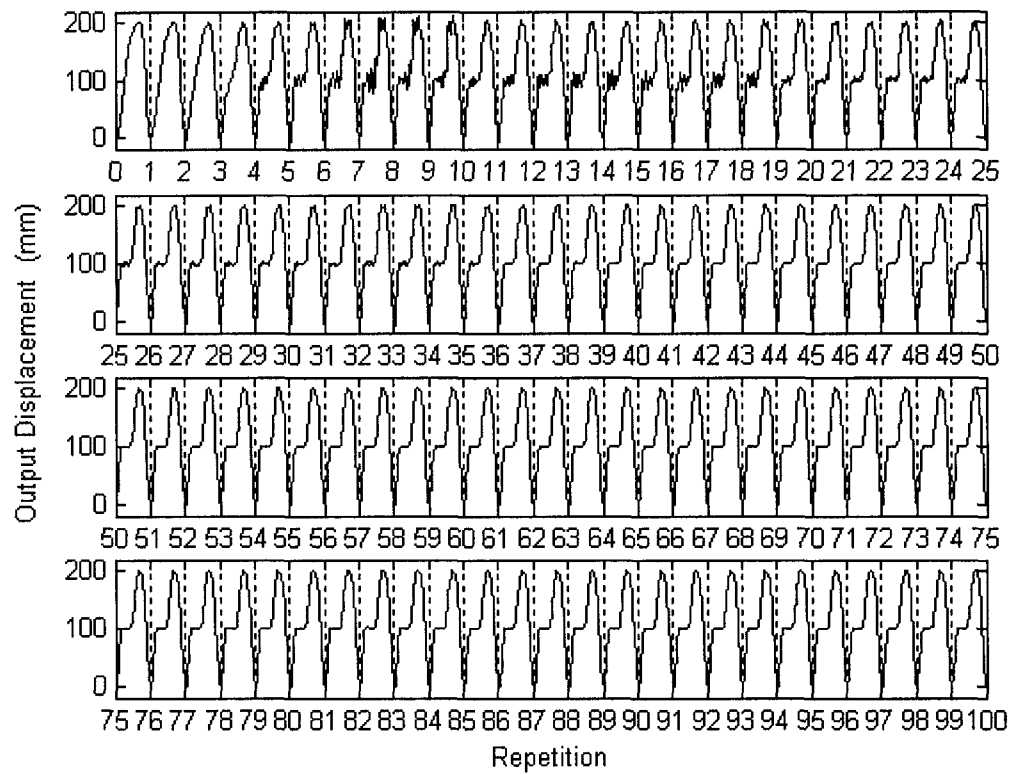


Figure 3.20: Output displacement versus repetitions using repetitive control

3.7 Discussion of results

Results of timing simple path generation show that the absolute error decreases rapidly in the first five repetitions, and then it decreases irregularly for the rest of the repetitions. The large error at the beginning occurs because the first repetition's input is relatively far away from the desired input. However, the quick drop of the error is due to bringing the overall trend of the input speed to the desired speed, which makes the error drop significantly to some low levels. The spike that appears at the tenth repetition is due to increasing the weight matrix that concerns about output error. The fluctuating region after the tenth repetition indicates that the vibrated system is hardly trying to match the desired output. The region after the 50th repetition shows that the system does reach the steady state and the error decreases insignificantly.

The steady state input angles in learning and repetitive methods are almost the same because the desired output is exactly the same in both cases. In fact, since the initial and final conditions of the desired output are precisely the same at each repetition and the learning method converges the actual output to the desired output, then the learning method becomes in the long run the same as the repetitive method. This means that there is no need to rest the system for a long time before starting new repetition because the final conditions have already come very close to the initial conditions.

Figures 3.7 and 3.11 show that the actual output in both control methods matches the desired output in around fifty repetitions.

The results of timing dwell path generation show irregular convergence. The absolute error plot shows that it has non-smooth decreasing. Many spikes appear due to increases in the weighting matrix. This result is expected since the desired output is uncommon for a slider-crank mechanism driving a vibrated mass.

For a second time, the input angles of learning and repetitive methods are alike for the same reason as in the previous case.

Notice that the excessive vibration at the extreme positions of the slider is more obvious for the repetitive method than for the learning method, since in learning method the system is allowed to stop at each repetition to match the initial conditions.

Figures 3.16 and 3.20 show the convergence progress of output motion to the desired motion. Observe the discontinuity of the output displacement in the learning control case at the beginning of each repetition due to stopping the system to bring it to zero initial conditions.

Chapter 4

Case 2: Constant Output Velocity

Constant output velocity is one of the most famous problems discussed in mechanisms. In some practical uses, the constant output velocity is certainly needed to perform some specific tasks. At present, the common constant input speed mechanisms are not sufficient to provide this kind of motion. Therefore, the variable input speed mechanisms become the solution for this challenging problem. Variable input speed mechanisms are preferred to old-fashioned constant input speed mechanisms because of the simplicity and accuracy of these new kinds of mechanisms.

The system used is exactly the same as that used for case 1. The learning and repetitive control methods in this case have the same procedures and concepts that were used in the previous case.

The task that needs to be done in this case is to obtain a constant output velocity of the attached mass for a part of the rising time. The return motion is free from any desired motion except that the mechanism goes smoothly to avoid any excessive vibrations at the end of the repetition.

4.1 Applying learning and repetitive control methods

In both control methods, the system start with constant input speed as an initial estimation of the desired input speed. There are 50 sampled points for describing the input angles of the mechanism. This number of sampled points is used to certify Nyquist frequency as discussed in chapter 3.

For this system, the output velocity of the slider is the function needed to be learned; therefore, it is described as,

$$\dot{Y}_i = \underline{A}_i x_i(0) + \underline{B}_i U_i$$

where \dot{Y} is the output velocity vector, A and B are the parameter matrices, x is the initial conditions vector, and U is the input angles vector, all at the i^{th} repetition. The above equation, which is used for the repetitive method, is the general case where the initial conditions are changeable.

Learning the output velocity is a sensitive case and undoubtedly harder than learning the output displacement. Therefore, the weight matrix Q, which corresponded to minimizing the output error, needs to be treated carefully. If Q is set large from the first repetition, then the system will behave unsteadily and the error will be tremendous, which makes the learning process unsuccessful. Thus, Q

is set initially very small, and then, it is increased gradually every twenty repetitions to perform the learning and optimizing processes as efficiently as possible.

Producing constant output velocity in a fraction of the motion's cycle requires setting the weighting matrix Q as zero matrix, except those elements that correspond to the designated points that belong to the constant output velocity region. Also, the desired output vector has to be equal to the desired output velocity. The modifications of the input angles that refer to the zero elements in matrix Q are irrelevant to both the output displacement and the output velocity at these points. The input angles for the zero elements will be modified by the propagation of modifying the concerned points that occur in the constant output velocity region. This modifying process makes the output motion smooth at the unconcerned regions to prepare the system to have constant output velocity at the concerned region.

In order to bring the output motion to the desired motion, the cost function that needs to be minimized must be formed specifically to ensure that it will compel the actual output velocity to converge to the desired output velocity. Otherwise, the system will not converge properly to the desired motion and some fluctuations in the output velocity will appear, making the output velocity unstable. Therefore, the cost function that needs to be minimized is

$$J = \frac{1}{2} \mathbf{e}_{i+1}^T \underline{\mathbf{Q}} \mathbf{e}_{i+1} + \frac{1}{2} \delta \mathbf{U}_{i+1}^T \underline{\mathbf{S}} \delta \mathbf{U}_{i+1}$$

$$\mathbf{e}_{i+1} = \mathbf{V}^* - \dot{\mathbf{Y}}$$

where \mathbf{V}^* is the desired constant output velocity. Performing the necessary work in minimizing this cost function results in,

$$\mathbf{U}_{i+1} = \mathbf{U}_i + \delta \mathbf{U}_{i+1}$$

$$\delta \mathbf{U}_{i+1} = \left(\underline{\mathbf{B}}_i^T \underline{\mathbf{Q}} \underline{\mathbf{B}}_i + \underline{\mathbf{S}} \right)^{-1} \underline{\mathbf{B}}_i^T \underline{\mathbf{Q}} \left(\mathbf{V}^* - \dot{\mathbf{Y}}_i - \underline{\mathbf{A}}_i (\mathbf{x}_{i+1}(0) - \mathbf{x}_i(0)) \right)$$

where \mathbf{U} and $\delta \mathbf{U}$ are the input angles and the difference in the input angle between any two consecutive repetitions at the $i^{\text{th}} + 1$ repetition, respectively. The percentage error that shows the convergence progression is defined as,

$$e = 100 \left| \frac{\mathbf{V}^* - \dot{\mathbf{Y}}_j}{\mathbf{V}^*} \right|_{\max} \% \quad , \quad p_1 \leq j \leq p_2$$

where p_1 and p_2 are the start and end points respectively of the constant output velocity region. In this studied case, the desired output velocity is 0.6 m/s, starting at 0.18 sec and ending at 0.42 sec. The desired output velocity is determined

thoughtfully to keep some stable angular velocity of the mechanism. It is nearly the average speed in the forward stroke of the output slider. Selecting higher or lower desired output velocity will speed up or lower down the angular velocity of the mechanism during the concerned region of desired output velocity, which leads to more vibrations of the attached mass. Moreover, it is important to have transient regions before and after the concerned region. These transient regions are used to prepare the system to move into or out of the constant output velocity region. The transient regions used in this case are very short because the overall period of the system is one second. Therefore, they are considered a one-time step of 0.02 sec.

4.2 Results of constant output velocity

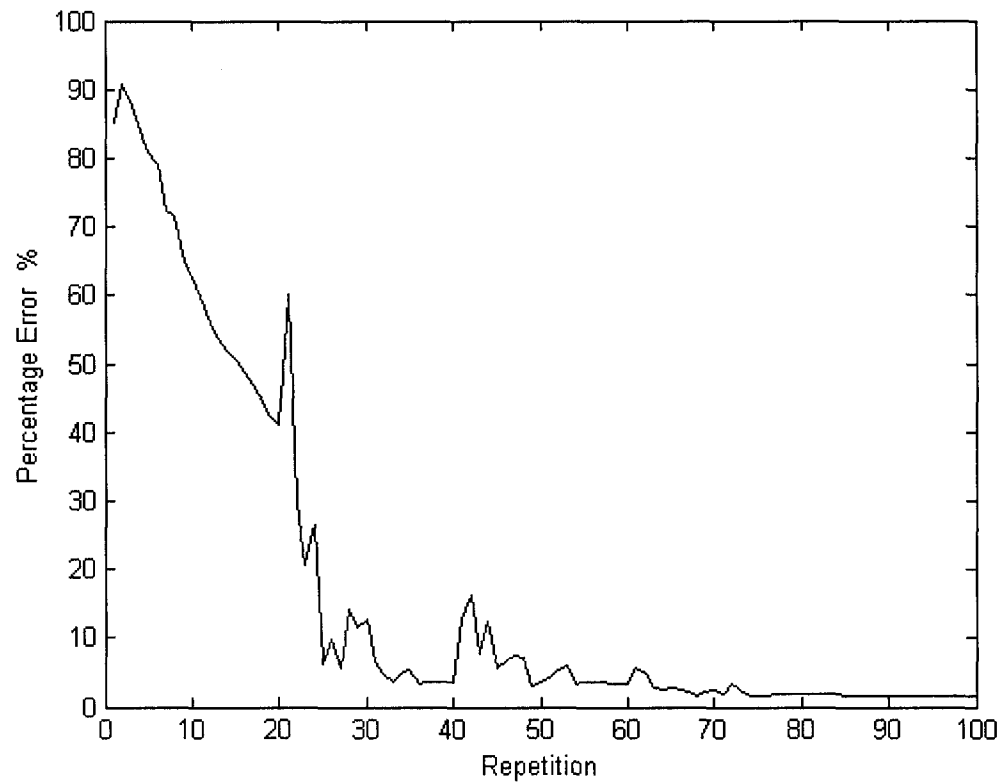


Figure 4.1: Percentage error versus repetitions using learning control

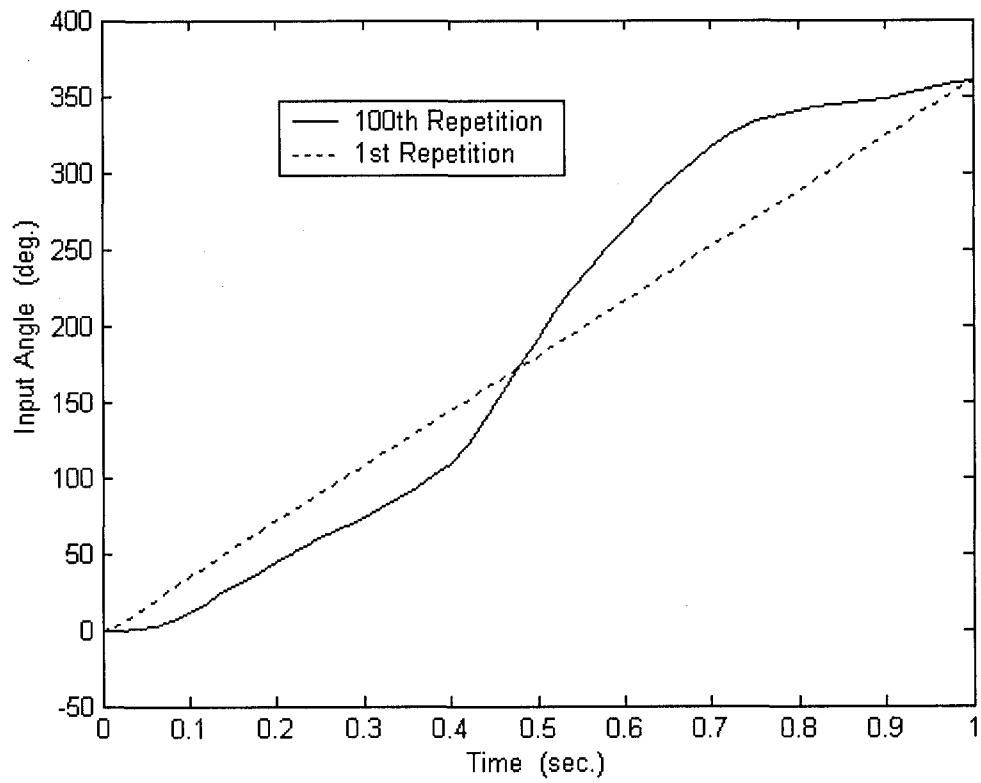


Figure 4.2: Input angle versus time using learning control

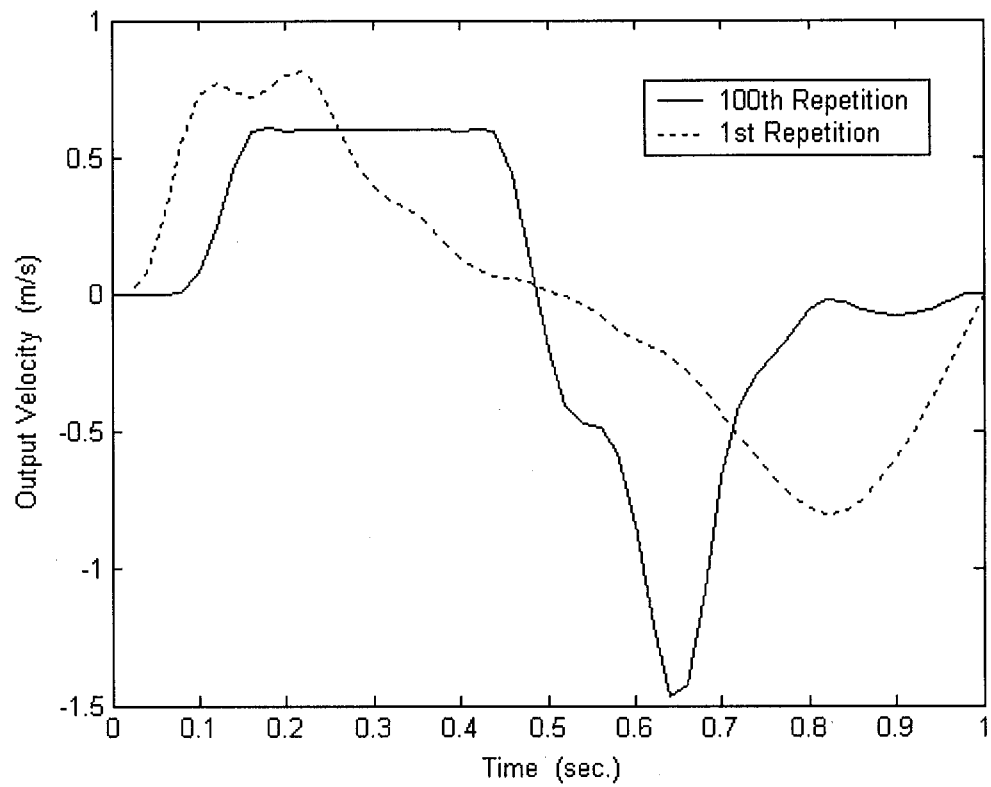


Figure 4.3: Output velocity versus time using learning control

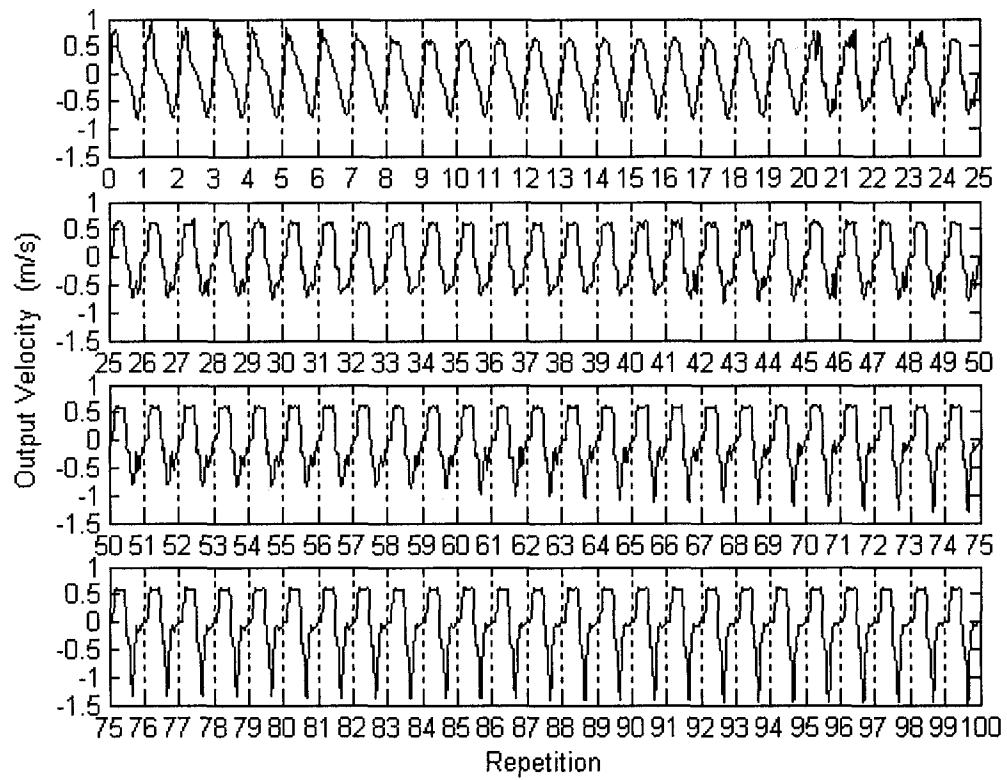


Figure 4.4: Output velocity versus repetitions using learning control

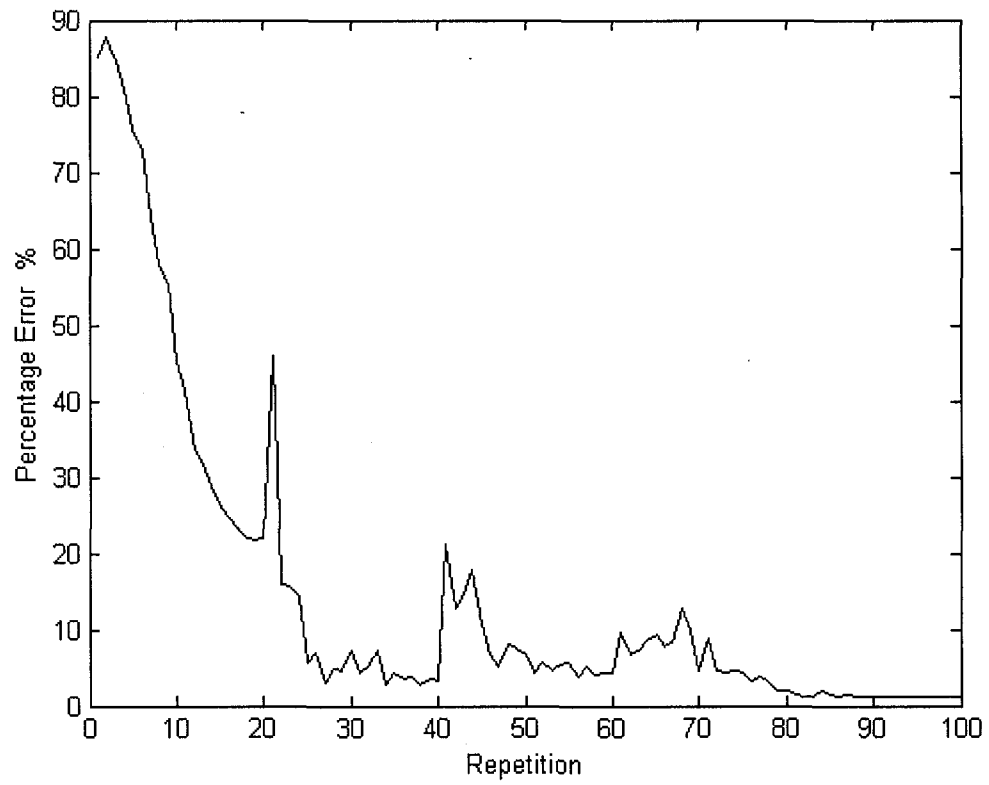


Figure 4.5: Percentage error versus repetitions using repetitive control

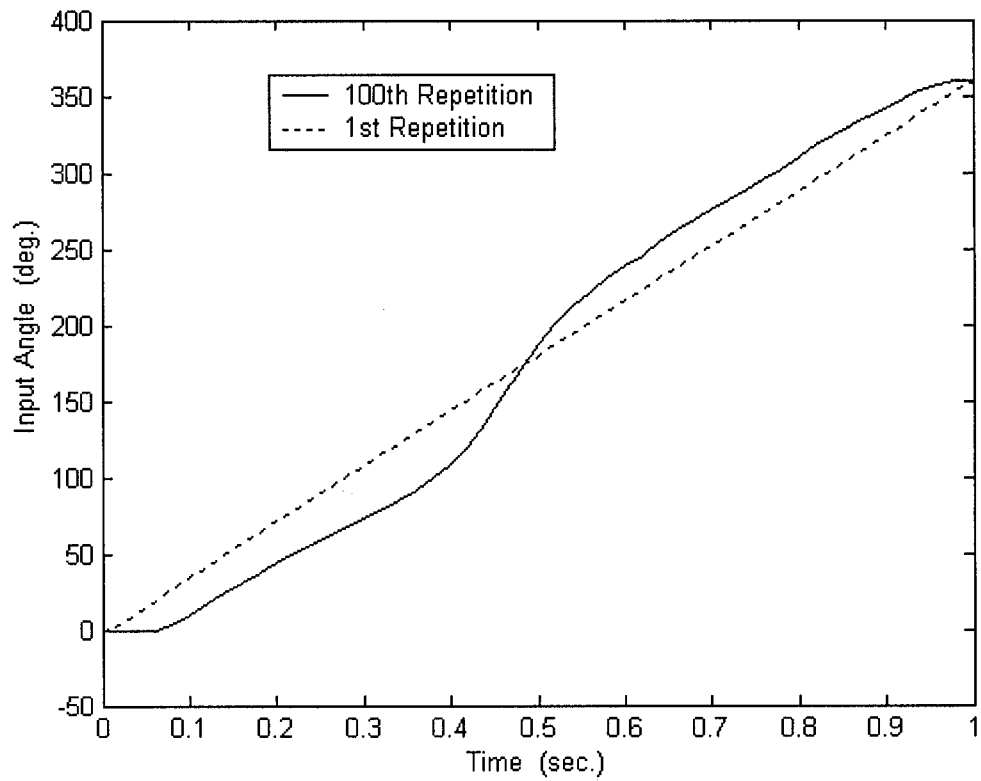


Figure 4.6: Input angle versus time using repetitive control

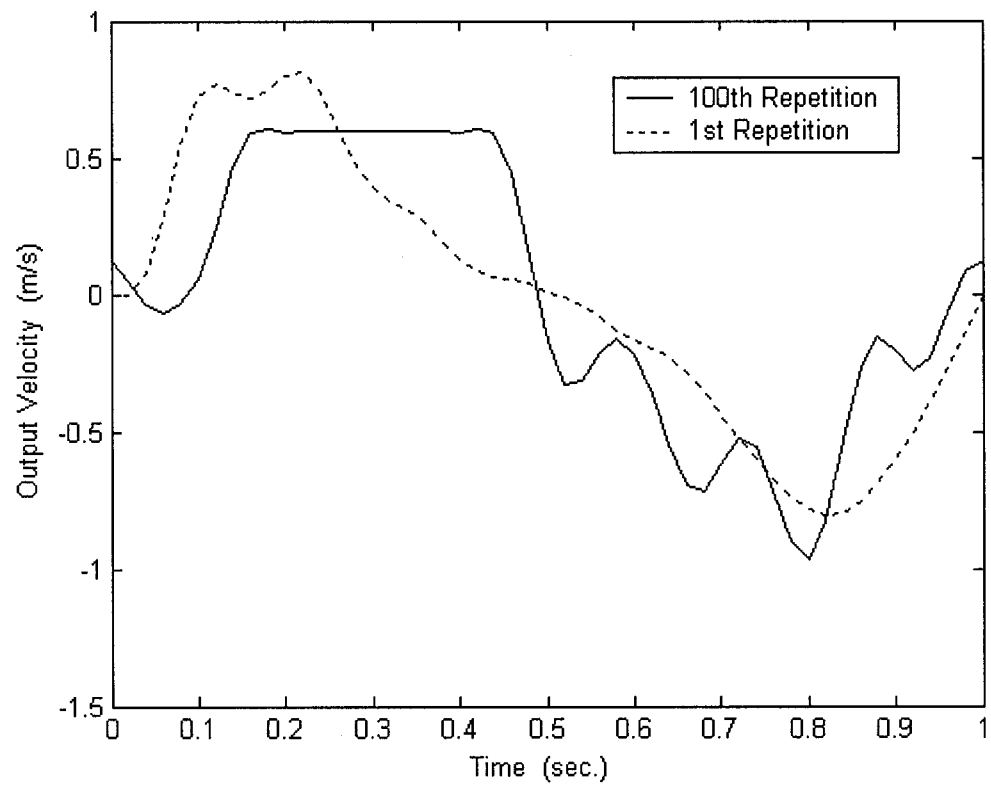


Figure 4.7: Output velocity versus time using repetitive control

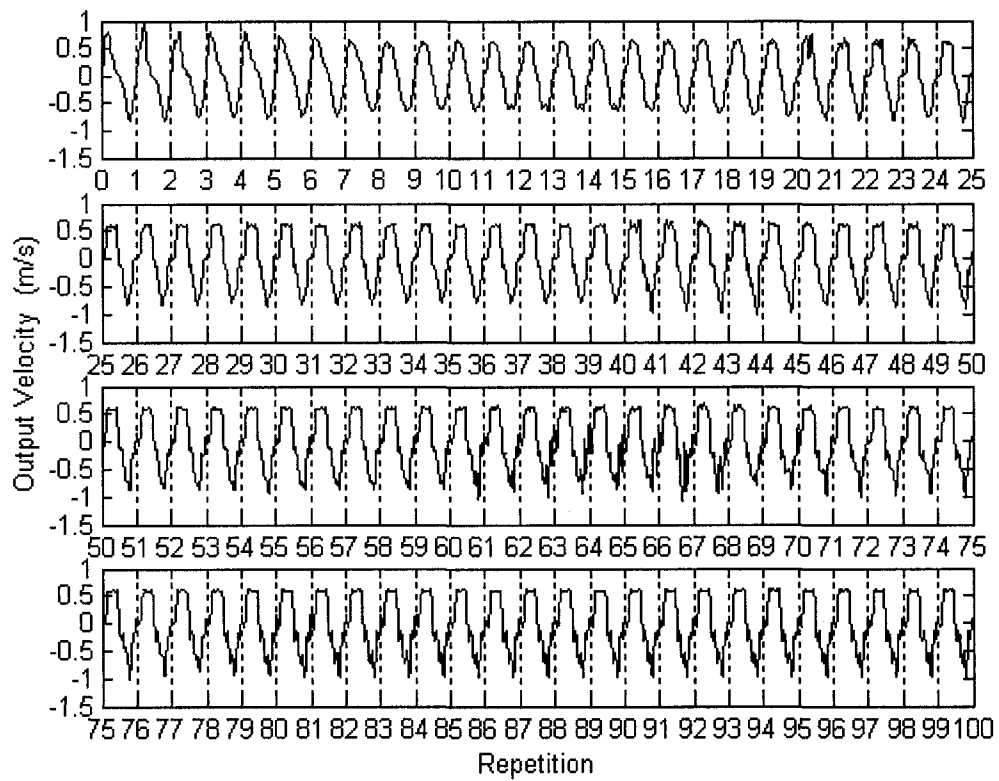


Figure 4.8: Output velocity versus repetitions using repetitive control

4.3 Discussion of results

The results show that the error was too high at the end of the first repetition, which means that the output velocity was far from what was desired. Also, they showed that the drop in the error started from the end of the third repetition, when the control methods started learning the system's behavior. The rapid drop in the error at the end of the first twenty repetitions illustrates how fast these control methods modify the input to bring the actual output velocity to the desired output velocity. The spike shown at the 20th repetition indicates the increasing of the weighting matrix Q . When Q increases, the differences in the input between any two consecutive repetitions increase. Up to the 20th repetition, the control methods still are incapable of doing large modifications since Q is small and the output motion shows little change through repetitions. However, when Q increases at the 20th repetition, the control methods quickly learn how the system behaves, and they recover the sudden jump in the error in a few repetitions. This phenomenon happens again insignificantly at the 40th and 60th repetitions.

Both methods need around 80 repetitions to bring the system close enough to the desired output, and eventually they bring the system to the steady state. Moreover, the learning control shows more progress in decreasing the error than the repetitive method because, as mentioned, it starts all repetitions from rest, which means it does not apply any effort to stop the excessive vibrations.

The input angle and the output velocity plots show that both methods converge to almost the same solution, especially for the rising region where the constant velocity region occurs. This is because both methods have the same desired output in the rising region, and they are free to act at the return region since there is no specific desired output.

Figure 4.3 and 4.7 show the output velocity at the 1st and 100th repetitions for both control methods. The repetitive control method shows more fluctuation in the output velocity, which means more vibrations of the attached mass. This is because the return region is not concerned about how the system behaves.

Figures 4.4 and 4.8 show the convergence progress of output velocity to that which is desired. The system shows fluctuation in the output velocity at the concerned region at the beginning of motion until the identifying process develops to modify the input for producing constant output velocity. Notice that the percentage error at the 100th repetition is less than 2%.

Chapter 5

Case 3: Minimizing Output Acceleration

When the slider-crank mechanism is used in reciprocating engines, the magnitude of the force provided by the slider becomes a crucial matter. In most applications, the slider-crank mechanism works frequently to convert the input rotational motion of the motor into some arbitrary reciprocal rectilinear output motion, without any preference of the position or the velocity of the slider during the motion. Thus, it is useful to run the mechanism in such a manner that minimizes some destructive factors.

According to Newton's second law of motion, the force is directly proportional to the acceleration. Therefore, minimizing output acceleration is a fundamental objective to smooth the motion and avoid impacts and shocks that could happen during motion, which consequently destroy the machine in the long run.

The system used in this case is the same as that used in case 1. Same concepts of using learning control and repetitive control methods were applied to this case. The objective of this case is to run the slider-crank mechanism in a way that minimizes the output acceleration of the attached mass.

5.1 Applying learning and repetitive control methods

Dealing with output acceleration of vibrational systems is much harder than treating output displacement or output velocity. It is an extremely sensitive case since the output acceleration is a highly fluctuating function varying widely during motion. Changing the input must be done very carefully and thoughtfully since the output acceleration shows tremendous changes for any little change of the input.

The system initially is fed with a constant input speed, which is the first estimation of the final desired input. This initial input is going to be modified as the control methods learn more about the system's behavior. The weight matrix Q is started very low and then it is increased every 40 repetitions. This long run for each increment step of Q is done because the control methods deal with a sensitive function, which is the output acceleration. So they need more repetitions to recognize the effect of the new bigger changes in the input on this sensitive function. Also, it is necessary to properly adjust the parameter matrix to learn the system's output and to work the necessary modifications.

Minimizing the output acceleration does not require any specific desired output reference, which means that the vector Y^* , which represents the desired output, becomes zero vector. When Y^* is zero, then the output acceleration will converge to match what is desired, but, in fact, the minimizing process eventually will reach its limit and the system at that time attains the lowest possible output acceleration.

Observe that it is important to specify some input angles to be greater than zero and keep them unchanged. Otherwise, the system will get to zero input angles in order to minimize the output acceleration, which is the trivial case. Therefore, the middle input angle point, which occurs at the mid period time must be set at 180° and it must remain unchanged during the modification process to ensure that the mechanism will not reach the trivial solution and will perform complete rotary motion.

Since specifying the cost function requires determining the output acceleration correctly, the best way to calculate it is to differentiate the output displacement twice with respect to time by some approximate numerical method. In this case, the simplest method that could be used with sufficient accuracy is the three forward, backward, or central points difference method, depending on the position of the point. For this system, the output displacement of the slider is the function that is learned through repetitions; therefore, it is described as,

$$Y_i = \underline{A}_i x_i(0) + \underline{B}_i U_i$$

where Y is the output displacement vector, A and B are the parameter matrices, x is the initial conditions vector, and U is the input angles vector, all at the i^{th} repetition.

The above equation, which is used for the repetitive method, is the general case where the initial conditions are changeable.

The cost function that needs to be minimized can be written as follows:

$$J = \frac{1}{2} \mathbf{e}_{i+1}^T \underline{\mathbf{Q}} \mathbf{e}_{i+1} + \frac{1}{2} \delta \mathbf{U}_{i+1}^T \underline{\mathbf{S}} \delta \mathbf{U}_{i+1}$$

$$\mathbf{e}_{i+1} = \mathbf{Y}^* - \underline{\mathbf{D}} \mathbf{Y}_{i+1}$$

$$\mathbf{Y}^* = [0 \ 0 \ \dots \ 0 \ 0]^T$$

$$\underline{\mathbf{D}} = \frac{1}{\Delta^2 t} \begin{bmatrix} 1 & -2 & 1 & 0 & 0 & \dots & 0 & 0 \\ 0 & 1 & -2 & 1 & 0 & 0 & \dots & 0 \\ 0 & 0 & 1 & -2 & 1 & 0 & \dots & 0 \\ \vdots & & & \ddots & \ddots & & & \vdots \\ 0 & \dots & 0 & 1 & -2 & 1 & 0 & 0 \\ 0 & \dots & 0 & 0 & 1 & -2 & 1 & 0 \\ 0 & 0 & \dots & 0 & 0 & 1 & -2 & 1 \end{bmatrix}$$

Since the desired vector is zero and all input points have the same importance, then the cost function can be simplified as

$$J = \frac{1}{2} q Y_{i+1}^T \underline{M} Y_{i+1} + \frac{1}{2} s \delta U_{i+1}^T \delta U_{i+1}$$

$$\underline{M} = \underline{D}^T \underline{D}$$

where q and s are the weighting elements of the terms of minimizing error and minimizing input change respectively.

In fact, simulation results show that identifying and minimizing this cost function is too hard and takes a long time. Therefore, a new term, which depends on the input angular acceleration, is introduced to this cost function to make the identifying and minimizing processes easier and more efficient. The new cost function is

$$J = \frac{1}{2} q_1 Y_{i+1}^T \underline{M} Y_{i+1} + \frac{1}{2} q_2 U_{i+1}^T \underline{M} U_{i+1} + \frac{1}{2} s \delta U_{i+1}^T \delta U_{i+1} \quad 5.1$$

and the optimized input becomes

$$U_{i+1} = U_i + \delta U_{i+1}$$

$$\delta U_{i+1} = - \left(q_1 \underline{B}_i^T \underline{M} \underline{B}_i + q_2 \underline{M} + s \underline{I} \right)^{-1} \underline{H}$$

$$\underline{H} = q_1 \underline{B}_i^T \underline{M} \left(\underline{Y}_i + \underline{A}_i (x_{i+1}(0) - x_i(0)) \right) + q_2 \underline{M} U_i$$

where I is the identity matrix, and $\frac{q_2}{q_1}$ initially is set to be 1% and is decreased in the course of the repetitions. The acceleration function, which gives an indication of how the system converges to the optimum motion, is defined as follows

$$\text{Acceleration Function} = \sum_{i=1}^p \ddot{Y}_i^2$$

where \ddot{Y}_i is the output acceleration of the attached mass at the i^{th} point. Minimizing this summation brings the peak output acceleration to some low level. However, this cost function does not minimize the peak output acceleration to the minimum level, but it makes it as low as possible.

Notice that in this case the damping ratio is increased to 0.5 to minimize the high fluctuation in the output acceleration, which subsequently makes the learning process easier and much more efficient.

5.2 Results of minimizing output acceleration

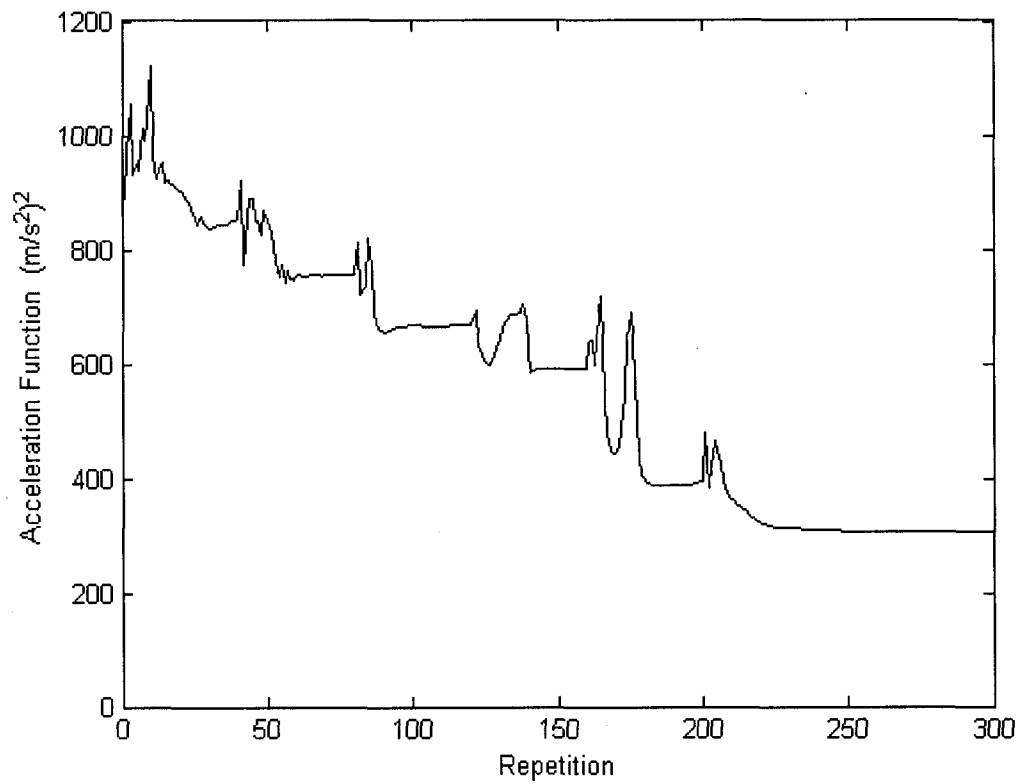


Figure 5.1: Acceleration function versus repetitions using learning control

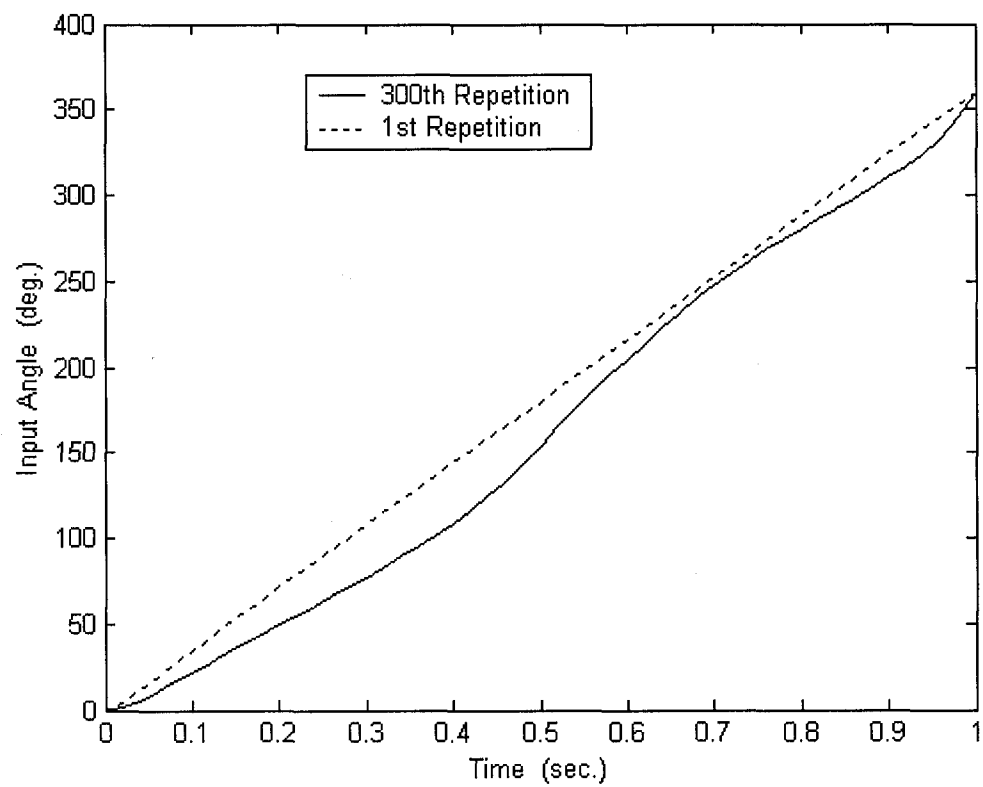


Figure 5.2: Input angle versus time using learning control

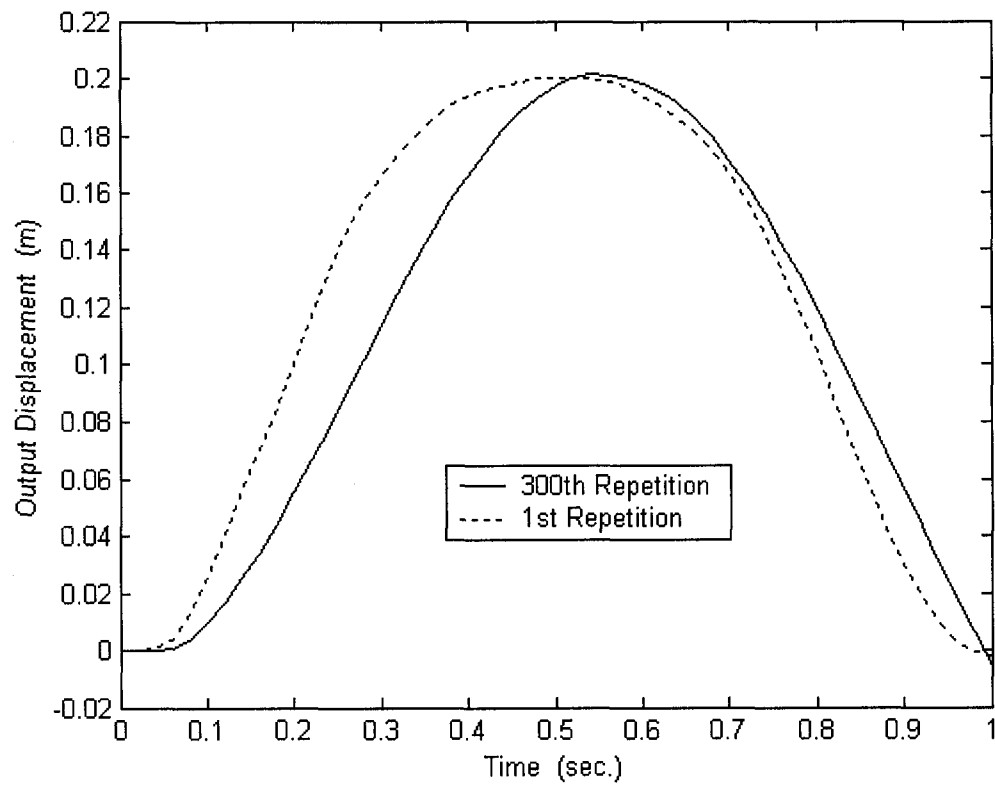


Figure 5.3: Output displacement versus time using learning control

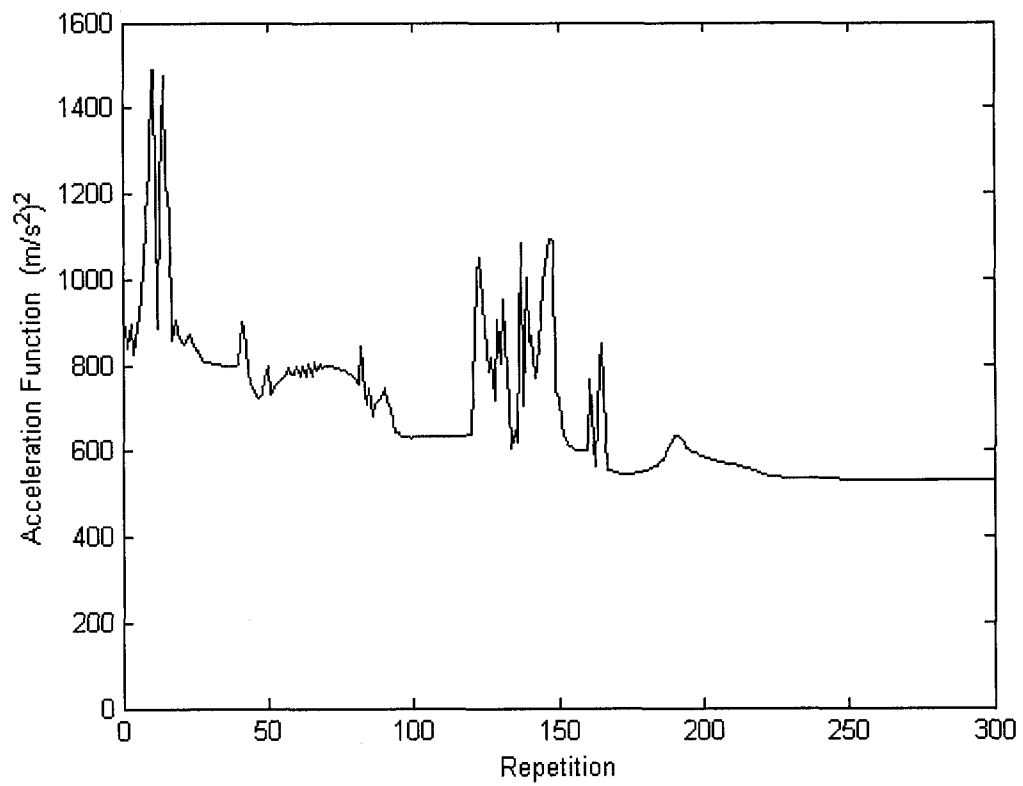


Figure 5.4: Acceleration function versus repetitions using repetitive control

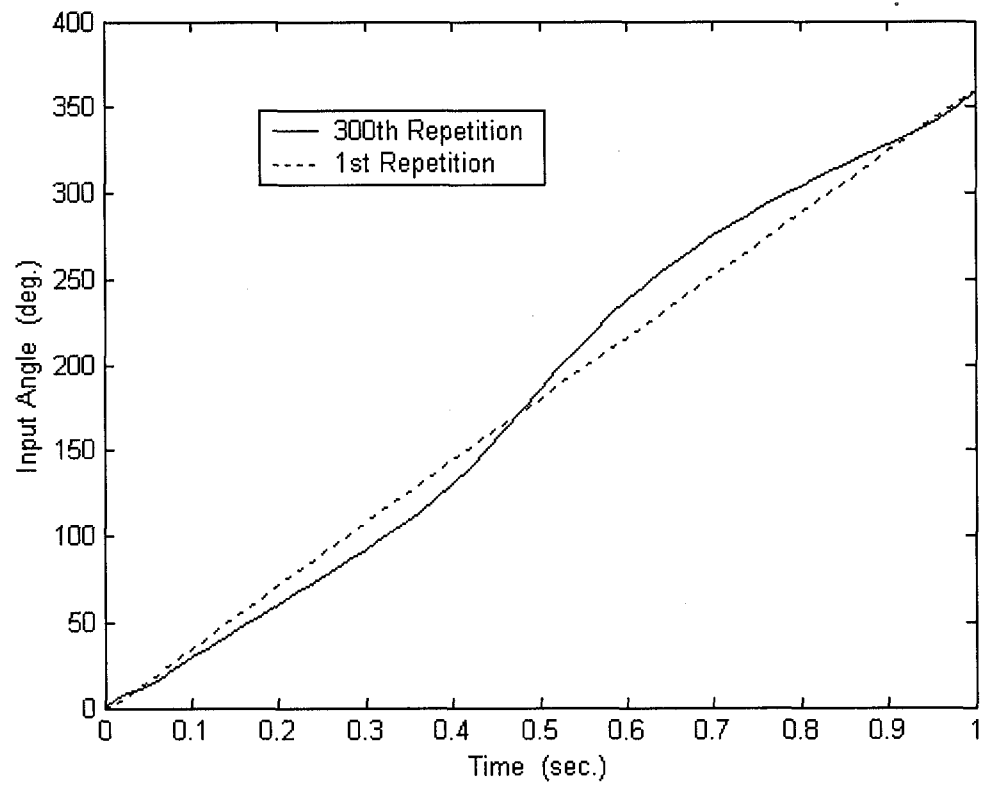


Figure 5.5: Input angle versus time using repetitive control

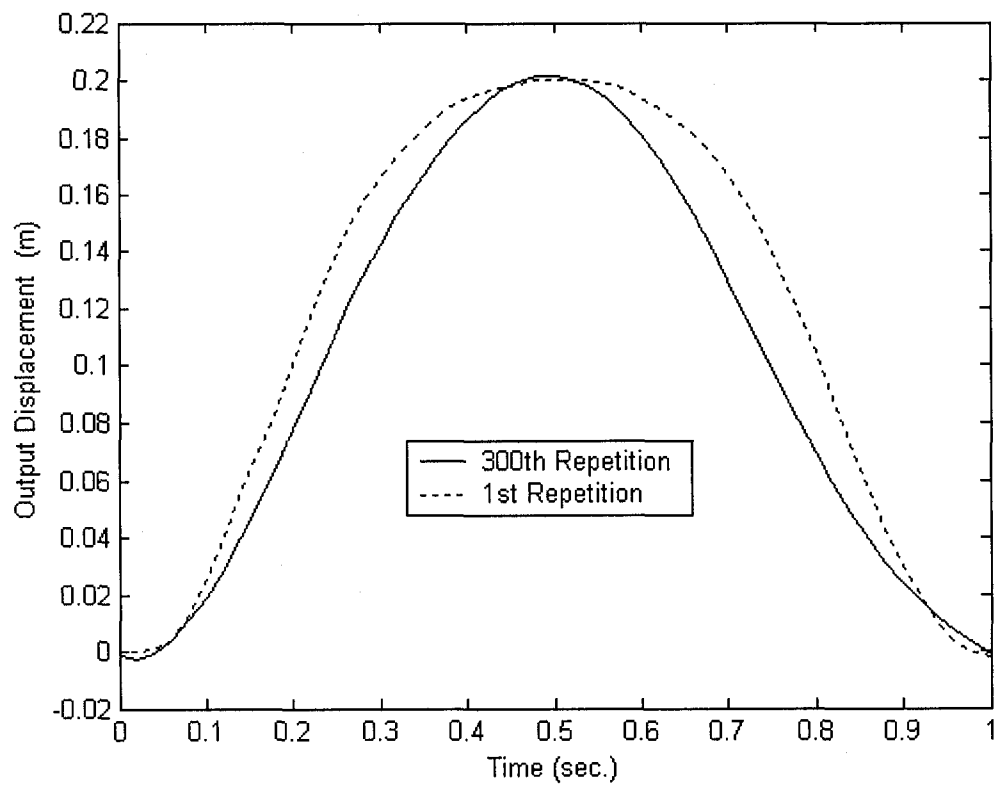


Figure 5.6: Output displacement versus time using repetitive control

5.3 Discussion of results

The results show that the learning and repetitive control methods are sufficient in minimizing the output acceleration. The acceleration function in both cases was minimized to the lowest possible level. The overall trend of the acceleration function is looks like steps decreasing due to the increase of the weight of minimizing acceleration every 40 repetitions, which makes the system take few repetitions after each increment to learn the system's behavior for the new weight, and then start minimizing the output acceleration for the rest of the repetitions until the next weight increment. However, sometimes the system needs more than few repetitions to identify the new behavior as shown in figure 5.4 for the repetitions from 120 to 150. This is because this specific increment seems to be just high enough to make the system have irregular converging. At the same time, reducing this increment could make the system take more time to reach the optimum solution. Therefore, this high increment was acceptable since the system did not show very large jumps in the acceleration function and it is still below the highest value.

Although the system started with very small weight minimizing the acceleration, the acceleration function increased for the first twenty repetitions. This is because the control methods were doing the required modifications knowing little about the system's behavior and nothing can be done to prevent the jumps that occur after the first repetition. Also, the system cannot be started with zero weights to avoid these

jumps because the control methods need to learn the system's behavior for different inputs, even if these inputs have small differences. Otherwise, the control methods would have learned well about the system but for the single and unchanged input, which also produces jumps once the control methods start changing the input. Therefore, it is important to optimize the initial weights at equation 5.1 to attain minimum jumps and necessary learning.

The case of repetitive control shows higher jumps in the acceleration function because the system has a continuous motion, which makes the attached mass vibrate more, as it appeared significantly in the acceleration function. Also, this increased vibration causes the steady state of the acceleration function is higher in repetitive control.

The output displacement plots show that the system tends to produce straight paths that are constant speed with minimum acceleration. This is obviously shown in the case of learning control since the final conditions are insignificant. This kind of motion is also shown in the repetitive control case especially at the rise region, but with a curved path at the end of the repetition to smooth the motion, minimize the excessive vibrations, and minimize the output acceleration of the attached mass, at the end and start any two consecutive repetitions.

Chapter 6

Case 4: Minimizing Dissipated Energy

The dissipation in energy is always happening in mechanical systems. This fact means that the total internal energy of any closed dynamic system is vanishing as long as the system is in motion. The dissipation is due to the dynamic friction that occurs between any movable surfaces in contact. This dynamic friction has an enormous effect in converting the useful mechanical energy that appears as kinetic or potential energies into useless heat energy that disappears into the atmosphere. In more complicated dynamic systems, there are other sources that consume the useful mechanical energy such as damping, which occurs in the springs, dampers, or bendable parts. Moreover, the electrical elements such as resistors, which are used in electromechanical systems, or some electrical phenomenon, such as back electromotive force (EMF), would also cause dissipation in the internal energy of the system. However, to keep the dynamic system in motion, an input energy must be supplied to compensate for the waste in energy. Therefore, minimizing dissipated energy in the systems is important issue since it means minimizing the input power to the system.

In this studied case, the learning and repetitive control methods are used to run the system in a way that minimizes the dissipation in the internal energy. The block diagram of controlling this system is shown in figure 3.1.

6.1 Applying learning and repetitive control methods

The objective of this case is to find the best variable input speed that makes the system run with minimum dissipated energy. In this system, the dissipation in energy occurs due to the Coulomb friction between moving surfaces, motor back EMF voltage, and viscosity in the dashpot. The Coulomb friction cannot be avoided, since it is constant as long as there is motion. Therefore, the energy function that shows how the system is making progress in minimizing wasted energy is represented as a summation of two integrals for both damping and back EMF.

$$\begin{aligned} \int_0^{X_{\text{final}}} c\dot{y} dy + \int_0^{T_{\text{final}}} \frac{V_{\text{EMF}}^2}{R_s} dt &= \int_0^{T_{\text{final}}} \left(c\dot{Y}^2 + \frac{V_{\text{EMF}}^2}{R_s} \right) dt \\ &= \int_0^{T_{\text{final}}} \left(c\dot{Y}^2 + \frac{(K_e \psi)^2}{R_s} \right) dt = \int_0^{T_{\text{final}}} \left(c\dot{Y}^2 + \frac{(K_e N\dot{\theta})^2}{R_s} \right) dt \end{aligned}$$

$$\text{Energy Function} = \int_0^{T_{\text{final}}} \left(c \dot{Y}^2 + \frac{N^2 K_e^2}{R_s} \dot{\theta}^2 \right) dt$$

where c is the damping constant, \dot{Y} is the output velocity of the slider, V_{EMF} is the motor's back EMF voltage, R_s is the armature resistance, K_e is the motor back EMF constant, ψ is the speed of the motor, N is the gear ratio, $\dot{\theta}$ is the angular velocity of the mechanism, and the integral is calculated for each repetition. Since there are equal time steps, then this energy function is simplified to a power function by taking the summation of the integrant divided by the time step Δt .

$$\text{Power Function} = \sum_{i=1}^p c \dot{Y}_i^2 + \frac{N^2 K_e^2}{R_s} \dot{\theta}_i^2$$

The simplified power function depends on two variables: the input angular velocity and the output velocity of the slider. For simplicity, the control methods are learning only the output velocity instead of learning the whole power term. Therefore, the output velocity of the slider is the function needs to be learned and it is described as,

$$\dot{Y}_i = \underline{A}_i x_i(0) + \underline{B}_i U_i$$

where A and B are the parameter matrices, x is the initial conditions vector, and U is the input angles vector, all at the i^{th} repetition. The above equation, which is used for the repetitive method, is the general case where the initial conditions are changeable. The input angular velocity is obtained by differentiating the input angles with respect to time. Separating the entire power term into sub-terms is the simplest and most efficient way to learn the system's behavior. Although learning the whole term of dissipated power can give more accurate results, it takes much more time and the case becomes more sensitive and much harder to be identified. Therefore, the cost function that needs to be minimized becomes

$$J = \frac{1}{2} c \dot{Y}_{i+1}^T \dot{Y}_{i+1} + \frac{1}{2} \frac{N^2 K_e^2}{R_s} (\underline{D} U_{i+1})^T (\underline{D} U_{i+1}) + \frac{1}{2} s \delta U_{i+1}^T \delta U_{i+1}$$

$$\underline{D} = \frac{1}{\Delta t} \begin{bmatrix} -1.5 & 2 & -0.5 & 0 & 0 & \dots & 0 & 0 \\ 0 & -0.5 & 0 & 0.5 & 0 & 0 & \dots & 0 \\ 0 & 0 & -0.5 & 0 & 0.5 & 0 & \dots & 0 \\ \vdots & & & \ddots & \ddots & & & \vdots \\ 0 & \dots & 0 & -0.5 & 0 & 0.5 & 0 & 0 \\ 0 & \dots & 0 & 0 & -0.5 & 0 & 0.5 & 0 \\ 0 & 0 & \dots & 0 & 0 & 0.5 & -2 & 1.5 \end{bmatrix}$$

where s is the weighting factor of minimizing the input's differences and D is the differentiating matrix used for calculating the input angular velocity. Observe that in this case the weighting factor of minimizing the power term is constant and equal to one, while s is changed during motion to control the converging process. It starts from 0.2 and is decreased every ten repetitions by 99%. This means that s is almost negligible after the tenth repetition and the whole minimizing effort is put on the power term. Minimizing this cost function, as discussed in appendix A, results in these equations.

$$U_{i+1} = U_i + \delta U_{i+1}$$

$$\delta U_{i+1} = - \left(c \underline{B}_i^T \underline{B}_i + \frac{N^2 K_e^2}{R_s} \underline{M} + s \underline{I} \right)^{-1} \left(c \underline{B}_i^T \left(\dot{Y}_i + \underline{A}_i (x_{i+1}(0) - x_i(0)) \right) + \frac{N^2 K_e^2}{R_s} \underline{M} U_i \right)$$

$$\underline{M} = \underline{D}^T \underline{D}$$

These equations are the general optimized input that was used in the repetitive control method, while the optimized input for the learning control method where the initial conditions term is ignored, is as follows:

$$\delta U_{i+1} = - \left(c \underline{B}_i^T \underline{B}_i + \frac{N^2 K_e^2}{R_s} \underline{M} + s \underline{I} \right)^{-1} \left(c \underline{B}_i^T \dot{\underline{Y}}_i + \frac{N^2 K_e^2}{R_s} \underline{M} \underline{U}_i \right)$$

In order to avoid the trivial stationary solution that leads to zero dissipation in energy, an end condition is set unchanged and equal to 360° to ensure that the mechanism will make complete revolutions and will not stop. Therefore, the weight s that corresponds to the final point is set too high and unchanged during the optimizing process.

6.2 System's model

The model used is a rigid slider-crank mechanism driven by a motor as shown in figure 6.1. The system moves in the horizontal plane where the weights are ignored. The slider's mass is included in the mass of the driven link, thus, the center of gravity of this link is not at the mid point. Vibrational elements are involved to connect the slider with a fixed point. These vibrational elements are used to provide some variable load on the mechanism, depending on the position and velocity of the slider. The complete derivation of the governing equations for this system is provided in appendix C and the system's governing equations are in this form:

$$\begin{bmatrix} \bar{I}_1 + m_2 R_1^2 & -m_2 R_1 r_2 C_{\theta+\phi} & -R_1 C_\theta \\ -m_2 R_1 r_2 C_{\theta+\phi} & I_2 + m_2 r_2^2 & R_2 C_\phi \\ R_1 C_\theta & -R_2 C_\phi & 0 \end{bmatrix} \begin{bmatrix} \ddot{\theta} \\ \ddot{\phi} \\ \lambda \end{bmatrix} = \begin{bmatrix} E_1 \\ E_2 \\ R_1 \dot{\theta}^2 S_\theta - R_2 \dot{\phi}^2 S_\phi \end{bmatrix}$$

$$E_1 = \frac{NK_t}{R_s} (V - K_e N \dot{\theta}) - c R_1 S_\theta (R_1 \dot{\theta} S_\theta + R_2 \dot{\phi} S_\phi) - m_2 R_1 r_2 \dot{\phi}^2 S_{\theta+\phi} - k(R_1 + R_2 - R_1 C_\theta - R_2 C_\phi) R_1 S_\theta$$

$$E_2 = -c R_2 S_\phi (R_1 \dot{\theta} S_\theta + R_2 \dot{\phi} S_\phi) - m_2 R_1 r_2 \dot{\theta}^2 S_{\theta+\phi} - k(R_1 + R_2 - R_1 C_\theta - R_2 C_\phi) R_2 S_\phi$$

$$V = K_p (\theta_r - \theta) + K_d (\dot{\theta}_r - \dot{\theta})$$

where S and C denote the sine and cosine of the angles, \bar{I}_1 is the total moment of inertia of the motor shaft, gears and driving link, K_t is the motor torque constant, V is the motor input voltage, θ_r is the reference input angle, K_p is the proportional controller gain, K_d is the derivative controller gain.

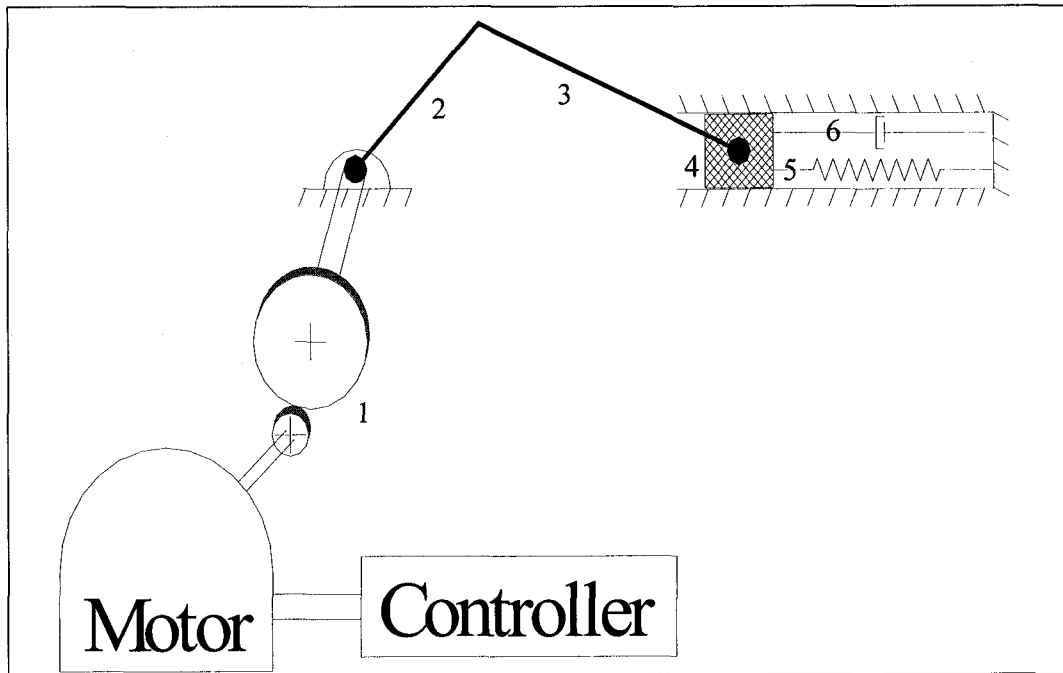


Figure 6.1: Rigid slider-crank mechanism

6.3 System's specifications

The proportional gain (K_p) is 100, while the derivative gain (K_d) is 1.1. The motor specifications are as follows:

K_t : Motor torque constant,	0.0189 N.m/amp.
K_e : Motor back EMF,	0.0189 V.s/rad
R_s : Armature resistance,	1.08 Ω
T_{PK} : Peak torque,	0.2232 N.m
S_{NL} : No load speed,	627.6 rad/s
T_F : Friction torque,	0.0042 N.m

6.3.1 Specifications of the rigid slider-crank mechanism

1. Gears, gear ratio (N) = 6.
2. Crank link.
3. Driven link.

Table 6.1: Links specifications of the rigid slider-crank mechanism

Link #	Length (m)	Mass (Kg)	Moment of inertia (Kg.m ²)
2	0.10	0.062832	$770.66 \times 10^{-6}^*$
3	0.15	0.18850	441.79×10^{-6}

* Moment of inertia of motor's shaft and gears are included in moment of inertia of link 2.

4. Slider.
5. Spring, $k = 37.699 \text{ N/m}$.
6. Dashpot, $c = 0.37699 \text{ Kg/s}$, damping ratio (ζ) = 0.1.

6.4 Results of minimizing dissipated energy

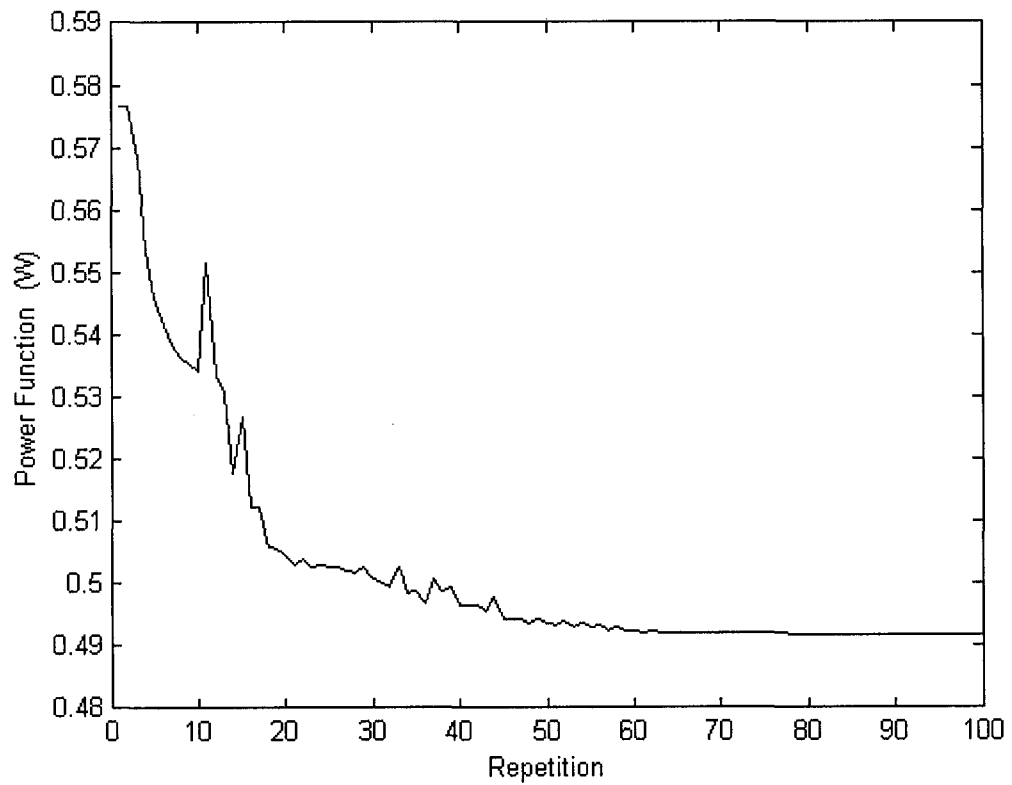


Figure 6.2: Power function versus repetitions using learning control

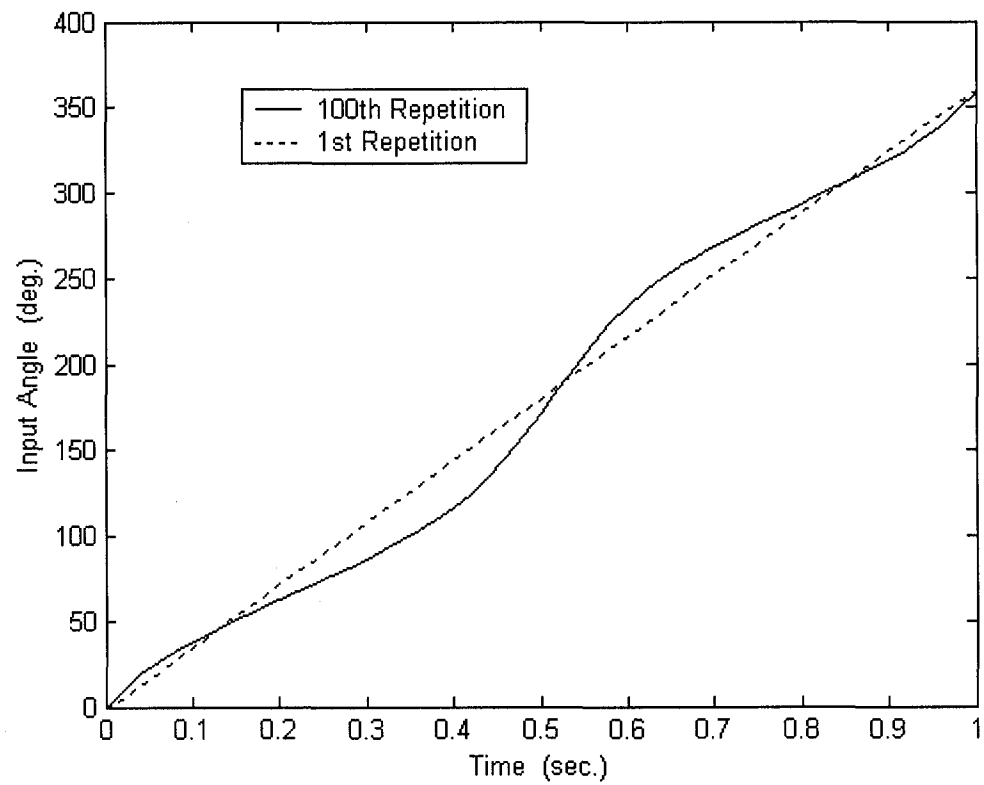


Figure 6.3: Input angle versus time using learning control

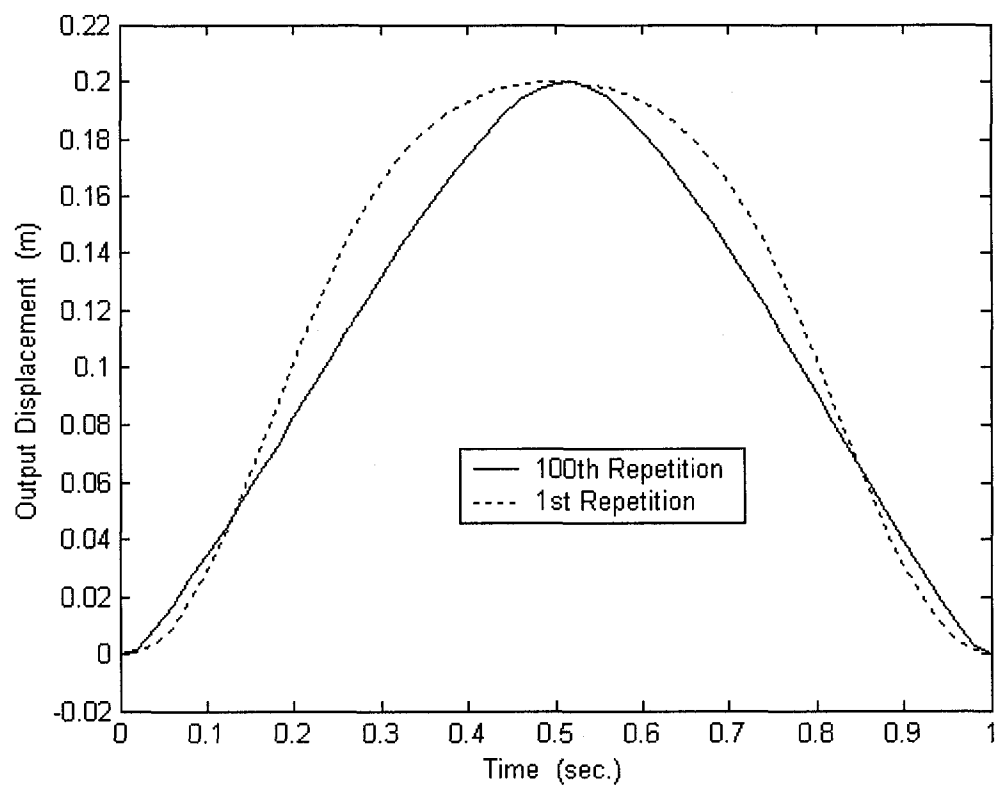


Figure 6.4: Output displacement versus time using learning control

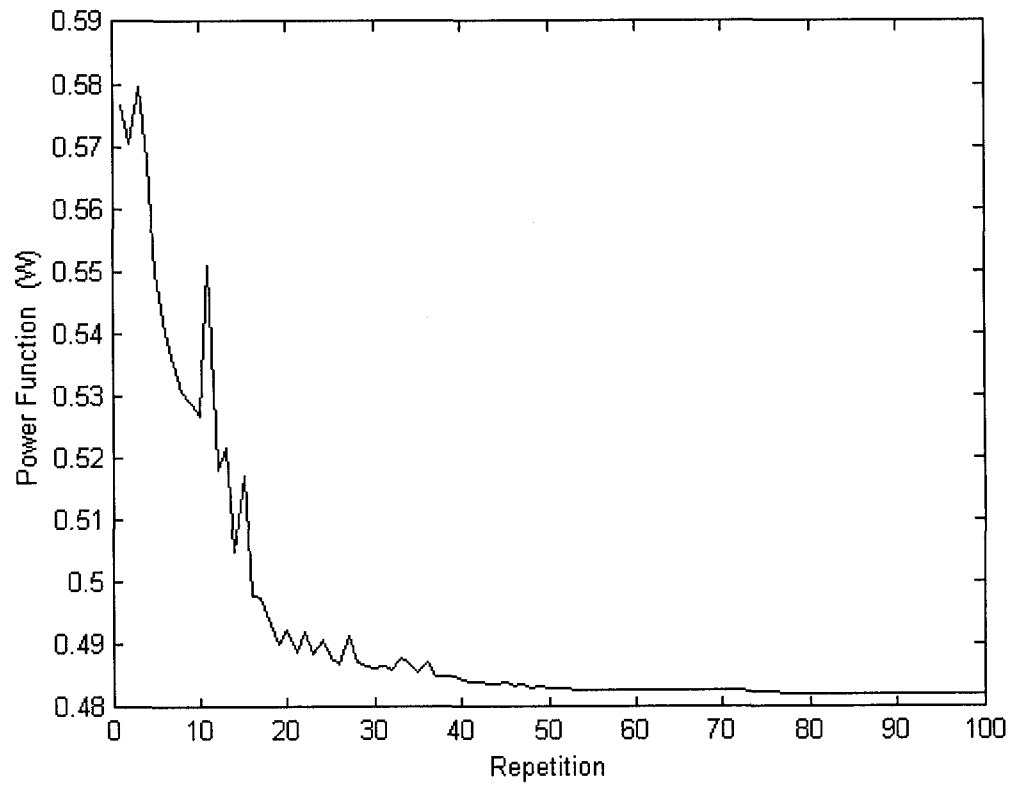


Figure 6.5: Power function versus repetitions using repetitive control

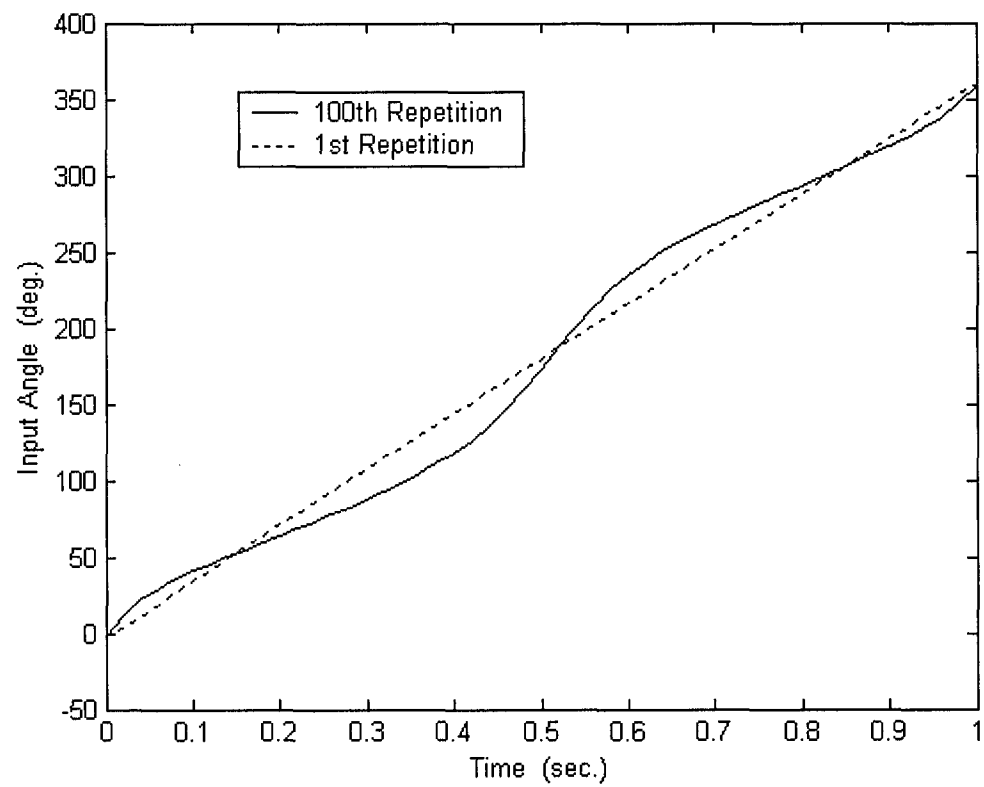


Figure 6.6: Input angle versus time using repetitive control

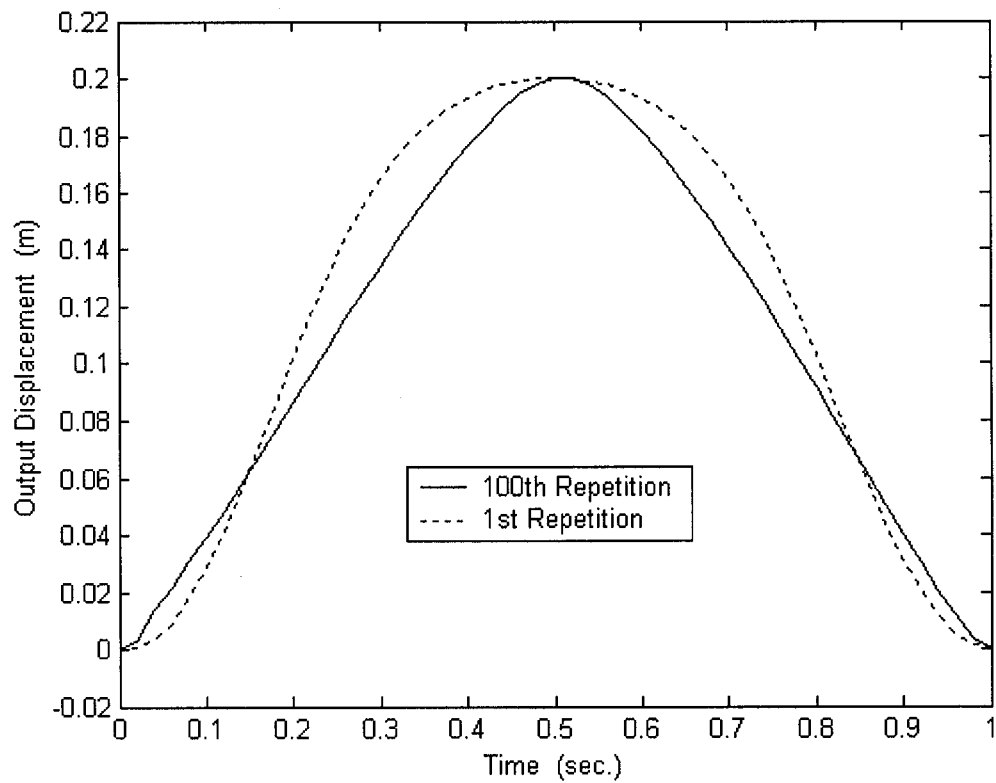


Figure 6.7: Output displacement versus time using repetitive control

6.5 Discussion of results

The plots of the power function for both control methods show that the system was converging to the optimum motion that minimizes the dissipation in energy. The spikes that appear are due to increasing the effort of minimizing the power term. When this term got more effort, the input had more changes that needed to be recognized by the learning process. The total reduction of the power function in both control methods was within 17% of the initial power function. This is because the initial input angles were close enough to the ones desired; therefore, there was no significant improvement in minimizing the power function. The repetitive method had a minimum power function that was 2% less than that for the learning method. This is because the learning method started each cycle with zero velocity, which means it needed to accelerate itself to compensate for the slower speed at the beginning and complete the whole cycle within the limited period time. This small acceleration during motion caused an increase in the damping term in the power function, which subsequently made the learning control method have greater power function than the repetitive control method.

The input angles and output displacements for both control methods were almost the same. The methods modified the input such that it generated nearly constant output velocity in rise and return segments. This minimized the dissipated energy at the dashpot by evenly distributing the dissipation rate along the period time.

Also, because the output velocity was approximately constant, it can be concluded that the dominant term in the power function is the damping.

The higher slope of the input angles around the middle of the cycle, as shown in figures 6.3 and 6.6, indicates an increase in the input speed. The even distribution of the power waste leads to minimum overall waste. Therefore, the system tended to speed up the mechanism at around 180° because at that position the slider has the least output velocity regardless of the input speed, which means least the energy is dissipated through the damper. Thus, the system increased the power lost through the motor to maintain, approximately, a constant rate of energy waste.

Chapter 7

Case 5: Minimizing Input Torque

When the case discussed in chapter 6 was minimizing the dissipated energy in order to somehow minimize the required power, this case directly minimizes the required power by minimizing the input torque to the mechanism. Minimizing input torque to the mechanism is an important factor in minimizing the size of the motor. In many applications, the slider-crank mechanism has to do some monotonous work that is irrelevant to the timing of the output. Within these kinds of applications, minimizing required input torque becomes an important issue in saving energy. Minimizing the total input torque also implies minimizing the torque peak, which accordingly reduces the size of the motor that is used or decreases the number of motors that may be needed in performing heavy-duty jobs. Mostly all the applications that require linkages mechanisms with variable load on the machine consume more power than exactly what they need. Generally, simple systems that contain constant input speed motors without any control unpredictably spend more power in driving machines to overcome some hindrances could be avoided in some way. However, simplicity is not the first priority in designing and constructing machines. Sometimes saving energy is the main concern in building machines. Therefore, minimizing the required input torques becomes the way to save energy consumption.

The objective of this case is to minimize the input torque that is needed to drive the slider-crank mechanism by varying the input speed of the motor. This mechanism carries variable load depending on the position and the velocity of the slider. The system used is exactly the same as that used in the case of minimizing dissipated energy as shown in figure 6.1.

7.1 Applying learning and repetitive control methods

Minimizing the peak torque by the analytical or numerical analysis in dynamic systems is a tricky problem since the exact and real behavior of the system is too hard to be obtained. Usually, the experimental examination of the dynamic systems gives an exact form of the required torque, but not in this case. Therefore, an indirect technique is employed, which minimizes the summation of the input torque at every time steps. This indirect procedure will minimize the peak input torque.

In this case, the torque function demonstrating the system's progression to converge to the optimum solution is,

$$\text{Torque Function} = \sum_{j=1}^p T_j^2$$

where T is the input torque to the mechanism and p is the total number of the time steps. The cost function that is used to determine the optimum input at each repetition can be written as:

$$J = \frac{1}{2} q T_{i+1}^T T_{i+1} + \frac{1}{2} s \delta U_{i+1}^T \delta U_{i+1}$$

$$T_{i+1} = \underline{A} x_{i+1}(0) + \underline{B} U_{i+1}$$

where q is the weight of minimizing the input torque, and s is the weight of minimizing the changes of the input during optimizing process. It is found that the input torque is extremely sensitive to the changes in the input. Any small changes in the input speed lead to large changes in the input torque. Moreover, in some middle repetitions the torque shows some fluctuations that are hard to be learned promptly in order to perform the proper adjustments to the input speed. Therefore, a new term representing the time derivative of the input torque is introduced to the cost function to make the whole learning and optimizing processes much more efficient. The modified cost function becomes,

$$J = \frac{1}{2} q_1 T_{i+1}^T T_{i+1} + \frac{1}{2} q_2 \dot{T}_{i+1}^T \dot{T}_{i+1} + \frac{1}{2} s \delta U_{i+1}^T \delta U_{i+1}$$

$$\dot{T}_{i+1} = \underline{D} T_{i+1}$$

$$\underline{D} = \frac{1}{\Delta t} \begin{bmatrix} -1.5 & 2 & -0.5 & 0 & 0 & \dots & 0 & 0 \\ 0 & -0.5 & 0 & 0.5 & 0 & 0 & \dots & 0 \\ 0 & 0 & -0.5 & 0 & 0.5 & 0 & \dots & 0 \\ \vdots & & & \ddots & \ddots & & & \vdots \\ 0 & \dots & 0 & -0.5 & 0 & 0.5 & 0 & 0 \\ 0 & \dots & 0 & 0 & -0.5 & 0 & 0.5 & 0 \\ 0 & 0 & \dots & 0 & 0 & 0.5 & -2 & 1.5 \end{bmatrix}$$

and the modified input angles become:

$$\delta U_{i+1} = - \left(q_1 \underline{B}_i^T \underline{B}_i + q_2 \underline{B}_i^T \underline{M} \underline{B}_i + s \underline{I} \right)^{-1} \left(q_1 \underline{B}_i^T + q_2 \underline{B}_i^T \underline{M} \right) (\underline{T}_i + \underline{A}_i (\underline{x}_{i+1}(0) - \underline{x}_i(0)))$$

where \underline{I} is the identity matrix. The torque time derivative term that is introduced to the cost function provides the system with smooth input torque that is able to be tracked and learned very easily. This added term stops the fluctuation in the torque that will appear in the absence of this term. The s weighting factor is set to be one all the time, where q_1 and q_2 start very small and then are increased by multiplying

them by 5 every 50 repetitions. The ratio $\frac{q_2}{q_1}$ is constant all the time and equal to

0.01. In order to avoid the trivial stationary solution that leads to zero input torque, an end condition is set unchanged and equal to 360° to ensure that the mechanism will make complete revolutions and will not stop. Therefore, the weight s that

corresponds to the final point is set too high and remains unchanged during the optimizing process.

7.2 Results of minimizing input torque

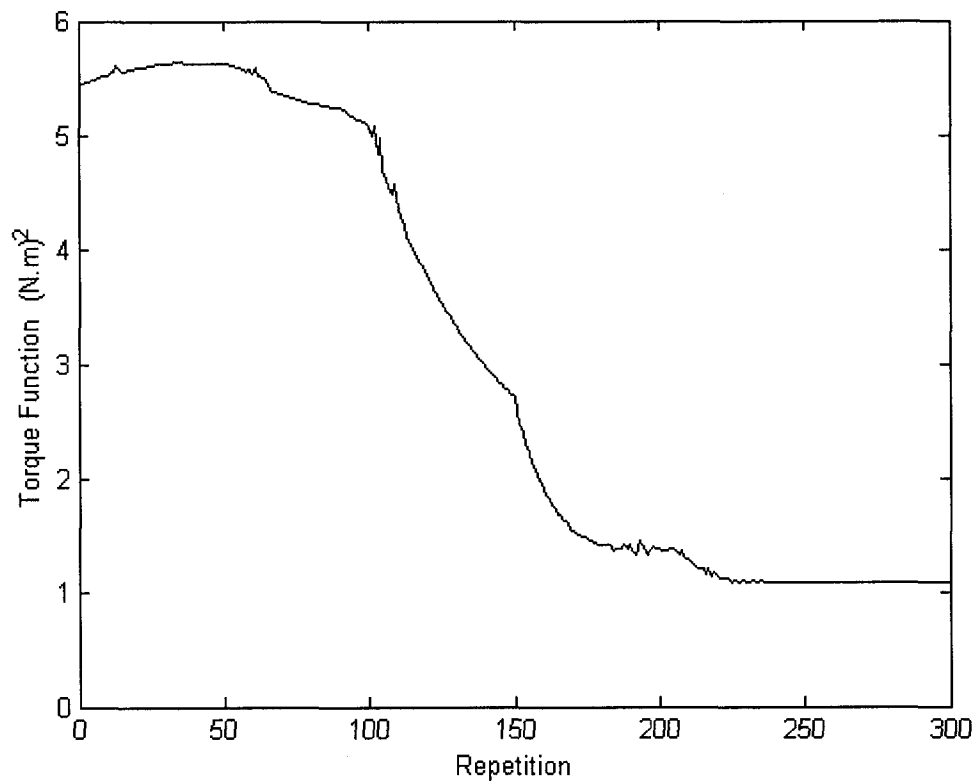


Figure 7.1: Torque function versus repetitions using learning control

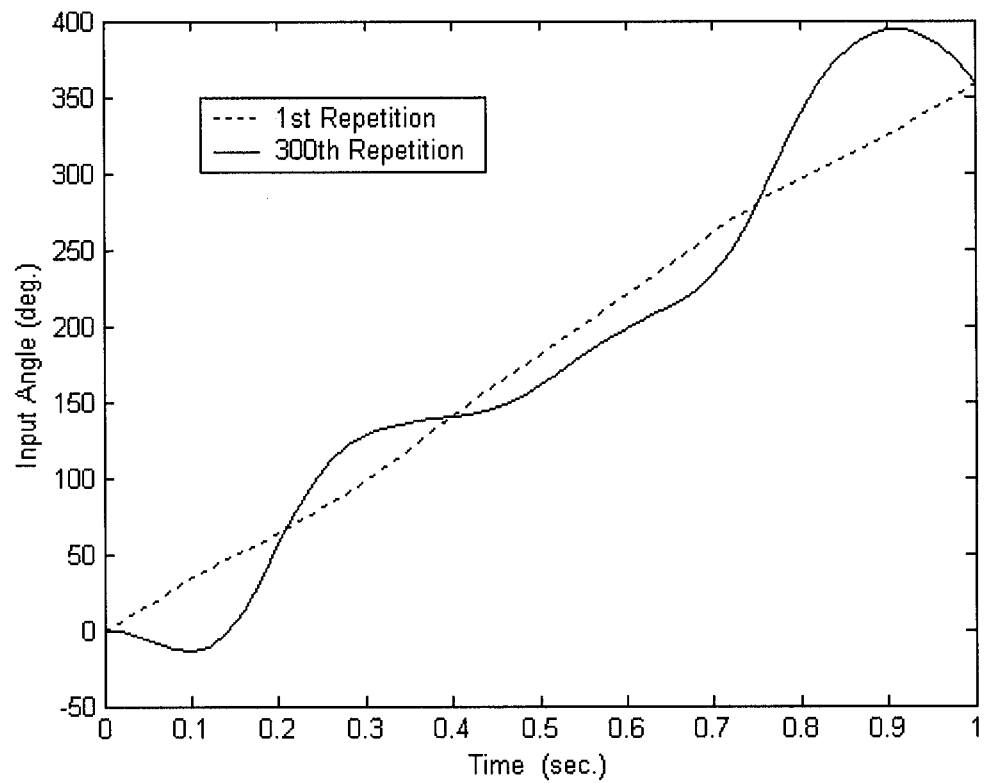


Figure 7.2: Input angles versus time using learning control

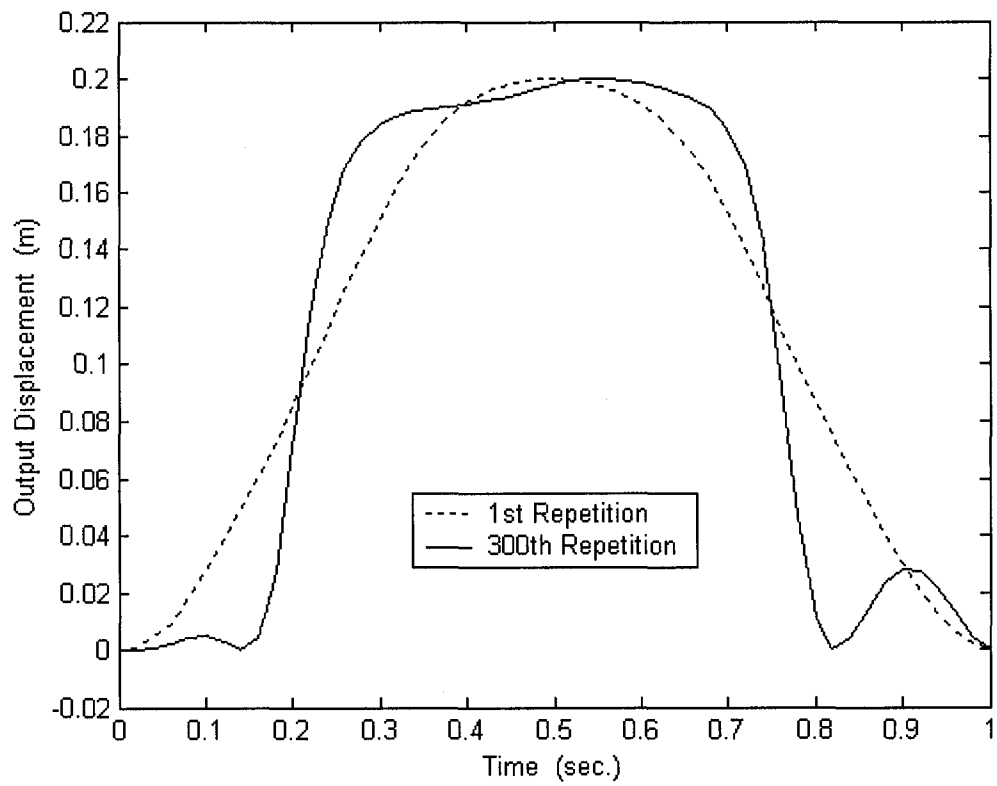


Figure 7.3: Output displacement versus time using learning control

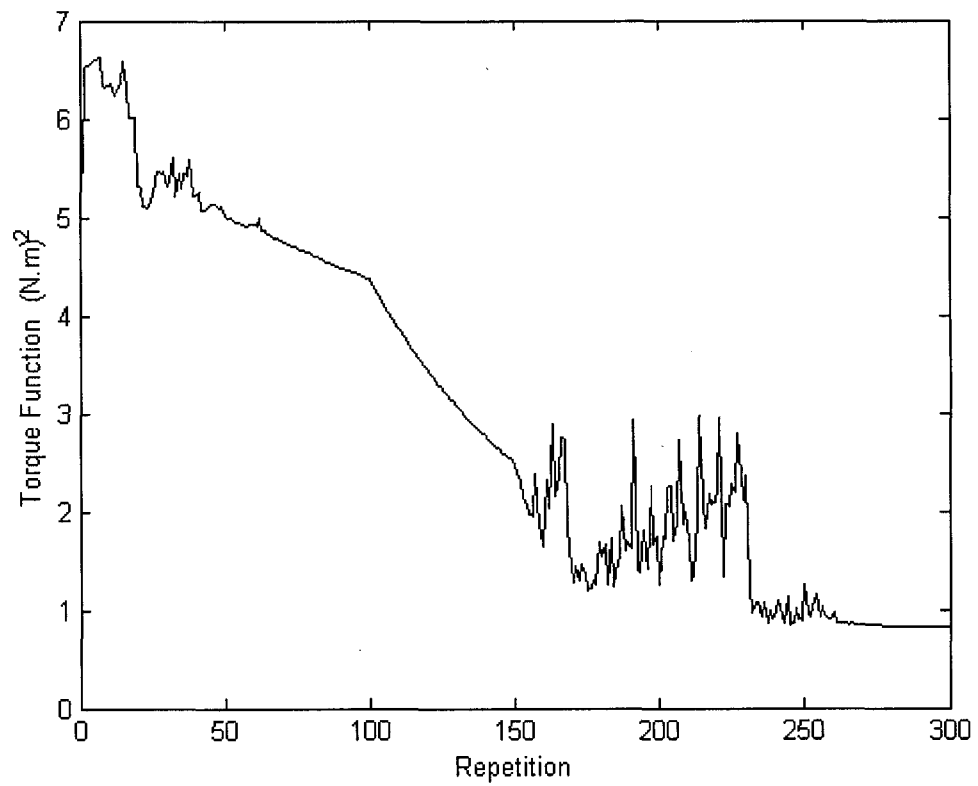


Figure 7.4: Torque function versus repetitions using repetitive control

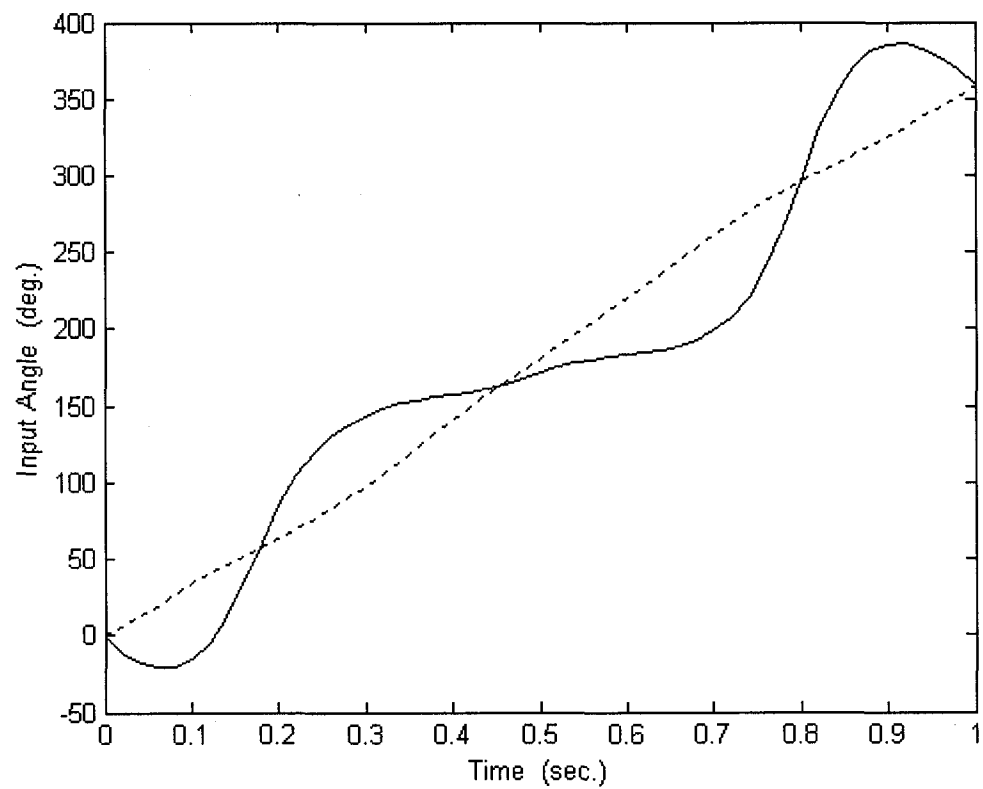


Figure 7.5: Input angles versus time using repetitive control

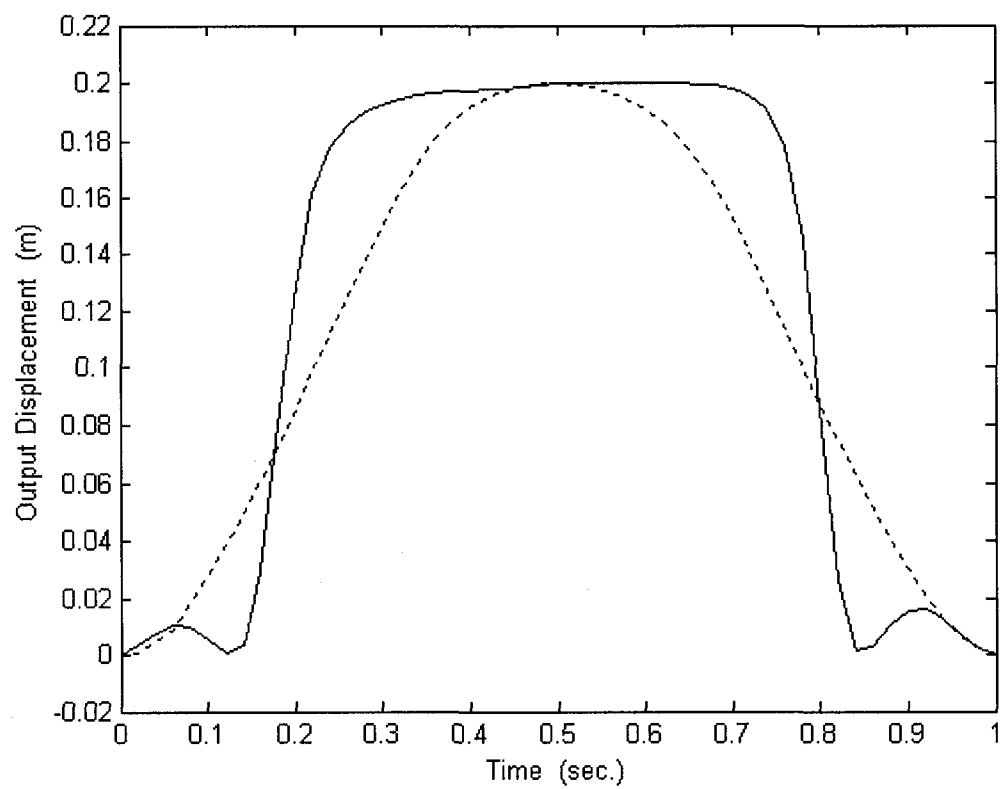


Figure 7.6: Output displacement versus time using repetitive control

7.3 Discussion of results

In minimizing input torque, both control methods required more than two hundred repetitions to achieve the preferred input. The learning control method has much faster and smoother progression in minimizing input torque. Although both control methods had the same minimizing weights and procedures, the difference in the convergence progression is caused by the continuity of the system's motion. In this case, the starting initial conditions had a significant effect on the learning process, which was an essential part in converging the system to the desired motion. In addition, the shape of the input angles and the output displacement emphasized how the initial conditions affected the system convergence. Starting from the same initial conditions made the learning process more efficient in the case of the learning control method since it was depending on the input angles only, whereas the repetitive control method was depending on the input angles and the changeable initial conditions.

As expected, the repetitive control method had a steady torque function lower than that for the learning control method because the latter method had to stop and restart the system at every new cycle, which required more torque to start up the system. On the other hand, the continuous motion in the case of the repetitive control made the system conserve some of its energy for the next repetitions. In other words, when the learning control method started each cycle with zero initial conditions, which is zero kinetic and potential energies, the repetitive control

method was starting each cycle with some positive mechanical energy that was used in driving the system for the next repetitions.

The torque function in both control methods shows somewhat of smooth elbows at the 50th, 100th, 150th and 200th repetitions due to the change of the minimizing weights at these repetitions. These changes in the weights forced the system to make more changes in the input to trim down the torque function.

Figure 7.4 shows some spikes in the torque function between the 150th and 250th repetitions because the system was struggling in identifying and recognizing the new changes in the input angles. It seems that this specific change in the minimizing weights was just high enough and needed many repetitions to bring the system to the regular convergence. Conversely, reducing these changes could make the system take more time to reach the optimum solution. Regardless, this high increment was acceptable since the system did not show very large jumps in the torque function and it was still much lower than its initial value.

Although the system started from very small minimizing weights in the case of repetitive method, the torque function increased for the first twenty repetitions. This was because the control methods were doing the required modifications knowing little about the system's behavior and nothing could be done to prevent the jumps that occurred after the first repetition. Also, the system could not be

started with zero weights to avoid these jumps because the control methods needed to learn the system's behavior for different inputs, even if these inputs had small differences. Otherwise, the control methods would have learned accurately about the system's behavior but for the single and unchanged input, which also produces jumps once the control methods start changing the input.

The plots of the input angles show surprising results for both control methods. The mechanism started each repetition by going backward and then changed direction to move forward. This occurred to store some energy in the spring and retrieve it when it moved forward. This stored energy gives more power to the system to move forward with minimum required torque. Moreover, this back and forth movement was done to minimize the required torque when the driving crank becomes vertical.

The output displacement plots show two jumps at the beginning and the end of the cycle due to the change of the direction of the input speed, which made the slider go forward and backward. The partly flat region in the middle of the output displacement plot indicated slow velocity of the slider when it came to the crank dead-center position. The system did a smart trick at around 180° where the spring had the maximum pulling force. The mechanism minimized the total required input torque to overcome the forces of the spring and the dashpot by slowing down

the input speed to minimize the effect of the dashpot, since the spring force was the maximum at that position and nothing could be done to reduce it.

The little increase in the slope of the output displacement just after the middle point denoted an increase in the output velocity. This was due to an increase in the angular velocity of the mechanism just after 180° because the slider had just reversed its motion to coincide with the forces of the flexible elements. At that position, the pulling forces against the motion became pulling forces in the direction of the motion, which subsequently increased the output velocity instantaneously.

Chapter 8

Case 6: Flexible Six-Bar Mechanism Used in Scanning Machine

Up to this point, a thorough investigation was done of the learning and repetitive control methods in controlling a slider-crank mechanism. All previous cases are considered as introductory cases to the real applications of using learning and repetitive control methods. In this case, these control methods are used in controlling a six-bar mechanism for scanning purposes.

Scanning machines are mostly used with computers and printers since their applications have become more important lately. Although the scanning machines belong to the electrical appliances and they work with digital equipment, the mechanical function is an essential part in their performance. As the mechanical components work efficiently, the whole performance of the scanning machine becomes more efficient. Certainly, its motion depends on some connected links forming a mechanism that regulates the whole motion of the machine. The main characteristic of this operating mechanism is that it produces a constant output velocity in order to make the scanning process applicable. Otherwise, the scanning tip that is carried by the mechanism would not identify the letters or colors that are in the scanned document. Therefore, maintaining constant velocity of the scanning head is the first priority in synthesizing scanning machines.

Controlling scanning machines by a simple controller is an advantageous technique. But with taking into account the random vibrations and the flexibility of all components of the machine, the simple control will not satisfy the requirement of getting a precise constant velocity. Thus, using advanced and effective techniques, such as learning and repetitive control methods in order to attain the desired accuracy, is only the way. As shown in the previous chapters, these methods proved their outstanding performance when they are used for controlling linkages mechanisms.

8.1 Constant input speed scanning machine

In 1991, Hodges and Pisano published a technical paper on the synthesis of planar straight line constant velocity scanning mechanisms. It was dedicated to the study of using a rigid six-bar Stephenson mechanism in scanning machines as shown in figure 8.1.

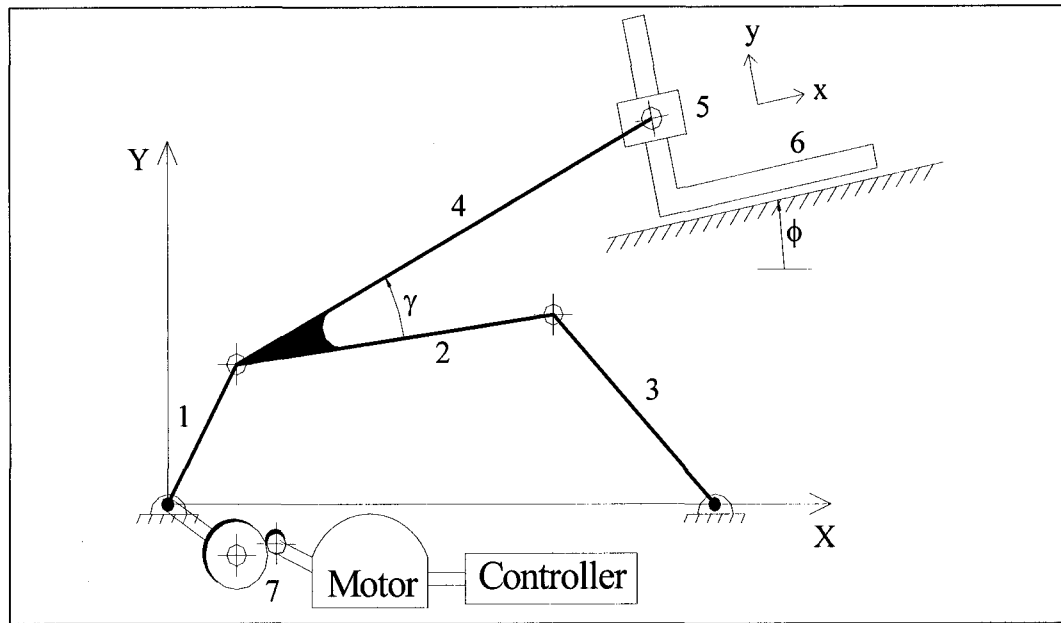


Figure 8.1: Six-bar Stephenson mechanism

Although this mechanism has six links, it belongs to the four-bar mechanisms. According to the Grashof condition, it is a crank-rocker mechanism, in which the input link is the shortest and it completes full rotations, while other links pivoted to the ground in an oscillating motion. The constant input speed of the driving link provides the driven links with a swinging motion, making links 2 and 3 oscillate, which subsequently makes the slider go in a reciprocating motion on any arbitrary plane.

Hodges and Pisano showed kinematically that with constant input speed to the mechanism, a constant output velocity could be obtained from the slider that is attached to the mechanism. After a grid search of various combinations of lengths

and angles, they ended up with the best dimensions of the mechanism. The final kinematics results showed that the mechanism could provide some constant output velocity for a scan fraction equal to 0.505, which is about 182° of the input angles, and a velocity error within 4% of the normalized output velocity as shown in figure 8.2. The upper plot shows the normalized output velocity versus input angles where the flat region indicates the constant output velocity for the slider from 68° to 250° . The lower plot shows the constant output velocity region, where the flat region in the upper plot is magnified and the fluctuation in the output velocity becomes clearer. As shown in this figure, even the kinematics results, which are a preliminary investigation, show that it is impossible to get an exact constant output velocity, and definitely, a margin of error has to be considered.

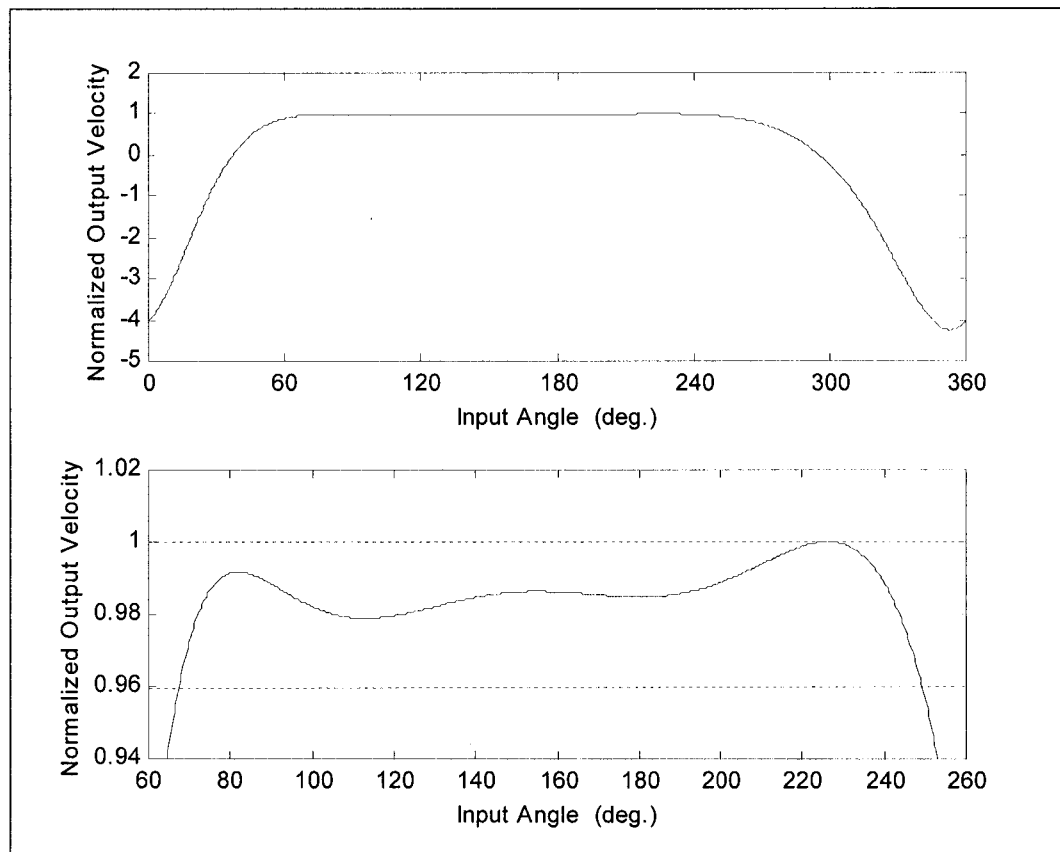


Figure 8.2: Normalized output velocity versus input angle

Therefore, the objective of this case is to prove that using learning and repetitive control methods in controlling this mechanism gives much more better results in producing constant output velocity in both kinematics and dynamics analyses with taking into account the flexibility of the links.

8.2 Applying learning and repetitive control methods

As discussed in previous chapters, the learning and repetitive control methods learn and optimize the input speed of the mechanism to minimize the velocity error as

much as possible. Since this mechanism is already synthesized for producing constant output velocity with constant input speed, the control methods make a little change in the input speed to attain the desired output and reduce the velocity error.

The control scheme is exactly the same as that employed in the previous cases as shown in figure 3.1. The learning and repetitive control methods that are used in this case follow the same procedure employed in chapter four in the case of constant output velocity. Generally, the learning process relates the input angles of the mechanism to the horizontal output velocity of the slider that is moving in the tilted plane as shown in figure 8.1. Therefore, the horizontal output velocity of the slider is the function needed to be learned; and it is described as,

$$\dot{Y}_i = \underline{A}_i x_i(0) + \underline{B}_i U_i$$

where \dot{Y} is the output velocity vector, A and B are the parameter matrices, x is the initial conditions vector, and U is the input angles vector, all at the i^{th} repetition. The above equation, which is used for the repetitive method, is the general case where the initial conditions are changeable.

Producing constant output velocity in a fraction of the motion's cycle requires setting the weighting matrix Q_1 as zero matrix, except those elements that correspond to the designated points that belong to the constant output velocity region. Also, the desired output vector has to be equal to the desired output velocity. The modifications of the input angles that refer to the zero elements in matrix Q_1 are irrelevant to both the output displacement and the output velocity at these points. The input angles related to the zero elements in matrix Q_1 , which correspond to the points outside the constant output velocity region, can be modified according to any preferred criterion. In this case, those exterior points are modified so that they minimize the input angular acceleration in order to smooth the input speed of the mechanism. Moreover, this modifying process makes the output motion smoother at the unconcerned regions to prepare the system to have constant output velocity at the concerned region.

In order to bring the output motion to the desired motion, the cost function that needs to be minimized must be formed specifically to ensure that it will compel the actual output velocity to converge to the desired output velocity. Otherwise, the system will not converge properly to the desired motion and some fluctuations in the output velocity will appear, making the output velocity unstable. Therefore, the cost function that needs to be minimized is

$$J = \frac{1}{2} \mathbf{e}_{i+1}^T \underline{\mathbf{Q}}_1 \mathbf{e}_{i+1} + \frac{1}{2} (\underline{\mathbf{D}} \mathbf{U}_{i+1})^T \underline{\mathbf{Q}}_2 (\underline{\mathbf{D}} \mathbf{U}_{i+1}) + \frac{1}{2} s \delta \mathbf{U}_{i+1}^T \delta \mathbf{U}_{i+1}$$

$$J = \frac{1}{2} \mathbf{e}_{i+1}^T \underline{\mathbf{Q}}_1 \mathbf{e}_{i+1} + \frac{1}{2} (\underline{\mathbf{D}} \mathbf{U}_i + \underline{\mathbf{D}} \delta \mathbf{U}_{i+1})^T \underline{\mathbf{Q}}_2 (\underline{\mathbf{D}} \mathbf{U}_i + \underline{\mathbf{D}} \delta \mathbf{U}_{i+1}) + \frac{1}{2} s \delta \mathbf{U}_{i+1}^T \delta \mathbf{U}_{i+1}$$

$$\mathbf{e}_{i+1} = \mathbf{V}^* - \dot{\mathbf{Y}}_i - \underline{\mathbf{A}}_i (\mathbf{x}_{i+1}(0) - \mathbf{x}_i(0)) - \underline{\mathbf{B}}_i \delta \mathbf{U}_{i+1}$$

$$\underline{\mathbf{Q}}_2 = q_2 \mathbf{I}$$

$$\underline{\mathbf{D}} = \frac{1}{\Delta^2 t} \begin{bmatrix} 1 & -2 & 1 & 0 & 0 & \dots & 0 & 0 \\ 0 & 1 & -2 & 1 & 0 & 0 & \dots & 0 \\ 0 & 0 & 1 & -2 & 1 & 0 & \dots & 0 \\ \vdots & & & \ddots & \ddots & & & \vdots \\ 0 & \dots & 0 & 1 & -2 & 1 & 0 & 0 \\ 0 & \dots & 0 & 0 & 1 & -2 & 1 & 0 \\ 0 & 0 & \dots & 0 & 0 & 1 & -2 & 1 \end{bmatrix}$$

where s is the weight of minimizing the changes in the input angles, \mathbf{I} is the identity matrix, $\delta \mathbf{U}$ is the difference in the input angles between any two consecutive repetitions, and \mathbf{V}^* is the desired constant output velocity. Performing the necessary work in minimizing this cost function results in,

$$U_{i+1} = U_i + \delta U_{i+1}$$

$$\delta U_{i+1} = (\underline{B}_i^T \underline{Q}_1 \underline{B}_i + \underline{M} + s \underline{I})^{-1} H$$

$$H = \underline{B}_i^T \underline{Q}_1 \left[\underline{V}^* - \dot{\underline{Y}}_i - \underline{A}_i (\underline{x}_{i+1}(0) - \underline{x}_i(0)) \right] - \underline{M} U_i$$

$$\underline{M} = \underline{D}^T \underline{Q}_2 \underline{D}$$

The weight s is set to be equal to 1 all the time, q_2 is constant and equal to 10^{-6} , and the weight of Q_1 for the non-zero elements is set initially 0.01 and is increased by 2 every ten repetitions. The percentage error that shows the convergence progression is defined as,

$$e = 100 \left| \frac{\underline{V}^* - \dot{\underline{Y}}_j}{\underline{V}^*} \right|_{\max} \% \quad , \quad p_1 \leq j \leq p_2$$

where p_1 and p_2 are the start and end points respectively of the constant output velocity region. In this case, the desired output velocity is 0.6 m/s, starting at 0.2 sec and ending at 0.66 sec. The desired output velocity is determined carefully to keep some stable angular velocity of the mechanism. In addition, this constant velocity has to cover the scanned page, which is 27 cm in length, in that period of time. Selecting higher or lower desired output velocity will speed up or lower the

angular velocity of the mechanism during the concerned region of desired output velocity, which leads to more vibrations of the whole system. Moreover, it is important to have transient regions before and after the concerned region. These transient regions are used to prepare the system to move into or out of the constant output velocity region. The transient regions used in this case are very short because these kinds of applications do not allow for big margins for practical reasons, and because the entire period of the mechanism is short as well. Therefore, the transient regions are considered a one-fourth time step, which is 0.005 sec.

Selecting the number of time steps is governed by the frequency of the system. According to Nyquist frequency, the sampling points have to be at least two times the maximum frequency of the system to make sure that aliasing is excluded. Therefore, in order to determine the maximum frequency of the vibrated links, an exact formula is used to determine the natural frequency of links 2 and 4. However, since the crank link is attached to the whole mechanism, this directly affects the frequency of this link. Therefore, in order to determine the natural frequency of the crank link properly, it is assumed that the crank link carries a mass at the pinned end, which represents the effect of the motion of the other links on the crank link. The determination of this mass is performed by employing the energy method, where the kinetic energy of the assumed mass is equivalent to the total kinetic energy of the mechanism excluding the crank link.

The analytical formulas of determining the natural frequency of the links 1, 2 and 4 are

$$f_1 = \frac{1}{2\pi} \sqrt{\frac{3E_1 I_1}{R_1^3 (M_1 + 0.23m_1)}}$$

$$f_2 = \frac{1}{2\pi} \sqrt{\frac{96E_2 I_2}{R_2^3 m_2}}$$

$$f_4 = \frac{1}{2\pi} \sqrt{\frac{3E_4 I_4}{R_4^3 (M_5 + 0.23m_4)}}$$

where f in Hz, E is the modulus of elasticity, I is the moment of inertia of the cross sectional area, R is the link's length, m is the mass of the link, and M is the mass attached to the link. Observe that M_1 needs to be calculated from the system's total kinetic energy, while M_5 is already involved in the system.

Applying the numbers in the above formulas shows that the natural frequencies of links 2 and 4 are 152.6 Hz and 18.70 Hz respectively. Since the natural frequency of the crank link is determined from the real performance of the system, it cannot be determined exactly before running the system. However, an approximate computation based on the constant speed of the mechanism showed that f_1 is smaller than f_2 . Thus, f_2 is considered as the maximum natural frequency of the system. The exact calculations of f_1 at the end of simulating the system show that

the natural frequency of the crank link is between 12.246 and 76.371 Hz. This variation of the natural frequency of that link occurs because the kinetic energy, which dominates the natural frequency, varies during motion.

Although the Nyquist frequency requires two times the maximum frequency, the number of time steps is set at 800, which is more than five times the maximum frequency to make sure that aliasing is totally avoided.

8.3 System's model

In this case, the system does not contain any individual vibrational elements. The flexibility of the system is embedded in the elastic links that are able to be bent and that vibrate during motion. The whole mechanism is made of some plastic material, which makes the links more flexible. Constructing this mechanism from a plastic material is one of the great improvements of using learning and repetitive control methods since control methods take into account the vibrations and bending of the links in the learning process of the system's behavior.

In order to analyze the system during motion, few assumptions are made to simplify the complexity of this flexible mechanism. The driven link, which is link number 3 in figure 8.1, is assumed rigid and unable to be bent during motion because it does not carry any external load and does not directly affect the output motion of the slider. All other links are assumed flexible and bendable due to the

bending moments that they may carry during action. They are considered as continuous cantilevers that vibrate laterally in the plane of motion. The method of assumed mode shapes is used in analyzing and simulating these flexible links during motion. Only the first mode of vibration is considered because this first mode has the dominant magnitude among higher mode shapes. The pre-investigation of a simple vibrated cantilever showed that the normalized magnitude of the first mode was greater than 85% of the entire magnitude of vibration. Therefore, taking into account only the first mode guarantees a high level of accuracy.

With reference to figure 8.1, the mode shapes of links 1 and 4 are the same since they have the same boundary conditions, which are assumed to be clamped-free cantilevers. The driving link is clamped to the motor shaft and free at the other end, while link 4 is clamped to the coupler with a fixed angle γ and free at the other end. However, the coupler is connected to two links; therefore, it is assumed to be pinned-pinned cantilever. The three mode shapes are in the form:

$$\Psi_1(x) = \sin(\omega_1 x) - \sinh(\omega_1 x) - \left\{ \frac{\sin(\omega_1) + \sinh(\omega_1)}{\cos(\omega_1) + \cosh(\omega_1)} \right\} \{ \cos(\omega_1 x) - \cosh(\omega_1 x) \}$$

$$\Psi_2(x) = \sin(\omega_2 x)$$

$$\Psi_4(x) = \sin(\omega_4 x) - \sinh(\omega_4 x) - \left\{ \frac{\sin(\omega_4) + \sinh(\omega_4)}{\cos(\omega_4) + \cosh(\omega_4)} \right\} \{ \cos(\omega_4 x) - \cosh(\omega_4 x) \}$$

$$\omega_1 = \frac{1.875104}{R_1}, \omega_2 = \frac{\pi}{R_2}, \omega_4 = \frac{1.875104}{R_4}$$

and the deflections of the links are in form:

$$y_i = \Psi_i(x) q_i(t), \quad i=1,2,4$$

where q is the magnitude function or the time-dependent coordinate.

Lagrange's equations are used in deriving the governing equations of the system. Describing the kinetic and potential energy of the system is the essential part in deriving the governing equations. The total energy of the system is found by summing up the individual total energies of all links and parts. Observe that the potential energy due to gravity is disregarded because the whole motion is assumed in the horizontal plane. Therefore, the potential energy is only the internal energy in the flexible links due to bending. Determining the total energy of the flexible links is done by integrating the kinetic energy and potential energy terms along the link's length, while the energies of the rigid parts are determined by definite terms. The complete detailed derivation of the governing equations is provided in appendix D.

Although the main objective of this case is to use the control methods in operating the scanning machine, examining the strength of the mechanism during action is the most important issue in synthesizing the scanning machine. Otherwise, the whole machine may fail and collapse during motion due to exceeding the allowable stresses on the system's parts. Therefore, it is important to determine the safety factor of this mechanism to make sure that this machine is operating safely. The most suitable theory that can be applied in determining the safety factor is the strain-energy theory. The safety factor can be predicted by comparing the strain-energy stored in the flexible links with the maximum allowable strain-energy corresponding to the yielding strength. The strain-energy per unit volume is defined as

$$U_s = \frac{\sigma^2}{2E}$$

and also it can be expressed as

$$U_s = \frac{EI}{2AR} \int_0^R y''^2 dx = \frac{EIq^2}{2AR} \int_0^R \Psi''^2 dx$$

therefore,

$$\sigma = Eq \sqrt{\frac{I}{AR} \int_0^R \Psi''^2 dx}$$

$$n = \frac{S_y}{\sigma} = \frac{S_y}{Eq_{\max} \sqrt{\frac{I}{AR} \int_0^R \Psi''^2 dx}}$$

where n is the safety factor, S_y is the yield strength, q_{\max} is the maximum absolute magnitude function, A is the cross sectional area, and R is the link's length. As a result, the minimum safety factor of this machine used in both control methods is 5.5, which means it will not fail during motion.

8.3.1 Specifications of the system

The mechanism's links are made of CARILON® Thermoplastic Polymer DP R1000. It has applications in the appliance, automotive, electrical, and other industries due to its balance of stiffness, toughness, chemical resistance, and easy processing. Table 8.1 shows some properties of this material.

Table 8.1: Physical and mechanical properties of
CARILON® Thermoplastic Polymer DP R1000

Density	1240 Kg/m ³
Yield tensile strength	64 MPa
Modulus of elasticity	2 GPa

A PD controller was used to control the motor. The proportional gain (K_p) is 30000, while the derivative gain (K_d) is 10. The motor specifications are as follows:

K_t : Motor torque constant,	0.74 N.m/amp.
K_e : Motor back EMF,	0.74 V.s/rad
R_s : Armature resistance,	0.5 Ω
T_{PK} : Peak torque,	24.0 N.m
S_{NL} : No load speed,	628.3 rad/s

With reference to figure 8.1, the mechanism components and specifications are:

1. Crank link.
2. Coupler link.
3. Driven link.
4. Driven dyad.
5. Connecting slider, $m_5 = 0.5097$ Kg
6. Output slider, $m_6 = 0.5606$ Kg

7. Gears,

gear ratio (N) = 20.

Table 8.2: Links specifications of the flexible six-bar Stephenson mechanism

Link #	Length (m)	Cross sectional area (mm ²)	Mass (Kg)	Area moment of inertia (m ⁴)
1	0.1424	706.9	0.1248	0.1590×10^{-6}
2	0.5696	1964	1.387	1.227×10^{-6}
3	0.6408	78.54	0.06241	$8.542 \times 10^{-3*}$ (Kg.m ²)
4	1.068	3849	5.097	4.714×10^{-6}

* Moment of inertia of link 3 is the mass moment of inertia around the pivoted end.

The ground link is 0.356 m, which is the distance between the two pivots of links 1 and 3. The internal damping ratio (ζ) of the flexible links is assumed to be 0.1. Angles γ and ϕ are 340° and 240° , respectively. The mass moment of inertia of the motor's shaft and the smaller gear (I_m) is 560.6×10^{-6} Kg.m², while it is for the bigger gear (I_G) is 18.65×10^{-3} Kg.m². The mechanism's average input speed is 60 rpm.

8.4 Results of the six-bar scanning machine

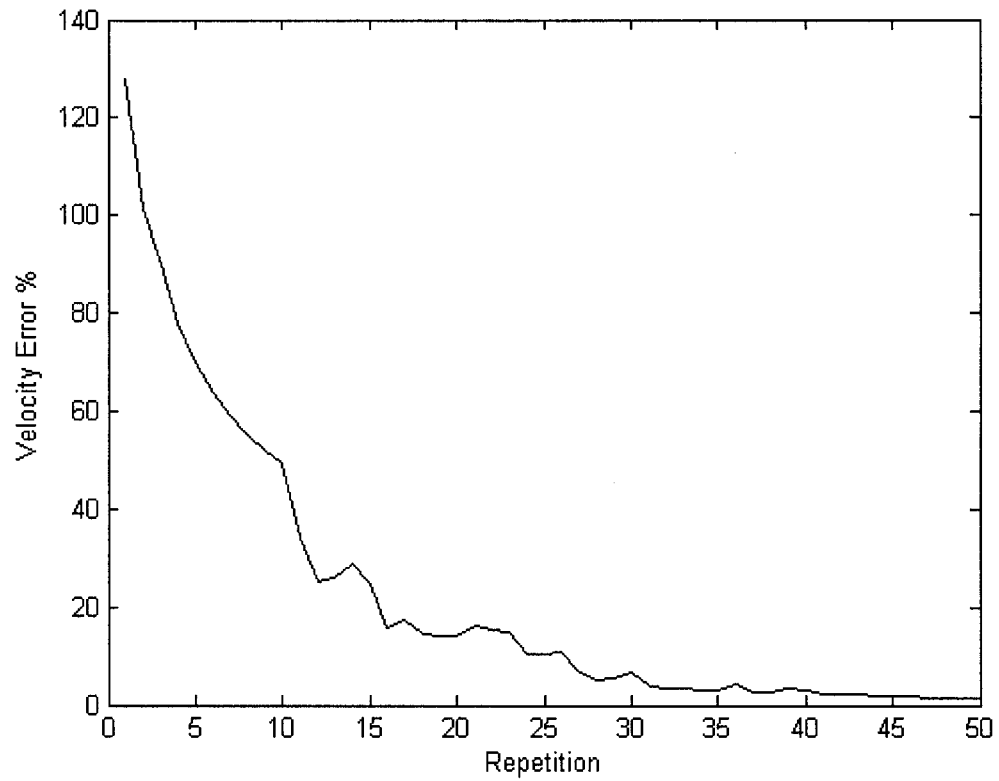


Figure 8.3: Velocity error versus repetitions using learning control

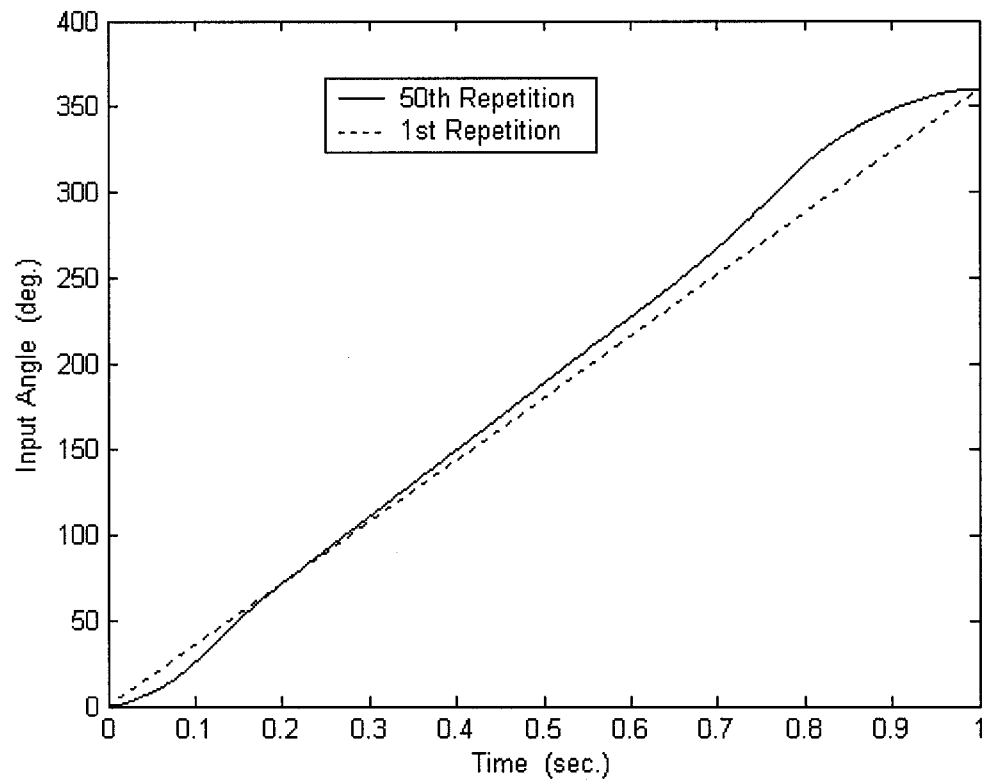


Figure 8.4: Input angles versus time using learning control

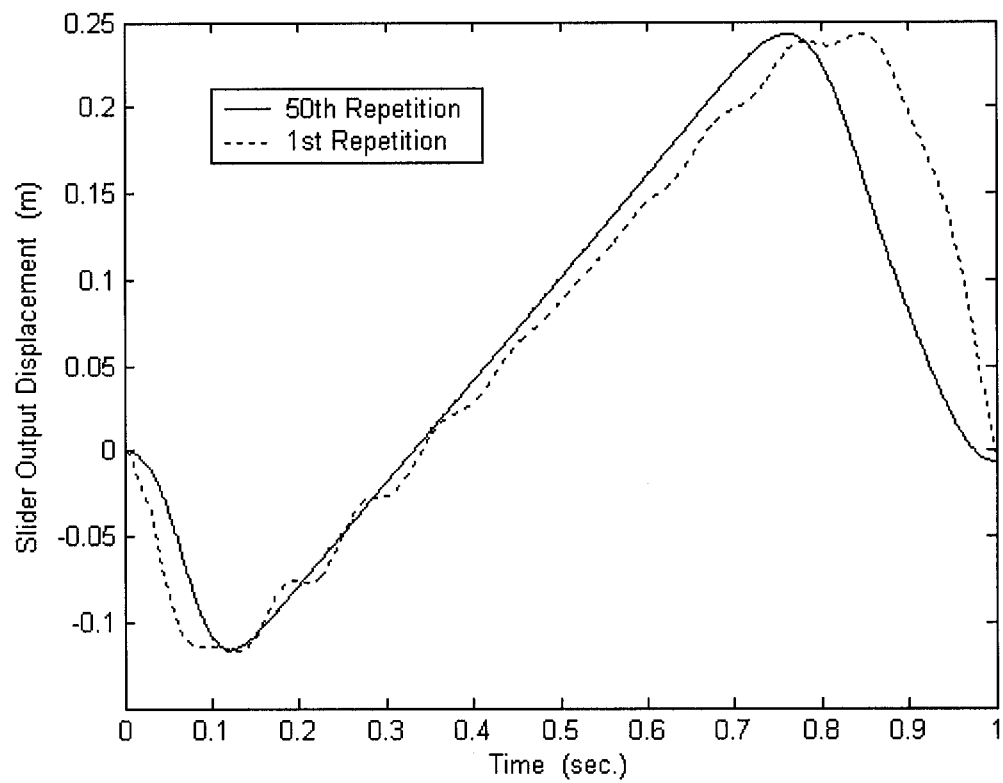


Figure 8.5: Output displacement of the slider versus time using learning control

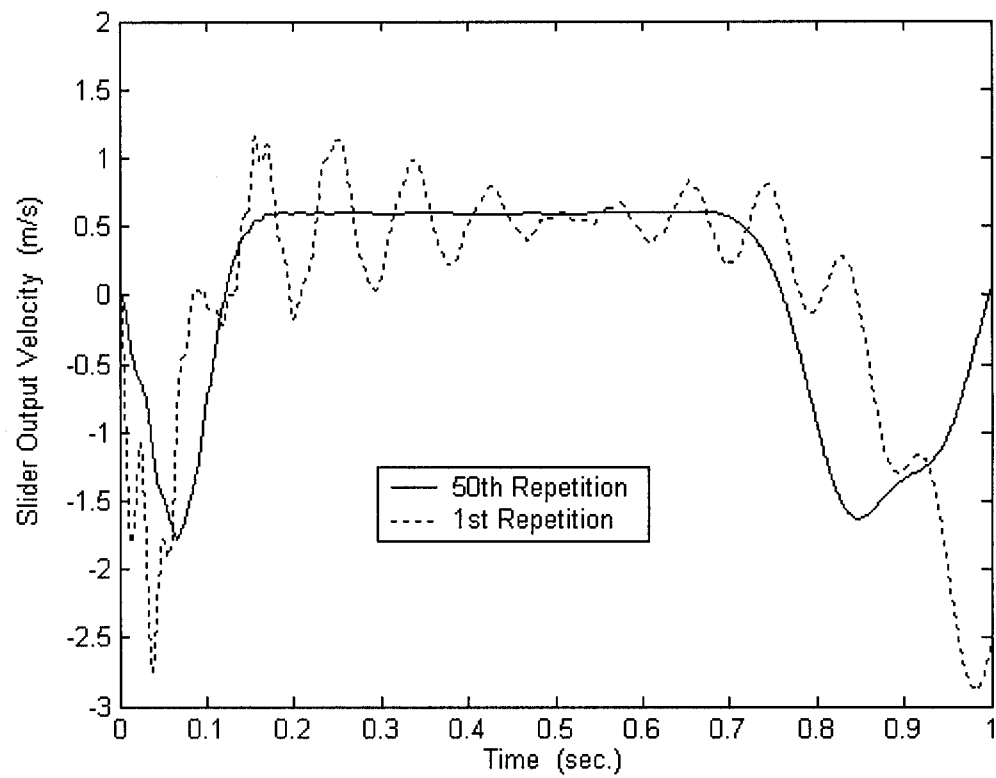


Figure 8.6: Output velocity of the slider versus time using learning control

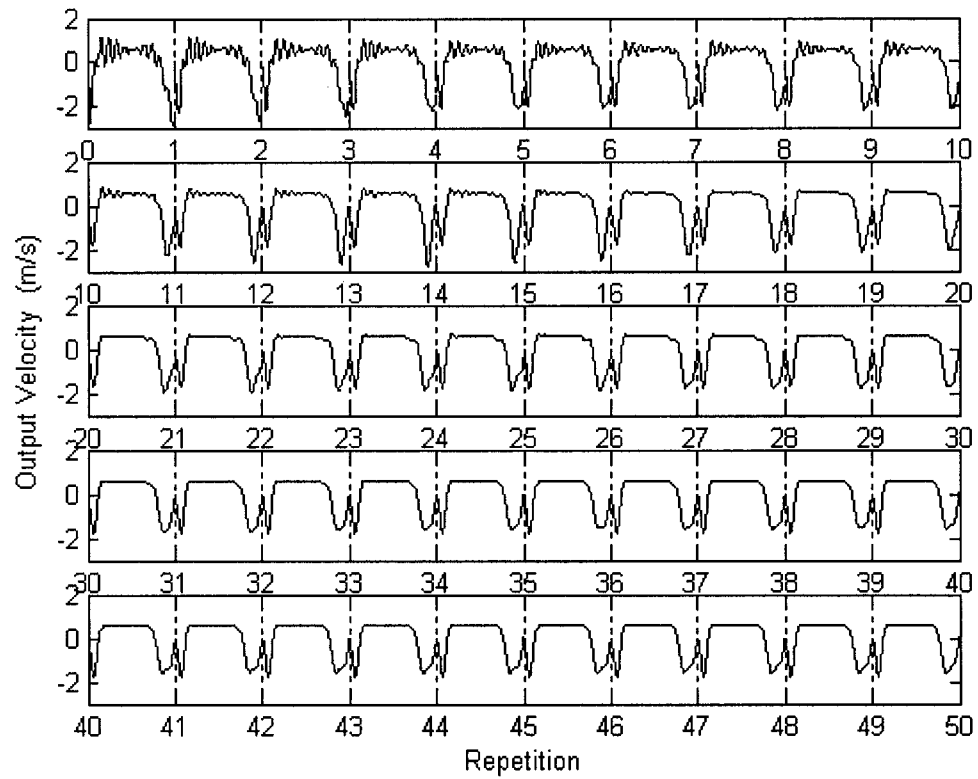


Figure 8.7: Output velocity of the slider versus repetitions using learning control

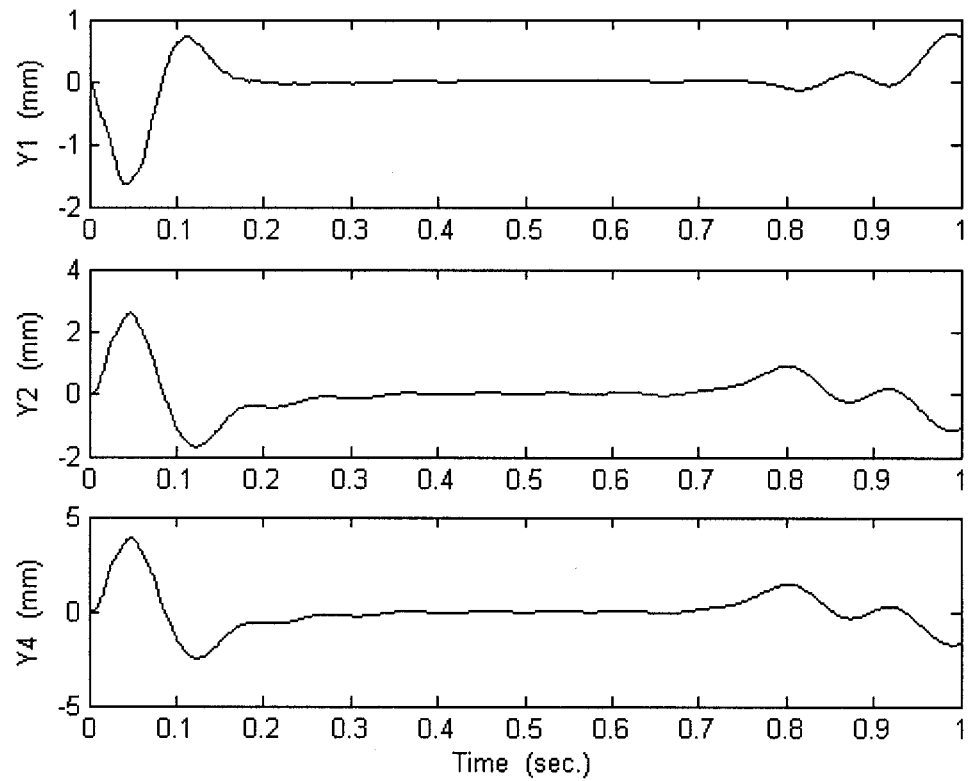


Figure 8.8: Maximum deflection of the flexible links 1, 2 and 4 versus time using learning control

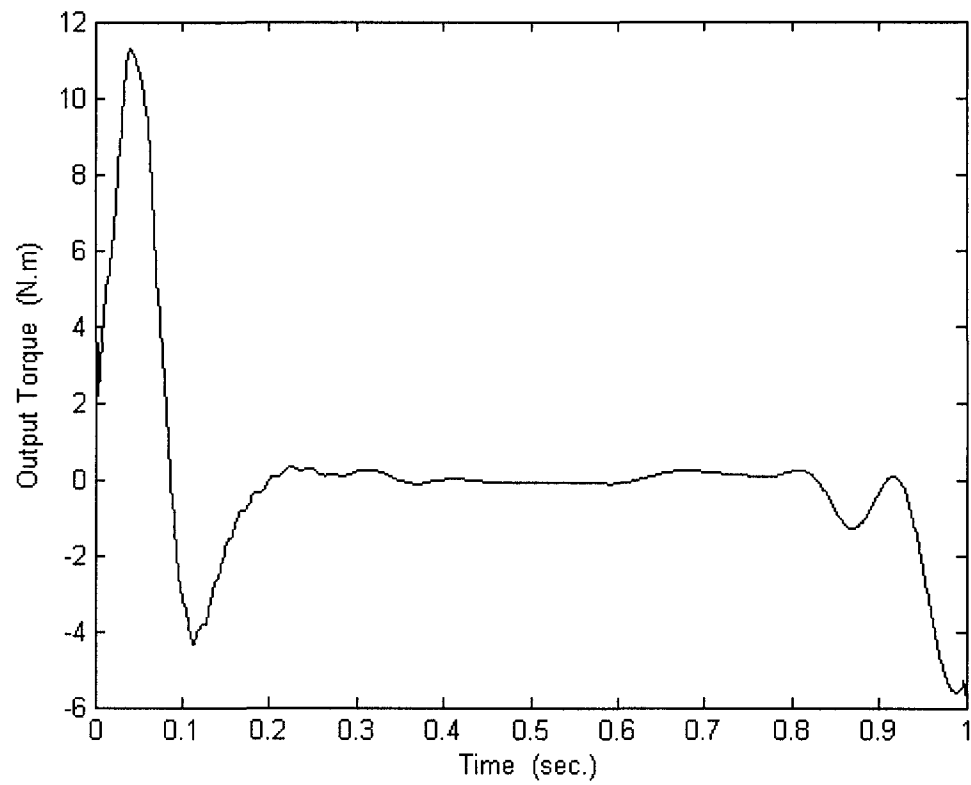


Figure 8.9: Motor's output torque to the mechanism versus time using learning
control

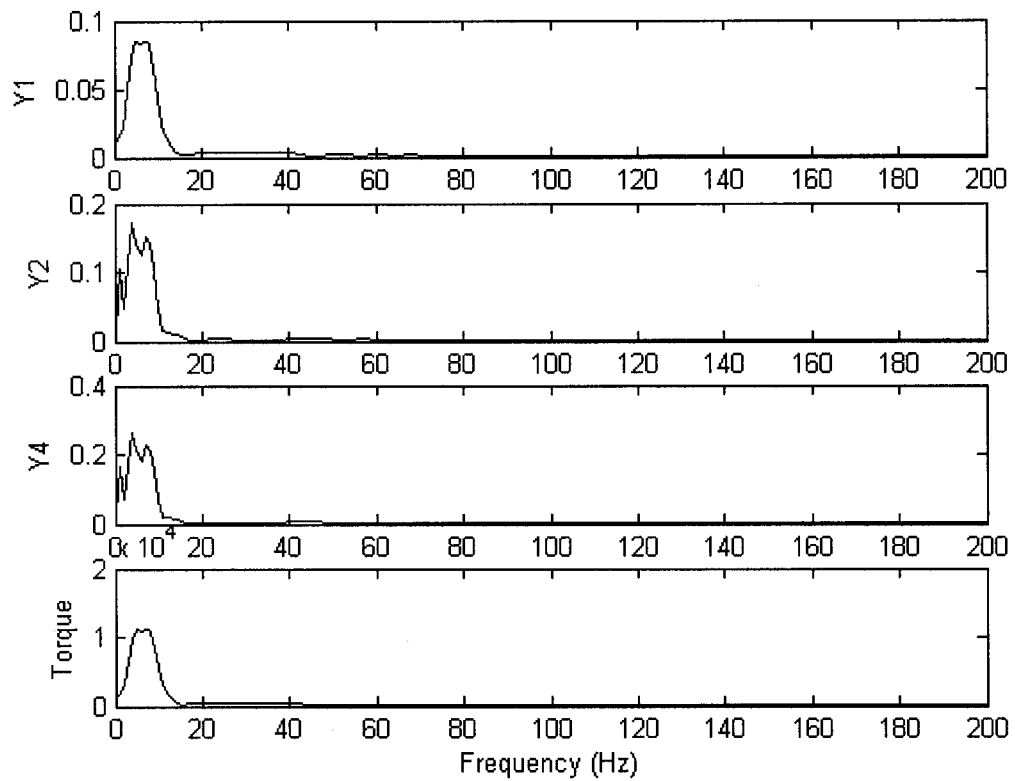


Figure 8.10: Frequency content of the flexible links 1, 2 and 4, and the input torque using learning control

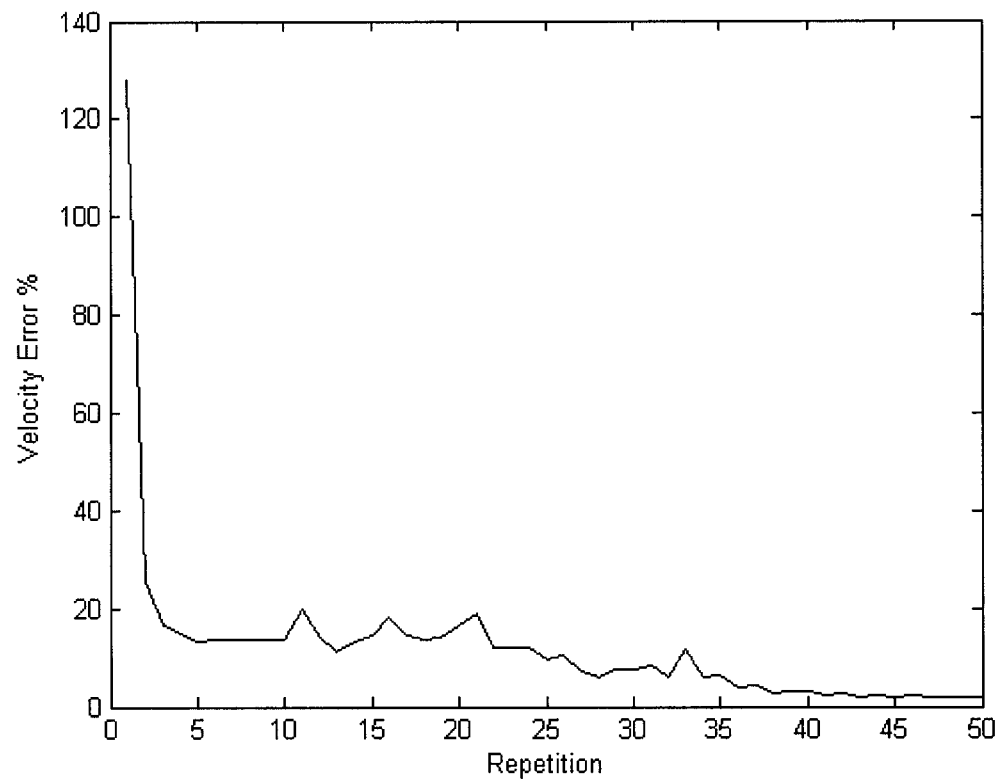


Figure 8.11: Velocity error versus repetitions using repetitive control

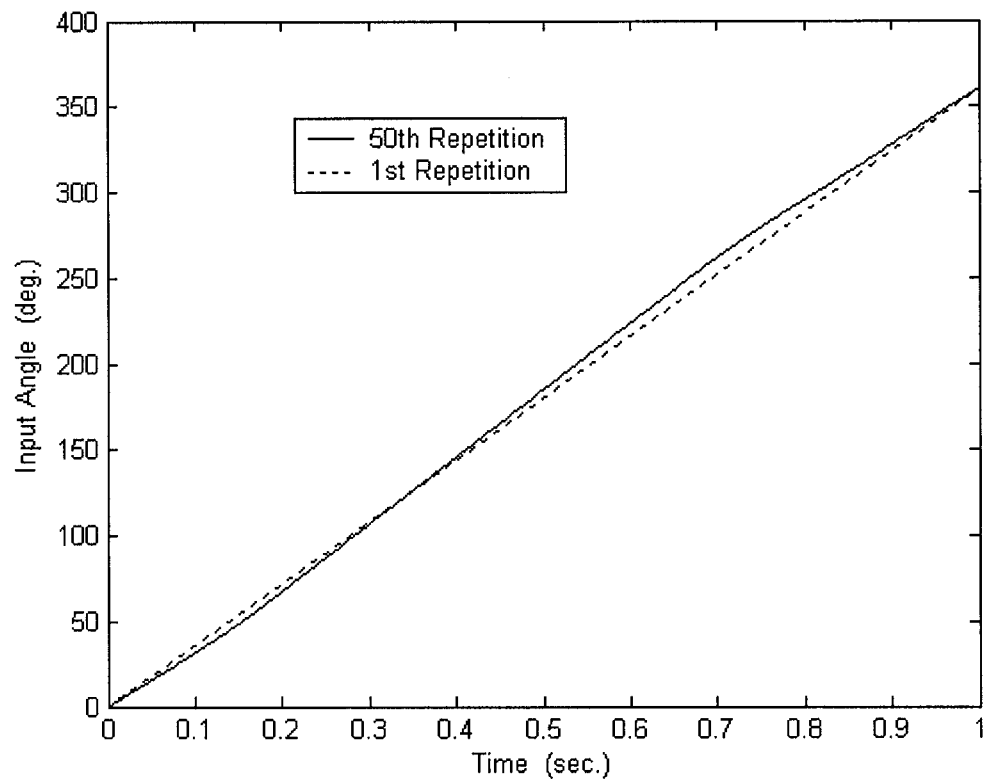


Figure 8.12: Input angles versus time using repetitive control

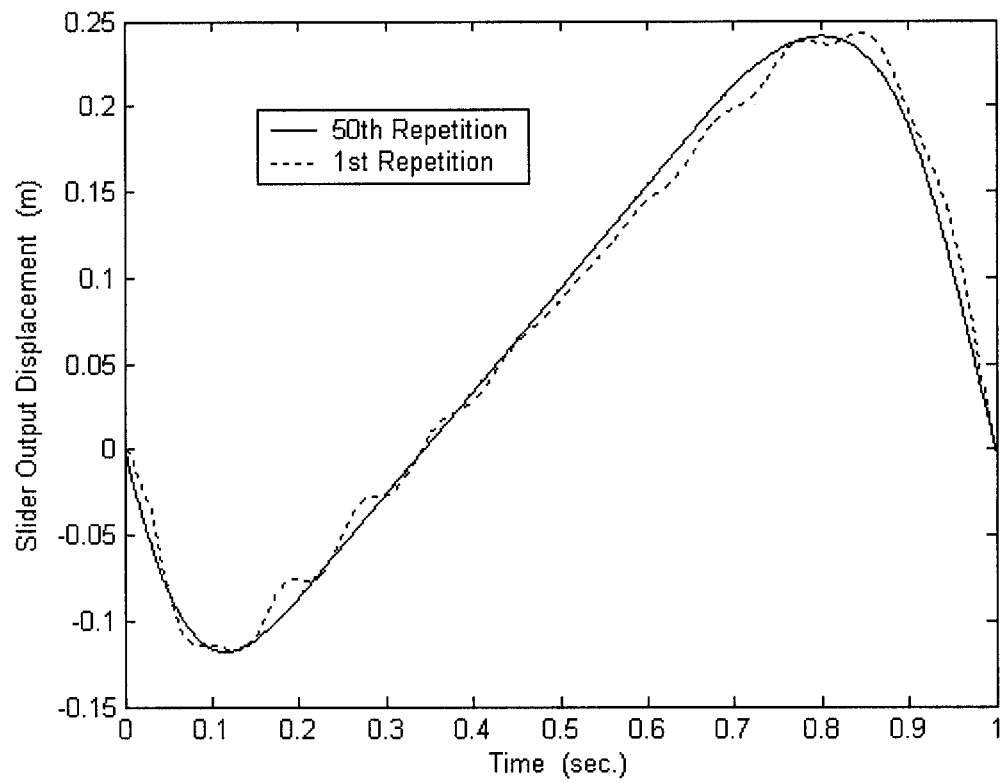


Figure 8.13: Output displacement of the slider versus time using repetitive control

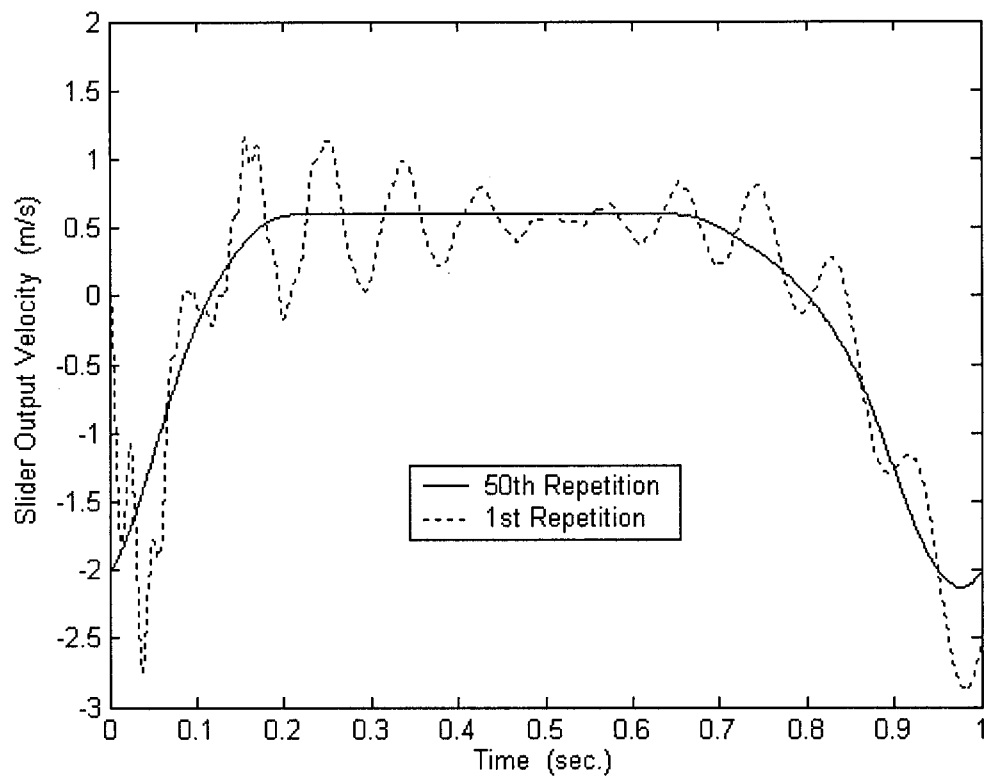


Figure 8.14: Output velocity of the slider versus time using repetitive control

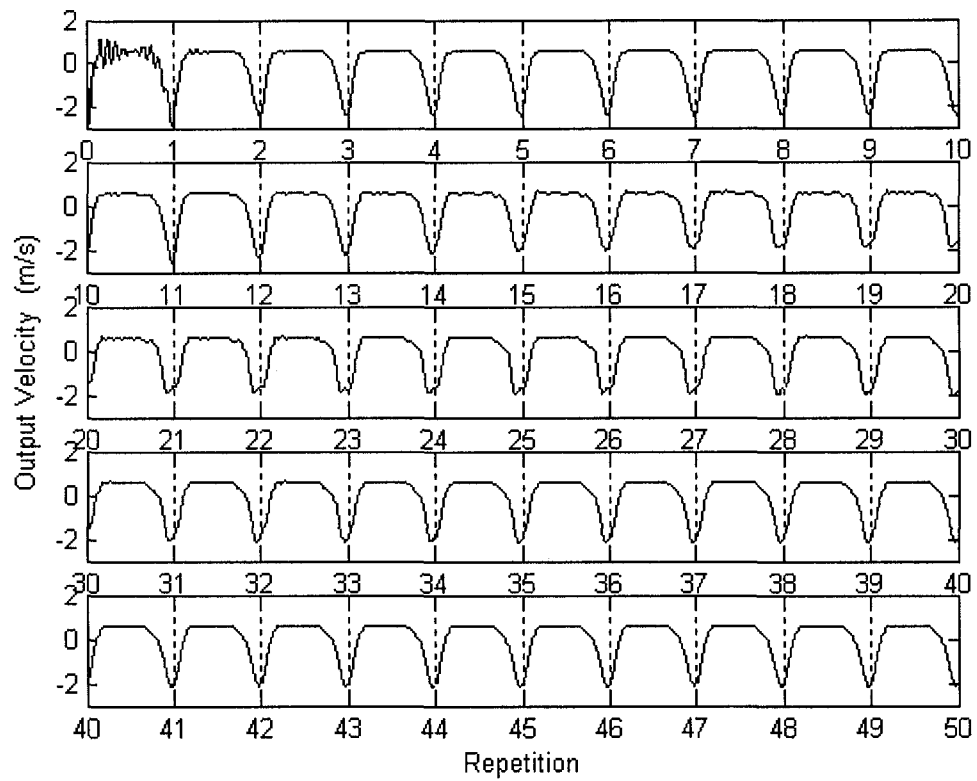


Figure 8.15: Output velocity of the slider versus repetitions using repetitive control

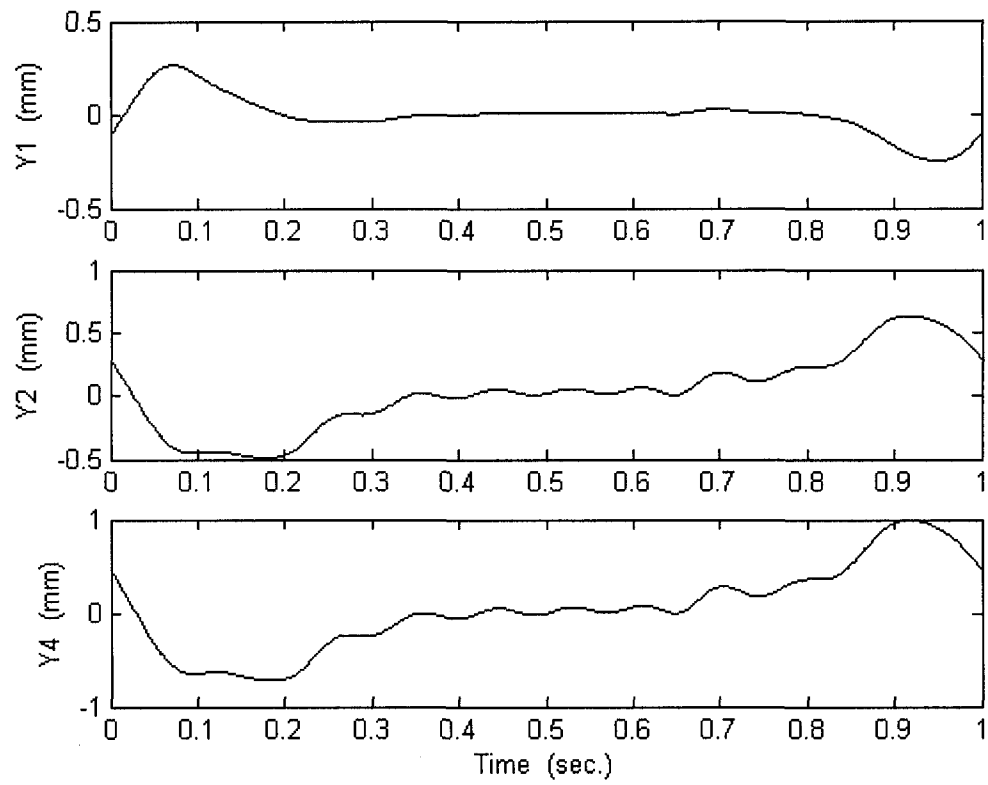


Figure 8.16: Maximum deflection of the flexible links 1, 2 and 4 versus time using repetitive control

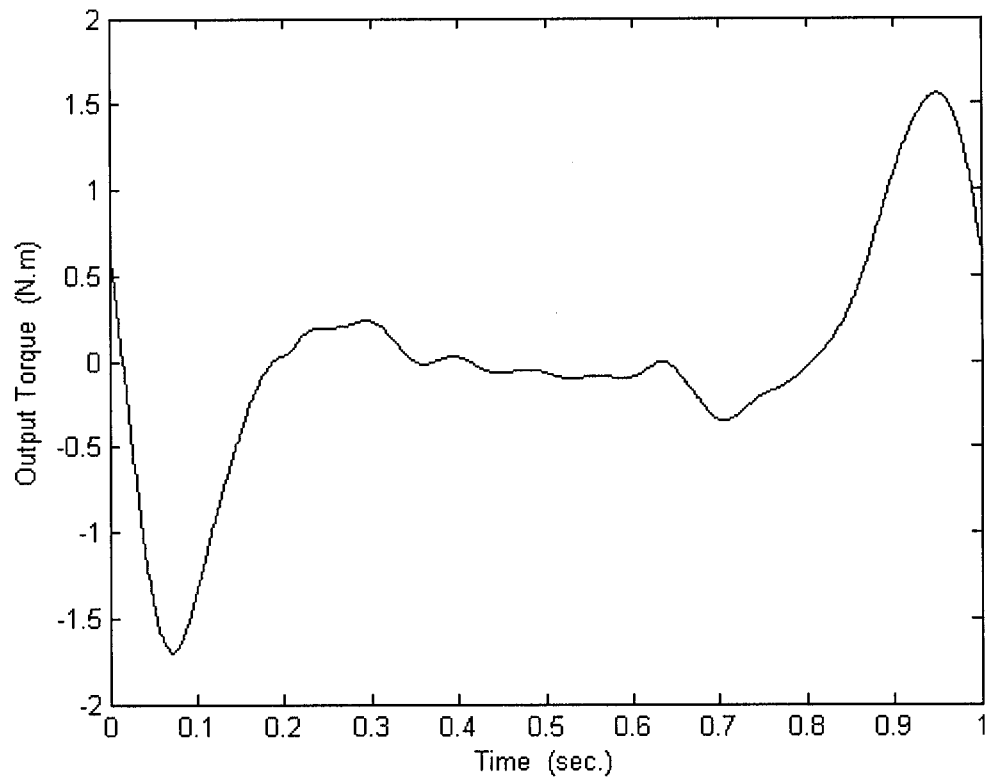


Figure 8.17: Motor's output torque to the mechanism versus time using repetitive control

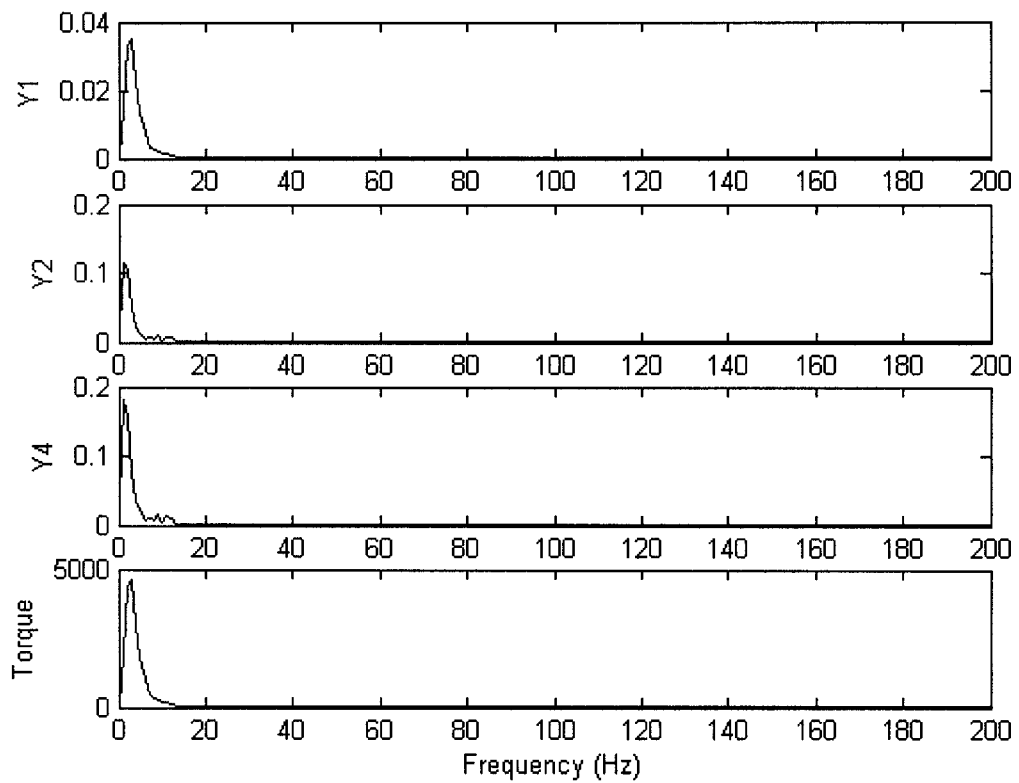


Figure 8.18: Frequency content of the flexible links 1, 2 and 4, and the input torque using repetitive control

8.5 Discussion of results

The results show an excellent enhancement of using the control methods in bringing the system to the desired output motion. The learning and repetitive control methods decreased the velocity error from 128% to less than 2%, which is an extremely large improvement of employing these control methods. The velocity error shows a quick drop in the first ten repetitions, and then it turns on irregular decreasing until it reaches the steady state error. This happens because the system minimizes the high fluctuation in the output velocity at the first repetitions, which means bringing the overall trend of the output velocity to what is desired. And then it starts to reduce this error as much as possible. The velocity error in the learning method shows less decrease at the first repetitions because it was starting the system at each cycle from rest, which generates vibrations in the flexible links more than the case of keeping the system in continuous motion.

The plots of the input angles show that the repetitive control did not make large changes in modifying the input angles and they still have an approximate constant speed. On the other hand, the learning control method made more changes to the input angles by producing smooth angular acceleration and deceleration at the start and the end of each cycle, respectively. Starting the system with smooth angular acceleration was done to minimize the vibrations caused by sudden changes in the velocity, while ending the cycle smoothly with zero velocity was done to bring the scanning machine to the initial position to prepare it for the next scanning period.

Figures 8.5 and 8.13 show the output displacement of the slider on the tilted plane. They show the vacillation of the slider's motion at the 1st repetition and the constant and stable motion at the 50th repetition.

The slider's output velocity shows the significant improvement of using the learning and repetitive control methods. The plots show the big difference between the shaky velocity at the 1st repetition and the constant velocity at the 50th repetition. As mentioned before, the repetitive case has more steady velocity and less vibration because of the continuity of motion.

Figure 8.7 and 8.15 show the converging progression of the output velocity to the desired velocity. In fifty repetitions, the control methods learned how to drive the system so that the vibrations of the flexible links were absorbed and made them behave as rigid links. Once more, the continuous motion in the case of repetitive control had a considerable effect in minimizing the vibrations as shown in these figures. Observe that the output velocity plot is continuous for all repetitions in the repetitive control case, while it shows discontinuity at the first repetitions of the learning control case. The later repetitions show continuous plots because the system learned enough about bringing the system to the same initial state, so that the system started each cycle with almost the same final state of the previous cycle.

Generally, the maximum deflection of the bendable links in the case of repetitive control is smaller by around three times than the case of learning control. This is an expected result attributed to the continuity of motion. The links 2 and 4 have the same trend of deflections since they are connected to each other rigidly, and they are under the same excitation. Observe that in the learning control, the deflections are starting from zero because the whole system starts from rest. Although the system comes to the zero velocity at the end of the cycle, the links are still deflected, and they take a little time to come to the rest. The shape of the deflection reflects the effect of the driving torque on that links. When the driving torque starts moving the crank link, this link deflects outward the motion because of its inertia, and then it changes its deflection's direction as the internal elasticity pulls back the link. The same thing occurs at the end of motion when the moment is reducing the speed of the crank link.

Starting the mechanism from rest and bringing it again to rest require large torques to control this heavy and large mechanism as shown in figure 8.9. The middle region shows less required torque since the mechanism goes in almost constant speed. However, the relatively high torques which appear in the beginning and the end of the case of repetitive control, are due to the large inertia of the other links that influence the crank link. Comparing the required torques for both control methods shows that the case of learning method requires a torque that is about 15

times larger than that which is needed in the case of repetitive method because of the discontinuity of the motion in the learning control case.

The frequency content of the input torque to the mechanism and the flexible links show that the input torque has less frequency than the natural frequencies of these links. Thus, the dominant frequency in vibrating the links, is the same as the frequency of the input torque, and the magnitudes of the natural frequencies for these links have almost vanished.

Chapter 9

Case 7: Flexible Slider-Crank Mechanism Used in Scanning Machine

In the previous chapter, the learning and repetitive control methods proved indisputably that they are able to enhance and improve any process that is needed to be controlled. There is no need to feed the controller by the inputs, since the control methods do the whole job from the first step of learning the system to the final step of optimizing the inputs. However, developing machines and making them more efficient is an important stage in doing research and studies. These developments are not limited by just increasing the efficiency of their performance; many other points may be considered. Size reduction, cutting down the complexity, and production growth are also important issues. But the question is would a control method result in all these improvements? And would it do so sufficiently? The answer is yes, by the power of the repetitive control method. Since big machines are designed complexly in order to perform certain jobs, simple and small machines can be used with the repetitive control to do the same job. Moreover, these simple machines could produce more, compared to large and complex machines.

In this case, a flexible slider-crank mechanism, which is one of the simplest mechanisms, is used instead of the six-bar Stephenson mechanism in scanning

machines, as shown in figure 9.1. By properly controlling it, the slider-crank mechanism produces two regions of constant output velocity during forward and backward strokes for increasing the number of scanned pages per cycle. The mechanism's links are assumed bendable and able to vibrate during motion. Furthermore, the comparison between the two mechanisms used in scanning machines will show how the repetitive control method enhances the usage of machinery.

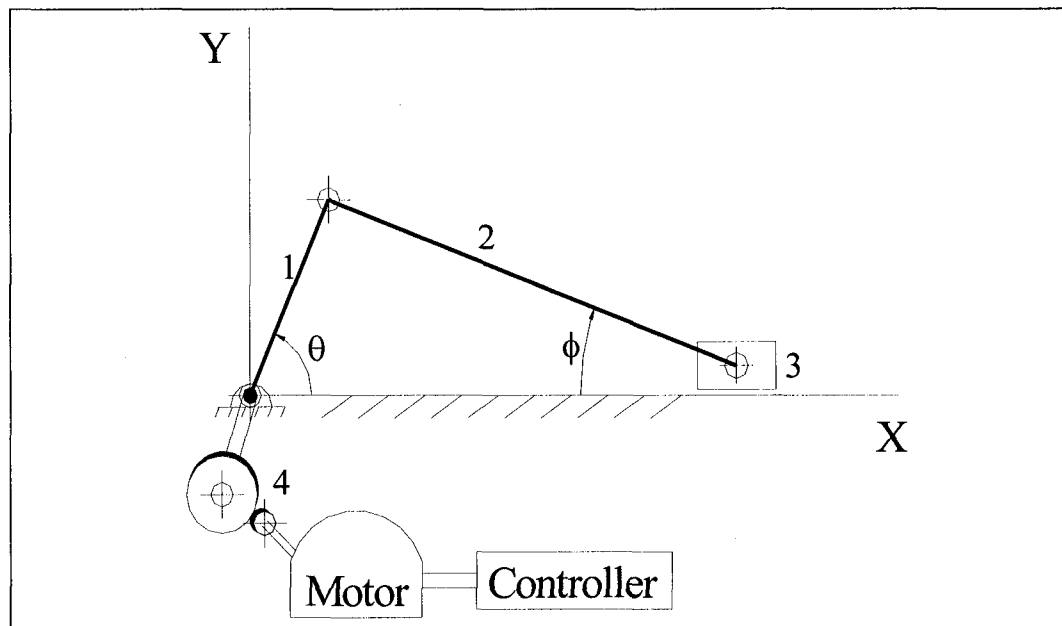


Figure 9.1: Flexible slider-crank mechanism

9.1 Applying learning and repetitive control methods

The procedure used in this case in applying the control methods is the same as that used in chapter 8. Generally, the control methods learn the relation between the

input angles and the output velocity. Then, they optimize the input angles in order to minimize the error. The exception here is that this mechanism has two separate constant velocity regions. Therefore, the weighting matrices have two sets of points these correspond to the concerned regions, and three more sets of points that correspond to the transient regions that are between the constant output velocity regions.

The general form of the output velocity used in the repetitive case can be expressed as

$$\dot{Y}_i = \underline{A}_i x_i(0) + \underline{B}_i U_i$$

where \dot{Y} is the output velocity vector, A and B are the parameter matrices, x is the initial conditions vector, and U is the input angles vector, all at the i^{th} repetition.

The cost function that needs to be minimized is expressed by

$$J = \frac{1}{2} e_{i+1}^T \underline{Q}_1 e_{i+1} + \frac{1}{2} (\underline{D} U_{i+1})^T \underline{Q}_2 (\underline{D} U_{i+1}) + \frac{1}{2} s \delta U_{i+1}^T \delta U_{i+1}$$

$$J = \frac{1}{2} e_{i+1}^T \underline{Q}_1 e_{i+1} + \frac{1}{2} (\underline{D} U_i + \underline{D} \delta U_{i+1})^T \underline{Q}_2 (\underline{D} U_i + \underline{D} \delta U_{i+1}) + \frac{1}{2} s \delta U_{i+1}^T \delta U_{i+1}$$

$$e_{i+1} = V^* - \dot{Y}_i - \underline{A}_i (x_{i+1}(0) - x_i(0)) - \underline{B}_i \delta U_{i+1}$$

$$\underline{Q}_2 = q_2 \underline{I}$$

$$\underline{D} = \frac{1}{\Delta^2 t} \begin{bmatrix} 1 & -2 & 1 & 0 & 0 & \dots & 0 & 0 \\ 0 & 1 & -2 & 1 & 0 & 0 & \dots & 0 \\ 0 & 0 & 1 & -2 & 1 & 0 & \dots & 0 \\ \vdots & & & \ddots & \ddots & & & \vdots \\ 0 & \dots & 0 & 1 & -2 & 1 & 0 & 0 \\ 0 & \dots & 0 & 0 & 1 & -2 & 1 & 0 \\ 0 & 0 & \dots & 0 & 0 & 1 & -2 & 1 \end{bmatrix}$$

where Q_1 is the weighting matrix of minimizing the error in the velocity, s is the weight of minimizing the changes in the input angles, q_2 is the weight of minimizing the angular acceleration of the mechanism, I is the identity matrix, δU is the difference in the input angles between any two consecutive repetitions, and V^* is the desired output velocity.

Producing constant output velocity in fractions of the motion's cycle requires setting the weighting matrix Q_1 as zero matrix, except those elements that correspond to the designated points that belong to the constant output velocity regions. The modifications of the input angles that refer to the zero elements in matrix Q_1 are irrelevant to both the output displacement and the output velocity at these points. The input angles related to the zero elements in matrix Q_1 , which correspond to the points outside the constant output velocity regions, can be modified according to any preferred criterion. In this case, the exterior points are

modified so that they minimize the angular acceleration in order to smooth the input speed of the mechanism. Moreover, this modifying process makes the output motion smoother at the unconcerned regions to prepare the system to have constant output velocity at the concerned region.

Performing the necessary work in minimizing this cost function results in,

$$U_{i+1} = U_i + \delta U_{i+1}$$

$$\delta U_{i+1} = (\underline{B}_i^T \underline{Q}_1 \underline{B}_i + \underline{M} + s \underline{I})^{-1} \underline{H}$$

$$\underline{H} = \underline{B}_i^T \underline{Q}_1 \left[\underline{V}^* - \dot{\underline{Y}}_i - \underline{A}_i (\underline{x}_{i+1}(0) - \underline{x}_i(0)) \right] - \underline{M} \underline{U}_i$$

$$\underline{M} = \underline{D}^T \underline{Q}_2 \underline{D}$$

The weight s is set to be equal to 1 all the time, q_2 is constant and equal to 5×10^{-6} , and the weight of Q_1 for the non-zero elements is set initially 0.01 and is changed every ten repetitions according to this relation

$$\underline{Q}_1|_{\text{new}} = \underline{Q}_1|_{\text{old}} + \frac{(\text{rpt})^2}{200}$$

where rpt is the number of the current repetition where the change occurs. The percentage error that shows the convergence progression is defined as,

$$e=100 \left| \frac{V^* - \dot{Y}_j}{V^*} \right|_{\max} \% , \quad \begin{array}{l} p_1 \leq j \leq p_2 \\ p_3 \leq j \leq p_4 \end{array}$$

where p_1 , p_2 , p_3 and p_4 are the start and end points of the constant output velocity regions. In this case, the desired output velocities in the forward stroke is 1 m/s, starting at 0.12 sec. and ending at 0.40 sec., while the desired output velocities in the backward stroke is -1 m/s, starting at 0.60 sec. and ending at 0.88 sec. The desired output velocity is determined carefully to maintain stable angular velocity of the mechanism. In addition, this constant velocity has to cover the scanned page, which is 27 cm in length, in that period of time. Selecting higher or lower desired output velocity will speed up or lower the angular velocity of the mechanism during the concerned region of desired output velocity, which leads to more vibrations in the whole system. Moreover, it is important to have transient regions before and after the concerned region. These transient regions are used to prepare the system to move into or out of the constant output velocity regions. The transient regions used in this case are short in length because these kinds of applications do not allow for big margins for practical reasons, and because the

entire displacement of the stroke is short as well. Therefore, the transient regions are considered to be 5 mm.

Since performing the control methods takes a number of repetitions depending on the simplicity of the case, it is impractical to keep the system running all leading repetitions until it reaches the desired output, whenever the system needs to be used. Actually, in the case of the learning control method, where the initial conditions are constant at all cycles, the system does not require the preliminary cycles. It just starts the motion directly with optimum input speed. However, this cannot be done when the case is the repetitive control, because the initial state of the system is changeable. But, if the final conditions of the system are set properly during the optimizing process, then the system can use the optimum input speed directly every time it starts from rest using fewer repetitions in reducing the error.

In this case, the final position of the crank link is set at 360° , so that the crank's rotations will not shift during angles modifying process, and so that the system will be forced to start from the rest-position, which is the horizontal position of the crank link. At the end of the optimizing process, when the desired input angles are obtained, the system starts again from rest with these optimum inputs to find out the required repetitions needed to make the system reach the desired output.

Selecting the number of time steps is governed by the frequency of the system. According to Nyquist frequency, the sampling points have to be at least two times the maximum frequency of the system to make sure that aliasing is excluded. Therefore, in order to determine the maximum frequency of the vibrated links, an exact formula is used to determine the natural frequency of link 2. However, since the crank link is attached to the whole mechanism, this directly affects the frequency of this link. Therefore, a similar procedure of that used in chapter 8 is done to determine its natural frequency. The analytical formula of determining the natural frequencies of the links 1 and 2 are

$$f_1 = \frac{1}{2\pi} \sqrt{\frac{3E_1 I_1}{R_1^3 (M_1 + 0.23m_1)}}$$

$$f_2 = \frac{1}{2\pi} \sqrt{\frac{96E_2 I_2}{R_2^3 m_2}}$$

where f is in Hz, E is the modulus of elasticity, I is the moment of inertia of the cross sectional area, R is the link's length, m is the mass of the link, and M_1 is the mass attached to the crank link.

Applying the numbers in the above formulas shows that the natural frequency of link 2 is 23.527 Hz. The exact calculations of f_1 at the end of simulating the system show that the natural frequency of the crank link is between 1.8863 and 19.271 Hz.

Although the Nyquist frequency requires two times the maximum frequency, the number of time steps is set at 100, which is more than four times the maximum frequency to make sure that aliasing is totally avoided.

9.2 System's model

With reference to figure 9.1, the flexible slider-crank mechanism has two flexible links, which vibrate laterally in the plane of motion. The whole mechanism is made of a plastic material, which makes the links more flexible. These links are treated as continuous cantilevers that vibrate in their first mode shape. Once again, the method of assumed mode shapes is used in analyzing and simulating these flexible links during motion. The crank link is assumed to be a clamped-free cantilever, while the driven link is assumed to be a pinned-pinned cantilever. The driving link is clamped to the motor shaft and free at the other end. This assumption of the boundary conditions of the driven link is made because it is connecting the crank link and the slider by pinned joints. The two mode shapes are in the form:

$$\Psi_1(x) = \sin(\omega_1 x) - \sinh(\omega_1 x) - \left\{ \frac{\sin(\omega_1) + \sinh(\omega_1)}{\cos(\omega_1) + \cosh(\omega_1)} \right\} \{ \cos(\omega_1 x) - \cosh(\omega_1 x) \}$$

$$\Psi_2(x) = \sin(\omega_2 x)$$

$$\omega_1 = \frac{1.875104}{R_1}, \quad \omega_2 = \frac{\pi}{R_2}, \quad \omega_4 = \frac{1.875104}{R_4}$$

and the deflections of the links are in the form:

$$y_i = \Psi_i(x) q_i(t), \quad i=1,2$$

where q is the magnitude function or the time-dependent coordinate.

Lagrange's equations are used in deriving the governing equations of the system. The total energy of the system is found by summing up the individual total energies of all links and parts. Observe that the potential energy due to gravity is disregarded because the whole motion is assumed in the horizontal plane. Therefore, the potential energy is only the internal energy in the flexible links due to bending. Determining the total energy of the flexible links is done by integrating the kinetic energy and potential energy terms along the link's length, while the energy of the slider is determined by a definite term. The complete detailed derivation of the governing equations is provided in appendix E.

The determination of the safety factor is exactly the same as that described in chapter 8. The formula used in finding the safety factor is

$$n = \frac{S_y}{Eq_{\max} \sqrt{\frac{I}{AR} \int_0^R \Psi'^2 dx}}$$

where n is the safety factor, S_y is the yield strength, q_{\max} is the maximum absolute magnitude function, A is the cross sectional area, and R is the link's length. As a result, the minimum safety factor of this machine used in both control methods is 16.7.

9.2.1 Specifications of the system

The material used in this system is CARILON® Thermoplastic Polymer DP R1000, which has specifications shown in table 8.1.

A PD controller was used to control the motor. The proportional gain (K_p) is 100, while the derivative gain (K_d) is 1.7. The motor specifications are as follows:

K_t : Motor torque constant,	0.0137 N.m/amp.
K_e : Motor back EMF,	0.0137 V.s/rad
R_s : Armature resistance,	3.1 Ω
T_{PK} : Peak torque,	0.052 N.m

S_{NL} : No load speed, 822 rad/s

T_F : Friction torque, 0.0025 N.m

The mechanism components and specifications are:

1. Crank link.
2. Driven link.
3. Slider, $m_3 = 10.52$ g
4. Gears, gear ratio (N) = 1.

Table 9.1: Links specifications of the flexible six-bar Stephenson mechanism

Link #	Length (m)	Cross sectional Area (mm ²)	Mass (g)	Area moment of inertia (mm ⁴)
1	0.18	3.142	0.7012	2.356
2	0.27	3.142	1.052	2.356

The internal damping ratio (ζ) of the flexible links is assumed to be 0.1. The mass moment of inertia of the motor's shaft (I_m) is 9.89×10^{-7} Kg.m². The mechanism's average input speed is 60 rpm.

9.3 Results of flexible slider-crank mechanism

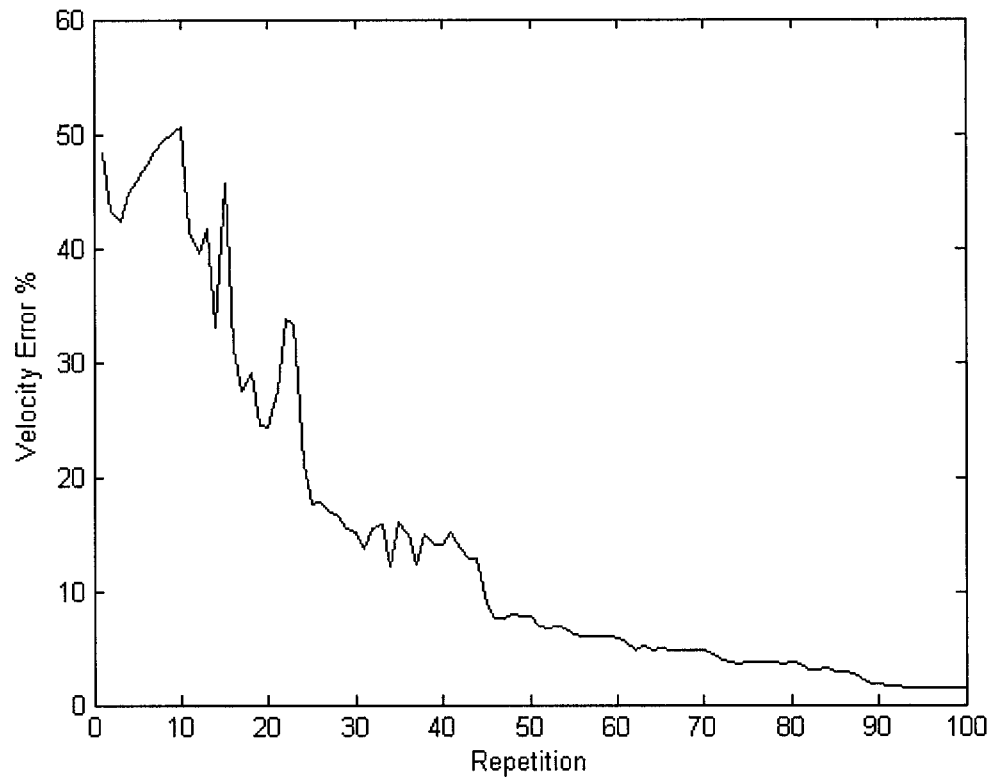


Figure 9.2: Velocity error versus repetitions using learning control

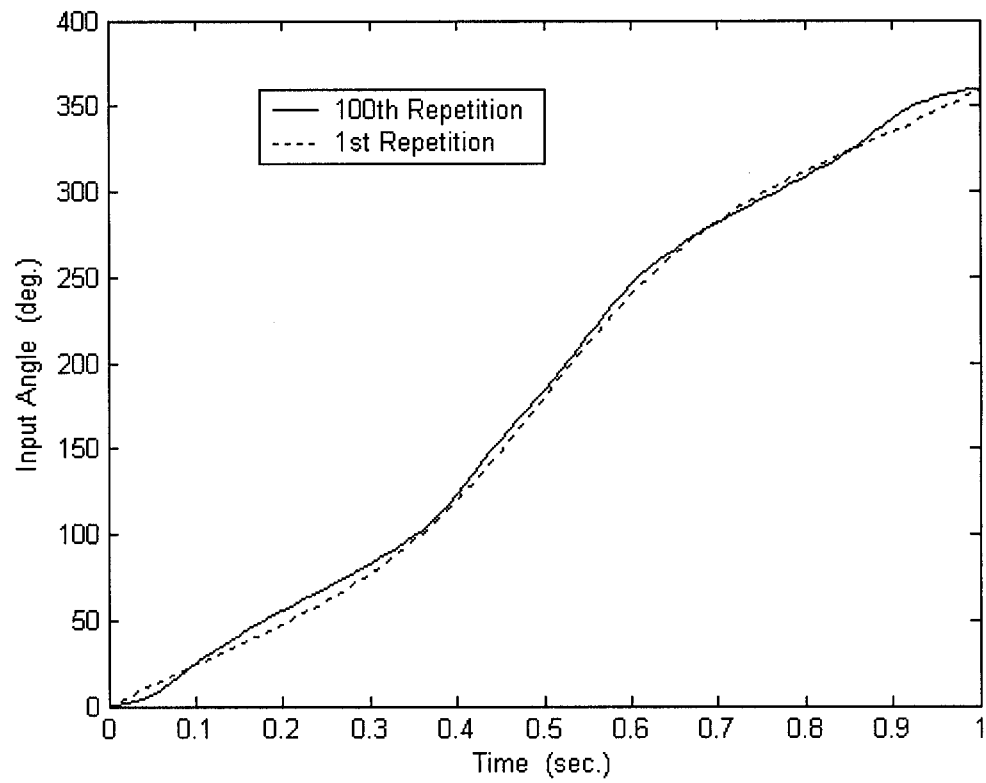


Figure 9.3: Input angles versus time using learning control

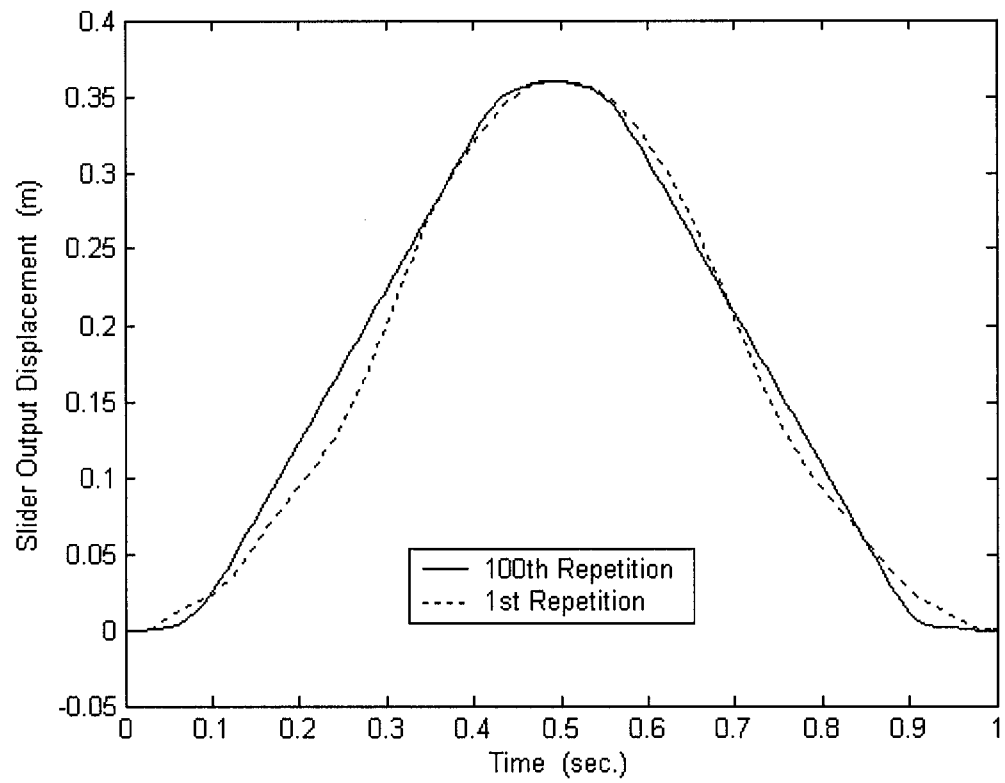


Figure 9.4: Output displacement of the slider versus time using learning control

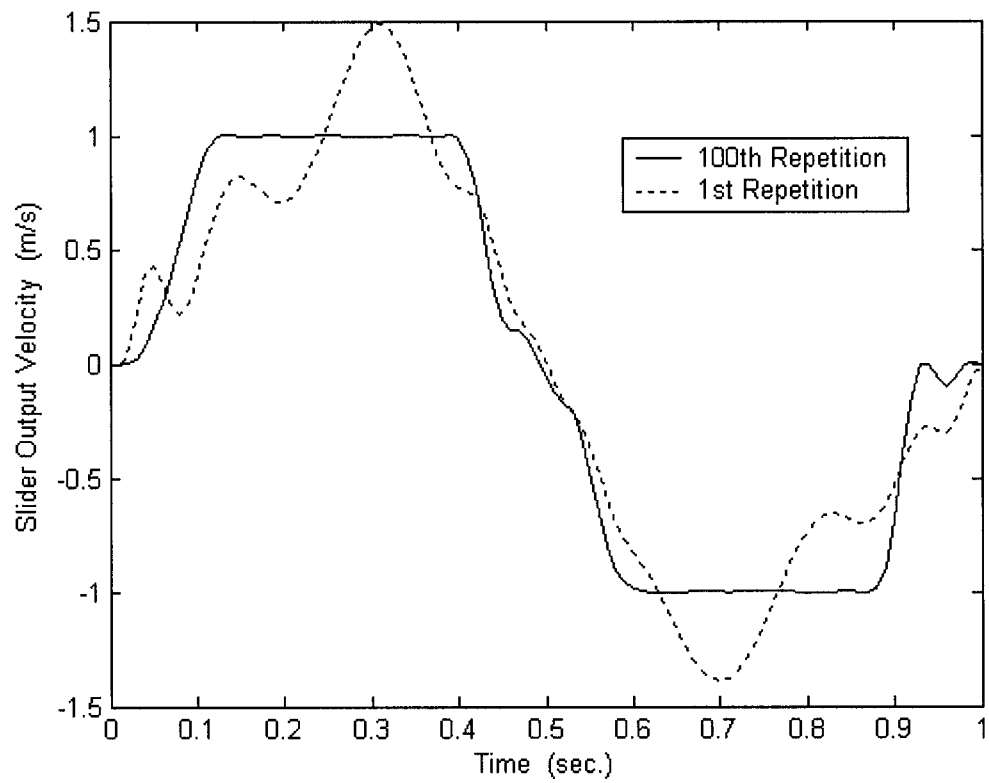


Figure 9.5: Output velocity of the slider versus time using learning control

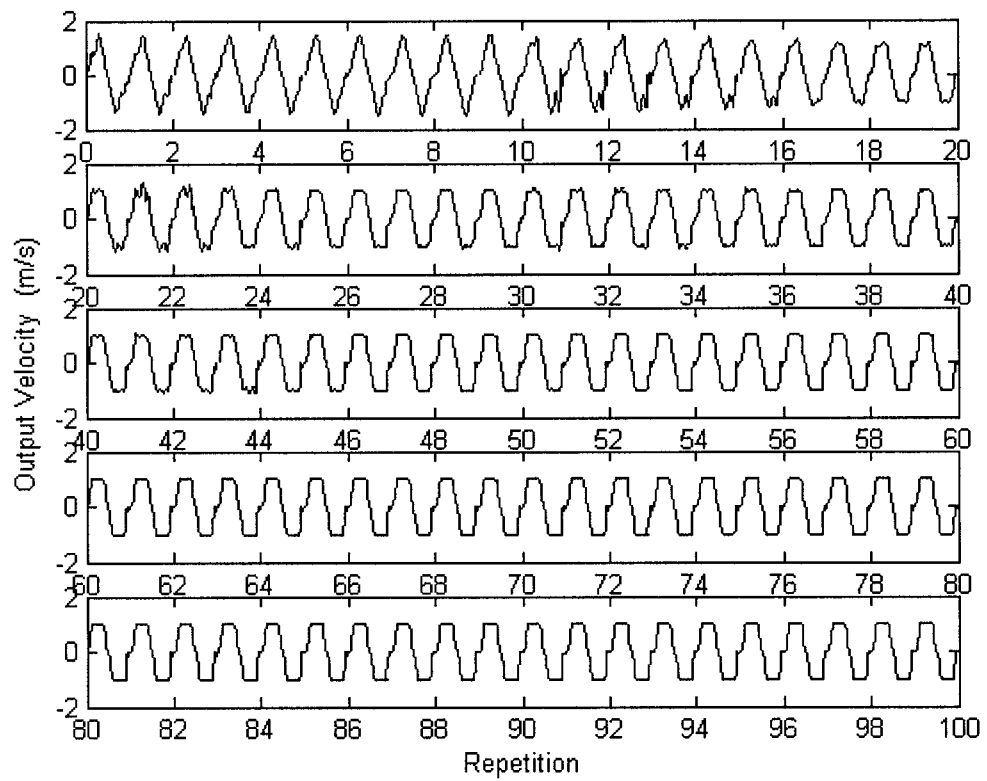


Figure 9.6: Output velocity of the slider versus repetitions using learning control

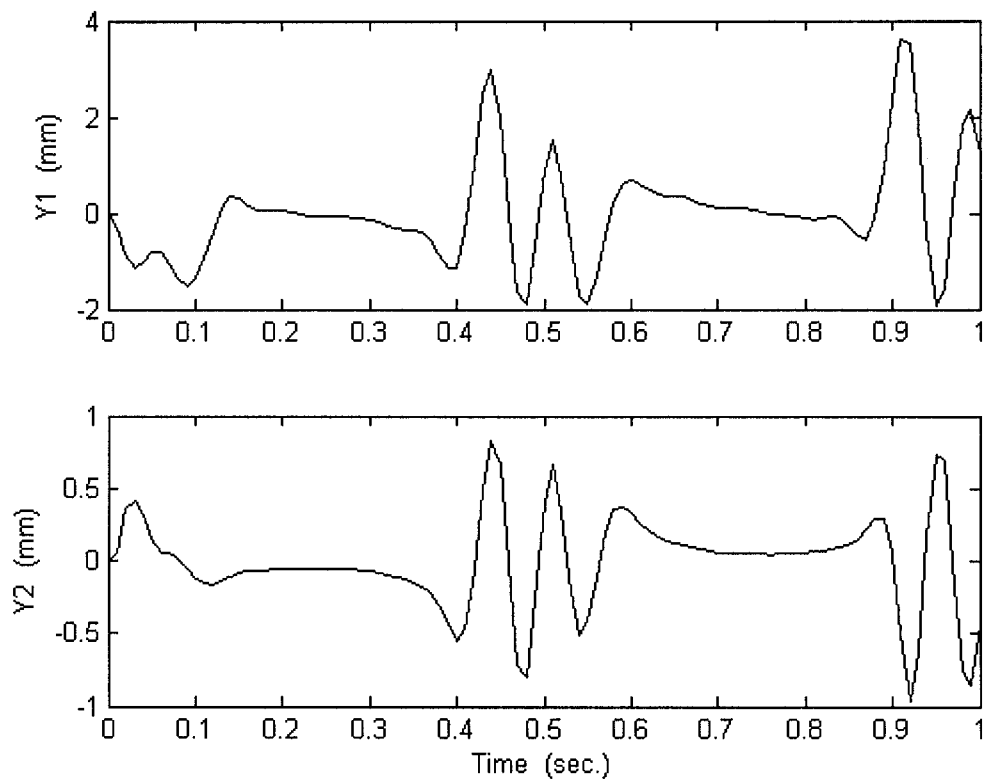


Figure 9.7: Maximum deflection of the flexible links 1 and 2 versus time
using learning control

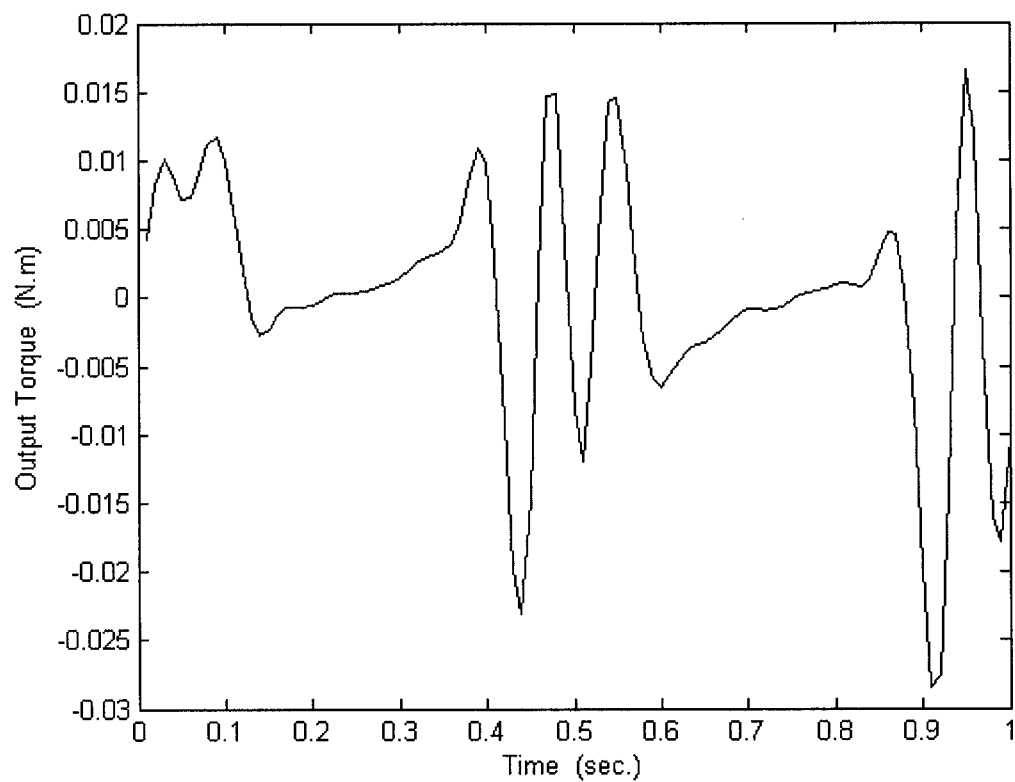


Figure 9.8: Motor's output torque to the mechanism versus time using learning control

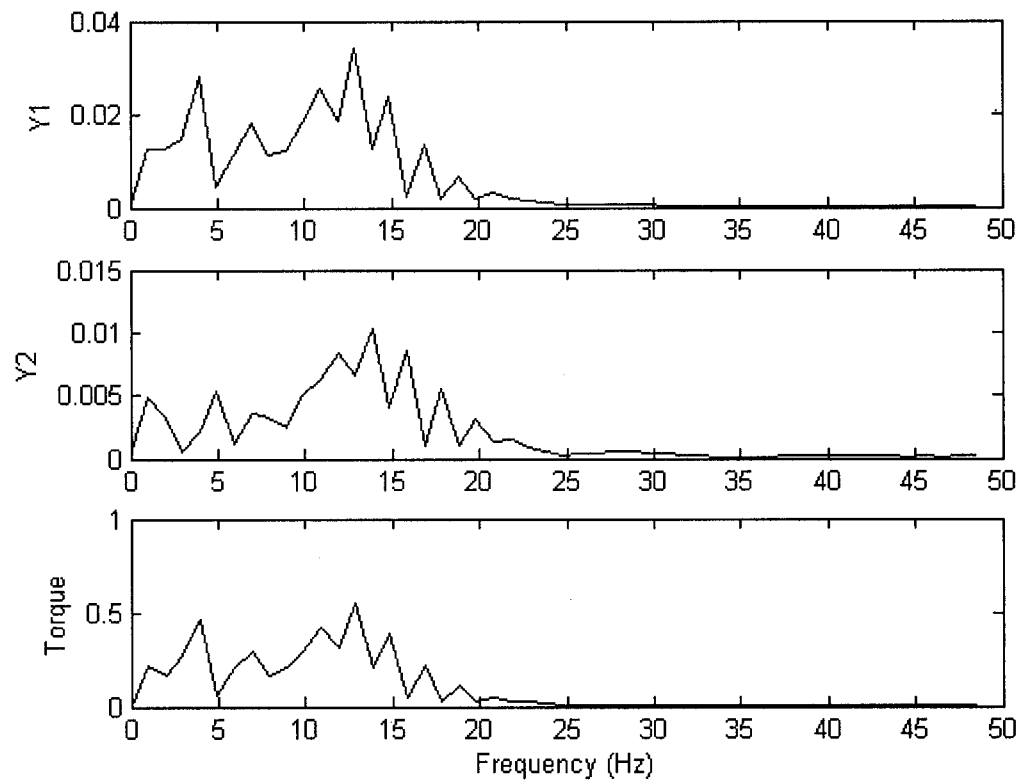


Figure 9.9: Frequency content of the flexible links 1 and 2, and the input torque
using learning control

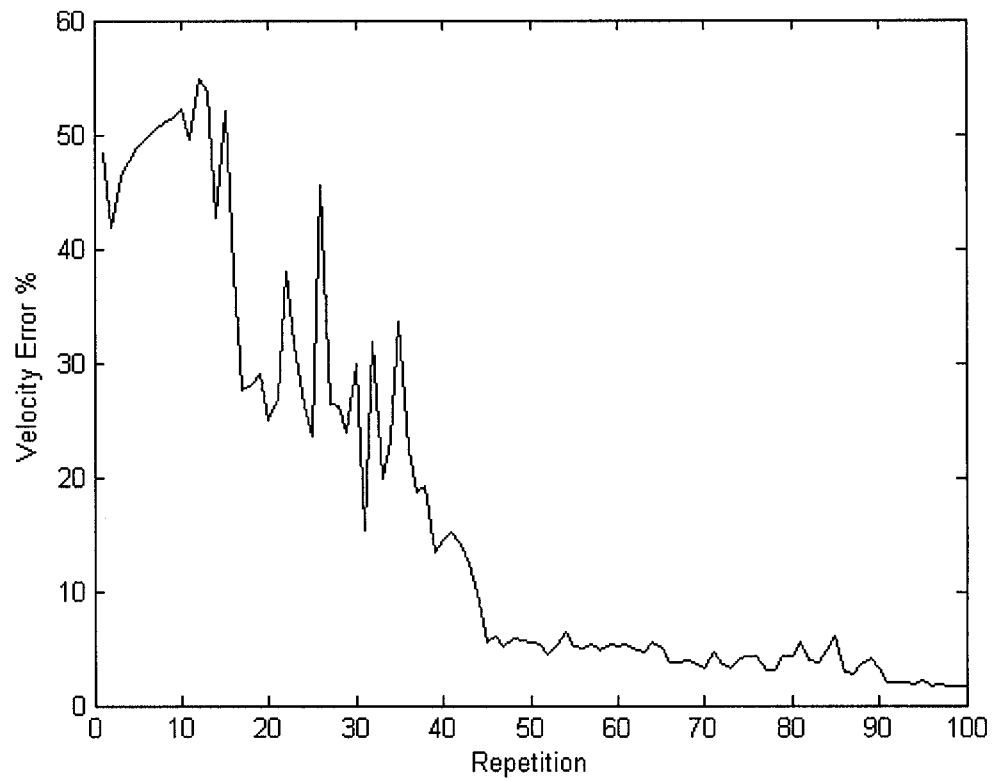


Figure 9.10: Velocity error versus repetitions using repetitive control

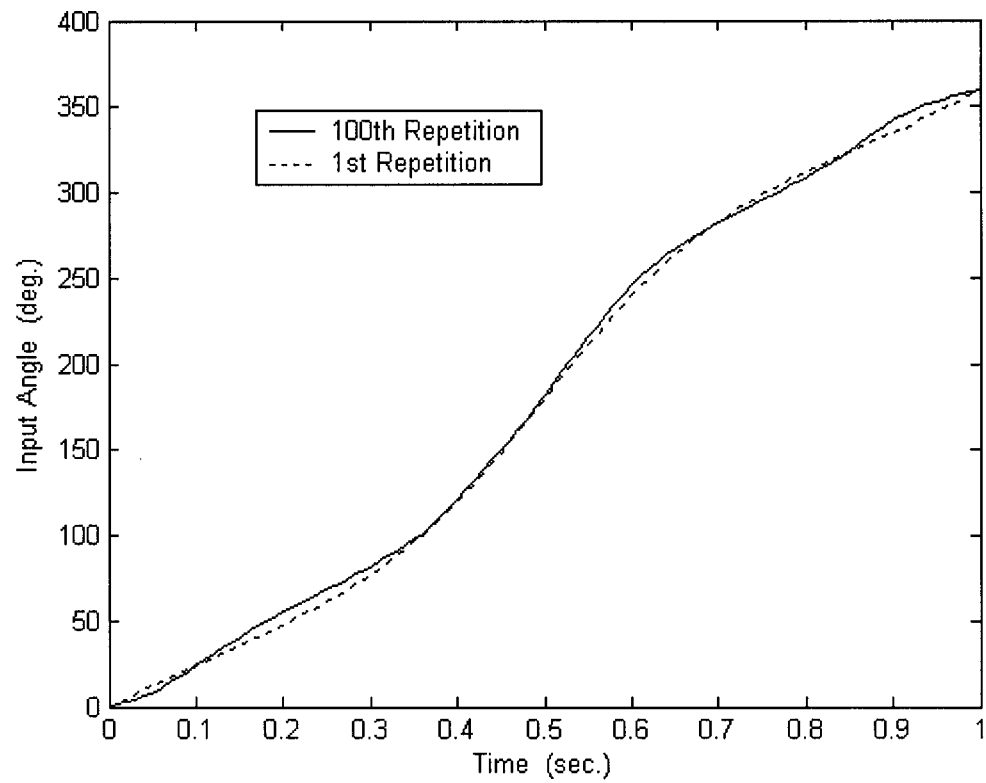


Figure 9.11: Input angles versus time using repetitive control

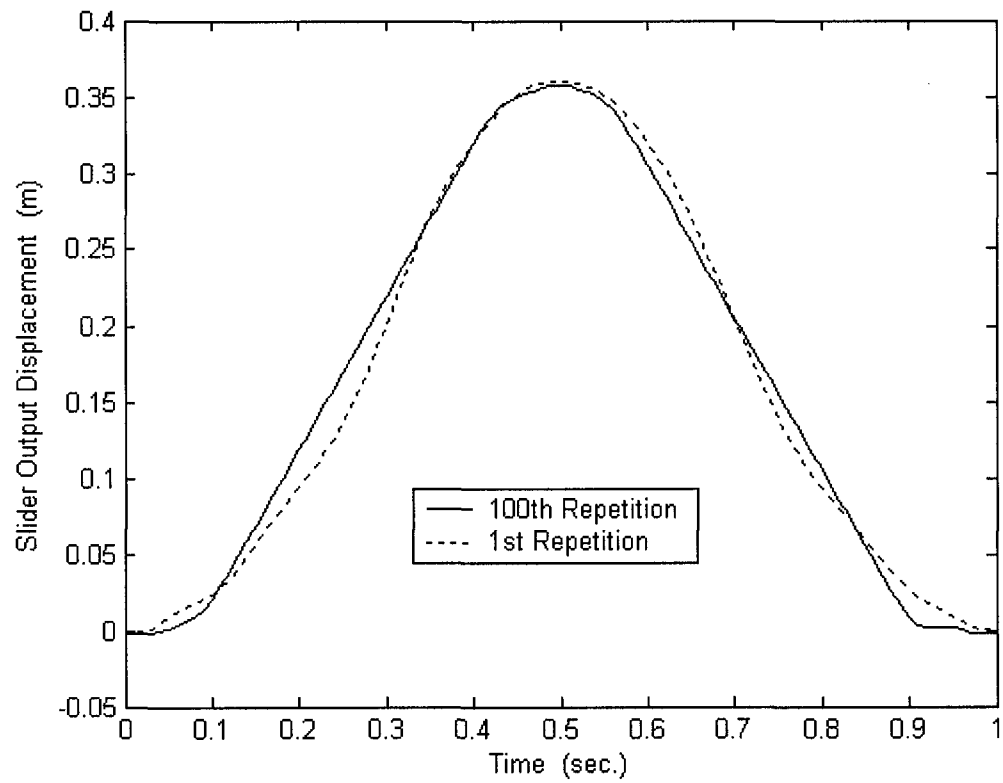


Figure 9.12: Output displacement of the slider versus time using repetitive control

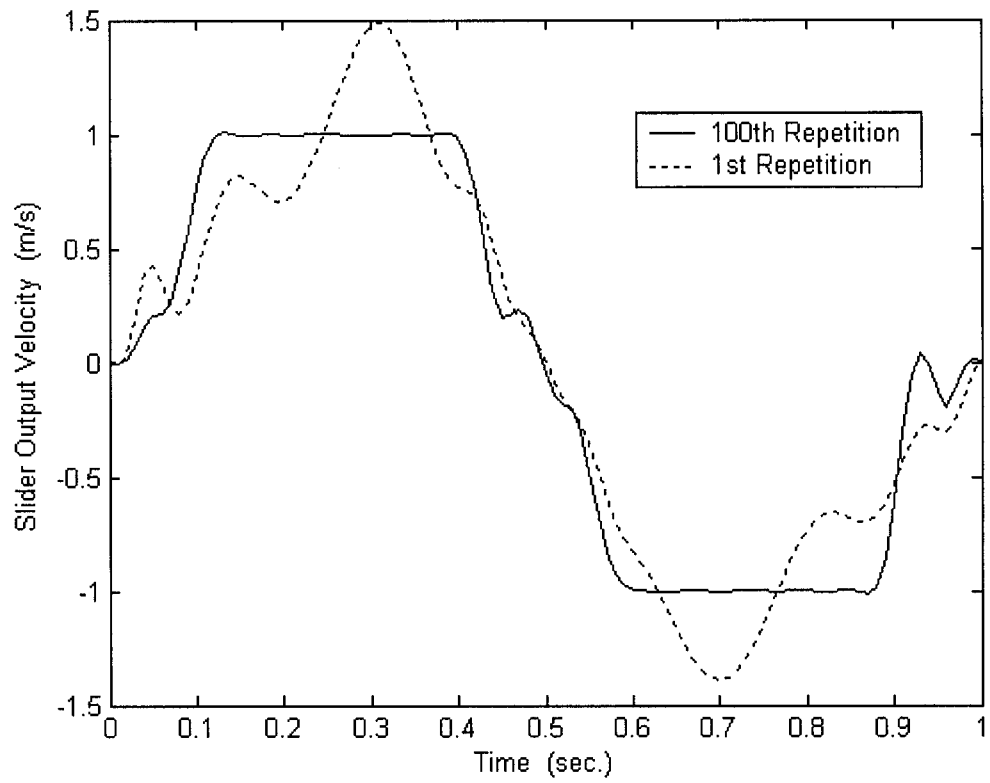


Figure 9.13: Output velocity of the slider versus time using repetitive control

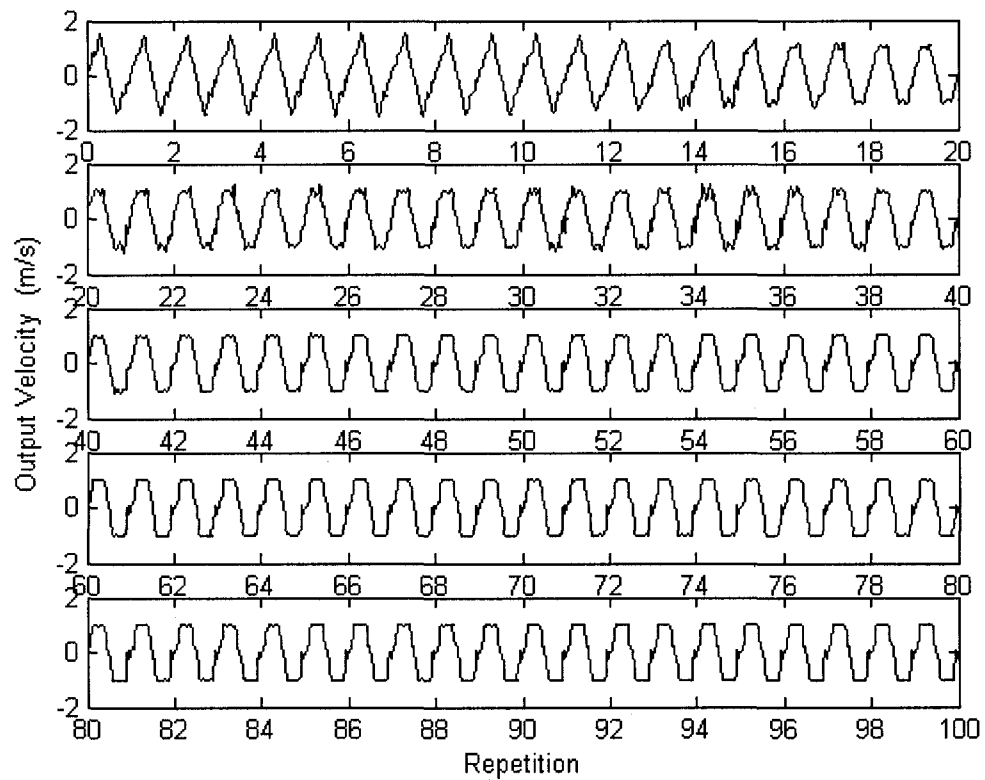


Figure 9.14: Output velocity of the slider versus repetitions using repetitive control

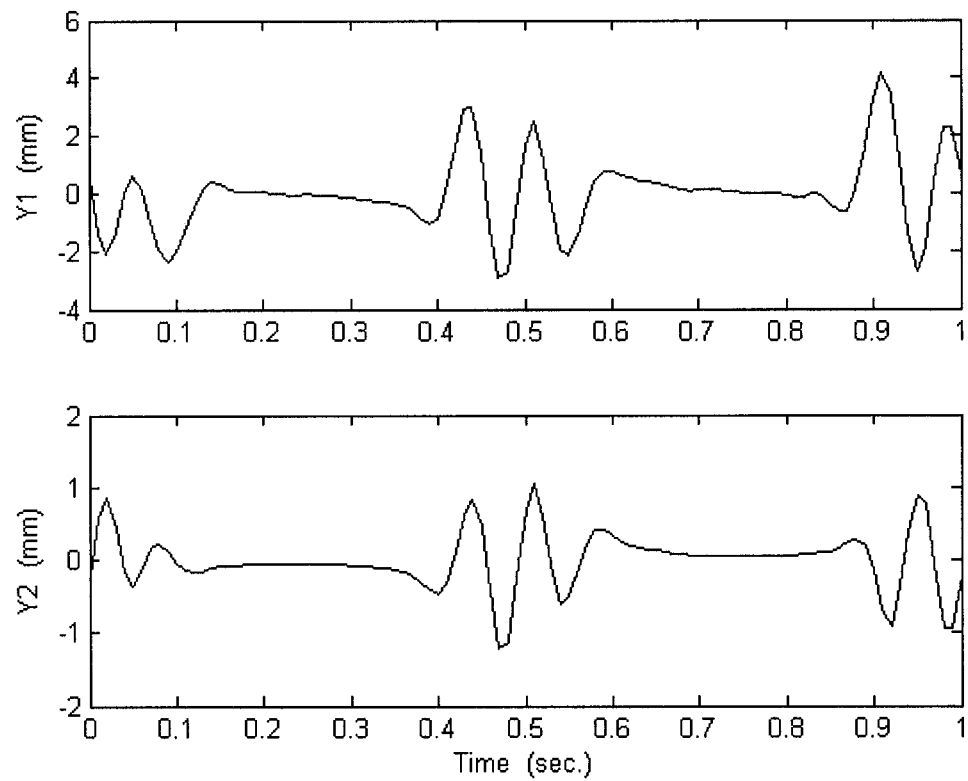


Figure 9.15: Maximum deflection of the flexible links 1 and 2 versus time
using repetitive control

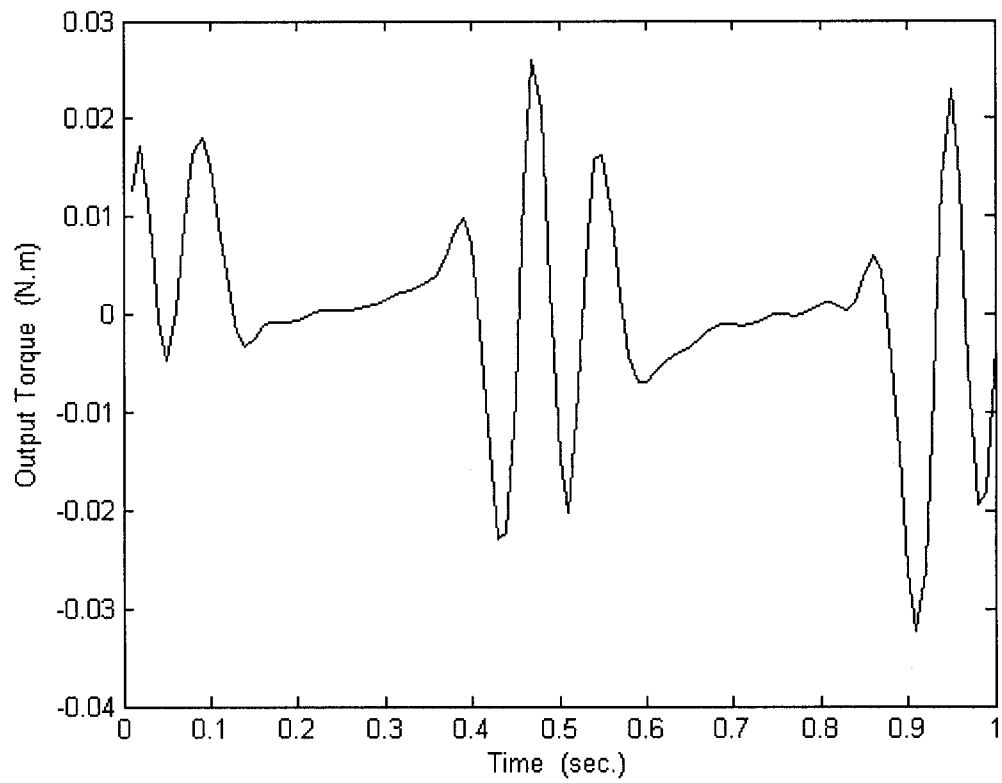


Figure 9.16: Motor's output torque to the mechanism versus time using repetitive control

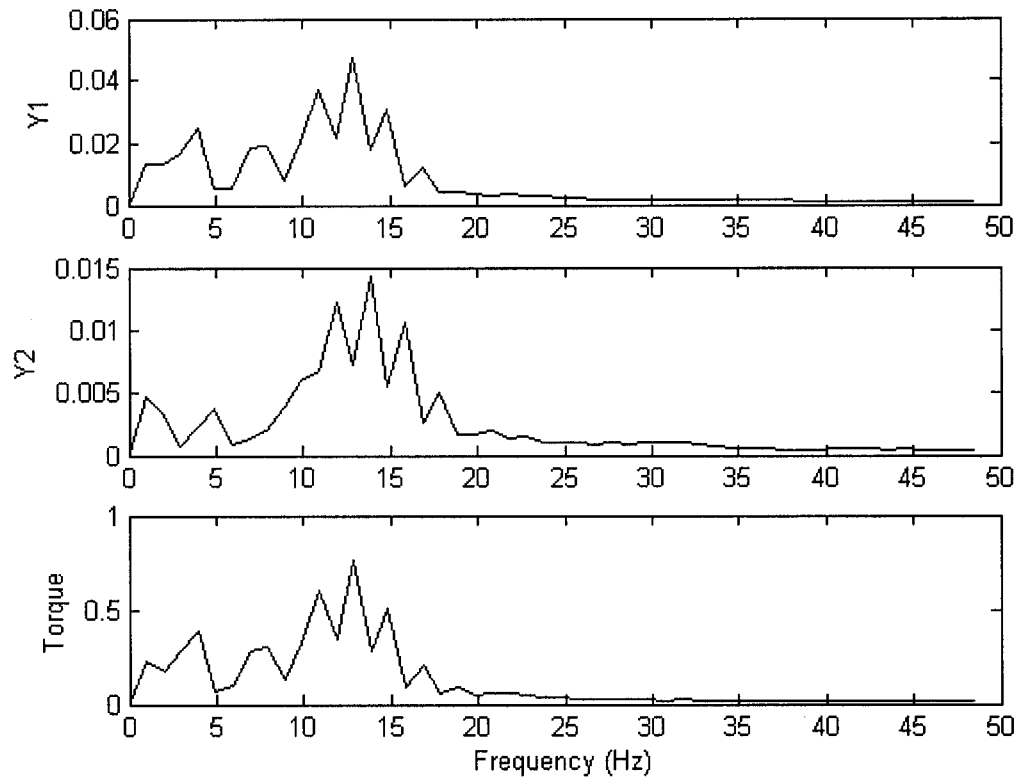


Figure 9.17: Frequency content of the flexible links 1 and 2, and the input torque
using repetitive control

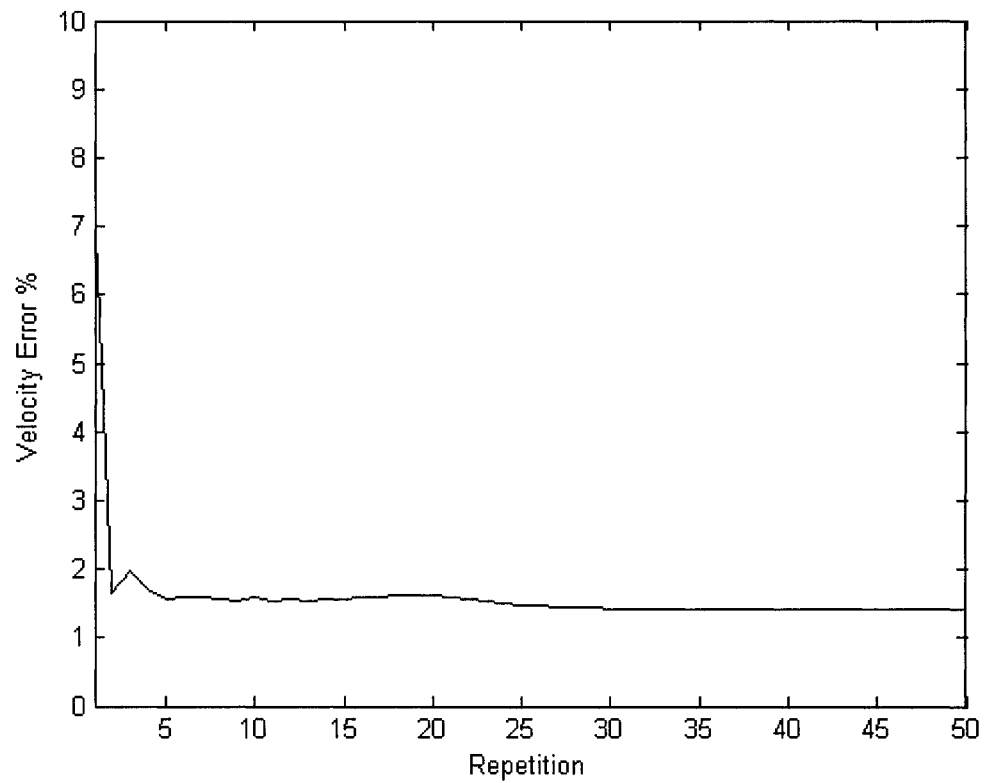


Figure 9.18: Velocity error versus repetitions of the final modified inputs
using repetitive control

Table 9.2: Comparison between the six-bar Stephenson mechanism
and the slider-crank mechanism used in scanning machines

Criterion	Six-bar Stephenson mechanism	Slider-crank mechanism	Improvement
Number of links	6	3	50%
Mechanism's mass	7.742 Kg	0.01227 Kg	0.16%
Mechanism's space	1.170 m ²	0.2268 m ²	19%
Motor's volume	3749 cm ³	50.57 cm ³	1.3%
Motor's weight	10.7 Kg	0.133 Kg	1.2%
Scanned pages per cycle	1	2	200%
Gear ratio	20	1	5%

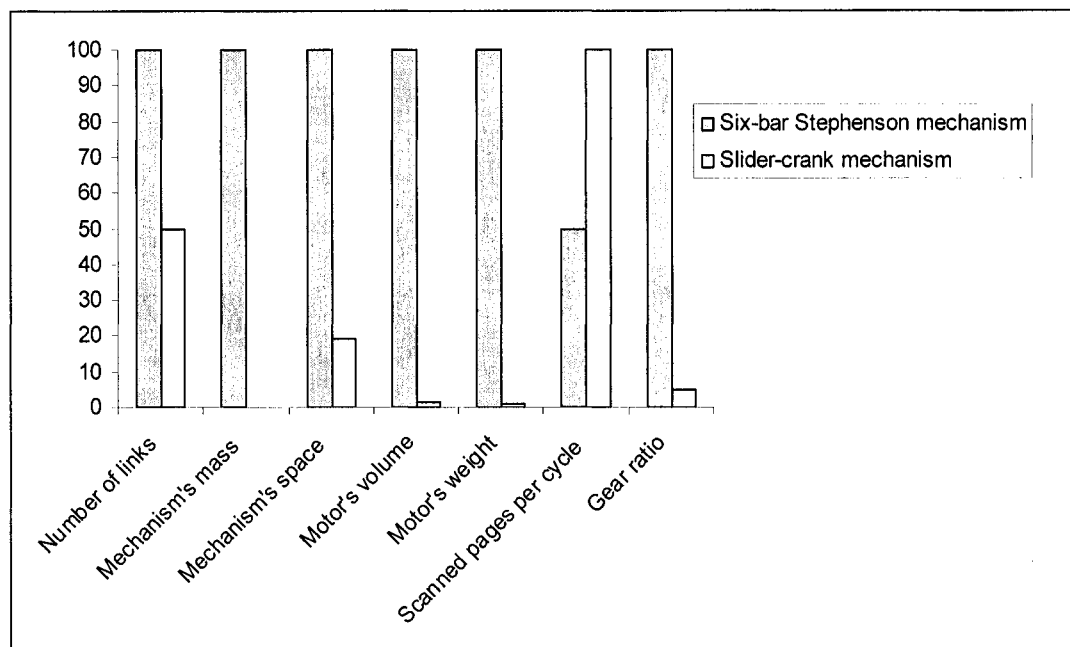


Figure 9.19: A comparison between the six-bar Stephenson mechanism and the slider crank mechanism, used in scanning machines

9.4 Discussion of results

The velocity error shows an irregular decrease until the 50th repetition because the weight of minimizing the error was increased while the control methods were still learning the system's behavior. When the error was reduced to less than 10% and the change in the inputs became very small, the velocity error showed relatively smooth convergence to the desired output. The final error in both control methods was less than 2%.

The plots of the input angles show that the system made minor modifications to the input angles because the system had started from some input angles that are close to the optimum ones. The input angles of the learning control show smooth acceleration of the mechanism at the beginning and smooth deceleration at the end in order to minimize the vibrations caused by sudden changes in the velocity. The high slope of the input angles at the middle of the cycle indicates an increase in the angular velocity. This occurs because the control methods speed up the mechanism at the regions outside the constant velocity regions, to ensure that the mechanism completes one revolution per sec. In addition, as the crank link comes closer to 180°, the output velocity of the slider becomes less sensitive to the input speed. Therefore, increasing the angular velocity of the crank link would stabilize the output velocity of the slider.

The output displacement shows flat segments at the beginning and the end of the cycle because the slider reaches the extreme positions at these instances, and the sensitivity of the output velocity becomes insignificant with respect to the changes in the input speed. A slight jump appears at the end of the cycle in the case of repetitive control because the system does not stop the motion, and some excessive vibration occurs at that time. However, since in the learning control case the system was forced to stop smoothly at the end of the cycle, the output displacement at that instant is flat and smooth. Observe that the constant output velocity regions are indicated by the straight paths occurring in the rise and return segments.

The slider output velocity shows the significant difference between the 1st and 100th repetitions. The fluctuation of the output velocity is replaced by some stable motion by adjusting the input speed of the mechanism through repetitions, and the major vibrations at the constant velocity regions are absorbed effectively. The small vibrations appearing in the unconcerned regions are due to less controllability at those positions or to less importance of the vibrations in disturbing the scanning process. Although the input speed is smooth at the end of the cycle, a slight drop in the output velocity occurs at that time because of the incidence of the excessive vibrations of the links.

Figures 9.6 and 9.14 show the convergence sequence of the output velocity to what is desired. In the earliest repetitions, the system does not show any constant output

velocity until about the 20th repetition, when the system started exhibiting some irregular constant velocity, which means that the learning process becomes more applicable after this number of repetitions.

The deflections occurring to the links increase at the middle and the end of the cycle because the mechanism starts increasing and decreasing the angular velocity at the middle and end respectively, which subsequently disturbs the shaking movements of the links. The maximum deflection in the crank link is about four times greater than it is in the driven link because the crank link is the one that is subjected to the input torque, while the driven link is free from any external loads. Notice that the maximum deflection of the crank link is greater than the diameter by two times. However, since the safety factor is around 16, there is no threat of rupture.

The output torque from the motor, which is driving the mechanism, shows some fluctuations, especially when the input speed is changed. The alternating of the sign at those regions occurs because of the need of strict control at those critical regions due to the acceleration of the mechanism and to the high inertia thrust of the driven link. This is also observed at the end of the motion, when the mechanism needs to reach the desired position and speed.

The frequency content of the vibrating links is consistent with the frequency of the input torque to the mechanism. Although the natural frequency of the crank link traverses the torque's frequency, the system does not reach the resonance because of the presence of internal damping. The same thing was observed for the driven link, where the frequency of the torque does not reach the natural frequency of the link, and the internal damping makes the vibration in the natural frequency vanish.

Figure 9.18 shows the velocity error versus repetitions when the final modified inputs are used in the case of repetitive control from the first repetition. The velocity error becomes less than 2% from the second repetition, which means that the scanning machine could start processing the job after one revolution of the mechanism. It also keeps the error within the acceptable limits for all upcoming cycles.

The comparison shown in table 9.2 and figure 9.19 shows how the use of the control methods improves the overall quality of the scanning machine. By employing the learning and repetitive control method, the required mechanism was simplified by reducing the number of links, the mechanism's mass and required space were considerably reduced, the motor's size and weight were significantly reduced, the large gears were replaced by small gears, and the productivity of the scanning machine was doubled.

Chapter 10

Conclusion

Applying learning and repetitive control methods in linkages mechanisms would lead to a great improvement for creating a new generation of mechanisms that are more efficient in performing jobs. These methods work successfully in minimizing the effect of vibrated elements and internal elasticity of the links, even when dealing with highly non-linear systems. Also, these control methods are capable of identifying any small disturbances or changes that could occur to the system during motion, and modify the inputs accordingly.

The learning and repetitive control methods rapidly learn how to bring the system to the desired motion in few repetitions, and definitely, this will minimize the energy required to keep the system tracking the desired motion. In addition, they work remarkably in controlling non-linear vibrated systems according to any specific criterion.

As shown in the previous cases, the control methods treat the system like a black box. They do not consider the internal actions between parts, as they relate the outputs to the inputs directly. This procedure simplifies the control scheme, since the interior processes are insignificant in learning the system's behavior.

The use of these control methods has also an influence on the overall characteristics of the systems. Besides reducing the error in controlling these systems, simpler and light machines can be used instead of larger ones. Also, the consumption of the input power can be reduced significantly by reducing the size and the number of the used motors.

Besides the studied cases, more tasks undoubtedly are able to be performed effectively by these methods. Moreover, they definitely will expand and extend the area of linkages mechanisms applications that were unable to be performed by the old-fashioned constant input speed mechanism.

Furthermore, one of the great advantages of using the repetitive control method is that the cyclical mechanical systems do not need to stop the motion for control purposes. The repetitive control modifies the inputs while the systems are running simultaneously, so they save time and energy.

More investigations, indeed, are needed to optimize the parameters that are involved in the learning and optimizing processes, and to improve the performance of the control methods.

Appendix A

Derivation of the Optimized Input

$$Y_{i+1} = \underline{A}_i x_{i+1}(0) + \underline{B}_i U_{i+1}$$

$$Y_{i+1} = \underline{A}_i x_{i+1}(0) + \underline{B}_i (U_i + \delta U_{i+1}) + \underline{A}_i (x_i(0) - x_i(0))$$

$$Y_{i+1} = [\underline{B}_i U_i + \underline{A}_i x_i(0)] + \underline{A}_i [x_{i+1}(0) - x_i(0)] + \underline{B}_i \delta U_{i+1}$$

$$Y_{i+1} = Y_i + \underline{A}_i [x_{i+1}(0) - x_i(0)] + \underline{B}_i \delta U_{i+1}$$

$$e_{i+1} = Y^* - Y_{i+1} = \underbrace{Y^* - Y_i - \underline{A}_i [x_{i+1}(0) - x_i(0)]}_{F_{i+1}} - \underline{B}_i \delta U_{i+1}$$

$$e_{i+1} = F_{i+1} - \underline{B}_i \delta U_{i+1}$$

$$J = \frac{1}{2} e_{i+1}^T \underline{Q} e_{i+1} + \frac{1}{2} \delta U_{i+1}^T \underline{S} \delta U_{i+1}$$

$$J = \frac{1}{2} (F_{i+1} - \underline{B}_i \delta U_{i+1})^T \underline{Q} (F_{i+1} - \underline{B}_i \delta U_{i+1}) + \frac{1}{2} \delta U_{i+1}^T \underline{S} \delta U_{i+1}$$

$$J = \frac{1}{2} \left(F_{i+1}^T \underline{Q} F_{i+1} - F_{i+1}^T \underline{Q} \underline{B}_i \delta U_{i+1} - \delta U_{i+1}^T \underline{B}_i^T \underline{Q} F_{i+1} + \delta U_{i+1}^T \underline{B}_i^T \underline{Q} \underline{B}_i \delta U_{i+1} + \delta U_{i+1}^T \underline{S} \delta U_{i+1} \right)$$

$$\frac{\partial J}{\partial (\delta U_{i+1})} = -\frac{1}{2} F_{i+1}^T \underline{Q} \underline{B}_i - \frac{1}{2} (\underline{B}_i^T \underline{Q} F_{i+1})^T + \delta U_{i+1}^T \underline{B}_i^T \underline{Q} \underline{B}_i + \delta U_{i+1}^T \underline{S}$$

$$\frac{\partial J}{\partial(\delta U_{i+1})} = -F_{i+1}^T \underline{Q} \underline{B}_i + \delta U_{i+1}^T \underline{B}_i^T \underline{Q} \underline{B}_i + \delta U_{i+1}^T \underline{S}$$

$$\frac{\partial J}{\partial(\delta U_{i+1})} = 0 \Rightarrow -F_{i+1}^T \underline{Q} \underline{B}_i + \delta U_{i+1}^T \underline{B}_i^T \underline{Q} \underline{B}_i + \delta U_{i+1}^T \underline{S} = 0$$

$$-\underline{B}_i^T \underline{Q} F_{i+1} + \underline{B}_i^T \underline{Q} \underline{B}_i \delta U_{i+1} + \underline{S} \delta U_{i+1} = 0$$

$$\delta U_{i+1} = (\underline{B}_i^T \underline{Q} \underline{B}_i + \underline{S})^{-1} \underline{B}_i^T \underline{Q} F_{i+1}$$

$$\delta U_{i+1} = (\underline{B}_i^T \underline{Q} \underline{B}_i + \underline{S})^{-1} \underline{B}_i^T \underline{Q} \{Y^* - Y_i - \underline{A}_i [x_{i+1}(0) - x_i(0)]\}$$

Appendix B

Derivation of the Equations of Motion of the Flexible Slider-Crank

Mechanism by Lagrange's Equations

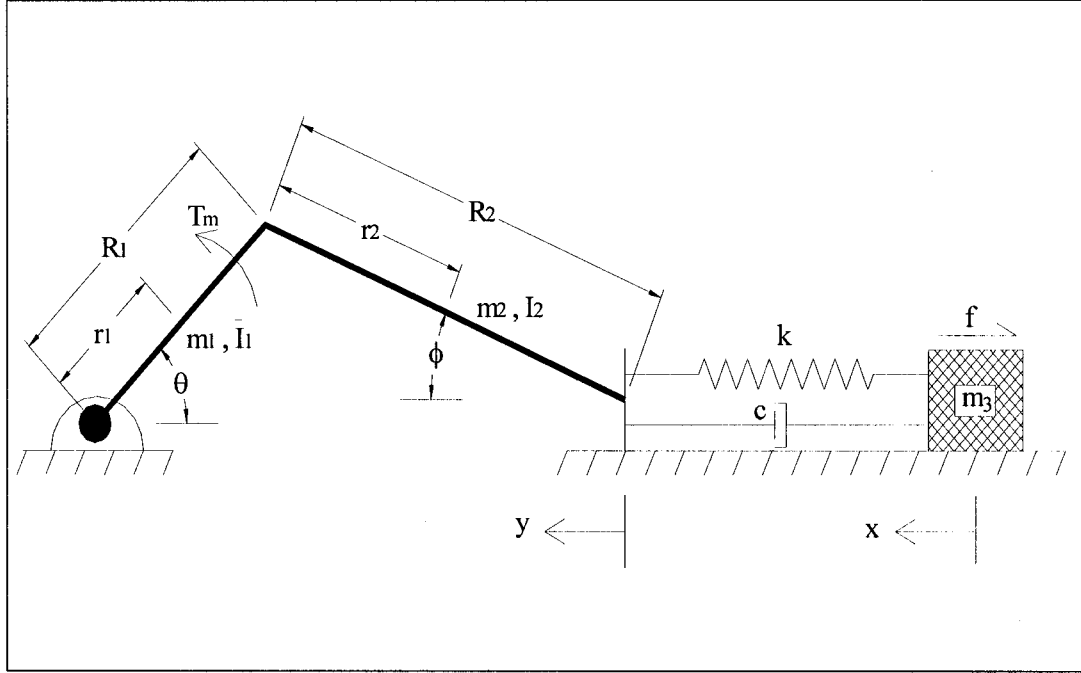


Figure B.1: Flexible slider-crank mechanism

$$\vec{P}_2 = R_1 e^{i\theta} + r_2 e^{-i\phi} = (R_1 C_\theta + r_2 C_\phi)_x + (R_1 S_\theta - r_2 S_\phi)_y$$

$$\vec{V}_2 = \dot{\vec{P}}_2 = (-R_1 \dot{\theta} S_\theta - r_2 \dot{\phi} S_\phi)_x + (R_1 \dot{\theta} C_\theta - r_2 \dot{\phi} C_\phi)_y$$

$$V_2^2 = R_1^2 \dot{\theta}^2 + r_2^2 \dot{\phi}^2 - 2R_1 r_2 \dot{\theta} \dot{\phi} C_{\theta+\phi}$$

$$\bar{y} = R_1 + R_2 - R_1 C_\theta - R_2 C_\phi$$

$$L = \frac{1}{2} \bar{I}_1 \dot{\theta}^2 + \frac{1}{2} I_2 \dot{\phi}^2 + \frac{1}{2} m_2 V_2^2 + \frac{1}{2} m_3 \dot{x}_3^2 - \frac{1}{2} k(y-x)^2 + \lambda(R_1 S_\theta - R_2 S_\phi)$$

$$L = \frac{1}{2} \bar{I}_1 \dot{\theta}^2 + \frac{1}{2} I_2 \dot{\phi}^2 + \frac{1}{2} m_2 (R_1^2 \dot{\theta}^2 + r_2^2 \dot{\phi}^2 - 2R_1 r_2 \dot{\theta} \dot{\phi} C_{\theta+\phi}) + \frac{1}{2} m_3 \dot{x}_3^2 - \frac{1}{2} k(R_1 + R_2 - R_1 C_\theta - R_2 C_\phi - x)^2 + \lambda(R_1 S_\theta - R_2 S_\phi)$$

$$\bar{I}_1 = N^2 J_m + J_M$$

$$\frac{d}{dt} \frac{\partial L}{\partial \dot{\theta}} = (\bar{I}_1 + m_2 R_1^2) \ddot{\theta} - m_2 R_1 r_2 C_{\theta+\phi} \ddot{\phi} + m_2 R_1 r_2 \dot{\phi} (\dot{\theta} + \dot{\phi}) S_{\theta+\phi}$$

$$\frac{\partial L}{\partial \theta} = m_2 R_1 r_2 \dot{\phi} \dot{\theta} S_{\theta+\phi} + \lambda R_1 C_\theta - k(R_1 + R_2 - R_1 C_\theta - R_2 C_\phi - x) R_1 S_\theta$$

$$\frac{d}{dt} \frac{\partial L}{\partial \dot{\phi}} = (I_2 + m_2 r_2^2) \ddot{\phi} - m_2 R_1 r_2 C_{\theta+\phi} \ddot{\theta} + m_2 R_1 r_2 \dot{\theta} (\dot{\theta} + \dot{\phi}) S_{\theta+\phi}$$

$$\frac{\partial L}{\partial \phi} = m_2 R_1 r_2 \dot{\phi} \dot{\theta} S_{\theta+\phi} - \lambda R_2 C_\phi - k(R_1 + R_2 - R_1 C_\theta - R_2 C_\phi - x) R_2 S_\phi$$

$$\frac{d}{dt} \frac{\partial L}{\partial \dot{x}} = m_3 \ddot{x}$$

$$\frac{\partial L}{\partial x} = k(R_1 + R_2 - R_1 C_\theta - R_2 C_\phi - x)$$

$$\frac{d}{dt} \frac{\partial L}{\partial \dot{\lambda}} = 0$$

$$\frac{\partial L}{\partial \lambda} = R_1 S_\theta - R_2 S_\phi$$

$$\delta W = Q_\theta \delta \theta + Q_\phi \delta \phi + Q_x \delta x$$

$$\delta W = T_m \delta \psi - f \delta x - c(\dot{y} - \dot{x}) \delta(y - x)$$

$$T_m = \frac{K_t}{R_s} (V - K_e N \dot{\theta})$$

$$\psi = N\theta$$

$$f = \mu m_3 g \operatorname{sign}(\dot{x})$$

$$\dot{y} = R_1 \dot{\theta} S_\theta + R_2 \dot{\phi} S_\phi$$

$$\delta y = \delta(R_1 + R_2 - R_1 C_\theta - R_2 C_\phi) = R_1 S_\theta \delta \theta + R_2 S_\phi \delta \phi$$

$$\delta W = T_m N \delta \theta - f \delta x - c(R_1 \dot{\theta} S_\theta + R_2 \dot{\phi} S_\phi - \dot{x})(R_1 S_\theta \delta \theta + R_2 S_\phi \delta \phi - \delta x)$$

$$Q_\theta = N T_m - c R_1 S_\theta (R_1 \dot{\theta} S_\theta + R_2 \dot{\phi} S_\phi - \dot{x})$$

$$Q_\phi = -c R_2 S_\phi (R_1 \dot{\theta} S_\theta + R_2 \dot{\phi} S_\phi - \dot{x})$$

$$Q_x = -\mu m_3 g \operatorname{sign}(\dot{x}) + c(R_1 \dot{\theta} S_\theta + R_2 \dot{\phi} S_\phi - \dot{x})$$

$$\frac{d}{dt} \frac{\partial L}{\partial \dot{\theta}} - \frac{\partial L}{\partial \theta} = Q_{\theta}$$

$$\begin{aligned} & (\bar{I}_1 + m_2 R_1^2) \ddot{\theta} - m_2 R_1 r_2 C_{\theta+\phi} \ddot{\phi} + m_2 R_1 r_2 \dot{\phi}^2 S_{\theta+\phi} - \lambda R_1 C_{\theta} \\ & + k(R_1 + R_2 - R_1 C_{\theta} - R_2 C_{\phi} - x) R_1 S_{\theta} = \frac{NK_1}{R_s} (V - K_e N \dot{\theta}) - c R_1 S_{\theta} (R_1 \dot{\theta} S_{\theta} + R_2 \dot{\phi} S_{\phi} - \dot{x}) \end{aligned}$$

$$\frac{d}{dt} \frac{\partial L}{\partial \dot{\phi}} - \frac{\partial L}{\partial \phi} = Q_{\phi}$$

$$\begin{aligned} & (I_2 + m_2 r_2^2) \ddot{\phi} - m_2 R_1 r_2 C_{\theta+\phi} \ddot{\theta} + m_2 R_1 r_2 \dot{\theta}^2 S_{\theta+\phi} + \lambda R_2 C_{\phi} + k(R_1 + R_2 - R_1 C_{\theta} - R_2 C_{\phi} - x) R_2 S_{\phi} \\ & = -c R_2 S_{\phi} (R_1 \dot{\theta} S_{\theta} + R_2 \dot{\phi} S_{\phi} - \dot{x}) \end{aligned}$$

$$\frac{d}{dt} \frac{\partial L}{\partial \dot{x}} - \frac{\partial L}{\partial x} = Q_x$$

$$m_3 \ddot{x} - k(R_1 + R_2 - R_1 C_{\theta} - R_2 C_{\phi} - x) = -\mu m_3 g \text{sign}(\dot{x}) + c(R_1 \dot{\theta} S_{\theta} + R_2 \dot{\phi} S_{\phi} - \dot{x})$$

$$\frac{d}{dt} \frac{\partial L}{\partial \dot{\lambda}} - \frac{\partial L}{\partial \lambda} = 0 \rightarrow \frac{d^2}{dt^2} \left(\frac{d}{dt} \frac{\partial L}{\partial \dot{\lambda}} - \frac{\partial L}{\partial \lambda} \right) = 0$$

$$R_1 C_{\theta} \ddot{\theta} - R_1 \dot{\theta}^2 S_{\theta} - R_2 C_{\phi} \ddot{\phi} + R_2 \dot{\phi}^2 S_{\phi} = 0$$

$$\begin{bmatrix} \bar{I}_1 + m_2 R_1^2 & -m_2 R_1 r_2 C_{\theta+\phi} & 0 & -R_1 C_\theta \\ -m_2 R_1 r_2 C_{\theta+\phi} & I_2 + m_2 r_2^2 & 0 & R_2 C_\phi \\ 0 & 0 & m_3 & 0 \\ R_1 C_\theta & -R_2 C_\phi & 0 & 0 \end{bmatrix} \begin{bmatrix} \ddot{\theta} \\ \ddot{\phi} \\ \ddot{x} \\ \lambda \end{bmatrix} \\
= \begin{bmatrix} E_1 \\ E_2 \\ -\mu m_3 g \text{sign}(\dot{x}) + c(R_1 \dot{\theta} S_\theta + R_2 \dot{\phi} S_\phi - \dot{x}) + k(R_1 + R_2 - R_1 C_\theta - R_2 C_\phi - x) \\ R_1 \dot{\theta}^2 S_\theta - R_2 \dot{\phi}^2 S_\phi \end{bmatrix}$$

$$E_1 = \frac{NK_t}{R_s} (V - K_e N \dot{\theta}) - c R_1 S_\theta (R_1 \dot{\theta} S_\theta + R_2 \dot{\phi} S_\phi - \dot{x}) - m_2 R_1 r_2 \dot{\phi}^2 S_{\theta+\phi} - k(R_1 + R_2 - R_1 C_\theta - R_2 C_\phi - x) R_1 S_\theta$$

$$E_2 = -c R_2 S_\phi (R_1 \dot{\theta} S_\theta + R_2 \dot{\phi} S_\phi - \dot{x}) - m_2 R_1 r_2 \dot{\theta}^2 S_{\theta+\phi} - k(R_1 + R_2 - R_1 C_\theta - R_2 C_\phi - x) R_2 S_\phi$$

$$V = K_p (\theta_r - \theta) + K_d (\dot{\theta}_r - \dot{\theta})$$

S: Sin

C: Cos

\bar{I}_1 : Total moment of inertia of the motor shaft, gears and driving link.

J_m : Moment of inertia of the motor shaft and the small gear.

J_M : Moment of inertia of the driving link and the large gear.

P_2 : Displacement of the center of gravity of the driven link.

V_2 : Velocity of the center of gravity of the driven link.

K_t : Motor torque constant.

K_e : Motor back EMF constant.

R_s : Armature resistance.

V : Motor input voltage.

N : Gear ratio (>1).

$\dot{\psi}$: Motor speed.

θ_r : Reference input angle.

K_p : Proportional controller gain.

K_d : Derivative controller gain.

Appendix C

Derivation of the Equations of Motion of the Rigid Slider-Crank

Mechanism by Lagrange's Equations

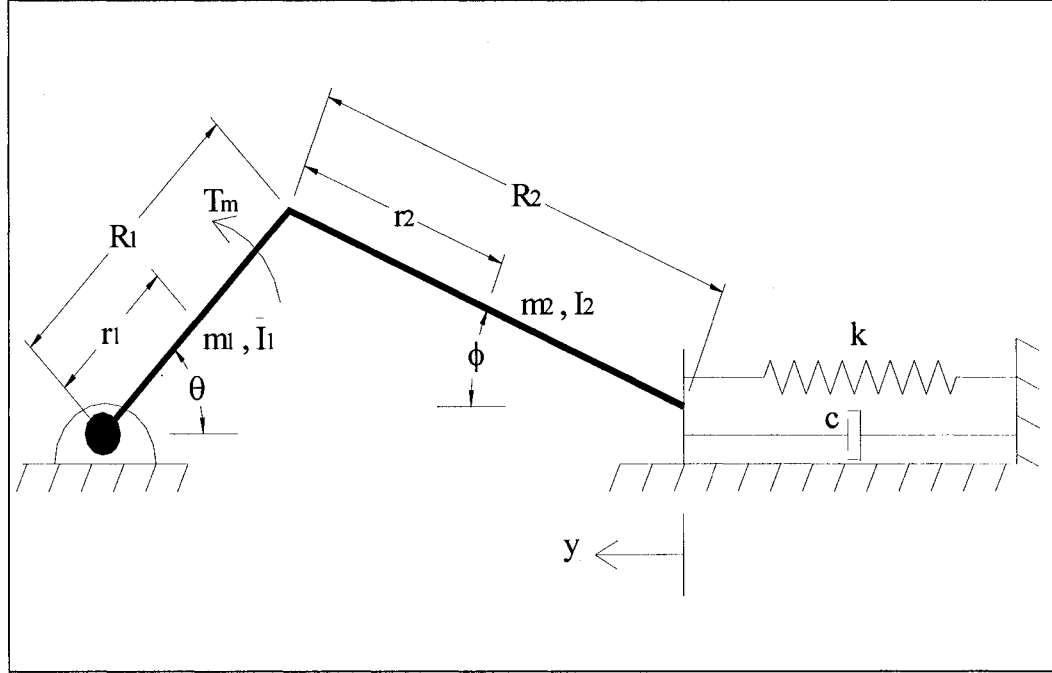


Figure C.1: Rigid slider-crank mechanism

$$\vec{P}_2 = R_1 e^{i\theta} + r_2 e^{-i\phi} = (R_1 C_\theta + r_2 C_\phi)_x + (R_1 S_\theta - r_2 S_\phi)_y$$

$$\vec{V}_2 = \dot{\vec{P}}_2 = (-R_1 \dot{\theta} S_\theta - r_2 \dot{\phi} S_\phi)_x + (R_1 \dot{\theta} C_\theta - r_2 \dot{\phi} C_\phi)_y$$

$$V_2^2 = R_1^2 \dot{\theta}^2 + r_2^2 \dot{\phi}^2 - 2R_1 r_2 \dot{\theta} \dot{\phi} C_{\theta+\phi}$$

$$\bar{y} = R_1 + R_2 - R_1 C_\theta - R_2 C_\phi$$

$$L = \frac{1}{2} \bar{I}_1 \dot{\theta}^2 + \frac{1}{2} I_2 \dot{\phi}^2 + \frac{1}{2} m_2 V_2^2 - \frac{1}{2} k y^2 + \lambda (R_1 S_\theta - R_2 S_\phi)$$

$$L = \frac{1}{2} \bar{I}_1 \dot{\theta}^2 + \frac{1}{2} I_2 \dot{\phi}^2 + \frac{1}{2} m_2 (R_1^2 \dot{\theta}^2 + r_2^2 \dot{\phi}^2 - 2 R_1 r_2 \dot{\theta} \dot{\phi} C_{\theta+\phi}) \\ - \frac{1}{2} k (R_1 + R_2 - R_1 C_\theta - R_2 C_\phi)^2 + \lambda (R_1 S_\theta - R_2 S_\phi)$$

$$\bar{I}_1 = N^2 J_m + J_M$$

$$\frac{d}{dt} \frac{\partial L}{\partial \dot{\theta}} = (\bar{I}_1 + m_2 R_1^2) \ddot{\theta} - m_2 R_1 r_2 C_{\theta+\phi} \ddot{\phi} + m_2 R_1 r_2 \dot{\phi} (\dot{\theta} + \dot{\phi}) S_{\theta+\phi}$$

$$\frac{\partial L}{\partial \theta} = m_2 R_1 r_2 \dot{\phi} \dot{\theta} S_{\theta+\phi} + \lambda R_1 C_\theta - k (R_1 + R_2 - R_1 C_\theta - R_2 C_\phi) R_1 S_\theta$$

$$\frac{d}{dt} \frac{\partial L}{\partial \dot{\phi}} = (I_2 + m_2 r_2^2) \ddot{\phi} - m_2 R_1 r_2 C_{\theta+\phi} \ddot{\theta} + m_2 R_1 r_2 \dot{\theta} (\dot{\theta} + \dot{\phi}) S_{\theta+\phi}$$

$$\frac{\partial L}{\partial \phi} = m_2 R_1 r_2 \dot{\phi} \dot{\theta} S_{\theta+\phi} - \lambda R_2 C_\phi - k (R_1 + R_2 - R_1 C_\theta - R_2 C_\phi) R_2 S_\phi$$

$$\frac{d}{dt} \frac{\partial L}{\partial \dot{\lambda}} = 0$$

$$\frac{\partial L}{\partial \lambda} = R_1 S_\theta - R_2 S_\phi$$

$$\delta W = Q_{\theta} \delta \theta + Q_{\phi} \delta \phi$$

$$\delta W = T_m \delta \psi - c \dot{y} \delta y$$

$$T_m = \frac{K_t}{R_s} (V - K_e N \dot{\theta})$$

$$\psi = N \theta$$

$$\dot{y} = R_1 \dot{\theta} S_{\theta} + R_2 \dot{\phi} S_{\phi}$$

$$\delta y = \delta (R_1 + R_2 - R_1 C_{\theta} - R_2 C_{\phi}) = R_1 S_{\theta} \delta \theta + R_2 S_{\phi} \delta \phi$$

$$\delta W = T_m N \delta \theta - c (R_1 \dot{\theta} S_{\theta} + R_2 \dot{\phi} S_{\phi}) (R_1 S_{\theta} \delta \theta + R_2 S_{\phi} \delta \phi)$$

$$Q_{\theta} = N T_m - c R_1 S_{\theta} (R_1 \dot{\theta} S_{\theta} + R_2 \dot{\phi} S_{\phi})$$

$$Q_{\phi} = -c R_2 S_{\phi} (R_1 \dot{\theta} S_{\theta} + R_2 \dot{\phi} S_{\phi})$$

$$\frac{d}{dt} \frac{\partial L}{\partial \dot{\theta}} - \frac{\partial L}{\partial \theta} = Q_{\theta}$$

$$\begin{aligned} & (\bar{I}_1 + m_2 R_1^2) \ddot{\theta} - m_2 R_1 r_2 C_{\theta+\phi} \ddot{\phi} + m_2 R_1 r_2 \dot{\phi}^2 S_{\theta+\phi} - \lambda R_1 C_{\theta} \\ & + k (R_1 + R_2 - R_1 C_{\theta} - R_2 C_{\phi}) R_1 S_{\theta} = \frac{N K_t}{R_s} (V - K_e N \dot{\theta}) - c R_1 S_{\theta} (R_1 \dot{\theta} S_{\theta} + R_2 \dot{\phi} S_{\phi}) \end{aligned}$$

$$\frac{d}{dt} \frac{\partial L}{\partial \dot{\phi}} - \frac{\partial L}{\partial \phi} = Q_{\phi}$$

$$\begin{aligned} & (I_2 + m_2 r_2^2) \ddot{\phi} - m_2 R_1 r_2 C_{\theta+\phi} \ddot{\theta} + m_2 R_1 r_2 \dot{\theta}^2 S_{\theta+\phi} + \lambda R_2 C_{\phi} \\ & + k(R_1 + R_2 - R_1 C_{\theta} - R_2 C_{\phi}) R_2 S_{\phi} = -c R_2 S_{\phi} (R_1 \dot{\theta} S_{\theta} + R_2 \dot{\phi} S_{\phi}) \end{aligned}$$

$$\frac{d}{dt} \frac{\partial L}{\partial \dot{\lambda}} - \frac{\partial L}{\partial \lambda} = 0 \rightarrow \frac{d^2}{dt^2} \left(\frac{d}{dt} \frac{\partial L}{\partial \dot{\lambda}} - \frac{\partial L}{\partial \lambda} \right) = 0$$

$$R_1 C_{\theta} \ddot{\theta} - R_1 \dot{\theta}^2 S_{\theta} - R_2 C_{\phi} \ddot{\phi} + R_2 \dot{\phi}^2 S_{\phi} = 0$$

$$\begin{bmatrix} \bar{I}_1 + m_2 R_1^2 & -m_2 R_1 r_2 C_{\theta+\phi} & -R_1 C_{\theta} \\ -m_2 R_1 r_2 C_{\theta+\phi} & I_2 + m_2 r_2^2 & R_2 C_{\phi} \\ R_1 C_{\theta} & -R_2 C_{\phi} & 0 \end{bmatrix} \begin{bmatrix} \ddot{\theta} \\ \ddot{\phi} \\ \lambda \end{bmatrix} = \begin{bmatrix} E_1 \\ E_2 \\ R_1 \dot{\theta}^2 S_{\theta} - R_2 \dot{\phi}^2 S_{\phi} \end{bmatrix}$$

$$\begin{aligned} E_1 = \frac{NK_t}{R_s} (V - K_e N \dot{\theta}) - c R_1 S_{\theta} (R_1 \dot{\theta} S_{\theta} + R_2 \dot{\phi} S_{\phi}) - m_2 R_1 r_2 \dot{\phi}^2 S_{\theta+\phi} \\ - k(R_1 + R_2 - R_1 C_{\theta} - R_2 C_{\phi}) R_1 S_{\theta} \end{aligned}$$

$$\begin{aligned} E_2 = -c R_2 S_{\phi} (R_1 \dot{\theta} S_{\theta} + R_2 \dot{\phi} S_{\phi}) - m_2 R_1 r_2 \dot{\theta}^2 S_{\theta+\phi} \\ - k(R_1 + R_2 - R_1 C_{\theta} - R_2 C_{\phi}) R_2 S_{\phi} \end{aligned}$$

$$V = K_p (\theta_r - \theta) + K_d (\dot{\theta}_r - \dot{\theta})$$

S: Sin

C: Cos

\bar{I}_1 : Total moment of inertia of the motor shaft, gears and driving link.

J_m : Moment of inertia of the motor shaft and the small gear.

J_M : Moment of inertia of the driving link and the large gear.

P_2 : Displacement of the center of gravity of the driven link.

V_2 : Velocity of the center of gravity of the driven link.

K_t : Motor torque constant.

K_e : Motor back EMF constant.

R_s : Armature resistance.

V: Motor input voltage.

N: Gear ratio (>1).

$\dot{\psi}$: Motor speed.

θ_r : Reference input angle.

K_p : Proportional controller gain.

K_d : Derivative controller gain.

Appendix D

Derivation of the Equations of Motion of the Flexible Six-Bar

Stephenson Mechanism by Lagrange's Equations

Part 1: Determining the critical damping of a simple cantilever

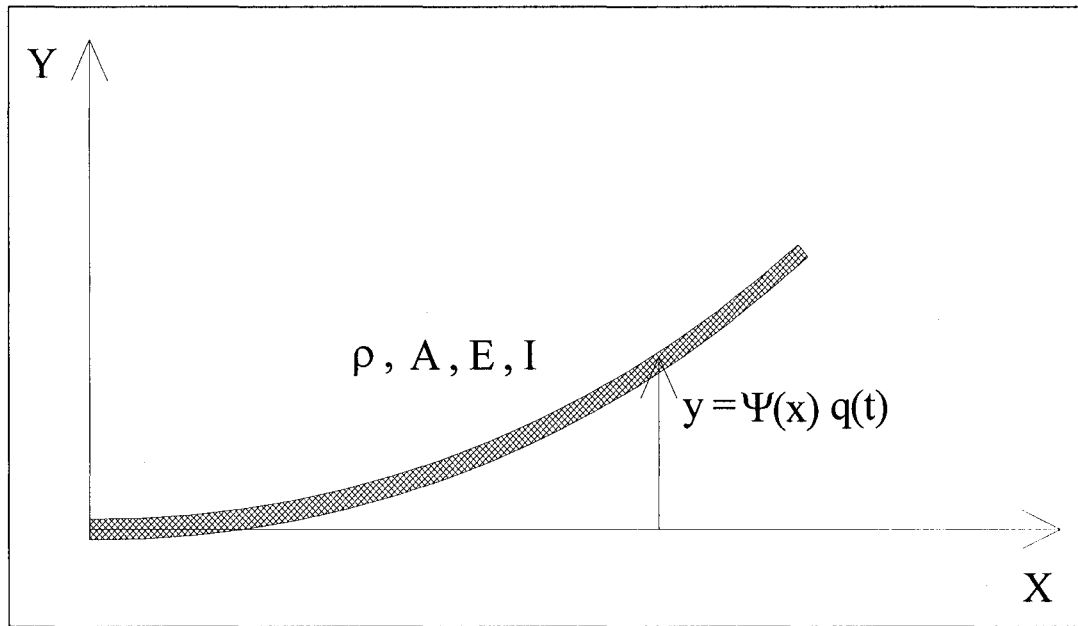


Figure D.1: A flexible cantilever deflected on the X-Y plane

The internal critical damping of a flexible continuous clamped-free cantilever (Figure D.1) that goes under free vibrations can be obtained by deriving the governing equations from the Lagrange's equations. By employing the assumed mode shapes method and considering only the first mode shape of vibration, the Lagrangian of the cantilever can be written as

$$L = \frac{1}{2} \rho A \int_0^R \dot{y}^2 dx - \frac{1}{2} EI \int_0^R y''^2 dx = \frac{1}{2} \rho A \dot{q}^2 \int_0^R (\Psi(x))^2 dx - \frac{1}{2} EI q^2 \int_0^R (\Psi''(x))^2 dx$$

where ρ is the volume density, A is the cross sectional area, R is the cantilever's length, y is the deflection, E is the modulus of elasticity, I is the area moment of inertia of the cross section around its center line, Ψ is the first mode shape, and q is the time dependent function.

By differentiating the Lagrangian and considering the non-conservative work done by the internal damping, one obtains:

$$\frac{d}{dt} \frac{\partial L}{\partial \dot{q}} - \frac{\partial L}{\partial q} = Q$$

$$\partial W_{\text{Damping}} = - \left(\int_0^R c \dot{q} \Psi^2(x) dx \right) \partial q = Q \partial q$$

$$\Rightarrow Q = -c \dot{q} \int_0^R \Psi^2(x) dx$$

$$\rho A \ddot{q} \int_0^R (\Psi(x))^2 dx + c \dot{q} \int_0^R \Psi^2(x) dx + EI q \int_0^R (\Psi''(x))^2 dx = 0$$

$$\left\{ c \int_0^R \Psi^2(x) dx \right\}^2 - 4 \left\{ \rho A \int_0^R (\Psi(x))^2 dx \right\} \left\{ EI \int_0^R (\Psi''(x))^2 dx \right\} = 0 \quad D.1$$

$$\Psi''(x) = \omega^2 \Psi(x)$$

and equation D.1 becomes

$$c^2 - 4\rho AEI\omega^4 = 0 \Rightarrow c = c_{cr.}$$

$$\Rightarrow c_{cr.} = 2\omega^2 \sqrt{\rho AEI} \quad D.2$$

$$\Rightarrow Q = -2\zeta\omega^2 \sqrt{\rho AEI} \dot{q} \int_0^R \Psi^2(x) dx$$

where $c_{cr.}$ is the critical damping.

Part 2: Lagrange's equations of motion

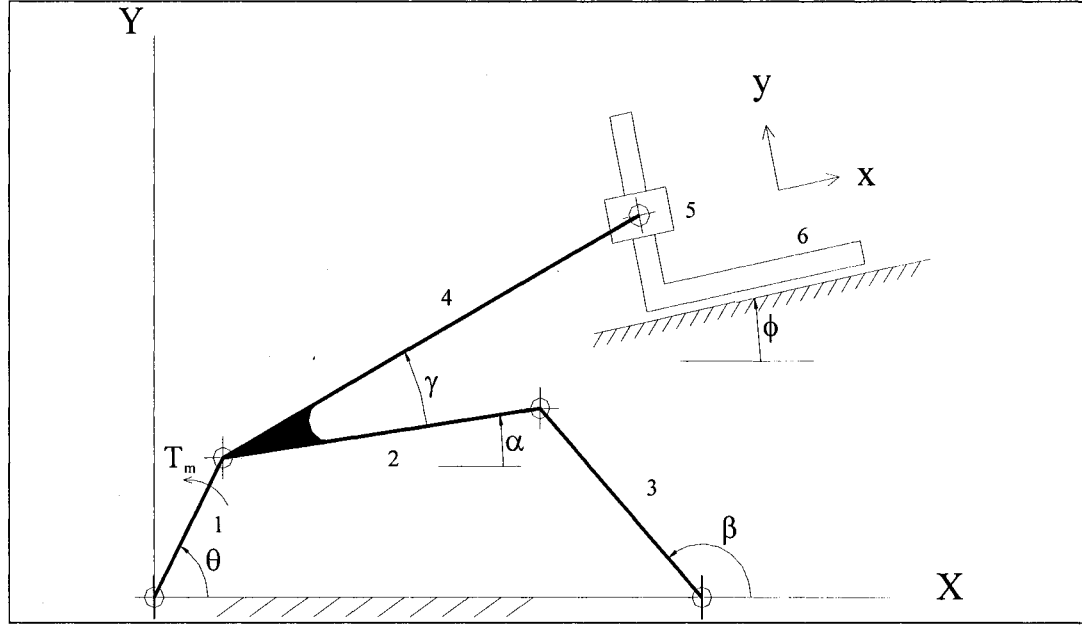


Figure D.2: The flexible Six-bar Stephenson Mechanism

$$y_i = \Psi_i(x)q_i(t) , \quad i=1,2,4$$

$$\Psi_1(x) = \sin(\omega_1 x) - \sinh(\omega_1 x) - \left\{ \frac{\sin(\omega_1) + \sinh(\omega_1)}{\cos(\omega_1) + \cosh(\omega_1)} \right\} \{ \cos(\omega_1 x) - \cosh(\omega_1 x) \}$$

$$\Psi_2(x) = \sin(\omega_2 x)$$

$$\Psi_4(x) = \sin(\omega_4 x) - \sinh(\omega_4 x) - \left\{ \frac{\sin(\omega_4) + \sinh(\omega_4)}{\cos(\omega_4) + \cosh(\omega_4)} \right\} \{ \cos(\omega_4 x) - \cosh(\omega_4 x) \}$$

$$\omega_1 = \frac{1.875104}{R_1} , \quad \omega_2 = \frac{\pi}{R_2} , \quad \omega_4 = \frac{1.875104}{R_4}$$

y is the deflection of the i^{th} link, ψ is the first mode shape of links 1, 2 and 4. The deflection y of each link is measured with respect to the local coordinate system that corresponds to the link's angle as shown in figure D.3. The position of any arbitrary point on link 1 with respect to the global coordinate system can be represented by a vector notation as shown in figure D.3 (a), as follows:

$$\vec{r}_1(x) = xe^{i\theta} + y_1 e^{i(\theta + \frac{\pi}{2})} = xe^{i\theta} + y_1 e^{i\theta} e^{i\frac{\pi}{2}}$$

$$\vec{r}_1(x) = xe^{i\theta} + iy_1 e^{i\theta} = (x + iy_1) e^{i\theta}$$

$$\vec{r}_1(x) = (x + iy_1)(C_\theta + iS_\theta) = (x + iq_1\Psi_1)(C_\theta + iS_\theta)$$

$$\vec{r}_1(x) = (xC_\theta - q_1\Psi_1S_\theta) + i(xS_\theta + q_1\Psi_1C_\theta)$$

where S and C are the sine and cosine of the angles.

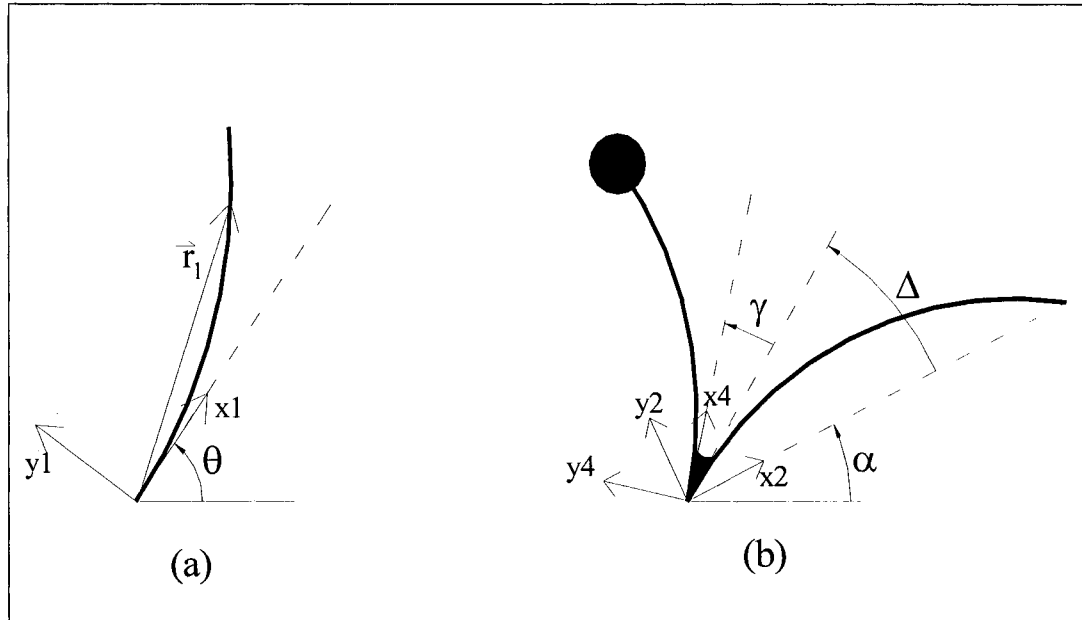


Figure D.3 (a,b): The deflected links with respect to the local coordinate system

By differentiating this vector with respect to time, one obtains the velocity vector of that point,

$$\vec{\dot{r}}_1(x) = (-x \dot{\theta} S_\theta - \dot{q}_1 \Psi_1 S_\theta - q_1 \Psi_1 \dot{\theta} C_\theta) + i(x \dot{\theta} C_\theta + \dot{q}_1 \Psi_1 C_\theta - q_1 \Psi_1 \dot{\theta} S_\theta)$$

$$\dot{r}_1^2(x) = x^2 \dot{\theta}^2 + \Psi_1^2 \dot{q}_1^2 + \Psi_1^2 q_1^2 \dot{\theta}^2 + 2x \Psi_1 \dot{\theta} \dot{q}_1$$

With the same procedure done to link 2, one obtains:

$$\vec{r}_2(x) = \vec{r}_1(R_1) + x e^{i\alpha} + y_2 e^{i(\alpha + \frac{\pi}{2})} = (R_1 + i y_{R_1}) e^{i\theta} + (x + i y_2) e^{i\alpha}$$

$$\vec{r}_2(x) = (R_1 C_\theta - q_1 \Psi_{R_1} S_\theta + x C_\alpha - q_2 \Psi_2 S_\alpha) + i(R_1 S_\theta + q_1 \Psi_{R_1} C_\theta + x S_\alpha + q_2 \Psi_2 C_\alpha)$$

$$\begin{aligned} \vec{\dot{r}}_2(x) = & (-R_1 \dot{\theta} S_\theta - \dot{q}_1 \Psi_{R_1} S_\theta - q_1 \Psi_{R_1} \dot{\theta} C_\theta - x \dot{\alpha} S_\alpha - \dot{q}_2 \Psi_2 S_\alpha - q_2 \Psi_2 \dot{\alpha} C_\alpha) \\ & + i(R_1 \dot{\theta} C_\theta + \dot{q}_1 \Psi_{R_1} C_\theta - q_1 \Psi_{R_1} \dot{\theta} S_\theta + x \dot{\alpha} C_\alpha + \dot{q}_2 \Psi_2 C_\alpha - q_2 \Psi_2 \dot{\alpha} S_\alpha) \end{aligned}$$

$$\begin{aligned} \dot{r}_2^2(x) = & x^2 \dot{\alpha}^2 + 2x \Psi_2 \dot{\alpha} \dot{q}_2 + \Psi_2^2 \dot{q}_2^2 + R_1^2 \dot{\theta}^2 + 2R_1 \Psi_{R_1} \dot{\theta} \dot{q}_1 + \Psi_{R_1}^2 \dot{q}_1^2 + \Psi_{R_1}^2 q_1^2 \dot{\theta}^2 \\ & + \Psi_2^2 q_2^2 \dot{\alpha}^2 + 2S_{\theta-\alpha} \{R_1 \Psi_2 q_2 \dot{\alpha} \dot{\theta} + \Psi_{R_1} \Psi_2 \dot{q}_1 q_2 \dot{\alpha} - x \Psi_{R_1} q_1 \dot{\alpha} \dot{\theta} - \Psi_{R_1} \Psi_2 q_1 q_2 \dot{\theta}\} \\ & + 2C_{\theta-\alpha} \{R_1 x \dot{\alpha} \dot{\theta} + R_1 \Psi_2 \dot{q}_2 \dot{\theta} + x \Psi_{R_1} \dot{q}_1 \dot{\alpha} + \Psi_{R_1} \Psi_2 \dot{q}_1 \dot{q}_2 + \Psi_{R_1} \Psi_2 q_1 q_2 \dot{\alpha} \dot{\theta}\} \end{aligned}$$

Notice that link 2 is assumed pinned-pinned, therefore, the initial angle (Δ) of that link at the left end is added to the angle of the clamped end of link 4. Since Δ is small enough, it is considered as the slope of link 2 at the left end.

$$\Delta = \Psi'_{20} q_2$$

$$\Psi'_{20} = \Psi'_2(0)$$

The velocity square term of link 4 that will be used in the Lagrangian becomes,

$$\begin{aligned} \dot{r}_4^2(x) = & x^2 (\dot{\alpha} + \Psi'_{20} \dot{q}_2)^2 + 2x\Psi_4 (\dot{\alpha} + \Psi'_{20} \dot{q}_2) \dot{q}_4 + \Psi_4^2 \dot{q}_4^2 + R_1^2 \dot{\theta}^2 + 2R_1 \Psi_{R_1} \dot{\theta} \dot{q}_1 \\ & + \Psi_{R_1}^2 \dot{q}_1^2 + \Psi_{R_1}^2 q_1^2 \dot{\theta}^2 + \Psi_4^2 q_4^2 (\dot{\alpha} + \Psi'_{20} \dot{q}_2)^2 \\ & + 2S_{\theta-\alpha-\Psi'_{20}q_2-\gamma} \{R_1 \Psi_4 q_4 (\dot{\alpha} + \Psi'_{20} \dot{q}_2) \dot{\theta} + \Psi_{R_1} \Psi_4 \dot{q}_1 q_4 (\dot{\alpha} + \Psi'_{20} \dot{q}_2) \\ & - x\Psi_{R_1} q_1 (\dot{\alpha} + \Psi'_{20} \dot{q}_2) \dot{\theta} - \Psi_{R_1} \Psi_4 q_1 \dot{q}_4 \dot{\theta}\} \\ & + 2C_{\theta-\alpha-\Psi'_{20}q_2-\gamma} \{R_1 x (\dot{\alpha} + \Psi'_{20} \dot{q}_2) \dot{\theta} + R_1 \Psi_4 \dot{q}_4 \dot{\theta} + x\Psi_{R_1} \dot{q}_1 (\dot{\alpha} + \Psi'_{20} \dot{q}_2) \\ & + \Psi_{R_1} \Psi_4 \dot{q}_1 \dot{q}_4 + \Psi_{R_1} \Psi_4 q_1 q_4 (\dot{\alpha} + \Psi'_{20} \dot{q}_2) \dot{\theta}\} \end{aligned}$$

The velocity squared term of the connecting slider (m_5) and the slider (m_6) are

$$V_5^2 = \dot{r}_4^2(R_4)$$

$$\begin{aligned}
V_5^2 = & R_4^2 (\dot{\alpha} + \Psi'_{20} \dot{q}_2)^2 + 2R_4 \Psi_4 (\dot{\alpha} + \Psi'_{20} \dot{q}_2) \dot{q}_4 + \Psi_4^2 \dot{q}_4^2 + R_1^2 \dot{\theta}^2 + 2R_1 \Psi_{R_1} \dot{\theta} \dot{q}_1 \\
& + \Psi_{R_1}^2 \dot{q}_1^2 + \Psi_{R_1}^2 q_1^2 \dot{\theta}^2 + \Psi_4^2 q_4^2 (\dot{\alpha} + \Psi'_{20} \dot{q}_2)^2 \\
& + 2S_{\theta-\alpha-\Psi'_{20}q_2-\gamma} \{R_1 \Psi_4 q_4 (\dot{\alpha} + \Psi'_{20} \dot{q}_2) \dot{\theta} + \Psi_{R_1} \Psi_4 \dot{q}_1 q_4 (\dot{\alpha} + \Psi'_{20} \dot{q}_2) \\
& - R_4 \Psi_{R_1} q_1 (\dot{\alpha} + \Psi'_{20} \dot{q}_2) \dot{\theta} - \Psi_{R_1} \Psi_4 q_1 \dot{q}_4 \dot{\theta}\} \\
& + 2C_{\theta-\alpha-\Psi'_{20}q_2-\gamma} \{R_1 R_4 (\dot{\alpha} + \Psi'_{20} \dot{q}_2) \dot{\theta} + R_1 \Psi_4 \dot{q}_4 \dot{\theta} + R_4 \Psi_{R_1} \dot{q}_1 (\dot{\alpha} + \Psi'_{20} \dot{q}_2) \\
& + \Psi_{R_1} \Psi_4 \dot{q}_1 \dot{q}_4 + \Psi_{R_1} \Psi_4 q_1 q_4 (\dot{\alpha} + \Psi'_{20} \dot{q}_2) \dot{\theta}\}
\end{aligned}$$

$$V_6 = V_{5x} C_\phi + V_{5y} S_\phi$$

$$\begin{aligned}
V_6 = & -R_1 \dot{\theta} S_{\theta-\phi} - \Psi_{R_1} (\dot{q}_1 S_{\theta-\phi} + q_1 \dot{\theta} C_{\theta-\phi}) - R_4 (\dot{\alpha} + \Psi'_{20} \dot{q}_2) S_{\alpha+\Psi'_{20}q_2+\gamma-\phi} \\
& - \Psi_{R_4} \{ \dot{q}_4 S_{\alpha+\Psi'_{20}q_2+\gamma-\phi} + q_4 (\dot{\alpha} + \Psi'_{20} \dot{q}_2) C_{\alpha+\Psi'_{20}q_2+\gamma-\phi} \}
\end{aligned}$$

$$\begin{aligned}
\dot{V}_6 = & -R_1 (\ddot{\theta} S_{\theta-\phi} + \dot{\theta}^2 C_{\theta-\phi}) - \Psi_{R_1} (\ddot{q}_1 S_{\theta-\phi} + 2\dot{q}_1 \dot{\theta} C_{\theta-\phi} + q_1 \ddot{\theta} C_{\theta-\phi} - q_1 \dot{\theta}^2 S_{\theta-\phi}) \\
& - R_4 (\ddot{\alpha} + \Psi'_{20} \ddot{q}_2) S_{\alpha+\Psi'_{20}q_2+\gamma-\phi} - R_4 (\dot{\alpha} + \Psi'_{20} \dot{q}_2)^2 C_{\alpha+\Psi'_{20}q_2+\gamma-\phi} \\
& - \Psi_{R_4} \{ \ddot{q}_4 S_{\alpha+\Psi'_{20}q_2+\gamma-\phi} + 2\dot{q}_4 (\dot{\alpha} + \Psi'_{20} \dot{q}_2) C_{\alpha+\Psi'_{20}q_2+\gamma-\phi} \\
& + q_4 (\ddot{\alpha} + \Psi'_{20} \ddot{q}_2) C_{\alpha+\Psi'_{20}q_2+\gamma-\phi} - q_4 (\dot{\alpha} + \Psi'_{20} \dot{q}_2)^2 S_{\alpha+\Psi'_{20}q_2+\gamma-\phi} \}
\end{aligned}$$

The Lagrangian of this system can be written as,

$$L = \sum_{i=1}^7 L_i$$

$$L_1 = \frac{1}{2} I_m (\dot{N}\dot{\theta})^2 + \frac{1}{2} I_G \dot{\theta}^2 + \frac{1}{2} \rho A_1 \int_0^{R_1} \dot{r}_1^2 dx - \frac{1}{2} E I_1 q_1^2 \int_0^{R_1} \Psi_1^2 dx$$

where I_m is the mass moment of inertia of the motor's shaft and the smaller gear, and I_G is the mass moment of inertia of the bigger gear.

$$L_i = \frac{1}{2} \rho A_i \int_0^{R_i} \dot{r}_i^2 dx - \frac{1}{2} E I_i q_i^2 \int_0^{R_i} \Psi_i^2 dx, \quad i=2,4$$

$$L_3 = \frac{1}{2} \bar{I}_3 \dot{\beta}^2$$

$$L_j = \frac{1}{2} m_j V_j^2, \quad j=5,6$$

$$L_7 = \lambda_1 \{ \bar{r}_1 (R_1)_y + \bar{r}_2 (R_2)_y - R_3 S_\beta \} + \lambda_2 \{ \bar{r}_1 (R_1)_x + \bar{r}_2 (R_2)_x - R_0 - R_3 C_\beta \}$$

$$L_1 = k_1 \dot{\theta}^2 + k_2 \dot{\theta} \dot{q}_1 + k_3 \dot{q}_1^2 + k_3 \dot{\theta}^2 q_1^2 - k_4 q_1^2$$

$$\begin{aligned} L_2 = & k_5 \dot{\alpha}^2 + k_6 \dot{\alpha} \dot{q}_2 + k_7 \dot{q}_2^2 + k_8 \dot{\theta}^2 + k_9 \dot{\theta} \dot{q}_1 + k_{10} \dot{q}_1^2 + k_{10} \dot{\theta}^2 q_1^2 + k_7 \dot{\alpha}^2 q_2^2 \\ & + S_{\theta-\alpha} \{ k_{11} \dot{\alpha} \dot{\theta} q_2 + k_{12} \dot{\alpha} \dot{q}_1 q_2 - k_{13} \dot{\alpha} \dot{\theta} q_1 - k_{12} \dot{\theta} q_1 \dot{q}_2 \} \\ & + C_{\theta-\alpha} \{ k_{14} \dot{\alpha} \dot{\theta} + k_{11} \dot{\theta} \dot{q}_2 + k_{13} \dot{\alpha} \dot{q}_1 + k_{12} \dot{q}_1 \dot{q}_2 + k_{12} q_1 q_2 \dot{\theta} \dot{\alpha} \} \end{aligned}$$

$$L_3 = \frac{1}{2} \bar{I}_3 \dot{\beta}^2$$

$$\begin{aligned}
L_4 = & k_{16}(\dot{\alpha} + \Psi'_{20}\dot{q}_2)^2 + k_{17}\dot{q}_4^2 + k_{18}\dot{q}_4(\dot{\alpha} + \Psi'_{20}\dot{q}_2) + k_{19}\dot{\theta}^2 + k_{20}\dot{\theta}\dot{q}_1 + k_{21}\dot{q}_1^2 \\
& + k_{21}\dot{\theta}^2 q_1^2 + k_{17}q_4^2(\dot{\alpha} + \Psi'_{20}\dot{q}_2)^2 + S_{\theta-\alpha-\Psi'_{20}q_2-\gamma} \{k_{22}(\dot{\alpha} + \Psi'_{20}\dot{q}_2)\dot{\theta}q_4 \\
& + k_{23}(\dot{\alpha} + \Psi'_{20}\dot{q}_2)\dot{q}_1q_4 - k_{24}(\dot{\alpha} + \Psi'_{20}\dot{q}_2)\dot{\theta}q_1 - k_{23}\dot{\theta}q_1\dot{q}_4\} \\
& + C_{\theta-\alpha-\Psi'_{20}q_2-\gamma} \{k_{26}(\dot{\alpha} + \Psi'_{20}\dot{q}_2)\dot{\theta} + k_{22}\dot{\theta}\dot{q}_4 + k_{24}(\dot{\alpha} + \Psi'_{20}\dot{q}_2)\dot{q}_1 + k_{23}\dot{q}_1\dot{q}_4 \\
& + k_{23}q_1q_4\dot{\theta}(\dot{\alpha} + \Psi'_{20}\dot{q}_2)\}
\end{aligned}$$

$$\begin{aligned}
L_5 = & \frac{1}{2}m_5 \{k_{28}(\dot{\alpha} + \Psi'_{20}\dot{q}_2)^2 + k_{29}\dot{q}_4^2 + k_{30}\dot{q}_4(\dot{\alpha} + \Psi'_{20}\dot{q}_2) + k_{31}\dot{\theta}^2 + k_{32}\dot{\theta}\dot{q}_1 + k_{33}\dot{q}_1^2 \\
& + k_{33}\dot{\theta}^2 q_1^2 + k_{29}q_4^2(\dot{\alpha} + \Psi'_{20}\dot{q}_2)^2 + 2S_{\theta-\alpha-\Psi'_{20}q_2-\gamma} [k_{34}(\dot{\alpha} + \Psi'_{20}\dot{q}_2)\dot{\theta}q_4 \\
& + k_{35}(\dot{\alpha} + \Psi'_{20}\dot{q}_2)\dot{q}_1q_4 - k_{36}(\dot{\alpha} + \Psi'_{20}\dot{q}_2)\dot{\theta}q_1 - k_{35}\dot{\theta}q_1\dot{q}_4] \\
& + 2C_{\theta-\alpha-\Psi'_{20}q_2-\gamma} [k_{38}(\dot{\alpha} + \Psi'_{20}\dot{q}_2)\dot{\theta} + k_{34}\dot{\theta}\dot{q}_4 + k_{36}(\dot{\alpha} + \Psi'_{20}\dot{q}_2)\dot{q}_1 \\
& + k_{35}\dot{q}_1\dot{q}_4 + k_{35}q_1q_4\dot{\theta}(\dot{\alpha} + \Psi'_{20}\dot{q}_2)]\}
\end{aligned}$$

$$L_6 = \frac{1}{2}m_6 V_6^2$$

$$\begin{aligned}
L_7 = & \lambda_1 \{R_1 S_\theta + \Psi_{R_1} q_1 C_\theta + R_2 S_\alpha + \Psi_{R_2} q_2 C_\alpha - R_3 S_\beta\} \\
& + \lambda_2 \{R_1 C_\theta - \Psi_{R_1} q_1 S_\theta + R_2 C_\alpha - \Psi_{R_2} q_2 S_\alpha - R_0 - R_3 C_\beta\}
\end{aligned}$$

$$\delta W = T_m N \delta\theta + \delta W_{\text{damping}}$$

From equations D.2,

$$\delta W_{\text{damping}} = -2\zeta\omega^2 \sqrt{\rho A E I} \dot{q} \int_0^R \Psi^2(x) dx$$

therefore,

$$\delta W = Q_\theta \delta\theta + Q_{q_1} \delta q_1 + Q_{q_2} \delta q_2 + Q_{q_4} \delta q_4$$

$$Q_\theta = T_m N$$

$$Q_{q_1} = -2\zeta\omega_1^2 \sqrt{\rho A_1 E_1 I_1} \dot{q}_1 \int_0^{R_1} \Psi_1^2(x) dx$$

$$Q_{q_2} = -2\zeta\omega_2^2 \sqrt{\rho A_2 E_2 I_2} \dot{q}_2 \int_0^{R_2} \Psi_2^2(x) dx$$

$$Q_{q_4} = -2\zeta\omega_4^2 \sqrt{\rho A_4 E_4 I_4} \dot{q}_4 \int_0^{R_4} \Psi_4^2(x) dx$$

$$k_1 = I_m N^2 + I_G + \frac{1}{2} \rho A_1 \int_0^{R_1} x^2 dx$$

$$k_2 = \rho A_1 \int_0^{R_1} x \Psi_1 dx$$

$$k_3 = \frac{1}{2} \rho A_1 \int_0^{R_1} \Psi_1^2 dx$$

$$k_4 = \frac{1}{2} E I_1 \int_0^{R_1} \Psi_1''^2 dx$$

$$k_5 = \frac{1}{2} \rho A_2 \int_0^{R_2} x^2 dx$$

$$k_6 = \rho A_2 \int_0^{R_2} x \Psi_2 dx$$

$$k_7 = \frac{1}{2} \rho A_2 \int_0^{R_2} \Psi_2^2 dx$$

$$k_8 = \frac{1}{2} \rho A_2 \int_0^{R_2} R_1^2 dx$$

$$k_9 = \rho A_2 \int_0^{R_2} R_1 \Psi_{R_1} dx$$

$$k_{10} = \frac{1}{2} \rho A_2 \int_0^{R_2} \Psi_{R_1}^2 dx$$

$$k_{11} = \rho A_2 \int_0^{R_2} R_1 \Psi_2 dx$$

$$k_{12} = \rho A_2 \int_0^{R_2} \Psi_{R_1} \Psi_2 dx$$

$$k_{13} = \rho A_2 \int_0^{R_2} x \Psi_{R_1} dx$$

$$k_{14} = \rho A_2 \int_0^{R_2} x R_1 dx$$

$$k_{15} = \frac{1}{2} E I_2 \int_0^{R_2} \Psi_2''^2 dx$$

$$k_{16} = \frac{1}{2} \rho A_4 \int_0^{R_4} x^2 dx$$

$$k_{17} = \frac{1}{2} \rho A_4 \int_0^{R_4} \Psi_4^2 dx$$

$$k_{18} = \rho A_4 \int_0^{R_4} x \Psi_4 dx$$

$$k_{19} = \frac{1}{2} \rho A_4 \int_0^{R_4} R_1^2 dx$$

$$k_{20} = \rho A_4 \int_0^{R_4} R_1 \Psi_{R_1} dx$$

$$k_{21} = \frac{1}{2} \rho A_4 \int_0^{R_4} \Psi_{R_1}^2 dx$$

$$k_{22} = \rho A_4 \int_0^{R_4} R_1 \Psi_4 dx$$

$$k_{23} = \rho A_4 \int_0^{R_4} \Psi_{R_1} \Psi_4 dx$$

$$k_{24} = \rho A_4 \int_0^{R_4} x \Psi_{R_1} dx$$

$$k_{26} = \rho A_4 \int_0^{R_4} x R_1 dx$$

$$k_{27} = \frac{1}{2} EI_4 \int_0^{R_4} \Psi_4''^2 dx$$

$$k_{28} = R_4^2$$

$$k_{29} = \Psi_{R_4}^2$$

$$k_{30} = R_4 \Psi_{R_4}$$

$$k_{31} = R_1^2$$

$$k_{32} = R_1 \Psi_{R_1}$$

$$k_{33} = \Psi_{R_1}^2$$

$$\begin{aligned}
k_{34} &= R_1 \Psi_{R_4} \\
k_{35} &= \Psi_{R_1} \Psi_{R_4} \\
k_{36} &= R_4 \Psi_{R_1} \\
k_{38} &= R_1 R_4
\end{aligned}$$

The Lagrange's equations for this system become,

$$\frac{d}{dt} \frac{\partial L}{\partial \dot{\theta}} - \frac{\partial L}{\partial \theta} = Q_\theta$$

$$E_1 \ddot{\theta} + E_2 \ddot{q}_1 + E_3 \ddot{\alpha} + E_4 \ddot{q}_2 + E_5 \ddot{q}_4 + E_6 + E_7 \lambda_1 + E_8 \lambda_2 = N T_m$$

$$T_m = \frac{K_t}{R_s} (V - K_e N \dot{\theta})$$

$$\begin{aligned}
E_1 &= 2[k_l + k_8 + k_{19} + (k_3 + k_{10} + k_{21})q_l^2] + m_5(k_{31} + k_{33}q_l^2) \\
&\quad + m_6(R_1 S_{\theta-\phi} + \Psi_{R_1} q_1 C_{\theta-\phi})^2
\end{aligned}$$

$$E_2 = k_2 + k_9 + k_{20} + m_5 k_{32} + m_6 (R_1 S_{\theta-\phi} + \Psi_{R_1} q_1 C_{\theta-\phi}) \Psi_{R_1} S_{\theta-\phi}$$

$$\begin{aligned}
E_3 &= (k_{11}q_2 - k_{13}q_1)S_{\theta-\phi} + (k_{14} + k_{12}q_1q_2)C_{\theta-\phi} + (k_{22}q_4 - k_{24}q_1)S_{\theta-\alpha-\Psi'_{20}q_2-\gamma} \\
&\quad + (k_{26} + k_{23}q_1q_4)C_{\theta-\alpha-\Psi'_{20}q_2-\gamma} \\
&\quad + m_5[(k_{34}q_4 - k_{36}q_1)S_{\theta-\alpha-\Psi'_{20}q_2-\gamma} + (k_{38} + k_{35}q_1q_4)C_{\theta-\alpha-\Psi'_{20}q_2-\gamma}] \\
&\quad + m_6(R_1 S_{\theta-\phi} + \Psi_{R_1} q_1 C_{\theta-\phi})(R_4 S_{\alpha+\Psi'_{20}q_2+\gamma-\phi} + \Psi_{R_4} q_4 C_{\alpha+\Psi'_{20}q_2+\gamma-\phi})
\end{aligned}$$

$$E_4 = k_{11}C_{\theta-\alpha} - k_{12}q_1S_{\theta-\alpha} + \Psi'_{20} \{ (k_{22}q_4 - k_{24}q_1 + m_5(k_{34}q_4 - k_{36}q_1))S_{\theta-\alpha-\Psi'_{20}q_2-\gamma} \\ + (k_{26} + k_{23}q_1q_4 + m_5(k_{38} + k_{35}q_1q_4))C_{\theta-\alpha-\Psi'_{20}q_2-\gamma} \\ + m_6(R_1S_{\theta-\phi} + \Psi_{R_1}q_1C_{\theta-\phi})(R_4S_{\alpha+\Psi'_{20}q_2+\gamma-\phi} + \Psi_{R_4}q_4C_{\alpha+\Psi'_{20}q_2+\gamma-\phi}) \}$$

$$E_5 = k_{22}C_{\theta-\alpha-\Psi'_{20}q_2-\gamma} - k_{23}q_1S_{\theta-\alpha-\Psi'_{20}q_2-\gamma} \\ + m_5(k_{34}C_{\theta-\alpha-\Psi'_{20}q_2-\gamma} - k_{35}q_1S_{\theta-\alpha-\Psi'_{20}q_2-\gamma}) \\ + m_6(R_1S_{\theta-\phi} + \Psi_{R_1}q_1C_{\theta-\phi})\Psi_{R_4}S_{\alpha+\Psi'_{20}q_2+\gamma-\phi}$$

$$E_6 = 4(k_3 + k_{21} + k_{10} + \frac{1}{2}m_5k_{33})q_1\dot{q}_1\dot{\theta} - \dot{\alpha}C_{\theta-\alpha}[(k_{11}q_2 - k_{13}q_1)\dot{\alpha} - 2k_{12}q_1\dot{q}_2] \\ + \dot{\alpha}C_{\theta-\alpha}[(k_{14} + k_{12}q_1q_2)\dot{\alpha} + 2k_{11}\dot{q}_2] \\ - (\dot{\alpha} + \Psi'_{20}\dot{q}_2)C_{\theta-\alpha-\Psi'_{20}q_2-\gamma}[(k_{22}q_4 - k_{24}q_1 + m_5(k_{34}q_4 - k_{36}q_1))(\dot{\alpha} + \Psi'_{20}\dot{q}_2) \\ - 2(k_{23} + m_5k_{35})q_1\dot{q}_4] \\ + (\dot{\alpha} + \Psi'_{20}\dot{q}_2)S_{\theta-\alpha-\Psi'_{20}q_2-\gamma}[(k_{26} + k_{23}q_1q_4 + m_5(k_{38} + k_{35}q_1q_4))(\dot{\alpha} + \Psi'_{20}\dot{q}_2) \\ + 2(k_{22} + k_{34})\dot{q}_4] \\ + m_6(R_1S_{\theta-\phi} + \Psi_{R_1}q_1C_{\theta-\phi})[R_1\dot{\theta}^2C_{\theta-\phi} + \Psi_{R_1}\dot{\theta}(2\dot{q}_1C_{\theta-\phi} - q_1\dot{\theta}S_{\theta-\phi}) \\ + R_4(\dot{\alpha} + \Psi'_{20}\dot{q}_2)^2C_{\alpha+\Psi'_{20}q_2+\gamma-\phi} \\ + \Psi_{R_4}(\dot{\alpha} + \Psi'_{20}\dot{q}_2)(2\dot{q}_4C_{\alpha+\Psi'_{20}q_2+\gamma-\phi} - q_4(\dot{\alpha} + \Psi'_{20}\dot{q}_2)S_{\alpha+\Psi'_{20}q_2+\gamma-\phi})]$$

$$E_7 = R_1S_{\theta} + \Psi_{R_1}q_1C_{\theta}$$

$$E_8 = -R_1C_{\theta} + \Psi_{R_1}q_1S_{\theta}$$

$$\frac{d}{dt} \frac{\partial L}{\partial \dot{q}_1} - \frac{\partial L}{\partial q_1} = Q_{q_1}$$

$$\begin{aligned}
& E_9 \ddot{\theta} + E_{10} \ddot{q}_1 + E_{11} \ddot{\alpha} + E_{12} \ddot{q}_2 + E_{13} \ddot{q}_4 + E_{14} + E_{15} \lambda_1 + E_{16} \lambda_2 \\
& = -2\zeta \omega_1^2 \sqrt{\rho A_1 E_1 I_1} \dot{q}_1 \int_0^{R_1} \Psi_1^2(x) dx
\end{aligned}$$

$$E_9 = k_2 + k_9 + k_{20} + m_5 k_{32} + m_6 \Psi_{R_1} S_{\theta-\phi} (R_1 S_{\theta-\phi} + \Psi_{R_1} q_1 C_{\theta-\phi})$$

$$E_{10} = 2(k_3 + k_{10} + k_{21}) + m_5 k_{33} + m_6 \Psi_{R_1}^2 S_{\theta-\phi}^2$$

$$\begin{aligned}
E_{11} = & k_{12} q_2 S_{\theta-\alpha} + k_{13} C_{\theta-\alpha} + k_{23} q_4 S_{\theta-\alpha-\Psi'_{20} q_2 - \gamma} + k_{24} C_{\theta-\alpha-\Psi'_{20} q_2 - \gamma} \\
& + m_5 (k_{35} q_4 S_{\theta-\alpha-\Psi'_{20} q_2 - \gamma} + k_{36} C_{\theta-\alpha-\Psi'_{20} q_2 - \gamma}) \\
& + m_6 \Psi_{R_1} S_{\theta-\phi} (R_4 S_{\alpha+\Psi'_{20} q_2 + \gamma - \phi} + \Psi_{R_4} q_4 C_{\alpha+\Psi'_{20} q_2 + \gamma - \phi})
\end{aligned}$$

$$\begin{aligned}
E_{12} = & k_{12} C_{\theta-\alpha} + \Psi'_{20} [(k_{23} + m_5 k_{35}) q_4 S_{\theta-\alpha-\Psi'_{20} q_2 - \gamma} + (k_{24} + k_{35}) C_{\theta-\alpha-\Psi'_{20} q_2 - \gamma} \\
& + m_6 \Psi_{R_1} S_{\theta-\phi} (R_4 S_{\alpha+\Psi'_{20} q_2 + \gamma - \phi} + \Psi_{R_4} q_4 C_{\alpha+\Psi'_{20} q_2 + \gamma - \phi})]
\end{aligned}$$

$$E_{13} = (k_{23} + m_5 k_{35}) C_{\theta-\alpha-\Psi'_{20} q_2 - \gamma} + m_6 \Psi_{R_1} \Psi_{R_4} S_{\theta-\phi} S_{\alpha+\Psi'_{20} q_2 + \gamma - \phi}$$

$$\begin{aligned}
E_{14} = & -k_{12}\dot{\alpha}^2 q_2 C_{\theta-\alpha} + 2k_4 q_1 - 2\left(k_3 + k_{10} + k_{21} + \frac{1}{2}m_5 k_{33}\right) q_1 \dot{\theta}^2 \\
& + \dot{\alpha} S_{\theta-\alpha} (k_{13}\dot{\alpha} + 2k_{12}\dot{q}_2) - k_{23} q_4 (\dot{\alpha} + \Psi'_{20}\dot{q}_2)^2 C_{\theta-\alpha-\Psi'_{20}q_2-\gamma} \\
& + (\dot{\alpha} + \Psi'_{20}\dot{q}_2) S_{\theta-\alpha-\Psi'_{20}q_2-\gamma} (k_{24}(\dot{\alpha} + \Psi'_{20}\dot{q}_2) + 2k_{23}\dot{q}_4) \\
& - k_{35} m_5 q_4 (\dot{\alpha} + \Psi'_{20}\dot{q}_2)^2 C_{\theta-\alpha-\Psi'_{20}q_2-\gamma} \\
& + m_5 (\dot{\alpha} + \Psi'_{20}\dot{q}_2) S_{\theta-\alpha-\Psi'_{20}q_2-\gamma} (2k_{35}\dot{q}_4 + k_{36}(\dot{\alpha} + \Psi'_{20}\dot{q}_2)) \\
& + m_6 \Psi_{R_1} S_{\theta-\phi} \left\{ R_1 \dot{\theta}^2 C_{\theta-\phi} + \Psi_{R_1} (2\dot{q}_1 \dot{\theta} C_{\theta-\phi} - q_1 \dot{\theta}^2 S_{\theta-\phi}) \right. \\
& + R_4 (\dot{\alpha} + \Psi'_{20}\dot{q}_2)^2 C_{\alpha+\Psi'_{20}q_2+\gamma-\phi} \\
& \left. + \Psi_{R_4} (\dot{\alpha} + \Psi'_{20}\dot{q}_2) (2\dot{q}_4 C_{\alpha+\Psi'_{20}q_2+\gamma-\phi} - q_4 (\dot{\alpha} + \Psi'_{20}\dot{q}_2) S_{\alpha+\Psi'_{20}q_2+\gamma-\phi}) \right\}
\end{aligned}$$

$$E_{15} = \Psi_{R_1} S_{\theta}$$

$$E_{16} = -\Psi_{R_1} C_{\theta}$$

$$\frac{d}{dt} \frac{\partial L}{\partial \dot{\alpha}} - \frac{\partial L}{\partial \alpha} = Q_{\alpha}$$

$$E_{17}\ddot{\theta} + E_{18}\ddot{q}_1 + E_{19}\ddot{\alpha} + E_{20}\ddot{q}_2 + E_{21}\ddot{q}_4 + E_{22} + E_{23}\lambda_1 + E_{24}\lambda_2 = 0$$

$$\begin{aligned}
E_{17} = & (k_{11}q_2 - k_{13}q_1) S_{\theta-\alpha} + (k_{14} + k_{12}q_1q_2) C_{\theta-\alpha} \\
& + [(k_{22} + m_5 k_{34})q_4 - (k_{24} + m_5 k_{36})q_1] S_{\theta-\alpha-\Psi'_{20}q_2-\gamma} \\
& + [k_{26} + m_5 k_{38} + (k_{23} + m_5 k_{35})q_1q_4] C_{\theta-\alpha-\Psi'_{20}q_2-\gamma} \\
& + m_6 (R_1 S_{\theta-\phi} + \Psi_{R_1} q_1 C_{\theta-\phi}) (R_4 S_{\alpha+\Psi'_{20}q_2+\gamma-\phi} + \Psi_{R_4} q_4 C_{\alpha+\Psi'_{20}q_2+\gamma-\phi})
\end{aligned}$$

$$E_{18} = k_{12}q_2 S_{\theta-\alpha} + k_{13}C_{\theta-\alpha} + (k_{23} + m_5 k_{35})q_4 S_{\theta-\alpha-\Psi'_{20}q_2-\gamma} \\ + (k_{24} + m_5 k_{36})C_{\theta-\alpha-\Psi'_{20}q_2-\gamma} \\ + m_6 \Psi_{R_1} S_{\theta-\phi} (R_4 S_{\alpha+\Psi'_{20}q_2+\gamma-\phi} + \Psi_{R_4} q_4 C_{\alpha+\Psi'_{20}q_2+\gamma-\phi})$$

$$E_{19} = 2(k_5 + k_{16}) + 2k_7 q_2^2 + 2k_{17} q_4^2 + m_5 (k_{28} + k_{29} q_4^2) \\ + m_6 (R_4 S_{\alpha+\Psi'_{20}q_2+\gamma-\phi} + \Psi_{R_4} q_4 C_{\alpha+\Psi'_{20}q_2+\gamma-\phi})^2$$

$$E_{20} = k_6 + \Psi'_{20} [2k_{16} + m_5 k_{28} + (2k_{17} + m_5 k_{29})q_4^2] \\ + \Psi'_{20} m_6 (R_4 S_{\alpha+\Psi'_{20}q_2+\gamma-\phi} + \Psi_{R_4} q_4 C_{\alpha+\Psi'_{20}q_2+\gamma-\phi})^2$$

$$E_{21} = k_{18} + m_5 k_{30} \\ + m_6 (R_4 S_{\alpha+\Psi'_{20}q_2+\gamma-\phi} + \Psi_{R_4} q_4 C_{\alpha+\Psi'_{20}q_2+\gamma-\phi}) \Psi_{R_4} S_{\alpha+\Psi'_{20}q_2+\gamma-\phi}$$

$$E_{22} = 4k_7 \dot{\alpha} q_2 \dot{q}_2 + \dot{\theta} C_{\theta-\alpha} (k_{11} \dot{\theta} q_2 + 2k_{12} \dot{q}_1 q_2 - k_{13} q_1 \dot{\theta}) \\ - \dot{\theta} S_{\theta-\alpha} (k_{14} \dot{\theta} + 2k_{13} \dot{q}_1 + k_{12} q_1 q_2 \dot{\theta}) + (4k_{17} + 2m_5) q_4 \dot{q}_4 (\dot{\alpha} + \Psi'_{20} \dot{q}_2) \\ + \dot{\theta} C_{\theta-\alpha-\Psi'_{20}q_2-\gamma} [(k_{22} + m_5 k_{34}) \dot{\theta} q_4 + 2(k_{23} + m_5 k_{35}) \dot{q}_1 q_4 - (k_{24} + m_5 k_{36}) q_1 \dot{\theta}] \\ - \dot{\theta} S_{\theta-\alpha-\Psi'_{20}q_2-\gamma} [(k_{26} + m_5 k_{38}) \dot{\theta} + 2(k_{24} + m_5 k_{36}) \dot{q}_1 + (k_{23} + m_5 k_{35}) q_1 q_4 \dot{\theta}] \\ + m_6 (R_4 S_{\alpha+\Psi'_{20}q_2+\gamma-\phi} + \Psi_{R_4} q_4 C_{\alpha+\Psi'_{20}q_2+\gamma-\phi}) [R_1 \dot{\theta}^2 C_{\theta-\phi} \\ + \Psi_{R_1} \dot{\theta} (2\dot{q}_1 C_{\theta-\phi} - q_1 \dot{\theta} S_{\theta-\phi}) + R_4 (\dot{\alpha} + \Psi'_{20} \dot{q}_2)^2 C_{\alpha+\Psi'_{20}q_2+\gamma-\phi} \\ + \Psi_{R_4} (\dot{\alpha} + \Psi'_{20} \dot{q}_2) (2\dot{q}_4 C_{\alpha+\Psi'_{20}q_2+\gamma-\phi} - q_4 (\dot{\alpha} + \Psi'_{20} \dot{q}_2) S_{\alpha+\Psi'_{20}q_2+\gamma-\phi})]$$

$$E_{23} = R_2 S_\alpha + \Psi_{R_2} q_2 C_\alpha$$

$$E_{24} = -R_2 C_\alpha + \Psi_{R_2} q_2 S_\alpha$$

$$\frac{d}{dt} \frac{\partial L}{\partial \dot{q}_2} - \frac{\partial L}{\partial q_2} = Q_{q_2}$$

$$\begin{aligned} & E_{25} \ddot{\theta} + E_{26} \ddot{q}_1 + E_{27} \ddot{\alpha} + E_{28} \ddot{q}_2 + E_{29} \ddot{q}_4 + E_{30} + E_{31} \lambda_1 + E_{32} \lambda_2 \\ & = -2\zeta \omega_2^2 \sqrt{\rho A_2 E_2 I_2} \dot{q}_2 \int_0^{R_2} \Psi_2^2(x) dx \end{aligned}$$

$$\begin{aligned} E_{25} = & k_{11} C_{\theta-\alpha} - k_{12} q_1 S_{\theta-\alpha} + \Psi'_{20} [((k_{22} + m_5 k_{34}) q_4 - (k_{24} + m_5 k_{36}) q_1) S_{\theta-\alpha-\Psi'_{20} q_2-\gamma} \\ & + ((k_{26} + m_5 k_{38}) + (k_{23} + m_5 k_{35}) q_1 q_4) C_{\theta-\alpha-\Psi'_{20} q_2-\gamma} \\ & + m_6 (R_4 S_{\alpha+\Psi'_{20} q_2+\gamma-\phi} + \Psi_{R_4} q_4 C_{\alpha+\Psi'_{20} q_2+\gamma-\phi}) (R_1 S_{\theta-\phi} + \Psi_{R_1} q_1 C_{\theta-\phi})] \end{aligned}$$

$$\begin{aligned} E_{26} = & k_{12} C_{\theta-\alpha} + \Psi'_{20} [(k_{23} + m_5 k_{35}) q_4 S_{\theta-\alpha-\Psi'_{20} q_2-\gamma} + (k_{24} + m_5 k_{36}) C_{\theta-\alpha-\Psi'_{20} q_2-\gamma} \\ & + m_6 \Psi_{R_1} S_{\theta-\phi} (R_4 S_{\alpha+\Psi'_{20} q_2+\gamma-\phi} + \Psi_{R_4} q_4 C_{\alpha+\Psi'_{20} q_2+\gamma-\phi})] \end{aligned}$$

$$\begin{aligned} E_{27} = & k_6 + \Psi'_{20} [2k_{16} + m_5 k_{28} + (2k_{17} + m_5 k_{29}) q_4^2 \\ & + m_6 (R_4 S_{\alpha+\Psi'_{20} q_2+\gamma-\phi} + \Psi_{R_4} q_4 C_{\alpha+\Psi'_{20} q_2+\gamma-\phi})^2] \end{aligned}$$

$$\begin{aligned} E_{28} = & 2k_7 + \Psi'^2_{20} [2k_{16} + m_5 k_{28} + (2k_{17} + m_5 k_{29}) q_4^2 \\ & + m_6 (R_4 S_{\alpha+\Psi'_{20} q_2+\gamma-\phi} + \Psi_{R_4} q_4 C_{\alpha+\Psi'_{20} q_2+\gamma-\phi})^2] \end{aligned}$$

$$E_{29} = \Psi'_{20} [k_{18} + m_5 k_{30} + m_6 \Psi_{R_4} S_{\alpha + \Psi'_{20} q_2 + \gamma - \phi} (R_4 S_{\alpha + \Psi'_{20} q_2 + \gamma - \phi} + \Psi_{R_4} q_4 C_{\alpha + \Psi'_{20} q_2 + \gamma - \phi})]$$

$$\begin{aligned} E_{30} = & 2\Psi'_{20} (2k_{17} + m_5 k_{29}) q_4 \dot{q}_4 (\dot{\alpha} + \Psi'_{20} \dot{q}_2) - 2k_7 \dot{\alpha}^2 q_2 + 2k_{15} q_2 \\ & - \dot{\theta} S_{\theta - \alpha} (k_{11} \dot{\theta} + 2k_{12} \dot{q}_1) - k_{12} \dot{\theta}^2 q_1 C_{\theta - \alpha} \\ & + \dot{\theta} \Psi'_{20} C_{\theta - \alpha - \Psi'_{20} q_2 - \gamma} [(k_{22} + m_5 k_{34}) q_4 \dot{\theta} + 2(k_{23} + m_5 k_{35}) \dot{q}_1 q_4 - (k_{24} + m_5 k_{36}) q_1 \dot{\theta}] \\ & - \dot{\theta} \Psi'_{20} S_{\theta - \alpha - \Psi'_{20} q_2 - \gamma} [(k_{26} + m_5 k_{38}) \dot{\theta} + 2(k_{24} + m_5 k_{36}) \dot{q}_1 + (k_{23} + m_5 k_{35}) q_1 q_4 \dot{\theta}] \\ & + m_6 \Psi'_{20} (R_4 S_{\alpha + \Psi'_{20} q_2 + \gamma - \phi} + \Psi_{R_4} q_4 C_{\alpha + \Psi'_{20} q_2 + \gamma - \phi}) [R_1 \dot{\theta}^2 C_{\theta - \phi} \\ & + \Psi_{R_1} \dot{\theta} (2\dot{q}_1 C_{\theta - \phi} - q_1 \dot{\theta} S_{\theta - \phi}) + R_4 (\dot{\alpha} + \Psi'_{20} \dot{q}_2)^2 C_{\alpha + \Psi'_{20} q_2 + \gamma - \phi} \\ & + \Psi_{R_4} (\dot{\alpha} + \Psi'_{20} \dot{q}_2) (2\dot{q}_4 C_{\alpha + \Psi'_{20} q_2 + \gamma - \phi} - q_4 (\dot{\alpha} + \Psi'_{20} \dot{q}_2) S_{\alpha + \Psi'_{20} q_2 + \gamma - \phi})] \end{aligned}$$

$$E_{31} = \Psi_{R_2} S_{\alpha}$$

$$E_{32} = -\Psi_{R_2} C_{\alpha}$$

$$\frac{d}{dt} \frac{\partial L}{\partial \dot{\beta}} - \frac{\partial L}{\partial \beta} = Q_{\beta}$$

$$\bar{I}_3 \ddot{\beta} + E_{33} \lambda_1 + E_{34} \lambda_2 = 0$$

$$E_{33} = -R_3 S_{\beta}$$

$$E_{34} = R_3 C_{\beta}$$

$$\frac{d}{dt} \frac{\partial L}{\partial \dot{q}_4} - \frac{\partial L}{\partial q_4} = Q_{q_4}$$

$$E_{35} \ddot{\theta} + E_{36} \ddot{q}_1 + E_{37} \ddot{\alpha} + E_{38} \ddot{q}_2 + E_{39} \ddot{q}_4 + E_{40} = -2\zeta \omega_4^2 \sqrt{\rho A_4 E_4 I_4} \dot{q}_4 \int_0^{R_4} \Psi_4^2(x) dx$$

$$E_{35} = (k_{22} + m_5 k_{34}) C_{\theta - \alpha - \Psi'_{20} q_2 - \gamma} - (k_{23} + m_5 k_{35}) q_1 S_{\theta - \alpha - \Psi'_{20} q_2 - \gamma} \\ + m_6 \Psi_{R_4} S_{\alpha + \Psi'_{20} q_2 + \gamma - \phi} (R_1 S_{\theta - \phi} + \Psi_{R_1} q_1 C_{\theta - \phi})$$

$$E_{36} = (k_{23} + m_5 k_{35}) C_{\theta - \alpha - \Psi'_{20} q_2 - \gamma} + m_6 \Psi_{R_4} \Psi_{R_1} S_{\alpha + \Psi'_{20} q_2 + \gamma - \phi} S_{\theta - \phi}$$

$$E_{37} = k_{18} + m_5 k_{30} \\ + m_6 \Psi_{R_4} S_{\alpha + \Psi'_{20} q_2 + \gamma - \phi} (R_4 S_{\alpha + \Psi'_{20} q_2 + \gamma - \phi} + \Psi_{R_4} q_4 C_{\alpha + \Psi'_{20} q_2 + \gamma - \phi})$$

$$E_{38} = \Psi'_{20} [k_{18} + m_5 k_{30} \\ + m_6 \Psi_{R_4} S_{\alpha + \Psi'_{20} q_2 + \gamma - \phi} (R_4 S_{\alpha + \Psi'_{20} q_2 + \gamma - \phi} + \Psi_{R_4} q_4 C_{\alpha + \Psi'_{20} q_2 + \gamma - \phi})]$$

$$E_{39} = 2k_{17} + m_5 k_{29} + m_6 \Psi_{R_4}^2 S_{\alpha + \Psi'_{20} q_2 + \gamma - \phi}^2$$

$$\begin{aligned}
E_{40} = & -(2k_{17} + m_5 k_{29}) q_4 (\dot{\alpha} + \Psi'_{20} \dot{q}_2)^2 + 2k_{27} q_4 \\
& - \dot{\theta} S_{\theta-\alpha-\Psi'_{20} q_2-\gamma} [(k_{22} + m_5 k_{34}) \dot{\theta} + 2(k_{23} + m_5 k_{35}) \dot{q}_1] \\
& - (k_{23} + m_5 k_{35}) \dot{\theta}^2 q_1 C_{\theta-\alpha-\Psi'_{20} q_2-\gamma} \\
& + m_6 \Psi_{R_4} S_{\alpha+\Psi'_{20} q_2+\gamma-\phi} \left\{ R_1 \dot{\theta}^2 C_{\theta-\phi} + \Psi_{R_1} \dot{\theta} (2\dot{q}_1 C_{\theta-\phi} - q_1 \dot{\theta} S_{\theta-\phi}) \right. \\
& + R_4 (\dot{\alpha} + \Psi'_{20} \dot{q}_2)^2 C_{\alpha+\Psi'_{20} q_2+\gamma-\phi} \\
& \left. + \Psi_{R_4} (\dot{\alpha} + \Psi'_{20} \dot{q}_2) (2\dot{q}_4 C_{\alpha+\Psi'_{20} q_2+\gamma-\phi} - q_4 (\dot{\alpha} + \Psi'_{20} \dot{q}_2) S_{\alpha+\Psi'_{20} q_2+\gamma-\phi}) \right\}
\end{aligned}$$

$$\frac{d}{dt} \frac{\partial L}{\partial \dot{\lambda}_1} - \frac{\partial L}{\partial \lambda_1} = 0$$

$$R_1 S_\theta + \Psi_{R_1} q_1 C_\theta + R_2 S_\alpha + \Psi_{R_2} q_2 C_\alpha - R_3 S_\beta = 0$$

$$\frac{d^2}{dt^2} (R_1 S_\theta + \Psi_{R_1} q_1 C_\theta + R_2 S_\alpha + \Psi_{R_2} q_2 C_\alpha - R_3 S_\beta) = 0$$

$$E_{41}\ddot{\theta}+E_{42}\ddot{q}_1+E_{43}\ddot{\alpha}+E_{44}\ddot{q}_2+E_{45}\ddot{\beta}+E_{46}=0$$

$$E_{41}=-R_1S_\theta-\Psi_{R_1}q_1C_\theta$$

$$E_{42}=-\Psi_{R_1}S_\theta$$

$$E_{43} = -R_2 S_\alpha - \Psi_{R_2} q_2 C_\alpha$$

$$E_{44} = -\Psi_{R_2} S_\alpha$$

$$E_{45} = R_3 S_\beta$$

$$E_{46} = -R_1 \dot{\theta}^2 C_\theta - \Psi_{R_1} (2\dot{q}_1 \dot{\theta} C_\theta - q_1 \dot{\theta}^2 S_\theta) - R_2 \dot{\alpha}^2 C_\alpha - \Psi_{R_2} (2\dot{q}_2 \dot{\alpha} C_\alpha - q_2 \dot{\alpha}^2 S_\alpha) + R_3 \dot{\beta}^2 C_\beta$$

$$\frac{d}{dt} \frac{\partial L}{\partial \dot{\lambda}_2} - \frac{\partial L}{\partial \lambda_2} = 0$$

$$R_1 C_\theta - \Psi_{R_1} q_1 S_\theta + R_2 C_\alpha - \Psi_{R_2} q_2 S_\alpha - R_0 - R_3 C_\beta = 0$$

$$\frac{d^2}{dt^2} (R_1 C_\theta - \Psi_{R_1} q_1 S_\theta + R_2 C_\alpha - \Psi_{R_2} q_2 S_\alpha - R_0 - R_3 C_\beta) = 0$$

$$E_{47} \ddot{\theta} + E_{48} \ddot{q}_1 + E_{49} \ddot{\alpha} + E_{50} \ddot{q}_2 + E_{51} \ddot{\beta} + E_{52} = 0$$

$$E_{47} = R_1 C_\theta - \Psi_{R_1} q_1 S_\theta$$

$$E_{48} = \Psi_{R_1} C_\theta$$

$$E_{49} = R_2 C_\alpha - \Psi_{R_2} q_2 S_\alpha$$

$$E_{50} = \Psi_{R_2} C_\alpha$$

$$E_{51} = -R_3 C_\beta$$

$$E_{52} = -R_1 \dot{\theta}^2 S_\theta - \Psi_{R_1} (2\dot{q}_1 \dot{\theta} S_\theta + q_1 \dot{\theta}^2 C_\theta) - R_2 \dot{\alpha}^2 S_\alpha \\ - \Psi_{R_2} (2\dot{q}_2 \dot{\alpha} S_\alpha + q_2 \dot{\alpha}^2 C_\alpha) + R_3 \dot{\beta}^2 S_\beta$$

The final equations of motion in matrix form are:

$$\begin{bmatrix} E_1 & E_2 & E_3 & E_4 & 0 & E_5 & E_7 & E_8 \\ E_9 & E_{10} & E_{11} & E_{12} & 0 & E_{13} & E_{15} & E_{16} \\ E_{17} & E_{18} & E_{19} & E_{20} & 0 & E_{21} & E_{23} & E_{24} \\ E_{25} & E_{26} & E_{27} & E_{28} & 0 & E_{29} & E_{31} & E_{32} \\ 0 & 0 & 0 & 0 & \bar{I}_3 & 0 & E_{33} & E_{34} \\ E_{35} & E_{36} & E_{37} & E_{38} & 0 & E_{39} & 0 & 0 \\ E_{41} & E_{42} & E_{43} & E_{44} & E_{45} & 0 & 0 & 0 \\ E_{47} & E_{48} & E_{49} & E_{50} & E_{51} & 0 & 0 & 0 \end{bmatrix} \begin{bmatrix} \ddot{\theta} \\ \ddot{q}_1 \\ \ddot{\alpha} \\ \ddot{q}_2 \\ \ddot{\beta} \\ \ddot{q}_4 \\ \lambda_1 \\ \lambda_2 \end{bmatrix}$$

$$= - \begin{bmatrix} E_6 - \frac{NK_t}{R_s} (V - K_e N \dot{\theta}) \\ E_{14} + 2\zeta\omega_1^2 \sqrt{\rho A_1 E_1 I_1} \dot{q}_1 \int_0^{R_1} \Psi_1^2(x) dx \\ E_{22} \\ E_{30} + 2\zeta\omega_2^2 \sqrt{\rho A_2 E_2 I_2} \dot{q}_2 \int_0^{R_2} \Psi_2^2(x) dx \\ 0 \\ E_{40} + 2\zeta\omega_4^2 \sqrt{\rho A_4 E_4 I_4} \dot{q}_4 \int_0^{R_4} \Psi_4^2(x) dx \\ E_{46} \\ E_{52} \end{bmatrix}$$

Appendix E

Derivation of the Equations of Motion of the Flexible Slider-Crank

Mechanism by Lagrange's Equations

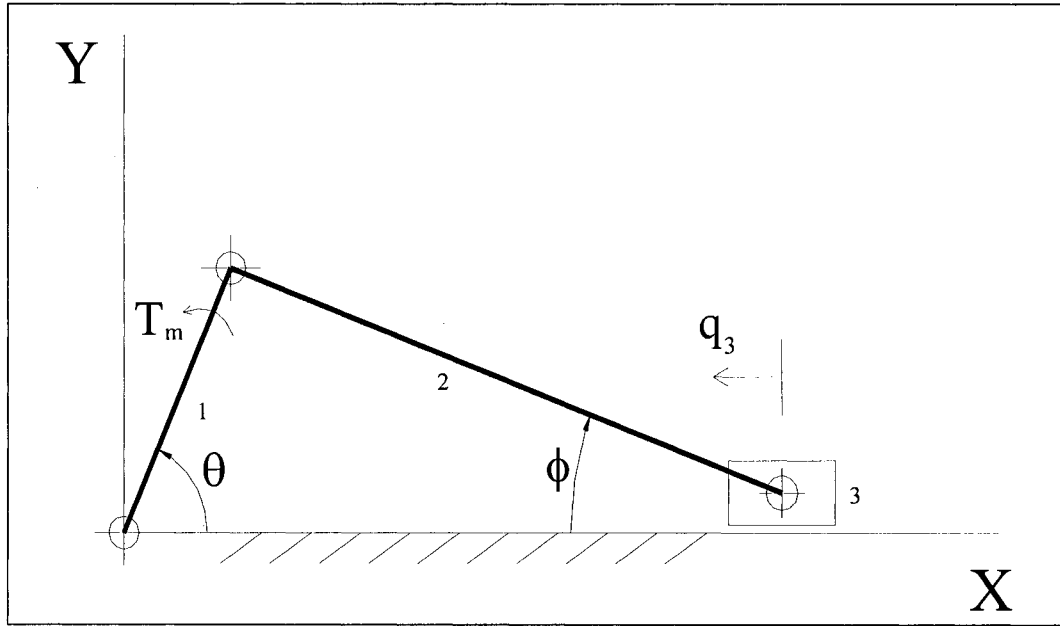


Figure E.1: Flexible slider-crank mechanism

The derivation of the governing equations of this mechanism and handling the flexible links are the same as that done in Appendix D for the flexible six-bar Stephenson mechanism. The boundary conditions for link 1 and 2 are assumed to be clamped-free and pinned-pinned respectively.

$$y_i = \Psi_i(x)q_i(t) , \quad i=1,2$$

$$\Psi_1(x) = \sin(\omega_1 x) - \sinh(\omega_1 x) - \left\{ \frac{\sin(\omega_1) + \sinh(\omega_1)}{\cos(\omega_1) + \cosh(\omega_1)} \right\} \{ \cos(\omega_1 x) - \cosh(\omega_1 x) \}$$

$$\Psi_2(x) = \sin(\omega_2 x)$$

$$\omega_1 = \frac{1.875104}{R_1}, \quad \omega_2 = \frac{\pi}{R_2}$$

$$\bar{r}_1 = x e^{i\theta} + y_1 e^{i(\theta + \frac{\pi}{2})} = x e^{i\theta} + y_1 e^{i\theta} e^{i\frac{\pi}{2}}$$

$$\bar{r}_1 = x e^{i\theta} + i y_1 e^{i\theta} = (x + i y_1) e^{i\theta}$$

$$\bar{r}_1 = (x + i y_1) (C_\theta + i S_\theta) = (x + i q_1 \Psi_1) (C_\theta + i S_\theta)$$

$$\bar{r}_1 = (x C_\theta - q_1 \Psi_1 S_\theta) + i (x S_\theta + q_1 \Psi_1 C_\theta)$$

$$\dot{\bar{r}}_1 = (-x \dot{\theta} S_\theta - \dot{q}_1 \Psi_1 S_\theta - q_1 \Psi_1 \dot{\theta} C_\theta) + i (x \dot{\theta} C_\theta + \dot{q}_1 \Psi_1 C_\theta - q_1 \Psi_1 \dot{\theta} S_\theta)$$

$$\dot{r}_1^2 = x^2 \dot{\theta}^2 + \Psi_1^2 \dot{q}_1^2 + \Psi_1^2 q_1^2 \dot{\theta}^2 + 2x \Psi_1 \dot{\theta} \dot{q}_1$$

$$\bar{r}_2 = (R_1 + R_2 - q_3) e^{i0} + x e^{i(\pi - \phi)} + y_2 e^{i(\frac{3\pi}{2} - \phi)}$$

$$\bar{r}_2 = R_1 + R_2 - q_3 + x e^{i\pi} e^{-i\phi} + y_2 e^{i(\frac{3\pi}{2})} e^{-i\phi}$$

$$\bar{r}_2 = R_1 + R_2 - q_3 - x e^{-i\phi} - i y_2 e^{-i\phi}$$

$$\vec{r}_2 = R_1 + R_2 - q_3 - (x + iy_2)e^{-i\phi}$$

$$\vec{r}_2 = R_1 + R_2 - q_3 - (x + iy_2)(C_\phi - iS_\phi)$$

$$\vec{r}_2 = (R_1 + R_2 - q_3 - xC_\phi - q_2\Psi_2S_\phi) + i(xS_\phi - q_2\Psi_2C_\phi)$$

$$\dot{\vec{r}}_2 = (-\dot{q}_3 + x\dot{\phi}S_\phi - \dot{q}_2\Psi_2S_\phi - q_2\Psi_2\dot{\phi}C_\phi) + i(x\dot{\phi}C_\phi - \dot{q}_2\Psi_2C_\phi + q_2\Psi_2\dot{\phi}S_\phi)$$

$$\dot{r}_2^2 = \dot{q}_3^2 + x^2\dot{\phi}^2 + \Psi_2^2\dot{q}_2^2 + \Psi_2^2q_2^2\dot{\phi}^2 - 2\dot{q}_3(x\dot{\phi}S_\phi - \Psi_2\dot{q}_2S_\phi - \Psi_2q_2\dot{\phi}C_\phi) - 2x\Psi_2\dot{\phi}\dot{q}_2$$

$$L = \frac{1}{2}\rho A_1 \int_0^{R_1} \dot{r}_1^2 dx + \frac{1}{2}\rho A_2 \int_0^{R_2} \dot{r}_2^2 dx + \frac{1}{2}m_3\dot{q}_3^2 - \frac{1}{2}EI_1 \int_0^{R_1} y_1^2 dx - \frac{1}{2}EI_2 \int_0^{R_2} y_2^2 dx \\ + \lambda_1(\vec{r}_1(R_1) - \vec{r}_2(R_2))_y + \lambda_2(\vec{r}_1(R_1) - \vec{r}_2(R_2))_x$$

$$L = k_1\dot{\theta}^2 + k_2\dot{\theta}\dot{q}_1 + k_3\dot{q}_1^2 + k_3\dot{\theta}^2q_1^2 + k_4\dot{\phi}^2 + k_5\dot{q}_2^2 + k_6\dot{\phi}\dot{q}_2 + k_7\dot{\phi}^2q_2^2 + k_{12}\dot{q}_3^2 \\ + \dot{q}_3(k_8\dot{\phi}S_\phi + k_9\dot{q}_2S_\phi + k_9q_2\dot{\phi}C_\phi) + \frac{1}{2}m_3\dot{q}_3^2 + k_{10}q_1^2 + k_{11}q_2^2 \\ + \lambda_1(R_1S_\theta + \Psi_{R_1}q_1C_\theta - R_2S_\phi) + \lambda_2(R_1C_\theta - \Psi_{R_1}q_1S_\theta - R_1 - R_2 + q_3 + R_2C_\phi)$$

$$k_1 = \frac{1}{2}\rho A_1 \int_0^{R_1} x^2 dx$$

$$k_2 = \frac{1}{2}\rho A_1 \int_0^{R_1} 2x\Psi_1 dx$$

$$k_3 = \frac{1}{2}\rho A_1 \int_0^{R_1} \Psi_1^2 dx$$

$$k_4 = \frac{1}{2} \rho A_2 \int_0^{R_2} x^2 dx$$

$$k_5 = \frac{1}{2} \rho A_2 \int_0^{R_2} \Psi_2^2 dx$$

$$k_6 = \frac{1}{2} \rho A_2 \int_0^{R_2} -2x \Psi_2 dx$$

$$k_7 = k_5$$

$$k_8 = \frac{1}{2} \rho A_2 \int_0^{R_2} -2x dx$$

$$k_9 = \frac{1}{2} \rho A_2 \int_0^{R_2} 2\Psi_2 dx$$

$$k_{10} = -\frac{1}{2} EI_1 \int_0^{R_1} \Psi_1''^2 dx$$

$$k_{11} = -\frac{1}{2} EI_2 \int_0^{R_2} \Psi_2''^2 dx$$

$$k_{12} = \frac{1}{2} \rho A_2 \int_0^{R_2} dx$$

$$\Psi_{R_1} = \Psi_1(R_1)$$

$$\frac{d}{dt} \frac{\partial L}{\partial \dot{\theta}} - \frac{\partial L}{\partial \theta} = Q_\theta$$

$$E_1 \ddot{\theta} + k_2 \ddot{q}_1 + E_2 + E_3 \lambda_1 + E_4 \lambda_2 = \frac{NK_t}{R_s} (V - K_e N \dot{\theta})$$

$$E_1 = 2(k_1 + k_3 q_1^2)$$

$$E_2=4k_3q_1\dot{q}_1\dot{\theta}$$

$$E_3=-R_1C_\theta+\Psi_{R_1}q_1S_\theta$$

$$E_4=R_1S_\theta+\Psi_{R_1}q_1C_\theta$$

$$\frac{d}{dt}\frac{\partial L}{\partial \dot{q}_1}-\frac{\partial L}{\partial q_1}=Q_{q_1}$$

$$k_2\ddot{\theta}+2k_3\ddot{q}_1+E_5+E_6\lambda_1+E_7\lambda_2=-2\zeta_1\omega_1^2\sqrt{\rho A_1E_1I_1}\dot{q}_1\int_0^{R_1}\Psi_1^2(x)dx$$

$$E_5=-2k_3q_1\dot{\theta}^2-2k_{10}q_1$$

$$E_6=-\Psi_{R_1}C_\theta$$

$$E_7=\Psi_{R_1}S_\theta$$

$$\frac{d}{dt}\frac{\partial L}{\partial \dot{\phi}}-\frac{\partial L}{\partial \phi}=Q_\phi$$

$$E_8\ddot{\phi}+k_6\ddot{q}_2+E_9\ddot{q}_3+E_{10}+E_{11}\lambda_1+E_{12}\lambda_2=0$$

$$E_8=2\left(k_4+k_7q_2^2\right)$$

$$E_9 = (k_8 S_\phi + k_9 q_2 C_\phi)$$

$$E_{10} = 4k_7 q_2 \dot{q}_2 \dot{\phi}$$

$$E_{11} = R_2 C_\phi$$

$$E_{12} = R_2 S_\phi$$

$$\frac{d}{dt} \frac{\partial L}{\partial \dot{q}_2} - \frac{\partial L}{\partial q_2} = Q_{q_2}$$

$$k_6 \ddot{\phi} + 2k_5 \ddot{q}_2 + E_{13} \ddot{q}_3 + E_{14} = -2\zeta \omega_2^2 \sqrt{\rho A_2 E_2 I_2} \dot{q}_2 \int_0^{R_2} \Psi_2^2(x) dx$$

$$E_{13} = k_9 S_\phi$$

$$E_{14} = -2k_7 q_2 \dot{\phi}^2 - 2k_{11} q_2$$

$$\frac{d}{dt} \frac{\partial L}{\partial \dot{q}_3} - \frac{\partial L}{\partial q_3} = Q_3$$

$$E_{15} \ddot{\phi} + E_{16} \ddot{q}_2 + E_{17} \ddot{q}_3 + E_{18} - \lambda_2 = 0$$

$$E_{15} = k_8 S_\phi + k_9 q_2 C_\phi$$

$$E_{16} = k_9 S_\phi$$

$$E_{17}=2k_{12}+m_3$$

$$E_{18}=k_8\dot{\phi}^2C_{\phi}+2k_9\dot{q}_2\dot{\phi}C_{\phi}-k_9q_2\dot{\phi}^2S_{\phi}$$

$$\frac{d}{dt}\frac{\partial L}{\partial \dot{\lambda}_1}-\frac{\partial L}{\partial \lambda_1}=0$$

$$E_{19}\ddot{\theta}+E_{20}\ddot{q}_1+E_{21}\ddot{\phi}+E_{22}=0$$

$$E_{19}=(R_1C_{\theta}-\Psi_{R_1}q_1S_{\theta})$$

$$E_{20}=\Psi_{R_1}C_{\theta}$$

$$E_{21}=-R_2C_{\phi}$$

$$E_{22}=-R_1\dot{\theta}^2S_{\theta}-2\Psi_{R_1}\dot{q}_1\dot{\theta}S_{\theta}-\Psi_{R_1}q_1\dot{\theta}^2C_{\theta}+R_1\dot{\phi}^2S_{\phi}$$

$$\frac{d}{dt}\frac{\partial L}{\partial \dot{\lambda}_2}-\frac{\partial L}{\partial \lambda_2}=0$$

$$E_{23}\ddot{\theta}+E_{24}\ddot{q}_1+E_{25}\ddot{\phi}+\ddot{q}_3+E_{26}=0$$

$$E_{23}=-R_1S_{\theta}-\Psi_{R_1}q_1C_{\theta}$$

$$E_{24}=-\Psi_{R_1}S_{\theta}$$

$$E_{25}=-R_2S_{\phi}$$

$$E_{26} = -R_1 \dot{\theta}^2 C_\theta - 2\Psi_{R_1} \dot{q}_1 \dot{\theta} C_\theta + \Psi_{R_1} q_1 \dot{\theta}^2 S_\theta - R_2 \dot{\phi}^2 C_\phi$$

The final equations of motion in matrix form are,

$$\begin{bmatrix} E_1 & k_2 & 0 & 0 & 0 & E_3 & E_4 \\ k_2 & 2k_3 & 0 & 0 & 0 & E_6 & E_7 \\ 0 & 0 & E_8 & k_6 & E_9 & E_{11} & E_{12} \\ 0 & 0 & k_6 & 2k_5 & E_{13} & 0 & 0 \\ 0 & 0 & E_{15} & E_{16} & E_{17} & 0 & -1 \\ E_{19} & E_{20} & E_{21} & 0 & 0 & 0 & 0 \\ E_{23} & E_{24} & E_{25} & 0 & 1 & 0 & 0 \end{bmatrix} \begin{bmatrix} \ddot{\theta} \\ \ddot{q}_1 \\ \ddot{\phi} \\ \ddot{q}_2 \\ \ddot{q}_3 \\ \lambda_1 \\ \lambda_2 \end{bmatrix}$$

$$= - \begin{bmatrix} E_2 - \frac{NK_t}{R_s} (V - K_e N \dot{\theta}) \\ E_5 + 2\zeta\omega_1^2 \sqrt{\rho A_1 E_1 I_1} \dot{q}_1 \int_0^{R_1} \Psi_1^2(x) dx \\ E_{10} \\ E_{14} + 2\zeta\omega_2^2 \sqrt{\rho A_2 E_2 I_2} \dot{q}_2 \int_0^{R_2} \Psi_2^2(x) dx \\ E_{18} \\ E_{22} \\ E_{26} \end{bmatrix}$$

References

- 1- H. Yan, W. Chen, "On the Output Motion Characteristics of Variable Input Speed Servo-Controlled Slider-Crank Mechanisms", *Journal of Mechanism and Machine Theory*, Vol. 35, pp. 541-561.
- 2- H. Yan, W. Chen, "A Variable Input Speed Approach for Improving the Output Motion Characteristics of Watt-Type Presses", *International Journal of Machine Tools & Manufacture*, Vol. 40, 675-690.
- 3- H. Yan, R. Soong, "Kinematic and Dynamic Design of Four-Bar Linkages by Links Counterweighing with variable Input Speed", *Journal of Mechanism and Machine Theory*, Vol. 36, pp. 1051-1071.
- 4- H. Yan, W. Chen, "Optimized Kinematic Properties for Stevenson-Type Presses with Variable Input Speed Approach", *Journal of Mechanical Design*, Vol. 124, June 2002, pp. 350-354.
- 5- A. Sherwood, "The Dynamic Synthesis of a Mechanism with Time-Dependent Output", *Journal of Mechanisms*, Vol. 3, pp. 35-40.
- 6- F. Wu, W. Zhang, Q. Li, P. Ouyang, "Integrated Design and PD Control of High-Speed Closed-Loop Mechanism", *Journal of Dynamic Systems, Measurement, and Control*, Vol. 124, December 2002, pp. 522-528.
- 7- H. Funabashi, F. Freudenstein, "Performance Criteria for High-Speed Crank-and-Rocker Linkages, Part I: Plane Crank-and-Rocker Linkages", *Journal of Mechanical Design*, Vol. 101, January 1979, pp. 20-25.

- 8- A. Garcia-Reynoso, W. Seering, "Vibration Characteristics of an Elastic Linkage with Elastic Input and Output Shafts", *Journal of Mechanisms, Transmissions, and Automation in Design*, Vol. 106, September 1984, pp. 272-277.
- 9- J. Song, E. Haug, "Dynamic Analysis of Planar Flexible Mechanisms", *Journal of Computer Methods in Applied Mechanics and Engineering*, Vol. 24, 1980, pp. 359-381.
- 10- A. Rao, "Dynamic Synthesis of 2 Degrees-of-Freedom Flexibly Coupled Slider-Link Mechanism for Harmonic Motion or Function-Generation", *Journal of Mechanism and Machine Theory*, Vol. 14, pp. 233-238.
- 11- J. Davidson, "Analysis and Synthesis of Slider-Crank Mechanism with a Flexibly-Attached Slider", *Journal of Mechanisms*, Vol. 5, pp. 239-247.
- 12- A. Liniecki, "Synthesis of a Slider-Crank Mechanism with Consideration of Dynamic Effects", *Journal of Mechanisms*, Vol. 5, pp. 337-349.
- 13- S. Arimoto, S. Kawamura, F. Miyazaki, "Bettering Operation of Robots by Learning", *Journal of Robotic Systems*, Vol. 1, 1984, pp. 123-140.
- 14- M. Chew, M. Phan, "Application of Learning Control Theory to Mechanisms: Part 1 – Inverse Kinematics and Parametric Errors Compensation", *Proc. Of the 23rd ASME Mechanisms Conference*, Minneapolis, MN, September 1994.
- 15- M. Chew, M. Phan, "Application of Learning Control Theory to Mechanisms: Part 1 – Reduction of Residual Vibrations in High-Speed Electromechanical

- Bonding Machines”, Proc. Of the 23rd ASME Mechanisms Conference, Minneapolis, MN, September 1994.
- 16- S. Oh, Z. Bien, “An Iterative Learning Control Method with Application for the Robot Manipulator”, IEEE Journal of Robotics and Automation, Vol. 4, No. 5, pp. 508-514.
- 17- R. Horowitz, “Learning Control of Robot Manipulators”, Journal of Dynamic Systems, Measurement, and Control, Vol. 115, June 1993, pp. 402-411.
- 18- W. Chang, “Repetitive Control of a High-Speed Cam-Follower System”, A thesis Presented to the graduate and Research Committee of Lehigh University, June 1996.
- 19- J. Mathews, “Numerical Methods”, Second Edition, Prentice Hall.
- 20- B. Kolman, “Introductory Linear Algebra with Applications”, Fourth Edition, Maxwell Macmillan.
- 21- B. Magrab, S. Azarm, B. Balachandran, J. Duncan, K. Herold, G. Walsh, “An Engineering Guide to MATLAB”, Prentice Hall.
- 22- I. Cochran, W. Cadwallender, “Analysis and Design of Dynamics Systems”, Third Edition, Addison Wesley.
- 23- J. Meriam, L. Kraige, “Engineering Mechanics, Dynamics”, Third Edition, J. W. Wiley.
- 24- H. Baruh, “Analytical Dynamics”, McGraw-Hill.
- 25- D. Greenwood, “Principles of Dynamics”, Second Edition, Prentice Hall.

- 26- Cyril M. Harris, "Shock and Vibration Handbook", Fourth Edition, McGraw-Hill.
- 27- S. Rao, "Mechanical Vibrations", Second Edition, Addison Wesley.
- 28- A. Shabana, "Vibration of Discrete and Continuous Systems", Second Edition, Springer.
- 29- L. Meirovitch, "Principles and Techniques of Vibrations", Prentice Hall.
- 30- C. Wilson, J. Sadler, W. Michels, "Kinematics and Dynamics of Machinery", 1983, Harper & Row.
- 31- A. Erdman, G. Sandor, S. Kota, "Mechanism Design: Analysis and Synthesis", Volume 1, Fourth Edition, Prentice Hall.
- 32- Norton, "Design of Machinery", Second Edition, McGraw-Hill.
- 33- G. Sandor, A. Erdman, "Advanced Mechanism Design: Analysis and Synthesis", Volume 2, Prentice Hall.
- 34- G. Franklin, J. Powell, M. Workman, "Digital Control of Dynamics System", Third Edition, Addison Wesley.
- 35- K. Ogata, "Modern Control Engineering", Second Edition, Prentice Hall.
- 36- K. Astrom, B. Wittenmark, "Adaptive Control", Second Edition, Addison Wesley.
- 37- R. Dorf, R. Bishop, "Modern Control Systems", Ninth Edition, Prentice Hall.
- 38- J. Shigley, C. Mischke, "Mechanical Engineering Design", Fifth Edition, McGraw-Hill.
- 39- P. Emanuel, "Motors, Generators, Transformers, and Energy", Prentice Hall.

Vita

Khaled Al-Ghanem was born in Kuwait in 1972. He received his B.S. degree in the mechanical engineering in 1996 from Kuwait University, Kuwait. He was granted a scholarship from Kuwait University for higher education in the United States. He received his M.S. degree in mechanical engineering in 1999 from Syracuse University, New York. Al-Ghanem continued study for the Ph.D. degree with Dr. Meng-Sang Chew at Lehigh University, Pennsylvania and received his Ph.D. in mechanical engineering in 2004.